Characterisation and Modulation of Drug Resistance in Lung Cancer Cell Lines

A thesis submitted for the degree of M.Sc.

By

Gráinne Dunne, B.Sc. (Hons)

The experimental work described in this thesis was carried out under the supervision of

Prof. Martin Clynes, Dr. Laura Breen and Dr. Robert O'Connor

National Institute for Cellular Biotechnology,
Dublin City University,
Glasnevin,
Dublin 9,
Ireland.

Acknowledgements

Firstly, thank you to my supervisors, Dr. Robert O'Connor and Prof. Martin Clynes for allowing me to undertake this project and for providing the support to see it through and to Dr. Laura for the endless help and support in and out of the lab.

Some of this work would also not have been possible without the help of Sandra with the drug quantifications, Mick and Paul with the membrane proteomics and Naomi with answering the never ending list of questions! Thank you guys, and to everyone in tox who helped me at some stage along the way.

There is a definite need to balance the insanity that accompanies any research project and so a huge thanks to all, who provided the friendships and laughs along the way! A special thanks to Laura, Naomi, Paula, Justine, Lisa and of course Sandra and Erica who never failed to make me laugh (at or with –either way it counts!). Also, not to forget the rest of the friends in tox and upstairs!

Thanks also; to my non-science friends, who never truly understood what I was moaning about but listened anyway!; to my family, who provide a constant source of support no matter what I do and of course Barry who has had to live with me during this!! I know this has been said before but…..patience of a saint comes to mind!

Characterisation and Modulation of Drug Resistance in Lung Cancer Cells

Abstract

Chemotherapy drug resistance is a major obstacle in the treatment of cancer. It can result from an increase in levels of cellular drug efflux pumps such as P-glycoprotein (P-gp). Using cellular models, this thesis aimed to investigate resistance in lung cancer cells while developing siRNA and membrane proteomic techniques and to increase our knowledge of the effect of lapatinib, a newly developed targeted therapy, in these resistant cells.

Lapatinib, a growth factor receptor tyrosine kinase inhibitor synergised with P-gp substrate cytotoxics in P-gp over-expressing resistant cells. However, lapatinib treatment, at clinically relevant concentrations, also increased levels of the P-gp drug transporter in a dose-responsive manner. Conversely, exposure to the epidermal growth factor (EGF), an endogenous growth factor receptor ligand, resulted in a decrease in P-gp expression. Using drug accumulation, efflux and toxicity assays we determined that alteration in P-gp levels by either lapatinib or EGF had little functional significance.

P-gp is not the only resistance mechanism so siRNA-mediated gene silencing was exploited to investigate the role of additional proteins with potential roles in resistance. Firstly, P-gp knockdown by siRNA was coupled with toxicity and accumulation assays to determine the impact of silencing this protein in the chosen resistant lung cells. Additional putative targets were chosen from microarray data identifying genes associated with the development of paclitaxel resistance. Of the three genes investigated, ID3, CRYZ and CRIP1, ID3 emerged as having a potential role in contributing to resistance in one of the resistant lung carcinoma cell lines investigated.

Many of the proteins important in resistance are membrane expressed but due to their size and hydrophobic nature, can be difficult to characterise. A 2D-LC-MS method was designed and employed to examine membrane proteins from the resistant lung cell models. Suitable parameters important in optimal identification of the proteins were determined. Large numbers of proteins were identified and comparisons made, highlighting those that were differentially expressed.

Chapter 1 Introduction

1.1. Cancer

Cancer is a major worldwide health problem that results in a huge loss of life every year. In 2002 it was estimated that there were 10.9 million new cancer cases, 6.7 million cancer associated deaths, and 24.6 million persons living with the disease, worldwide [1]. Cancer ultimately results from alterations in the control mechanisms that govern normal cell physiology. Some of the primary alterations contributing to malignancy are; a self-sufficiency in growth signalling; insensitivity to growth-inhibitory signalling; evasion of apoptosis (programmed cell death); inexhaustible replicative potential; sustained angiogenesis; and tissue invasion and metastasis [2]. Tumour formation interferes with the body's normal physiology, causing damage to internal organs and systems, and in many cases, ultimately results in death.

1.1.1. Lung cancer

Lung cancer was reported to be the most frequently diagnosed of the major cancers and the most common cause of cancer mortality in males by the World Health Organisation in 2001 [3]. A decreased incidence in lung cancer was observed in males throughout Europe in the decade spanning from the mid 1990s to the mid 2000s. However, an opposing effect was seen in females and ultimately this cancer is still very commonly diagnosed in Europe and associated with poor survival rates [4]. The majority of cases present with advanced disease and are typically associated with a less than 5 year survival duration. The disease can progress significantly before symptoms develop. However, there is generally an increase in occurrence of the common symptoms of expectoration and cough over time in clinical cases [5]. Cigarette smoke exposure is a major causative factor with approximately 87% of lung-cancer cases resulting from this single cause [6]. Lung cancers can be histologically classified into two main groups, non small cell lung cancer (NSCLC) and small cell lung cancer (SCLC) with 80% of cases falling into the first group and the remaining 20% into the second [7].

The staging of lung cancers is carried out in order to determine treatment regimes and to compare efficacies of new treatments across clinical trials. This is generally based on the (TNM) classification, where T represents the scale of the primary tumour, N represents the lymph node involvement and M represents the presence metastasis [8, 9].

1.1.1.1. Small Cell Lung Cancer (SCLC)

Small cell lung cancers are aggressive malignancies, with rapid growth and characterised by early metastasis. These tumours are normally centrally located and are strongly associated with smoking. Relapse is very common even after initial response to treatment [10, 11].

1.1.1.2. Non Small Cell Lung Cancer (NSCLC)

NSCLC include adenocarcinomas, squamous cell, large cell and bronchoalveolar carcinomas. Around 30% of NSCLC are made up by adenocarcinomas, including the bronchoalveolar carcinomas. These are typically peripheral tumours. Adenocarcinomas are associated with early development of metastasis and often the primary site remains symptomless [11]. Squamous cell carcinomas account for approximately 30% of all lung cancers and they are typically centrally located [5, 9]. Squamous-cell carcinomas, which are very common in Europe, and can be accompanied with late development of distant metastasis [11]. NSCLC is associated with poor prognosis and despite surgery being first line treatment, approximately 70% of patients present with unresectable disease [12].

1.1.2. Lung cancer treatments

The objective in cancer treatment is to control or eradicate the neoplasm and prevent its spread. Methods employed in the treatment of cancer include, surgery, radiation and chemotherapy or a combination of the above. Despite huge developments in cancer treatment, the outcome for many patients with advanced disease is still not promising.

Chemotherapy is the mainstay treatment for small cell lung cancer as surgery is often not an option due to most patients presenting with metastasis. Cisplatin, carboplatin, doxorubicin, vincristine, paclitaxel and docetaxel are among the active chemotherapy drugs approved in SCLC treatment. Single agent therapy produces a more short lived response and so combination therapy is the standard care. Although response rates are high (75-80%), most patients will suffer from relapsed disease [10, 11, 13].

Surgical resection is more commonly employed in non small cell lung cancer treatment and carried out where possible [11]. Many single anti-cancer agents have activity against NSCLC and these include cisplatin, carboplatin, paclitaxel, docetaxel,

vinorelbine and gemcitabine; however, a modest increase in response rates is seen with combinations and so platinum-based combinations form the standard care [14]. Paclitaxel or docetaxel in combination with cisplatin has been recommended as an option in first-line treatment of advanced NSCLC. More recently, targeted therapies have shown promise in the treatment of NSCLC. The epidermal growth factor receptor (EGFR) inhibitors erlotinib, gefitinib, and cetuximab have proved to have some clinical activity in non-small cell lung cancer [15]. Such agents will be discussed further in section 1.4.

Despite progress in the development of drugs that target unique cancer-specific pathways, chemotherapeutics yield significant survival advantages in many cancer types and so continue to be used in the clinic.

1.2. Chemotherapy

Cytotoxic drugs employed in the treatment of cancer include, anthracyclines, taxanes, vinca alkaloids and platinum compounds. These can be used as a monotherapy but are often administered in specific combinations. The discussion below focuses on agents employed in this study.

1.2.1. Anthracyclines

Anthracyclines are cytotoxic antibiotics that produce their effects primarily by acting directly on DNA. They include doxorubicin (adriamycin), daunorubicin and epirubicin. These drugs are the semi-synthetic derivative of the fermentation product of *Streptomyces pseucetius var. caesius.* They are broad spectrum anti-cancer agents, having potent activity against a wide variety of cancer types [16]. These agents cause breaks to double- or single- stranded DNA. In addition, they produce free radicals that damage macro-molecules and lipid membranes and they also poison Topoisomerase II, resulting in DNA damage, since topoisomerases function in DNA replication, chromosome condensation and chromosome segregation. Anthracyclines are frequently used in the treatment of breast cancer, leukaemias, lymphomas and sarcomas [17]. Structures of doxorubicin and epirubicin are shown in figure 1.1. Both doxorubicin and epirubicin often form part of standard care in adjuvant treatment of

breast cancer, with cardiotoxicity being the main life-threatening side effect to contend with [18].

Figure 1.1 Chemical structures of doxorubicin and epirubicin

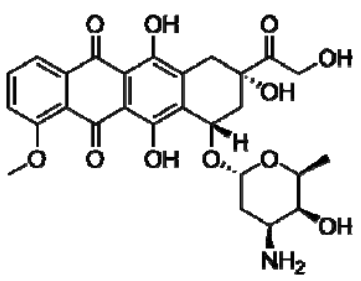

Doxorubicin

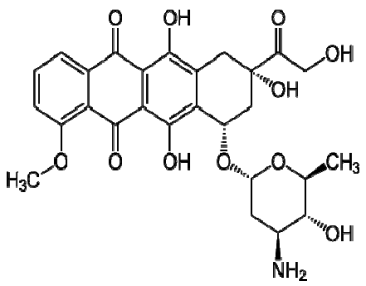

Epirubicin

1.2.2. Antimitotics

Anticancer drugs that target tubulin form a group of effective anticancer agents. These include taxanes and the vinca alkaloids. In the cellular cytoskeleton, tubulin polymerises to form microtubules and these are crucial in the development and maintenance of cell shape, in mediating intracellular transport, in cell signalling and in cell division and mitosis. The critical role of these proteins in cell division and mitosis makes them a good target for anticancer drugs. Taxanes are known as microtubule-stabilizing agents and vinca alkaloids as destabilizing agents [19].

1.2.2.1. Taxanes

Taxanes bind to β-tubulin in the microtubles causing accelerated polymerisation of the tubulin. The resultant microtubules are in a stabilized state and fail to depolymerise. This disruption to the normal function of microtubules results in cell cycle arrest between the prophase and anaphase stages [20]. Paclitaxel (taxol) was first isolated in 1971 from the pacific yew (*Taxus brevifolia*) and this was followed by the more potent semi-synthetic derivative, docetaxel. These agents demonstrate broad spectrum anticancer activity on cancers of the breast, lung, ovary, bladder and prostate and their structures are shown in figure 1.2. Despite their structural similarity, paclitaxel and docetaxel exhibit differences in their activity and toxicity

profiles. Docetaxel has greater affinity for β-tubulin, affecting centromere organisation and acts on cells in the S, G_2 and M phases of the cell cycle. Paclitaxel affects the mitotic spindle and so acts on cells in the G_2 and M phases of the cell cycle. Docetaxel exhibits a greater uptake into tumour cells, which may explain its increased potency compared with paclitaxel [21, 22].

Figure 1.2 Chemical structures of paclitaxel and docetaxel

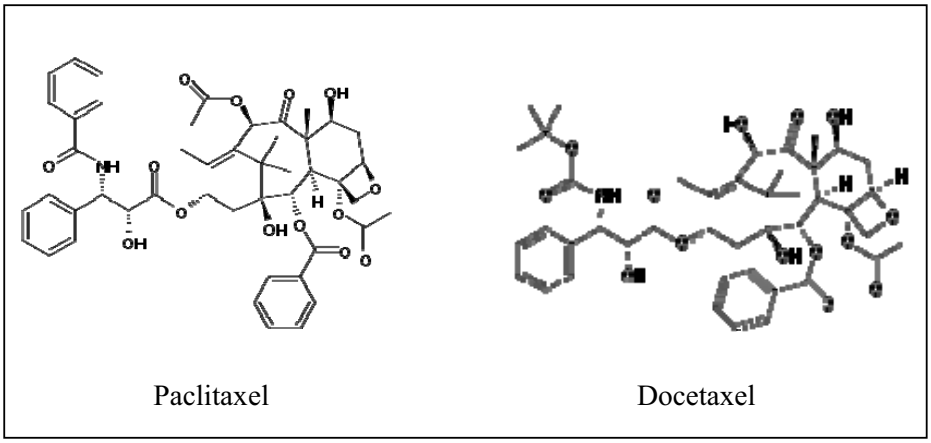

Paclitaxel Docetaxel

1.2.2.2. Vinca alkaloids

The vinca alkaloids, vinblastine and vincristine were the first plant-derived anticancer agents to progress into clinical use. They were isolated from the Madagascar periwinkle plant *Catharanthus roseus G.Don.* [23]. Their cytotoxic effects are concentration dependent. At lower concentrations they bind to high affinity sites at the ends of microtubules and prevent microtubule polymerization. When present in higher concentrations they bind to low affinity, high capacity sites resulting in disintegration of formed microtubules [21]. Vinblastine has uses in the treatment of systemic Hodgkin's disease and other lymphomas as well as in lung carcinoma and carcinoma of the testis [16]. Vincristine has also been included in treatment regimes for acute lymphoblastic leukaemia, hodgkin's disease, non-hodgkin's lymphoma and brain tumour and is frequently used in childhood malignancies. This drug has shown limited success in the treatment of lung cancer and breast cancer [24]. Vinorelbine is a newer vinca alkaloid and has shown much promise. In the USA it has been approved for treatment of non-small cell lung cancer (NSCLC) and has demonstrated considerable activity in breast cancer and squamous cell carcinoma of the head and

neck. In metastatic breast cancer studies, vinorelbine treatment has yielded promising results in combination with trastuzumab [21].

Figure 1.3 Chemical structures of vinblastine and vincristine

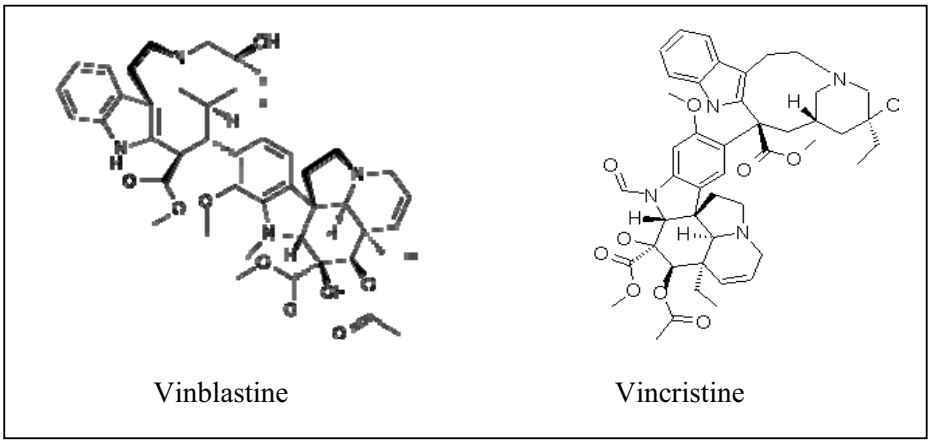

Vinblastine Vincristine

1.2.3. Other cytotoxic agents

There are many other chemotherapeutic agents also having clinical benefit as anti-cancer agents, including; alkylating agents, such as procarbazine and cisplatin; antimetabolites, such as methotrexate and pyrimidine antagonists, such as 5-fluorouracil (5-FU). Cisplatin, a platinum compound binds DNA through formation of interstrand cross-links and can kill cells at any stage of the cell cycle. Methotrexate is a folate antagonist that ultimately interferes with the formation of DNA, RNA and protein. 5-FU's actions include inhibition of DNA synthesis and alteration of RNA processing and function [16].

A lot of these drugs have been very successful in the treatment of many malignancies, they are, however, therapeutically limiting when faced with problems such as toxicity and resistance.

1.3. Chemotherapy resistance

Resistance to chemotherapy action has long been a problem in the treatment of cancer. This phenomenon is thought to account for treatment failure in over 90% of metastatic disease. Drug resistance may be intrinsic, occurring at the time of first line treatment, or acquired, developing after treatment with chemotherapeutics. There are

many mechanisms by which cancer cells can develop this resistance. These include; increased drug efflux and decreased drug uptake, drug inactivation, changes to drug target, handling of drug-induced damage and evasion of apoptosis [25]. Many different genes that contribute to various mechanisms of resistance have been identified. Their contribution includes; the amplification or over-expression of membrane drug transporters, such as P-gp; the altering of cellular proteins involved in detoxification, including glutathione S transferase; alteration of proteins involved in DNA repair, such as DNA topoisomerase II; and the activation or inactivation of oncogenes (HER-2, bcl-2, c-jun and ras) and tumour suppressor genes (p53), respectively [26]. Over-expression of growth factor receptors has been shown to play a role in resistance and this is discussed further in section 1.4.3.

Ultimately, the presence of the drug, at its required intracellular concentration, is vital for chemotherapeutic drug efficacy and so, much research has focused on resistance associated with drug efflux. Tumours can often develop resistance to drugs other than that they were treated with and this is termed multi-drug resistance.

1.3.1. Drug efflux pump-mediated resistance

Over 30 years ago, Juliano and Ling described the nature of a cellular protein conferring drug resistance. They showed that Chinese Hamster Ovary cells displayed cross-resistance to a range of amphiphilic drugs after they were selected for resistance to colchicine. This drug resistant state was as a result of a reduced rate of drug permeation. A cell surface glycoprotein, named P-glycoprotein (P-gp), was described and its levels correlated with the degree of drug-resistance in the cross-resistant ovary cells [27]. P-gp is said to be the product of the multi-drug resistance gene (MDR) and so is also known as MDR-1. This protein is an ATP-dependent transporter and a member of the ABC superfamily of transporter proteins.

The family of ABC transporters all contain ATP-binding domains or nucleotide—binding folds (NBF), which in turn contain characteristic motifs (Walker A and B motifs) separated by sequences of 90-120 amino acids found in all ATP-binding proteins. They use the energy from ATP binding to drive the transport of substances across the membrane. This transport occurs in a unidirectional manner and can be against substantial concentration gradients, ultimately moving drugs out of the cell.

Functional ABC proteins contain two NBFs which are located in the cytoplasm and two transmembrane domains. The transmembrane domains contain a number of membrane spanning α-helices which determine their substrate specificity [28, 29].

Members of the ABC superfamily of transporter proteins function in transporting a wide range of substrates, such as ions, phospholipids, steroids, polysaccharides, amino acids and peptides across biological membrane [30]. Many chemotherapy drugs in current use, such as anthracyclines, vinca alkaloids and taxanes, are transported by one or more of these protein pumps (Table 1.1). Tumour over-expression of these pumps can therefore greatly reduce treatment efficacy.

1.3.1.1. P-glycoprotein

P-gp, the product of the ABCB1/MDR1 gene, is a 170kDa transmembrane glycoprotein which belongs to the ABCB subfamily of the superfamily of ATP-binding cassette (ABC) proteins. Like other ABC transporters, it contains two transmembrane domains and two ATP binding sites. The transmembrane domains each span the membrane six times as shown schematically in Figure 1.4. P-glycoprotein can catalyse substrate-stimulated ATP hydrolysis at a rate comparable to other ion-translocating ATPases. Mutational analysis has shown that both ATP binding sites are needed for ATP hydrolysis and drug transport [31].

Figure 1.4 **Schematic of P-glycoprotein transmembrane drug efflux pump, illustration obtained from Sorrentino *et al.*, (2002) [32]**

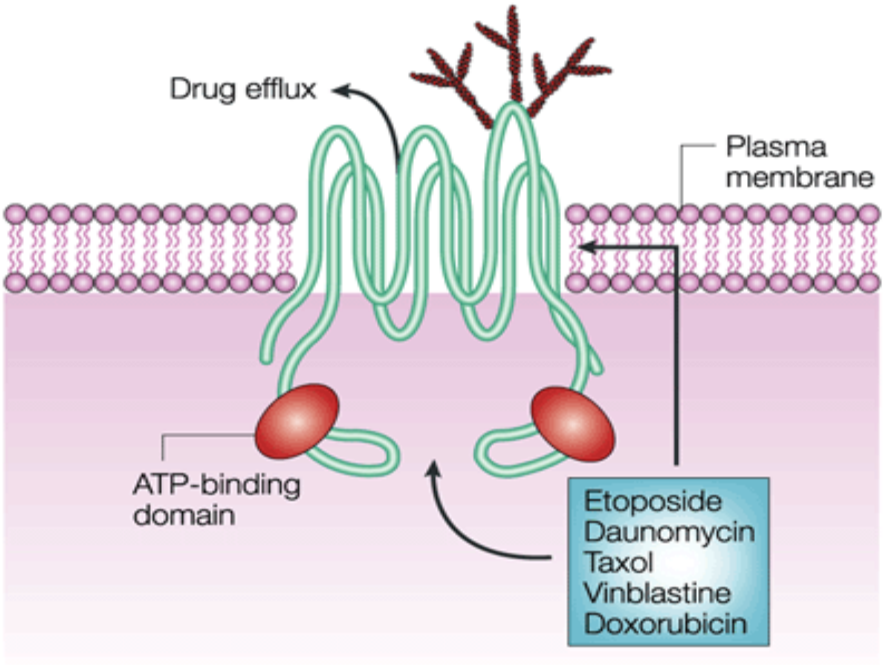

P-gp plays an important protective role in normal tissues. It is capable of transporting drugs from the cytoplasm and is present on the surface of epithelial cells from excretory organs and in endothelial cells in the blood-brain barrier. Studies on P-gp-knockout mice show a reduced body clearance of many drugs and so this protein acts to protect the host by reducing exposure to xenobiotics [33].

However, P-gp also plays an important role in multi-drug resistance and is the most studied and best characterised of all the drug transporter pumps. High levels of the MDR1 gene and protein have been found in cancers derived from the kidney, liver, colon, pancreas and adrenal glands. Some untreated cancers, including leukaemia, neuroblastoma and breast, show high levels of MDR1 mRNA and increased expression is often seen with chemotherapy treatments [34]. P-gp levels were shown to be positively correlated to levels of resistance in SKBR-3, MCF-7 and BT474 cell lines [35]. P-gp can transport a wide variety of anti-cancer agents. Substrates are usually organic molecules, containing aromatic groups, although they may be non-aromatic. Uncharged molecules are the most efficient to be transported, with more

acidic compounds transported at a lower rate. All substrates are amphipathic in nature. The hydrophobic nature of most P-gp substrate drugs allows them to readily diffuse across membranes into tissues. Drugs of interest which are actively transported by P-gp include doxorubicin, daunorubicin, epirubicin, paclitaxel, docetaxel, vinblastine and vincristine [28, 36].

1.3.1.2. MRP1

The discovery of P-gp led to more research into the phenomena of drug resistance; however, it was observed that several cell lines displayed the multi-drug phenotype in the absence of P-gp expression. This led to further investigations and a second pump was later described when the multi-drug resistance associated gene (ABCC1) was cloned in 1992. This gene encodes for multi-drug resistant protein 1 (MRP1) and is also a member of the ATP-binding cassette (ABC) superfamily of transporter proteins [37]. Subsequent members of the MRP (ABCC) family were identified.

This MRP1 transporter has a similar structure to P-gp, thus containing two hydrophobic membrane spanning domains and two cytosolic ATP binding domains, in addition to an N-terminal extension containing five putative transmembrane segments. It is thought that MRP1 co-transports some natural product chemotherapeutic drugs with gluthatione hence this peptide plays an important role in MRP1-mediated drug resistance. Over-expression of MRP1 has been found in multi-drug resistant cells lines from many different tissue and tumour types, including lung, colon, breast, bladder, prostate and thyroid carcinomas [29, 30].

1.3.1.3. BCRP

The breast cancer resistant pump (BCRP), a product of the ABCG2 gene, also known as MXR and ABCP, was identified more recently and is believed to contribute to some cases of multidrug resistance [38]. This member of the ABC transporter proteins is referred to as a half transporter as it contains only one ATP binding site and one transmembrane domain within one polypeptide and must dimerise to function. However, it can still transport a variety of drugs including daunorubicin, doxorubicin, mitoxantrone and prazosin. It has been shown to be over-expressed in a range of cell types, such as those derived from breast cancer, ovarian carcinoma, colon cancer and leukaemia causing multidrug resistance in the absence of P-gp and

MRP [39]. Table 1.1 outlines substrate specificity for the three drug transporter pumps, P-gp, MRP1 and BCRP.

Table 1.1 Substrates for ABC transporters, obtained from Sparreboom *et al.*, (2003) [28]

ABC Transporter Gene	Substrate
ABCB1 (P-gp)	Daunorubicin
	Doxorubicin
	Doxetaxel
	Paclitaxel
	Vinblastine
	Vincristine
	Mitoxantrone
	Topotecan
ABCC1 (MRP1)	Daunorubicin
	Doxorubicin
	Vincristine
	Methotrexate
ABCG2 (BCRP)	Daunorubicin
	Epirubicin
	Mitoxantrone
	Topotecan

1.3.2. Inhibitors of multidrug resistance

Due to their role in resistance, the drug transporter pumps present an attractive target for anti-resistance agents, and successful development of such drugs could lead to improved patient treatments. Modulators of the P-gp protein have been developed, however, with limited success. First-generation modulators include the calcium channel blocker verapamil and the immunosuppressant cyclosporin A. The problem with these agents is that, these drugs are required in high doses to achieve sufficient plasma concentrations needed to reverse MDR, and at these doses they are highly toxic. Their failure as P-gp modulators led to the development of second generation

agents which were stereoisomers or structural analogues of the first generation drugs. These did not work well in combination with anti-cancer drugs as they interfered with the pharmacokinetic and biodistribution properties of the chemotherapy drugs [40]. Third generation inhibitors of P-gp function were developed using structure-activity relationships and combinatorial chemistry. These include tariquidar and elacridar and have demonstrated some potential in the preclinical setting [41]. In a phase II clinical trial tariquidar showed limited ability to restore sensitivity to anthracycline or taxane chemotherapy in patients with advanced breast cancer [42].

More recently other agents have been developed and shown to have the ability to reverse MDR. Curcumin, a constituent of tumeric, has been shown to reduce the expression of P-gp by inhibiting the PI3K/Akt/NF-κB signalling pathway, thereby reversing doxorubicin resistance in L1210/Adr cells [43]. Other non-steroidal anti-inflammatory agents such as ibuprofen and NS-398 also have actions in over-coming P-gp mediated MDR in resistant cell lines [44]. A newly synthesized triaryl-substituted imidazole derivative, FG020326, can potentiate the cytotoxicity of paclitaxel, doxorubicin and vincristine in two P-gp over-expressing cell lines [45]. Carnosic acid, dihydroptychantol A and sipholenol A are other newly identified agents which have MDR reversing abilities [46-48].

Tyrosine kinase inhibitors have also recently emerged as agents with some activity in modulating multi-drug resistance ATP-binding cassette proteins and this is discussed further in section 1.4.5.

1.3.3. Genes associated with development of paclitaxel resistance

Microarray analysis carried out previously in our laboratory, identified genes associated with the development of paclitaxel resistance, by comparing genes present in three lung cell lines and those present in their paclitaxel selected resistant counterparts [49]. In this thesis, some of these genes were chosen for further investigation utilising siRNA mediated gene knockdown and are discussed below. Three genes were selected from the microarray data, ID3, CRYZ and CRIP1.

ID3 is a member of the ID (inhibition of DNA binding/differentiation) helix-loop-helix family of proteins whose main function is in regulating cell growth and

differentiation. They act as dominant-negative regulators of basic HLH transcription factors. Altered expression of the ID3 has been observed in various cancer cell lines from the lung, colon, and pancreas with high expression reported as being associated with aggressive mammary epithelial tumours [50, 51].

Zeta-crystallin (CRYZ) was first identified in guinea pig lenses and then in the lenses of other animals. It was later found in non-lenticular tissues of various species. It is a NADPH-dependent quinone reductase thereby amending oxidative damage in cells [52, 53].

CRIP1 encodes for cysteine-rich intestinal protein 1 and is a member of the LIM/double zinc finger protein family. It contains the LIM motif, a conserved region of histidine and cysteine residues and so has metal binding properties and is thought to have a role in zinc transport [54, 55]. More recently it has been described as a novel cancer biomarker exhibiting high levels of expression in many cancer types [56].

1.4. Targeted therapy

As traditional chemotherapeutics face problems with toxicity and lack of selectivity there has been a huge surge in focus on developing targeted therapeutics. Unlike chemotherapeutic drugs which are directed at rapidly dividing cells, the newer agents take advantage of and target, signalling pathways more specific to cancer cells. Therapies have been developed to target; the BCR-ABL protein, which is present and causative in a huge majority of chronic myeloid leukaemia (CML) patients; the mammalian target of rapamycin (mTOR), which is involved in protein synthesis and cell survival; the Raf/MEK/ERK signalling cascade, which mediates tumour cell proliferation and angiogenesis; the ubiquitin-proteasome pathway, which plays a vital role in regulating the degradation of proteins involved in cell cycle control and tumour cell proliferation; cyclin-dependant kinases, which form core components of the cell cycle machinery allowing tumour cells a selective growth advantage; VEGF, which promotes the formation of new blood capillaries and BCL-2, which has anti-apoptotic abilities [57]. The oncogenic activity of growth factors and their receptors makes their signalling an attractive pathway to manipulate with molecular-targeted

therapy and many agents have also been developed to target the epidermal growth factor receptors.

1.4.1. ErbB receptors

The Epidermal Growth Factor (EGF) receptor is a member of the ErbB family of transmembrane glycoprotein receptors that play an important role in managing cellular functions such as growth/proliferation, survival and differentiation [58]. EGFR is a 170kDa transmembrane glycoprotein containing an extracellular receptor domain and an intracellular domain with tyrosine kinase function [59]. The ErbB family of receptors has four members; EGFR also known as ErbB1/Her1, ErbB2/Her2, ErbB3/Her3 and ErbB4/Her4 to which many ligands bind [60].

Ligand binding induces receptor homo- and hetero- dimerization which in turn activates intracellular tyrosine kinase activity. Autophosphorylation of the tyrosine residues triggers downstream signalling pathways. Such pathways include those involving phospholipase C (PLCγ), ras, rho and rac, PI3 kinase (phosphatidylinositol 3' kinase), PLD (phospholipase D), some STAT (signal transducer and activator of transcription) isoforms and the proto-oncogene tyrosine kinase src [61]. PLCγ generates two second messengers, inositol triphosphate and diacylglycerol from the hydrolysis of phosphatidylinositol 4,5- bisphosphate, which causes the release of intracellular calcium and activation of protein kinase C [62]. This PLCγ-mediated signalling is required for ErbB-mediated motility. Ras activation leads to activation of erk MAP kinases which promotes proliferation and migration [61]. PI3K has an important role in mediating cell survival. PI3K activates the serine-threonine kinase c-AKT which promotes cell survival and blocks apoptosis. It is thought to do this through phosphorylation of the Bcl-2 family member BAD [63]. An overview of EGFR receptor signalling can be seen in figure 1.5. Dimerization is followed by internalisation which attenuates the signal. Cytosolic, ligand bound receptors are subsequently targeted for lysosomal degradation [64]. No ligands have been described for the ErbB2/HER-2 receptor and it is thought to act primarily as a co-receptor. HER-2 therefore forms heterodimers with other ErbB receptors and it has been shown that this can potentiate the signal [60]. These receptors and their ligands which, under normal conditions are tightly controlled are subject to deregulation during cancer pathogenesis [2].

Figure 1.5 **Schematic of the epidermal growth factor receptor signalling pathway, illustration adapted from Herbst *et al.*, (2004) [65]**

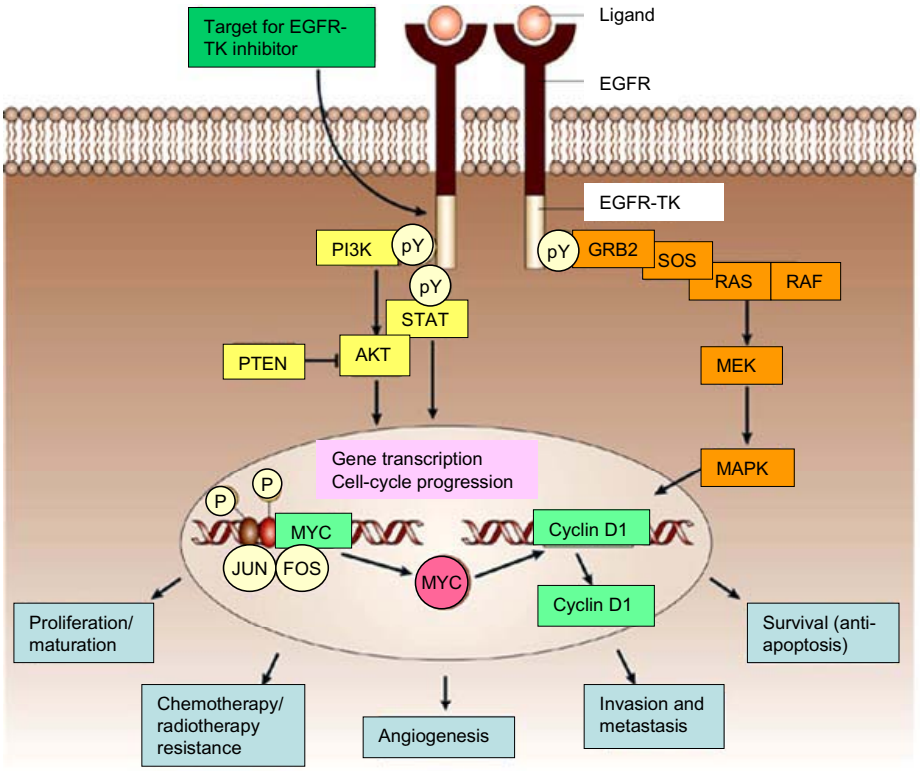

1.4.2. Growth factor receptors in cancer

EGFR is over-expressed in a large number of cancers including breast, lung, oropharyngeal and endometrial [66-69]. In a review by Nicholson *et al.,* (2001), it was reported that in 74 studies of head and neck, ovarian, cervical, bladder and oesophageal cancers 70% showed a strong association between elevated levels of EGFR and poor patient outcome. In breast, endometrial, colorectal and gastric cancers, a more moderate association between EGFR levels and poor prognosis was reported [70].

The tight regulation of EGFR signalling may be disrupted in a number of ways thereby contributing to a cancer phenotype. Such mechanisms include, increased ligand production, increased levels of the growth factor receptor, EGFR mutations,

leading to the formation of a constitutively active form of receptor, defective down-regulation of EGFR and cross-talk with heterologous receptor system [71].

EGFR over-expression in fibroblasts leads to cellular transformation and increased cell motility. This is believed to be as a result of spontaneous receptor dimerization due to the increased EGFR levels on the cell surface [72]. A number of cellular mechanisms can contribute to increased levels of the epidermal growth factor receptor and they include, EGFR gene amplification, increased promoter activity and deregulation at translational and post-translational levels. Mutations in the extracellular region of the EGFR can result in a constitutively active variant, while intracellular mutations can prolong the activity of ligand-bound receptors. Another mutation, affecting the cytosolic region allows the receptor escape degradation. Cross-talk between receptors often occurs and co-over-expression of multiple members of the ErbB family has been found in breast, brain, oral and ovarian cancer [71].

HER-2 which plays an important role in normal development is often over-expressed in cancers due to gene amplification. The HER-2 gene is reported to be amplified in 20-25% of primary tumours resulting in aggressive and deregulated signalling, ultimately causing a poorer prognosis for the patient [73, 74]. Immortalised human mammary epithelial cells which over-express HER-2, comparable to that observed in breast cancer cells, display anchorage-independent growth and invasion capabilities [75]. In another study, stimulation of HER-2 expressing cells with EGF related ligands resulted in an increased invasion, whereas stimulation in cells devoid of functional HER-2 did not display this increased invasion [76].

There are many ways in which normal growth factor signalling can be deregulated leading to an imbalance in cell proliferation motility and survival. Epidermal growth factors and their receptors have also been linked with chemotherapy resistance by promoting survival factors thus preventing cell apoptosis in the face of cytotoxic insults [77]. Taking all of this together ErbB receptors make attractive therapeutic targets in cancer cells.

1.4.3. Role and contribution of growth factor receptors in resistance

The Ras/Raf/MEK/ERK and PI3K/PTEN/AKT signalling pathways, which have been shown to be activated by growth factor receptor activation, have been implicated in drug resistance. However, their anti-apoptotic and drug resistance actions appear to vary in different cell lines. Raf/MEK/ERK signalling can result in phosphorylation of the anti-apoptotic mediator BAD and this allows Bcl-2 to form homodimers resulting in an anti-apoptotic response. The PI3K pathway has been shown to be abnormally active in prostate cancer cells and various tumours, such as, breast, lung, melanoma and leukaemia. It has been demonstrated that the expression of AKT in the MCF-7 breast cancer cell line conferred resistance to 4HT (4-hydroxyl tamoxifen) and doxorubicin [78]. Further evidence to support a role for the growth factor receptors in resistance was shown in an adriamycin-resistant MCF-7 breast cancer cell line, which exhibited an 8-12 fold increase in EGFR expression compared with the parental cell line [79].

It has been suggested that ErbB2 over-expression may have a role in resistance to chemotherapeutic agents. Chen *et al.* (2000), carried out studies into this phenomenon and showed that SKBR3 and BT474 cells which are described as moderately resistant to anti cancer drugs, express high levels of EGFR, ErbB2 and ErbB3. The BT20 cell line, which is said to be more resistant, had very high expression levels of EGFR. They also undertook transfection studies using NIH 3T3 cells, demonstrating that NIH 3T3-EGFR/ErbB2, co-expressing EGFR and ErbB2 (HER-2) and NIH 3T3-ErbB2/ErbB3, co-expressing ErbB2 and ErbB3, cells were strongly resistant to 5-fluorouracil, cytoxan, doxorubincin, taxol (paclitaxel) and vinorelbine. On the other hand, NIH 3T3 cells transfected with ErbB2 and ErbB3 alone were only slightly resistant and transfection with EGFR alone rendered cells moderately resistant, to the same agents. Co-expression of EGFR or ErbB3 with ErbB2 was therefore shown to enhance chemotherapy drug resistance in breast cancer cell lines [35]. One study suggests that the function of P-gp can be regulated by EGF through phospholipase C activity. EGF activation of its receptor was shown to transiently stimulate phosphorylation of P-gp which coincides with enhanced drug transport in MCF-7 drug resistant cells [80].

1.4.4. EGF-related growth factors

The EGF family of ligands for the epidermal growth factor receptors consists of six-structurally related proteins; EGF, TGF-α, amphiregulin (AR), heparin-binding EGF (HB-EGF), betacellulin (BTC) and epiregulin (EPR). They all contain a conserved EGF-like domain and their soluble forms are derived from their integral membrane precursors through proteolysis [81]. EGF and TGF-α both exhibit high expression levels in the nervous system and at the early stages of embryonic development and enhanced synthesis has been observed on several tumour types [82]. These growth factors exert their actions by binding to the cell surface growth factor receptors which have intrinsic tyrosine kinase activity. An experiment carried out in T47D cells by Beerli and Hynes (1995), demonstrated the activities of the individual growth factors to the different growth factor receptors and results are shown in Table 1.2 [83].

Table 1.2 Activation of ErbB receptors by EGF-like growth factors in T47D, adapted from Beerli *et al.*, (1996) [83].

Factor	ErbB-1	ErbB-2	ErbB-3	ErbB-4
EGF	+++	++	+	-
TGF-α	+++	++	+	-
HB-EGF	+++	++	++	+
AR	+	-	+	_
BTC	+++	++	+++	+++

1.4.5. Agents targeting growth factor receptors

There has been a great deal of research into potential agents targeting ErbB receptors and this has resulted in two therapeutic approaches; monoclonal antibodies and tyrosine kinase inhibitors of EGFR function. Monoclonal antibodies against EGFR have been generated to target the ligand-binding extracellular domain and thus block the binding of ligands. Tyrosine kinase inhibitors, which generally have a molecular weight between 300 and 500Da, act on the intracellular tyrosine kinase domain. They were generated by screening small molecules from natural or synthetic compound

libraries which compete for the Mg-ATP binding of the catalytic domain of the EGFR tyrosine kinase domain [84].

1.4.5.1. Monoclonal antibodies

Trastuzumab (Herceptin™, Genentech), a recombinant humanised anti-HER2 antibody, exhibited positive preclinical and clinical data against HER-2 expressing breast cancer progression and has been approved for use in breast tumours over-expressing HER2 [85]. Cetuximab is an anti-EGFR chimeric (human-murine) monoclonal antibody and has also shown promise in cancer treatment. In NSCLC studies, cetuximab has shown some benefit [86] and it has been approved for use in the treatment of EGFR-expressing metastatic colorectal cancer [87].

1.4.5.2. Tyrosine kinase inhibitors

Tyrosine kinase inhibitors (TKIs) are largely synthetic compounds of low molecular weight that interfere with the receptors kinase activity, thus preventing recruitment of downstream signalling molecules. The first two natural tyrosine kinase inhibitors, quercetin and genistein were developed in the 1980s and currently there are approximately thirty inhibitors in clinical development for cancer. Receptor tyrosine kinases consist of an extracellular ligand binding domain, a hydrophobic transmembrane domain and a cytoplasmic domain containing a tyrosine kinase core. In addition to the epithelial growth factor receptors, they include insulin, platelet-derived endothelial, vascular endothelial and fibroblast, growth factor receptors. The catalytic domain of the receptor tyrosine kinases has proved the promising target. Minor differences in the ATP-binding domain between the different receptors are taken advantage of to develop highly selective inhibitors [88]. Erlotinib, gefitinib and lapatinib are three of the major tyrosine kinase inhibitors that have been approved for use in cancer treatment and so the following discussion focuses on these agents.

1.4.5.3. Gefitinib and erlotinib

Gefitinib (Iressa™, Astra Zeneca), a competitive inhibitor of ATP-binding which exhibits a high degree of selectivity for EGFR, was the first tyrosine kinase approved for second line treatment in NSCLC. It has been shown to inhibit EGFR tyrosine kinase activity and tumour growth inhibition was seen in mice with xenografts for

lung, breast, colon, and prostate tumours [89]. Anti-tumour responses were observed in advanced cancers of the lung in clinical trials and in 2003 and this formed the basis for an excelled approval for this drug for use in the treatment of patients with advanced NSCLC [90]. Exposure to this drug can arrest cells in the G1 phase of the cycle, and at increasing concentrations, it can induce apoptosis [91].

Erlotinib (Tarceva™, Genentech), a reversible inhibitor of EGFR tyrosine kinase activity, was approved for use in 2004 as a monotherapy in patients with advanced NSCLC after failure of at least one prior chemotherapy treatment program [92]. It exhibited promising anti-cancer actions in pre-clinical investigations where it inhibited the phosphorylation of the EGFR causing cell cycle arrest and induction of apoptosis and so progressed into clinical trials [93]. Erlotinib showed improvement in overall survival in the treatment of advanced and metastatic NSCLC after treatment failure of one or more chemotherapeutics and so was FDA approved for this purpose [94]. Further *in vitro* studies have shown it to induce inhibition of the cell growth and G1/S phase arrest in the NSCLC line H322. In these cells, erlotinib decreased cyclin –A and –E, and inhibited CDK-2 activity, all of which are proteins involved in the transition of cells from the G1 and S phase. It also was shown to induce $p27^{KIP1}$ a cyclin- dependent kinase (CDK) inhibitor [95]. Erlotinib, in combination with chemotherapy drugs is also being clinically investigated and is discussed later in this section. The structures for these two tyrosine kinase inhibitors are shown in figure 1.6.

Figure 1.6 Chemical structures of erlotinib and gefitinib

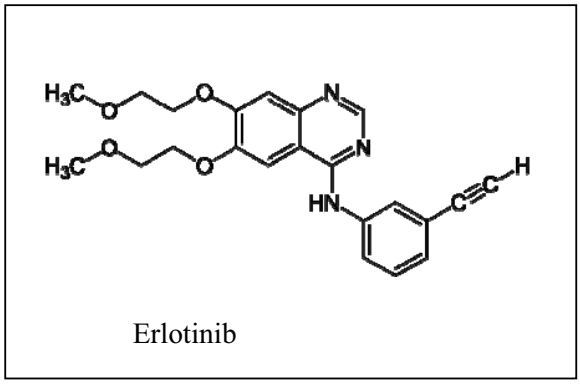

Erlotinib

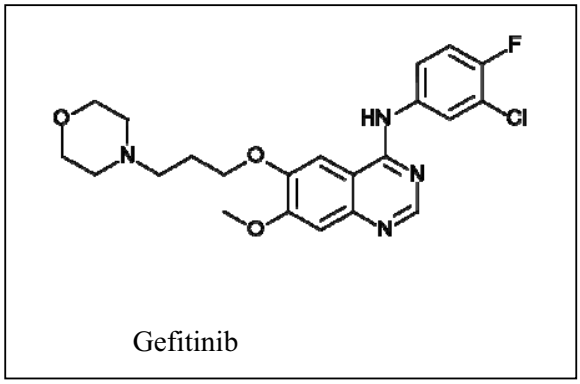

Gefitinib

1.4.5.4. Lapatinib

Lapatinib (GW572016) is a reversible, dual tyrosine kinase inhibitor that inhibits both EGFR/ErbB1 and HER-2/ErbB2. It interferes with downstream activation of Erk1/2 and MAP kinases which are convergence points of most mitotic signalling pathways. This drug also inhibits the PI3K/AKT pathway which plays a role in survival. The presence of exogenous EGF does not reverse the anti-proliferative actions of this drug. These effects, which lead to growth arrest and/or apoptosis, have been demonstrated *in vitro* and *in vivo* in human tumour xenografts [96]. Konecny *et al.* (2006), reported that lapatinib exhibited concentration-dependent anti-proliferative effects on thirty-one characterised human breast cancer cell lines. This response correlated with HER-2 expression [97]. In clinical trials lapatinib has shown some promise in the treatment of refractory metastatic breast cancer and as a first line agent in metastatic breast cancer [98]. It was approved for use by the U.S food and drug administration in March 2007 in combination with capecitabine for the

treatment of patients with human HER-2-overexpressing metastatic breast cancer who had received prior therapy including an anthracycline, a taxane, and trastuzumab [99]. Lapatinib shares the quinaolzine core found in other tyrosine kinase inhibitors and is administered as the monohydrate ditosylate derivative. The parent structure is shown in Figure 1.7.

Figure 1.7 Chemical structure of lapatinib

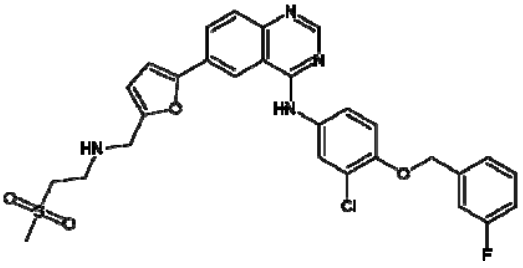

Lapatinib

1.4.6. Tyrosine kinase inhibitors and chemotherapy drug resistance

Evidence indicates tyrosine kinase inhibitors have the ability to chemosensitize cells, however, the exact nature of this inhibition is not always clearly understood. Some tyrosine kinase inhibitors are also substrates for drug transporter pumps. In 1997 two tyrosine kinase inhibitors, staurosporine and its derivate, CGP41251, were shown to reverse the decreased accumulation of rhodamine-123 in P-gp-mediated drug resistant promyelocytic leukaemia HL-60 cells [100]. Hegedus *et al.* (2002) showed that several tyrosine kinase inhibitors interact with, and are substrates for, MRP-1 and MDR1. This drug-pump interaction varied in transporter selectivity and specificity [101]. Increased intracellular accumulation of various drugs and agents, when combined with a tyrosine kinase inhibitor, therefore could be as a result of competition for transport by one or more of the transporter pumps. In this case, the small molecule targeted agent takes the place of the chemotherapy drug in the transporter system thereby leaving the cytotoxic to accumulate.

1.4.6.1. Gefitinib and erlotinib and chemotherapy resistance

Gefitinib was originally shown to reverse drug resistance in P-gp over-expressing lung and breast cancer cell lines. The drugs presence resulted in an increased intracellular accumulation of the P-gp substrate rhodamine-123. Gefitinib also increased ATPase activity in a pure P-gp-expressing membrane, indicating that it interacts directly with the pump [102]. Further studies observed that gefitinib directly inhibits P-gp activity at clinically relevant concentrations [103]. *In vivo* studies carried out in abcg2-/- and mdr1(a/b)-/- mice, showed an increased apparent bioavailability of topotecan and a decreased drug clearance after a single dose of gefitinib in these mice compared with untreated control animals [104]. Combinations of gefitinib with chemotherapeutics went on to be evaluated in the clinic and this is discussed further in section 1.4.7.

Erlotinib also appears to have some actions in modulating ABC transporters. One study indicates how erlotinib reversed BCRP-mediated resistance through direct inhibition of BCRP drug efflux [105]. A tyrosine kinase inhibitor GW282974A, which is an analogue of lapatinib was shown to circumvent drug resistance in two EGFR over-expressing resistant ovarian cancer cell lines when given in combination with chemotherapy drugs and this was associated with a reduction in the downstream signalling molecule phosphorylated ERK [106]. More recently the BCR-ABL tyrosine kinase inhibitor, Nilotinib (AMN107, Tasigna®), has been reported to potentiate the cytotoxicity of BCRP and P-gp substrates mitoxantrone, doxorubicin, vincristine and paclitaxel and enhance the accumulation of paclitaxel in P-gp over-expressing cell lines [107].

1.4.6.2. Lapatinib and chemotherapy resistance

Lapatinib also has modulatory activity for some of the ABC binding cassette transporter proteins. It has been shown to potently enhance the accumulation of doxorubicin, docetaxel and epirubicin in P-gp- and BCRP- over-expressing lung and breast cell lines, but not in the P-gp negative cell lines. This, of course, resulted in greater toxicity of doxorubicin, docetaxel and epirubicin in the resistant cells. Lapatinib can stimulate P-gp and BCRP ATPase activity suggesting it may be a substrate. However, it was also shown to directly inhibit verapamil-induced P-gp

ATPase activity and so can also be described as an inhibitor of P-gp activity [108-110].

1.4.7. TKIs in combination therapy

The above evidence would indicate that combination therapies with tyrosine kinase inhibitors and classical chemotherapy drugs may be a powerful tool in overcoming drug resistance. There is currently a major focus on research and clinical trials with tyrosine kinase inhibitors in combination with chemotherapy agents. Also, although these agents have shown promise in the clinic they are unlikely to substitute standard chemotherapy in first line treatments and they are more likely to be used for their additive and synergistic effects to existing therapies. There is much pre-clinical to phase III trials/research being carried out to see the benefits or downfalls of combination treatments with tyrosine kinase inhibitors and chemotherapeutic drugs. So far these studies have yielded both positive and negative results as outlined below.

1.4.7.1. Combination therapy with gefitinib or erlotinib

Pre-clinical studies investigating gefitinib combination therapies demonstrated an additive to synergistic effect with this TKI in combination with the topoisomerase inhibitor SN-38 in five out of seven lung cancer cell lines analysed. These five cell lines expressed wild type EGFR and the remaining two in which antagonistic effects were observed with the same treatment, expressed mutant EGFR. Interestingly, one of the EGFR mutant cell lines which had an acquired resistance to gefitinib after *in vitro* exposure responded to sequential treatment of the tyrosine kinase inhibitor and cytotoxic, whereby treatment with SN-38 followed by gefitinib resulted in a synergistic effect [111]. These finding indicate the potential for combination therapies with tyrosine kinase inhibitors and also highlight the importance of administration schedules. An *in vivo* study has illustrated that co-administration of gefitinib enhanced the efficacy of cytotoxic drugs in human tumour xenografts. The growth inhibitory actions of doxorubicin, taxanes and platinum agents were all improved when administered with gefitinib against A431 vulvar, A549 and LX-1 lung and TSU-PR1 and PC-3 prostate tumour xenografts in mice [112]. Studies were also carried out in breast cell lines, where findings showed positive synergistic effects with the combination of gefitinib and either paclitaxel or docetaxel in the EGFR and HER-2 positive cell line MCF7/ADR, however, additive antagonist effects were

observed in the EGFR positive cell line MDA-MB-231. These results also carried through to xenograft studies [113].

Positive pre-clinical data also supports the use of erlotinib in combination with chemotherapy agents in the clinic. It was shown to enhance the anti-tumour activity of irinotecan in a human colorectal tumour xenograft model [114]. Substantial anti-tumour activities were also observed with combinations of cisplatin and erlotinib in non-small cell lung cancer xenograft models [115]. Additive cytotoxic effects were seen in head and neck squamous cell carcinomas with a combination of docetaxel and erlotinib, in a dose- and sequence- dependent manner [116].

However positive, pre-clinical data has often failed to translate into the clinical setting. Clinical trials of gefitinib and erlotinib in combination with some chemotherapeutic agents in non small cell lung cancer have yielded disappointing results [117].

The INTACT phase III trial was one of the first to investigate the efficacy of gefitinib in combination therapy. Gefitinib in combination with gemcitabine and cisplatin was compared to placebo in combination with the same chemotherapy agents and assessed for overall survival and time to progression in patients with advanced NSCLC. No survival benefit was observed with gefitinib over placebo when combined with gemcitabine and cisplatin in the large (1093) population of chemotherapy-naive patients with advanced NSCLC analysed [118]. A second phase III trial of identical design was also set up to investigate gefitinib in combination with paclitaxel and carboplatin in advanced NSCLC. Gefitinib again added no benefit in survival or time to progression compared with placebo in combination with paclitaxel and carboplatin, in the 1037 patients with advanced NSCLC [119]. One report suggests gefitinib may have been more efficacious as a neo-adjuvant therapy [120]. A clinical trial in patients with untreated advanced NSCLC who were administered either erlotinib or a placebo together with cisplatin, demonstrated no statistically significant difference between the two groups in overall survival or progression [121]. Another study on patients with the same disease status showed no improvement in survival, time to progression or response rate, between those administered erlotinib in combination with paclitaxel and carboplatin and those who received chemotherapy alone [122]. However, a positive outcome was observed in patients with advanced pancreatic cancer, where erlotinib in combination with

gemcitabine improved overall and progression-free survival compared to gemcitabine monotherapy [121].

1.4.7.2. Combination therapy with lapatinib

Given its actions on the drug transporter pumps, lapatinib also holds promise in combination therapies with chemotherapeutics. From the studies to date there have been some positive findings with lapatinib combinations, however, as with gefitinib and erlotinib, some studies have proved somewhat negative. A study looking at the combination of lapatinib with capecitabine compared with capecitabine alone in patients with HER-2-positive, locally advanced or metastatic breast cancer resistant to trastuzumab was stopped early due to a significant improvement in the time to progression in patients receiving combination, and this treatment setting is now the approved use for lapatinib [123]. Lapatinib with paclitaxel has also shown promise in the breast cancer setting. This was shown in a phase II trial involving daily lapatinib and weekly paclitaxel administration in patients with inflammatory breast cancer [124]. A phase III trial was later carried out with this same combination. In the HER-2-negative or HER-2-untested cohort of metastatic breast cancer no benefit from the addition of lapatinib to paclitaxel was observed. However, it was concluded that in HER-2-positive patients the first-line therapy with paclitaxel-lapatinib significantly improved clinical outcomes [125]. The reporting of the outcomes from this clinical trial has been criticised and Amir *et al*, (2009) suggest the results may not be as promising as the article indicates [126].

In pre-clinical studies, a synergistic toxic effect was observed in two bladder cancer cell lines when lapatinib was introduced into a treatment regimen of gemcitabine and cisplatin. In this same study dosing schedules were examined and the optimal sequence was found to be lapatinib treatment before and during chemotherapy cycles [127]. Oxaliplatin/leucovorin/5-fluorouracil (5-FU) (FOLFOX4) is an effective treatment regimen in patients with advanced colorectal cancer. A phase I trial showed that the addition of lapatinib to this treatment to be tolerable and also there was evidence of clinical activity [128]. Another phase I clinical trial was carried out to evaluate the safety of lapatinib and docetaxel with pegfilgrastim in patients with advanced solid tumours. This combination was well tolerated, however, little clinical activity was observed [129]. Evidence suggests topotecan with lapatinib is also well

tolerated in patients with advanced solid tumours and warrants further study in clinical trials [130].

While a large number of clinical trials examining combination therapies have failed, it is important to keep in mind the potential impact of patient selection and of dosing schedules on results. The importance in choice of administration schedule has been demonstrated in a study involving the combination of gemcitabine and gefitinib in head and neck carcinoma. Chun and colleagues (2006) confirmed that gefitinib arrested cells in the G1 growth phase and gemcitabine arrested cells in S phase. The investigators therefore hypothesised that as gemcitabine requires entry to the S phase, administration of this chemotherapy drug followed by gefitinib would have greater synergy than the reverse or either agent alone. They demonstrated that when cells were treated with gemcitabine they entered S phase and after treatment with gefitinib they underwent apoptosis. Also, gemcitabine was shown to increase phosphorylated EGFR levels and subsequent gefitinib stopped this increase and was associated with decreased phosphorylated AKT levels, poly (ADP-ribose) polymerase cleavage and apoptosis [131]. Another study supporting these results was carried out using KYSE30 cells as a model of a human cancer cell line with EGFR expression. This study involved the anti-EGFR agents, gefitinib, ZD6474 and cetuximab given in different sequences with either a platinum derivative (cisplatin, carboplatin, oxaliplatin) or a taxane (docetaxel, paclitaxel). In the case of all drugs tested, only the schedules involving cytotoxic drug followed by inhibitor proved to be synergistic. In these cases an increased level of apoptosis and an accumulation of remaining cells in the G2/M phases of the cell cycle, were observed [132]. Conversely, if the tyrosine kinase inhibitor is enhancing the cytotoxicity of the chemotherapy drugs by competing as a substrate for the P-gp pump and thereby increasing accumulation of the drug, then it would seem co-administration of both agents would appear necessary.

The clinical findings have not been as compelling as might have been expected and it is difficult to predict whether combinations of tyrosine kinase inhibitors with chemotherapeutics will form part of many typical cancer treatment regimens in the future. However, some of the clinical trials have yielded positive results and pre-clinical data continues to produce many encouraging results. It therefore seems worth

while to maintain the research in this field to identify new and different combinations which may give better synergy and a greater understanding of how the drugs are acting together.

1.5. Membrane proteomics

Membrane proteomics encompasses the study and analysis of membrane proteins in the cell and is extremely useful in cancer research. It may prove particularly beneficial in the study of resistance due to the high number of important membrane proteins involved the various mechanisms of resistance.

1.5.1. Membrane proteins

Membrane proteins are a structurally and functionally diverse group of proteins and can be divided into two main groups; integral and peripheral. Integral membrane proteins are firmly associated with the membrane through hydrophobic interactions with them and the membrane lipids. Most integral membrane proteins span the entire phospholipid bilayer, containing one or more membrane spanning domains. The membrane spanning domains are usually found in α-helical bundle or β-barrel confirmation. The integral proteins containing membrane-spanning α-helical domains are embedded in membranes by hydrophobic interactions with the interior lipid component of the bilayer and most likely also by ionic interactions with the polar head groups of the phospholipids. Peripheral membrane proteins are more loosely associated through electrostatic interactions and hydrogen bonds and do not interact with the hydrophobic core of the phospholipid [133, 134].

The hypothesised structure of these membrane proteins in a biological membrane is shown in figure 1.8. The hydrophobic nature of the α-helical bundles common to integral membrane proteins makes these proteins difficult to isolate and analyse. Integral proteins require detergents, organic solvents or denaturants which interfere with the hydrophobic interactions to remove them from the membrane structure. Milder treatments can remove the peripheral membrane-associated proteins [133, 135].

Membrane proteins are involved in key cellular functions including, transport, cell-cell, cell-pathogen and cell-substrate interaction and recognition and cell communication and signalling [136]. They include growth factor receptors and ABC transporter proteins which have great relevance in cancer studies, as demonstrated above.

Figure 1.8 Membrane proteins in a biological membrane, illustration obtained from Lodish *et al.*, (2000) [134]

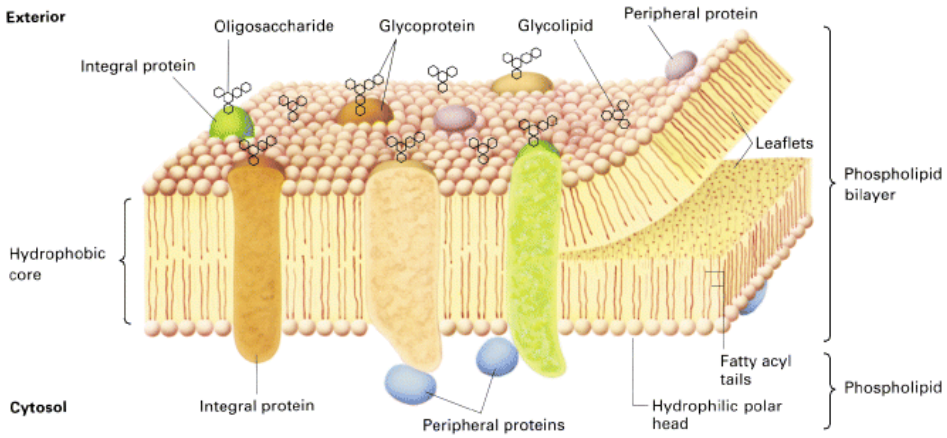

1.5.2. Proteomics

Proteomics describes the study and analysis of proteins expressed in cells or tissues, to which mass spectrometry now increasingly provides the analytical means. It is a hugely important tool in research and readily applied to studies of proteins involved in cancer. The process of proteomics combines separation techniques to separate proteins and peptides, analytical techniques for the identification and quantification, and bioinformatics for data management and analysis. Separation techniques include two-dimensional polyacrylamide gel electrophoresis (2-D PAGE) and liquid chromatography. Mass spectrometry (MS), which is now the analytical technique of choice, has greatly improved utility over the last decade and advanced bioinformatic tools have also been developed to complement equipment improvements and make sense of the increasingly complex data being generated [137, 138].

Large scale proteomic analysis of membrane proteins has proven difficult. 2-D PAGE is a capable and efficient separation method; it separates proteins based on mass and charge and can do this for thousands of proteins in one gel. However, separation of membrane proteins is a significant challenge and hydrophobic proteins such as membrane proteins are often under-represented in 2D-PAGE-based analysis. This may be due to the inability of detergents employed to efficiently solubilise hydrophobic proteins in the aqueous medium used for isoelectric focusing [138, 139]. Hydrophobic proteins are soluble in organic solvents and so the use of organic solvents to extract membrane proteins prior to electrophoresis has been investigated. This has offered some benefit with additional hydrophobic proteins being identified, however, proteins with predicted multi-transmembrane spanning domains are usually not found [140].

The shotgun proteomic approach has led to some advances in the area of membrane proteomics. In this case, proteins are dissolved in a surfactant medium or in an organic solvent, followed by enzymatic or chemical digestion and subsequent separation and analysis using liquid chromatography (LC) coupled with tandem mass spectrometry [141]. It has been reported that the presence of surfactants can suppress analyte ionization and hinder chromatographic separation hence the use of surfactant-free organic solvent-assisted solubilisation is beneficial in this field [139]. A workflow of a shotgun proteomics strategy can be seen in figure 1.9.

Figure 1.9 Workflow of LC/MS/MS-based shotgun proteomics strategy, illustration obtained from Motoyama *et al.*, (2008) [142]

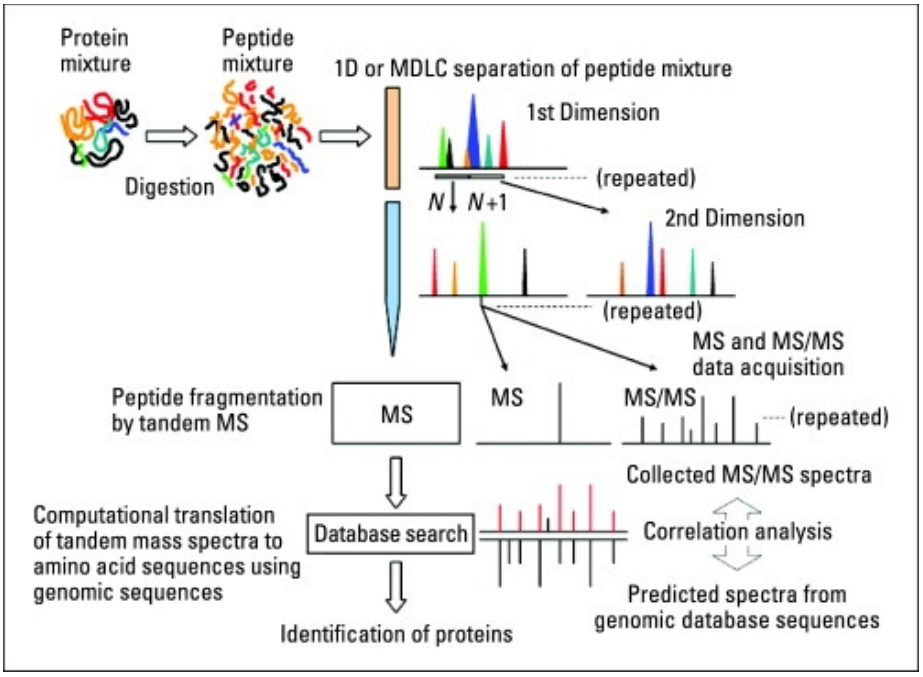

1.5.3. Liquid chromatography

Liquid chromatography (LC), referring to a chromatographic procedure in which the moving phase is a liquid, is ideally suited for the separation of macromolecules and ionic species of biomedical interest, labile natural products, and a wide variety of other high molecular weight and/or less stable compounds [143]. Liquid chromatography (LC) can be used successfully to separate peptides and can overcome some of the problems encountered with 2D-PAGE. Reversed-phase liquid chromatography (RPLC), which is based on distribution of the sample between a polar mobile phase and a non-polar stationary phase, is a widely employed separation method. In RP HPLC, compounds are separated based on their hydrophobic character. Ion-exchange LC is dependent on exchange of sample or buffer ions between the mobile phase buffer and charged groups on the stationary phase [144]. To deal with the increasing complexity of samples for analysis, multidimensional LC was developed and its use has increased immensely over the past number of years. This separation method combines two or more forms of LC, resulting in an increased

peak capacity thereby enhancing the resolving power to better fractionate peptides before being analysed by mass spectrometry [142].

1.5.4. Tandem mass spectrometry

Mass spectrometry analysis involves the separation of proteins and other analytes according to their mass-to-charge ratio (m/z). The mass spectrum is presented in Daltons (Da) per unit charge. This technique requires an ion source, a mass analyzer and a detector. A molecule is ionised and resulting gas-phase ions are propelled towards the mass analyzer by an electric field that resolves each ion according to its m/z ratio. The ions are then detected according to their abundance and the information is then forwarded to the computer for bioinformatic analysis [138, 145]. A variety of ionisation techniques can be employed including electron ionisation and chemical ionisation [145, 146].

In tandem mass spectrometry, a particular ion formed from the ionisation of the mixture by the first analysis is further fragmented to generate characteristic secondary (daughter) fragment ions and hence is also denoted as MS/MS. Tandem MS instruments include the triple quadrupole, ion-trap and the hybrid quadrupole-time-of-flight (Q-TOF) [147]. Tandem MS requires the fragmentation of precursor ions isolated by the first analyzer in order for the second analyzer to analyse the product ions. Collision-induced dissociation is the dissociation method almost universally used [145-147], although, electron transfer dissociation is a newer method also used in MS/MS. The tandem mass spectrometry (MS/MS) approach typically improves signal/noise ratio, giving increased sensitivity and accuracy and is a very useful for identifying proteins. Fragments are generated by cleavage of a bond in the peptide chain, where Cα-C, C-N or N-Cα bonds are cleaved to yield six types of fragments, namely a_n, b_n, c_n, x_n, y_n and z_n. The first three of these are formed when a positive charged is maintained by the N-terminal side and the later three when the positive charged is maintained by the C-terminal side. B_n and y_n fragments are favoured at low energy. The identity of consecutive amino acids can be determined using the mass difference between consecutive ions within a series [145].

Figure 1.10 Diagrammatic view of tandem mass spectrometry, illustration adapted from Glish *et al.*, (2003) [146].

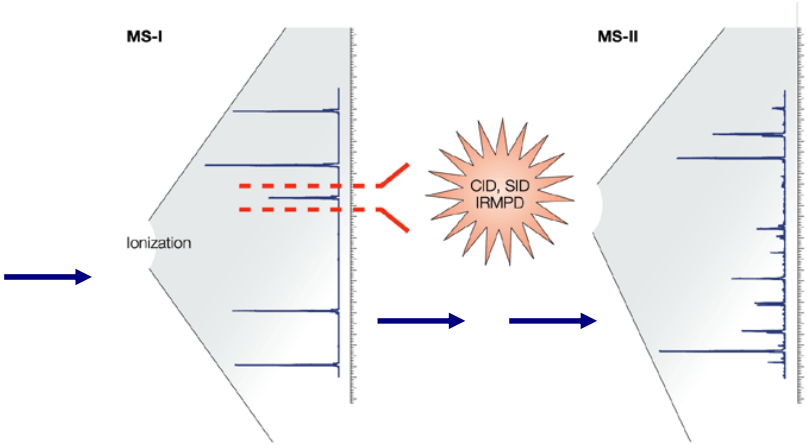

1.5.4.1. Collision induced dissociation (CID)

In CID, the parent ion collides with a neutral target (collision) gas and some of the kinetic energy of the parent ion can be converted to internal energy, which induces decomposition of the parent ion. This technique allows an increase in the number of precursor ions that fragment in the reaction region and also the number of fragmentation paths. CID involves two steps, the first step involves the initial collision between the ion and the target and the second step consists of the decomposition of the ion. A b- and y-type ion series is generated from this fragmentation [145, 146].

1.5.4.2. Electron transfer dissociation (ETD)

Electron transfer dissociation is a relatively new method of fragmentation. This method utilises ion/ion chemistry. It fragments peptides through the transferring of electrons from radical anions to protonated peptides. This induces fragmentation of the peptide backbone, causing cleavage of the Cα-N bond. This creates complementary c- and z-type ions [148, 149].

CID and ETD are both extremely useful methods in MS/MS and it is thought now that they are best used together to achieve a broader range of peptide fragmentation and identification. CID has limitations in that it does not cleave all the required bonds to get the full information available from peptide. It also has limited efficiency in

sequencing polypeptides due to overlap of the masses of N-terminal and C-terminal fragments. ETD can complement the actions of CID as it preferentially cleaves at different residues and has been found to be particularly suitable for the fragmentation of large polypeptides. It is therefore thought the best use of these techniques is to use them together [150, 151].

1.5.5. Applications of membrane proteomics

The development of membrane proteomics has allowed for a greater scope of research into integral membrane proteins and their roles in disease. Techniques in membrane proteomics have been used to investigate heart disease-associated changes in the cardiac membrane subproteome as well as in examining the patho-physiology associated with red blood cells [152, 153]. Cancer studies has also benefited from developments in membrane proteomics. Various methods have been utilised to identify membrane proteins associated with metastasis and disease progression [154, 155]. Membrane bound proteins such as receptors or ion channels are often ideal candidates for drug targeting which provides a further important application of membrane proteomics. Disease biomarkers, often prove to be membrane proteins and so these techniques are also relevant for biomarker discovery [156]. Large scale analysis of membrane proteins also has a role in research into multidrug resistance. Membrane proteomics therefore provides a vital tool in cancer research and could provide an alternative to Western blot if coupled with quantitative methods.

1.6. Aims

The aims of the thesis were to:

1) Investigate the therapeutic role of lapatinib in resistant lung cancer cell lines and examine its modulatory effect on drug-transporter levels in the cells. This was achieved through the examination of combination toxicity with lapatinib and chemotherapy drugs, and the close analysis of drug transporter levels in response to lapatinib treatment and the subsequent impact this may have on the cells.

2) Develop and make use of siRNA-based gene silencing techniques to investigate targets associated with resistance. Previously identified targets with potential roles in resistance were chosen and analysed for their effects on chemotherapy sensitivity in the cells.

3) Utilise a designed membrane proteomics method to establish its ability to successfully identify membrane proteins from complex samples. This method was then applied to other samples in order to identify potentially differentially expressed membrane proteins in resistant cells lines and their non-resistant variants.

Chapter 2 Materials and Methods

2.1 Cell culture

2.1.1. Cell lines

Table 2.1 outlines details and sources of the lung and breast tumour cell lines used in this thesis. All cells were maintained under standard culture conditions, 5% CO_2 at 37^{o}C and fed every 2-3 days. All cell lines were mycoplasma free; testing was carried out in-house every four months.

Table 2.1 Cell lines used in this thesis

Cell Line	Details-Histology	Source
A549	Lung adenocarcinoma	ATCC
A549-Taxol	Taxol-selected variant of A549 selected by Dr. Laura Breen	NICB [157]
BT474	Breast carcinoma	ATCC
DLKP	Lung squamous carcinoma	NICB [158]
DLKPA	Adriamycin-selected variant of DLKP selected by Dr. Alice Redmond	NICB [159]
NCI- H1299	Lung large cell carcinoma	ATCC
H1299-Taxol	Taxol-selected variant of H1299 selected by Dr. Laura Breen	NICB [157]
SKBR3	Breast adenocarcinoma	ATCC

NICB, National Institute for Cellular Biotechnology, DCU.
ATCC, American Type Culture Collection, Rockville, MD, USA.

2.1.2. Ultrapure water and sterilisation

Ultrapure water (UHP) used in media preparation and many solutions, was purified to a standard of 12-18 MΩ/cm resistance by a reverse osmosis system (Millipore Milli-RO 10 plus, Elgastat UHP). Sterile glassware was used for all cell culture related

work. This glassware was prepared by soaking in a 2% RBS-25 (AGB Scientific) for 1 hour, followed by washing in an industrial dishwasher using Neodisher detergent. Finally, the glassware was rinsed twice with UHP and sterilised by autoclave (2.3). Along with glassware all thermostable solutions were sterilised by autoclaving at 121°C for 20 minutes at 15 bar. Thermolabile solutions were sterilised by filtration through 0.22 µm sterile filters (Millipore, Millex-GV SLGV025BS).

2.1.3. Preparation of cell culture media

All 1X basal media for cell culture were prepared as follows: 10X media was added to sterile UHP water, buffered with HEPES (N-(2-Hydroxyethyl) piperazine-N-(2-ethanesulfonic acid) and $NaHCO_3$ as required and adjusted to pH 7.5 using sterile 1.5 N NaOH or 1.5 N HCL. The media was then filtered through sterile 0.22 µm bell filters (Gelman, 12158) and stored in sterile 500 ml bottles at 4°C. Sterility checks were performed on each bottle of media for bacterial, yeast and fungal contamination by inoculating Colombia blood agar plates (Oxoid, CM217), Thioglycollate broths (Oxoid, CM173) and Sabauraud dextrose (Oxoid, CM217) and incubating the plates at 37°C and 25°C. Basal media were stored at 4°C for up to three months. Supplements of 2 mM L-glutamine (Gibco, 11140-0350) were added to all basal media and 1ml 100X non-essential amino acids (Gibco, 11140-035) and 100 mM sodium pyruvate (Gibco, 11360-035) added to MEM. Additional components were added as described in table 2.2. Complete media were maintained at 4°C for a maximum of 1 month.

Table 2.2 Additional components in media.

Cell Line	Basal Media	FCS (%)	Additions
A549/A549-T	ATCC	5	N/A
DLKP/DLKP-A	ATCC	5	N/A
NCI H1299/H1299-T	RMPI 1640	5	Sodium pyruvate
SKBR3	RPMI 1640	10	Sodium pyruvate

2.1.4. Aseptic techniques

All cell culture work was carried out in a class II laminar airflow cabinet (Holten LaminAir). Experiments involving cytotoxic compounds were carried out in a

cytoguard (Holten LaminAir Maxisafe). Laminar flow cabinets were swabbed with 70% industrial methylated spirits (IMS) before and after use, as were all items brought into the cabinet. Only one cell line was used in the laminar at a time and on completion of work, the laminar was allowed 15 minutes to clear, so as to eliminate the possibility of cross contamination. The laminar cabinets were cleaned weekly using the industrial disinfectant Virkon (Antech International, P0550).

2.2. Basic culture techniques

2.2.1. Subculturing of cell lines

The cell culture medium was removed from the tissue culture flask and discarded into a sterile bottle. The flask was then rinsed out with 1 ml of trypsin/EDTA solution (0.25% trypsin (Gibco, 043-05090), 0.01% EDTA (Sigma, E9884) solution in PBS (Oxoid, BRI4a)) to ensure the removal of any residual media. Trypsin (1-5ml, depending on flask size) was added to the flask, which was then incubated at 37°C, for approximately 5 minutes, until all of the cells detached from the inside surface of the flask. The trypsin was deactivated by adding an equal volume of complete media to the flask. The cell suspension was removed from the flask and placed in a sterile universal container (Sterilin, 128a) and centrifuged at 1000 r.p.m. for 5 minutes. The supernatant was then discarded from the universal and the pellet was suspended in complete medium. A cell count was performed and an aliquot of cells was used to reseed a flask at the required density.

2.2.2. Assessment of cell number and viability

Cells were trypsinised, pelleted and resuspended in media. An aliquot of the cell suspension was then added to trypan blue (Gibco, 525) at a ratio of 5:1. After 3 minutes incubation at room temperature, a 10 µl aliquot of the mixture was then applied to the chamber of a glass coverslip enclosed haemocytometer. Cells in the 16 squares of the four grids of the chamber were counted. The average cell numbers per 16 squares were multiplied by a factor of 10^4 and the relevant dilution factor to determine the number of cells per ml in the original cell suspension. Non-viable cells stained blue, while viable cells excluded the trypan blue dye as their membrane

remained intact, and remained unstained. On this basis, % viability could be calculated.

2.2.3. Cryopreservation of cells

Cells for cryopreservation were harvested in the log phase of growth and counted as described in Section 2.2.2. Cell pellets were resuspended in a suitable volume of serum. An equal volume of a 10 – 20% DMSO/serum solution was added dropwise to the cell suspension. A total volume of 1ml of this suspension (which should contain approximately $7x10^6$ cells) was then placed in cryovials (Greiner, 122278) and immediately placed in the vapour phase of liquid nitrogen container (-80ºC). After three hours, the vials were removed from the vapour phase and transferred to the liquid phase for long-term storage (-196ºC).

2.2.4. Thawing of cryopreserved cells

5ml of fresh warmed medium was added to a sterile universal. The cryopreserved cells were removed from the liquid nitrogen and diluted with media using a Pasteur pipette. If required, the resulting cell suspension was centrifuged at 1,000 r.p.m. for 5 minutes. The supernatant was removed and the pellet resuspended in fresh culture medium. An assessment of cell viability on thawing was carried out (Section 2.2.2). Thawed cells were then added to an appropriately sized tissue culture flask with a suitable volume of growth medium and allowed to attach overnight. The following day, flasks were fed with fresh media.

2.2.5. Monitoring of sterility of cell culture solutions

Sterility testing was performed in the case of all cell culture media and cell culture-related solutions. Samples of prepared basal media were incubated at 37ºC for seven days. This facilitated the detection of bacteria, fungus and yeast contamination.

2.3. *In vitro* proliferation assays

Cells in the exponential phase of growth were harvested by trypsinisation. Cell suspensions containing 1 x 10^4 cells/ml were prepared in cell culture medium. 100 µl/well of the cell suspension was added to 96-well plates (Costar, 3599). Plates were agitated gently in order to ensure even dispersion of cells over the surface of the

wells. Cells were then incubated overnight. Cytotoxic drug dilutions were prepared at 2X their final concentration in cell culture medium. 100 µl of the drug dilutions were then added to each well. Plates were then mixed gently as above. Cells were incubated for a further 6-7 days until the control wells had reached approximately 80-90% confluency. Assessment of cell survival in the presence of drug was determined by the acid phosphatase assay (section 2.3.2). The concentration of drug which caused 50% cell kill (IC_{50} of the drug) was determined from a plot of the % survival (relative to the control cells) versus cytotoxic drug concentration.

Table 2.3 Drugs used in this thesis and their sources

Drug	MW (g/mol)	Storage	Source
Lapatinib (Ditosylate Monohydrate)	943.5	Room temperature in dark	Sequoia
Adriamycin (Doxorubicin)*	543.5	4ºC in dark	SVUH
Epirubicin*	579.9	4ºC in dark	SVUH
Paclitaxel (Taxol)*	853.9	Room temperature in dark	SVUH
Docetaxel (Taxotere)*	807.8	Room temperature in dark	SVUH
Vinblastine*	909.1	4ºC in dark	SVUH
Vincristine*	923	4ºC in dark	SVUH
5-Fluorouracil	130.1	Room temperature in dark	SVUH
Elacridar (GF120918)	600.1	-20ºC	Sequoia

* = Clinical formulation

SVUH = St. Vincents University Hospital

2.3.1. Lapatinib combination toxicity assays

Cells were set up as for *in vitro* proliferation assays (section 2.3). Following overnight incubation, cytotoxic and lapatinib drug dilutions were prepared at 4X their

final concentration in media. Volumes of 50 µl of the 4X chemotherapeutic drug and lapatinib dilutions were added to appropriate wells. All wells contained a total final volume of 200 µl (including controls). All agents were dissolved in DMSO, ethanol or media. Cells were incubated for a further 6 days. Cell number was assessed using the acid phosphatase assay (section 2.3.2).

2.3.2. Assessment of cell number - Acid phosphatase assay

A. Acid Phosphatase in 96-well plate format.

Following an incubation period of 6-7 days, media was removed from the plates. Each well on the plate was washed with 100 µl PBS. This was removed and 100 µl of freshly prepared phosphatase substrate (10 mM *p*-nitrophenol phosphate (Sigma 104-0) in 0.1 M sodium acetate (Sigma, S8625), 0.1% triton X-100 (BDH, 30632), pH 5.5) was added to each well. The plates were wrapped in tinfoil and incubated in the dark at 37°C for 1.5 hours. The enzymatic reaction was stopped by the addition of 50 µl of 1 M NaOH to each well. The plate was read in a dual beam plate reader at 405nm with a reference wavelength of 620nm (BIO-TEK®, Synergy HT).

B. Acid Phosphatase in 6-well plate format.

Following an incubation period of 72 hours, media was removed from the plates. Each well on the plate was washed with 1 ml PBS. This was removed and 2ml of freshly prepared phosphatase substrate (10 mM *p*-nitrophenol phosphate (Sigma 104-0) in 0.1 M sodium acetate (Sigma, S8625), 0.1% triton X-100 (BDH, 30632), pH 5.5) was added to each well. The plates were wrapped in tinfoil and incubated in the dark at 37°C for 2 hours. The enzymatic reaction was stopped by the addition of 1 ml of 1 M NaOH to each well. Plates were read in a dual beam plate reader at 405 nm with a reference wavelength of 620 nm.

2.4. TUNEL apoptosis assay

The apoptosis assay was carried out using the Guava® TUNEL kit (Guava Technologies).

2.4.1. Cell preparation

Cells were seeded in 24 well plates at a density of 2.5 x 10^4 per ml. One well was allowed for each condition and 1 ml of media was added to each well on top of cell solution. Plates were incubated overnight.

The following day media was removed and a 1ml solution of each drug condition or media control was added to assigned wells. The plates were then incubated for a further 72hrs.

2.4.2. Cell fixing

Media was removed and transferred to labelled eppendorf tubes. Each well was washed with 500µl PBS after which 50µl of trypsin was added. When the cells were detached 150µl media was added and solution pipetted up and down. The 200µl from each well was then transferred to its corresponding eppendorf and all were centrifuged at 300 x g for 5 min. The resulting supernatant was removed, the pellets resuspended in 150µl PBS and transferred to a 96-well round-bottom plate. To each well 50µl of 4% paraformaldehyde was added and plates were then incubated at 4^{o}C for 60 min.

Following this incubation, the plate was centrifuged at 300 x g for 5 min. Leaving 10-15µl the rest of the supernatant was discarded. The cells were resuspended in the remaining liquid and 200µl of ice-cold 70% ethanol was added. The plates were then incubated at -20^{o}C for 12 hrs.

2.4.3. Cell staining

The DNA labelling mix and anti-BrdU staining mix were made up as per manufacturer's specifications. 100µl of positive and negative controls were added to two wells on the round-bottom plate containing samples. The 24-well plate was centrifuged at 300 x g for 5-7 min. Supernatant was then aspirated and 200µl of Wash Buffer added. Again the plates were centrifuged as above and supernatant removed. This wash step was repeated a second time. Cells were then resuspended in 25µl of the DNA labelling mix, covered and incubated at 37^{o}C for 60 min. After this incubation cells were centrifuged again at 300 x g for 5-7 min and supernatant removed. 50µl of the anti-BrdU staining mix was added to resuspended cells and plates incubated for 30 min at room temperature in the dark. At the end of the incubation 150µl of Rinsing Buffer was added to each well and acquired on the

Guava® System. The Guava TUNEL Assay detects apoptosis-induced DNA fragmentation through a quantitative fluorescence assay. Terminal deoxynucleotidyl transferase (TdT) catalyzes the incorporation of bromo-deoxyuridine (BrdU) residues into the fragmented nuclear DNA at the 3'-hydroxyl ends. A TRITC-conjugated anti-BrdU antibody then labels the DNA fragments. The assay distinguishes two populations:non-apoptotic cells (TUNEL-negative) and apoptotic cells (TUNEL-positive). The guava uses flow cytometry and has six parameters (4 fluorescent colors, 2 light scatter) and has a blue laser (488nm excitation) for access to commonly used fluorescent dyes with absolute counting.

2.5. Lapatinib and EGF treatments

Cells were seeded at a density of 3 – 7 x 10^4 in 90mm tissue culture dishes and incubated over night. Medium was then removed and 1X lapatinib or EGF treatments added to dishes for as long as assay required and protein was then extracted as outlined in section 2.6.1. Lapatinib was diluted in DMSO to 1mM, with further dilutions being in media. A DMSO control, containing the same volume of DMSO as in lapatinib samples was also included. EGF treatments were made up in serum-free medium and the control cells for these treatments were therefore incubated with serum-free medium.

2.6. Western blotting techniques

2.6.1. Protein extraction

Cells were grown to 80-90% confluency in cell culture grade petri dishes. Media was removed and cells were washed twice with ice cold PBS. All procedures from this point forward were performed on ice. Cells were lysed with 500µl of RIPA (R0278, Sigma) lysis buffer and incubated on ice for 20 minutes. Table 2.4 below provides the details of the lysis buffer. Cells were then removed with a cell scraper and further homogenised by passing through a 21 G syringe. Sample lysates were centrifuged at 14000 rpm for 10 minutes at 4^{o}C. Supernatant containing extracted protein was transferred to a fresh chilled eppendorf tube. Protein concentration was quantified using the Biorad assay as detailed in Section 2.5.2. Samples were then stored in aliquots at -80°C.

Table 2.4 RIPA buffer components

Component
150 mM NaCl
1% Igepal CA-630
0.5% sodium deoxycholate
0.1% SDS
50 mM Tris, pH8.0

Table 2.5 RIPA lysis buffer 1ml stock

Volume	Component	Preparation
955 µl	RIPA buffer	
5 µl	100 mM PMSF	174 mg in 10ml ethanol
40 µl	25X protease inhibitors (P2714, sigma)	20 mM AEBSF, 10 mM EDTA, 1.3 mM Bestatin, 140 µM E-64, 10 µM Leupeptin, 3 µM Aprotinin

2.6.2. Protein quantification

Protein levels were determined using the Bio-Rad Quick Start™ Bradford Dye Reagent (Bio-Rad, 500-0205) as follows. A 2 mg/ml bovine serum albumin (BSA) solution (Sigma, A9543) was prepared freshly in lysis buffer. A protein standard curve (0, 0.2, 0.4, 0.6, 0.8 and 1.0 mg/ml) was prepared from the BSA stock with dilutions made in lysis buffer. The protein samples were diluted 1:10 with dH_2O. 5 µl of standards and samples were added in triplicate onto a 96-well plate. 250 µl of the Bio-Rad solution was added to each well. After 5 minutes incubation, absorbance was assessed at 570 nm. The concentration of the protein samples was determined from the plot of the absorbance at 570 nm versus concentration of the protein standard.

2.6.3. Gel electrophoresis

Proteins for analysis by Western blotting were resolved using SDS-polyacrylamide gel electrophoresis (SDS-PAGE). The stacking and resolving gels were prepared as illustrated in table 2.7 or precast 7.5% gels were used (Lonza, 5950).

Table 2.6 Preparation protocol for SDS-PAGE gels (2 x 0.75mm gels)

Components	7.5% Resolving Gel	5% Stacking Gel
Acrylamide stock	3.8 ml	840 µl
dH_2O	7.3 ml	2.84 Ml
1.875 M Tris-HCl pH 8.8	3.75 ml	-
1.25 M Tris-HCl pH 6.8	-	125 µl
10% SDS	150 µl	50 µl
10% NH_4- persulfate	60 µl	20 µl
TEMED	10 µl	5 µl

The acrylamide stock in table 2.7 consists of a 30% (29:1) ratio of acrylamide:bis-acrylamide (Sigma, A2792). In advance of samples being loaded in to the relevant sample wells, 20-40 µg of protein was diluted in 10x loading buffer. Molecular weight markers (Sigma, C4105) were loaded alongside samples. The gels were run at constant voltage (250V) and an amplitude of 20mA per gel until the bromophenol blue dye front reached the end of the gel, at which time sufficient resolution of the molecular weight markers was achieved.

2.6.4. Western blotting

Western blotting was performed by the method of Towbin *et al*. (1979) [160]. Once electrophoresis was complete, the SDS-PAGE gel was equilibrated in transfer buffer (25 mM Tris (Sigma, T8404), 192 mM glycine (Sigma, G7126), pH 8.3-8.5) for approximately 15 minutes. Five sheets of 3 mm filter paper (Whatman, 1001-824) were soaked in freshly prepared transfer buffer. These were then placed on the cathode plate of a semi-dry blotting apparatus (Bio-Rad, TransBlot®). Air pockets were removed from between the filter paper. Nitrocellulose membrane (GE Healthcare, RPN 3032D), which had been equilibrated in the same transfer buffer, was placed over the filter paper on the cathode plate. Air pockets were once again removed. The gels were then aligned on to the membrane. Five additional sheets of transfer buffer soaked filter paper were placed on top of the gel and all air pockets removed. The anode was carefully laid on top of the stack and the proteins were transferred from the gel to the membrane at a current of 300 mA at 15 V for 30-40 minutes, until all colour markers had transferred. Following protein transfer,

membranes were stained using PonceauS (Sigma, P7170) to ensure efficient protein transfer. The membranes were then blocked for 2 hours using 5% skimmed milk powder (BioRad, 170-6404) in PBS at RT. Membranes were incubated with primary antibody over-night at 4 °C (table 2.7). Antibodies were prepared in 1% skimmed milk powder in PBS. Primary antibody was removed after this period and the membranes rinsed 3 times with PBS containing 0.5% Tween 20 (Sigma P1379) for a total of 15-30 minutes. Secondary antibody (1 in 1,000 dilution of anti-mouse IgG peroxidase conjugate (Sigma, A4914)) in PBS, was added for 1.5 hour at room temperature. The membranes were washed thoroughly in PBS containing 0.5% tween for 15 minutes.

Table 2.7 List of primary, secondary antibodies and dilutions used

Primary Antibody	Dilution	Source
MDR-1/P-gp	1/250	ALX-801-002-C100, Alexis
MRP-1	1/100	sc-59607, Santa Cruz Biotechnology
BCRP	1/200	ALK-801-029-0250, Alexis
AKT	1/1000	9272, Cell Signaling Technology
MAPK	1/1000	9102, Cell Signaling Technology
Phosphorylated AKT (Ser 473)	1/1000	9271, Cell Signaling Technology
Phosphorylated MAPK (Tyr 204)	1/1000	9101, Cell Signaling Technology
β-actin	1:10,000	A5441, Sigma
Secondary Antibody	**Dilution**	**Source**
Anti-mouse	1/1000	A6782, Sigma
Anti-rabbit	1/500	A3574, Sigma

2.6.5. Enhanced chemiluminescence (ECL) detection

Immunoblots were developed using Luminol (Santa Cruz, sc-2048), which facilitated the detection of bound peroxidase-conjugated secondary antibody. Following the final washing membranes were incubated with the Luminol reagent (Santa Cruz, sc-2048). 3 ml of a 50:50 mixture of Luminol reagents was used to cover the membrane. The membrane was wrapped in clingfilm. The membrane was then exposed to autoradiographic film (Kodak, X-OMATS) for various times (from 10 seconds to 30

minutes depending on the signal). The exposed autoradiographic film was developed for 3 minutes in developer (Kodak, LX-24). The film was then washed in water for 15 seconds and transferred to a fixative (Kodak, FX-40) for 5 minutes. The film was then washed with water for 5-10 minutes and left to dry at room temperature.

2.7. RT-PCR analysis

2.7.1. Total RNA extraction

As with all RNA work, care was taken to reduce the impact of RNase enzymes. Gloves were changed regularly and RNase inhibitor (RNase Zap®, AM9780) was used to clean bench and instruments. Cells were seeded at 5 x 10^5 cells in a 6 well plate and incubated for 48 hours. Media was then removed and 750µl of TRI reagent (Sigma, T9424) was added to solubilise sample. Samples were allowed to stand at room temperature for 5-10 minutes. TRI reagent is a mixture of guanidine thiocyanate and phenol in a mono-phase solution. It effectively dissolves DNA, RNA and protein on lysis of cell culture samples.

200µl of chloroform per ml of TRI reagent was added to cell lysate. The samples were covered tightly, shaken vigorously for 15 seconds and allowed to stand at room temperature for 15 minutes. The resultant mixtures were centrifuged at 13,000 rpm for 15 minutes at 4ºC. Centrifugation separated the mixture into 3 phases: an organic phase (containing protein), an interphase (containing DNA) and a colourless upper aqueous phase (containing RNA). The aqueous phase was transferred to a fresh tube and 0.5 ml of ice-cold isopropanol per ml of TRI reagent was added. Samples were then mixed and allowed to stand at room temperature for 5-10 minutes.

The samples were centrifuged at 13,000 rpm for 30 minutes at 4ºC. The RNA precipitate formed a pellet. The supernatant was carefully removed and RNA pellet washed in 1 ml 75% ethanol. After removal of ethanol the RNA pellet was allowed to air-dry briefly. Depending on pellet size, it was resuspended in approximately 30µl DEPC-treated water and stored at -80ºC.

2.7.2. RNA quantification using Nanodrop

RNA was quantified spectrophotometrically at 260nm and 280nm using the NanoDrop®, (ND-1000 Spectrophotometer). A 1µl aliquot of suitably diluted RNA

was placed on the nanodrop. The nanodrop software calculated the amount of RNA present using the fact that an optical density of 1 at 260nm is equivalent to 40mg/ml RNA. The ratio of A_{260}/A_{280} was used to indicate the purity of the RNA in the sample.

2.7.3. Reverse transcription of RNA isolated from cell lines

A high-capacity cDNA reverse transcription kit was used (Applied biosystems, 4374966). The master mix (table 2.8) was made up to necessary volume, allowing 10µl per sample. 10µl of the master mix was added to PCR tubes, to which 10µl of RNA (1µg) sample was then added. The samples were briefly centrifuged to spin down contents and eliminate air bubbles. The samples were then subjected to the following PCR conditions: 25ºC for 10 minutes, 37ºC for 120 minutes and 85ºC for 5 minutes.

Table 2.8 Components of Master Mix for reverse transcription

Component	Volume (µl) per 20 µl reaction
10X RT Buffer	2.0
25X dNTP Mix (100 mM)	0.8
10X RT Random Primers	2.0
Multiscribe ™ Reverse Transcription	1.0
RNase Inhibitor	1.0
Nuclease-free H_2O	3.2

2.7.4. Polymerase Chain Reaction (PCR) analysis of cDNA

PCR reactions were set up as 50µl volumes. Each PCR reaction tube contained 45µl of the Platninum® PCR Supermix (Invitrogen, 11306-016); 1µl of cDNA and 2µl each of the forward and reverse target primers (table 2.9). The sequences of all primers used in this thesis are shown in table 2.8. The mixture was heated to 94ºC for

2 minutes (denatures the template and activates the RT enzyme). The cDNA was then amplified by PCR using the following conditions:

- 32 cycles: Denature 94ºC for 30 seconds
  Anneal 55ºC for 30 seconds
  Extend 72ºC for 1 minute
- Final extension of 72ºC for 10 minutes
- Hold temperature of 4ºC

Table 2.9 Primer sequences for PCR

Gene	Length (bp)	Tm (ºC)	Size (bp)	Sequence
B-actin		55ºC	228	
Forward	20			CGGGAAATCGTGCGTGACAT
Reverse	21			GGAGTTGAAGGTAGTTTCGTG
P-gp		55ºC	156	
Forward	20			GTTCAAACTTCTGCTCCTGA
Reverse	20			CCCATCATTGCAATAGCAGG
MRP1		55ºC	551	
Forward	23			AGTGGAACCCCTCTCTGTTTAAG
Reverse	23			CCTGATACGTCTTGGTCTTCATC

2.7.5. DNA electrophoresis

Gel electrophoresis was used to separate the amplified targets based on their size, which can then be identified using a DNA ladder. 5µl of a 10X loading buffer, consisting of 0.25% bromophenol blue (Sigma, B5525) and 30% glycerol in water, was added to each cDNA product. 10µl of target cDNA products and 2µl of

endogenous control cDNA were separated by electrophoresis at 100mV through a 2% agarose (Sigma, A9539) gel containing ethidium bromide (Sigma, E8751), using TAE (22.5 mM TRIS-HCL, 22.5 mM boric acid (Sigma, B7901) and 0.5 mM EDTA) as running buffer. Molecular weight markers (GeneRuler™, Fermentos, SM1333) were run, simultaneously. The resulting product bands were visualized when placed on a transilluminator (UVP Transilluminator) and images photographed.

2.8. Enzyme-Linked Immunosorbant Assays (ELISAs)

Protein lystates were extracted and quantified as for Western Blotting (Section 2.6.1, 2.6.2). Total EGFR and ErbB2 and phosphorylated EGFR and ErbB2 levels were measured using commercially available developmental sandwich ELISA assay kits (R&D Biosystems, DY1854, DY1129, DY1095, and DYC1768).

2.8.1. Total EGFR/ErbB2 and phosphorylated EGFR/ErbB2

In all cases the capture antibody was diluted to the working concentration specified in PBS without carrier protein. A treated 96-well plate (Nunc, 467466 F16 Maxisorp) was coated with 100 µl per well of the diluted capture antibody. The plate was sealed and incubated overnight at room temperature. The following day, each well was aspirated and washed with wash buffer (0.05% Tween in PBS, pH 7.2-7.4), repeating the process two times for a total of three washes. Complete removal of liquid at each step was essential for good performance. After the last wash, any remaining wash buffer was removed by inverting the plate and blotting it against clean paper towels. Plates were then blocked by adding 300 µl of blocking reagent to each well (1% BSA in PBS, pH 7.2 to 7.4). The plate was then incubated at room temperature for a minimum of 1 hour, followed by three washes.

Samples were diluted as per table 2.10 in reagent diluent. In the case of total EGFR and ErbB2, a seven point standard curve using 2-fold serial dilutions with highs of 2,000 and 4,000 pg/ml, respectively, was generated. For phosphorylated EGFR and ErbB2 a single standard/control of 10,000 and 3,000 pg/ml respectively, was made up. 100 µl of sample or standard was added in duplicate to plate. An adhesive strip was used to cover the plate and it was then incubated for 2 hours at room temperature. Three washes were then repeated as before. 100 µl of the detection

antibody diluted to specified working concentration in reagent diluent was then added to each well in all cases. The plate was covered again and incubated for 2 hours at room temperature. Three washes with were carried out as before.

For total EGFR/ErbB2 plates 100 µl of the working dilution of Streptavidin-HRP was added to each well. The plate was covered again and left to incubate for 20 minutes at room temperature, avoiding direct light. Wash buffer was used to perform three washes as before. To all plates 100 µl of substrate solution (R&D Systems, DY999) was added to each well, followed by incubation for 20 minutes at room temperature avoiding direct light. To end the reaction, 50 µl of stop solution (R&D Systems, DY994) was dispensed to each well, again, in all cases. Gentle agitation mixed the solutions and the optical density of each well was read immediately, using a microplate reader set to 450 nm. Wavelength correction was set to 540 nm or 570 nm. Total EGFR/ErbB2 levels were determined from a standard curve plotting absorbance *versus* concentration. Each level was then calculated as ng/mg total protein. For the phosphorylated proteins, values were expressed relative to standard/control sample.

Table 2.10 Quantity of protein used

Cell Line	Protein µg/100µl			
	EGFR	ErbB2	Phospho-EGFR	Phospho-ErbB2
A549-T	7.5	20	20	50
SKBR3	7.5	0.25	20	5
H1299-T	7.5	20	20	50

2.9. RNA interference (RNAi)

RNAi using small interfering RNAs (siRNAs) was carried out to silence specific genes. The siRNAs used were chemically synthesised (Ambion Inc). These siRNAs were 21-23 bps in length and were introduced to the cells via reverse transfection with the transfection agent siPORT™ *Neo*FX™ (Ambion Inc., 4511).

2.9.1. Transfection optimisation

In order to determine the optimal conditions for siRNA transfection, optimisation with kinesin siRNA (Ambion Inc., 16704) was carried out for each cell line. Cell suspensions were prepared at $1x10^5$, $3x10^5$ and $5x10^5$ cells per ml. Solutions of negative control and kinesin siRNAs at a final concentration of 30 nM were prepared in optiMEM (Gibco^{TM}, 31985). NeoFX solutions at a range of concentrations were prepared in optiMEM in duplicate and incubated at room temperature for 10 minutes. After incubation, either negative control or kinesin siRNA solution was added to each neoFX concentration. These solutions were mixed well and incubated for a further 10 minutes at room temperature. Replicates of 10 µl of the siRNA/neoFX solutions were added to wells of a 96-well plate. 100µl of the relevant cell concentrations were added to each well. The plates were mixed gently and incubated at 37°C for 24 hours. After 24 hours, the transfection mixture was removed from the cells and the plates were fed with fresh medium. The plates were assayed for changes in proliferation at 72 hours using the acid phosphatase assay (section 2.3.2). Optimal conditions for transfection were determined as the combination of conditions which gave the greatest reduction in cell number after kinesin siRNA transfection and also the least cell kill in the presence of transfection reagent alone.

Table 2.11 Optimised conditions for siRNA transfection

Cell line	Seeding density per 96-well	Seeding density per 6-well	Volume NeoFX per 96 well (µl)	Volume NeoFX per 6 well (µl)
A549/A549T	2.5×10^3	3×10^5	0.2	2
DLKPA	2×10^3	3×10^5	0.25	2

2.9.2. siRNA controls

Two siRNAs were chosen for each of the protein/gene targets and transfected into cells. For each set of siRNA transfections carried out, control, non-transfected (NT) cells and a scrambled (SCR) siRNA transfected control were used. Scrambled siRNA

are sequences that do not have homology to any genomic sequence. The scrambled non-targeting siRNA used in this study is commercially produced, and guarantees siRNA with a sequence that does not target known any gene product. It has also been functionally proven to have no significant effects on cell proliferation, morphology and viability. For each set of experiments investigating the effect of siRNA, the cells transfected with target-specific siRNAs were compared to cells transfected with scrambled siRNA. This took account of any effects due to the transfection procedure, reagents, and also any random effects of the scrambled siRNA. Kinesin was used as a control to assess the efficiency of the siRNA transfection. Kinesin plays an important role in cell division; facilitating cellular mitosis. Therefore, transfection of siRNA kinesin results in cell cycle arrest and efficient transfection is confirmed by significantly lower growth rates.

Table 2.10 List of siRNAs used

Target name	Ambion Ids
Scrambled	17010
Kinesin	14851
ABCB1 #1	4123
ABCB1 #2	3933
ID3 #1	122173
ID3 #2	122294
Crystallin-zeta #1	112817
Crystallin-zeta #2	146128
CRIP 1 #1	145761
CRIP 1 #2	215088

2.9.3. Confirmation of knockdown by Western blotting

Cells were seeded as per conditions outlined in table 2.9 in a 6-well plate, using 2µl NeoFX per well to transfect 100µl of 30nM siRNA and incubated for 24hrs. Medium

was removed and replaced with fresh media. At 72 hrs following transfection protein was extracted as per section 2.6.1 and analysed by Western blot (section 2.6).

2.9.4. Proliferation assays on siRNA transfected cells

As described in table 2.9, cells were seeded using 0.2 µl Neofx to transfect 30nM siRNA in a cell density of $2.5x10^3$ per well of a 96-well plate. Plates were again incubated for 24 hrs, after which the transfection medium was replaced with fresh media. Cells were allowed to grow until they reached 80-90% confluency, a total of 5 days. Cell number was assessed using the acid phosphatase assay (section 2.3.2).

2.9.5. Chemosensitivity assay on siRNA-transfected cells

Assays were set up as described above (section 2.9.3). 24 hrs after addition of fresh media, appropriate concentrations (2x) of chemotherapeutic drugs were added to the wells in replicates of 4 and incubated for 3 days. The plates were assayed for changes in proliferation at 96 hrs using the acid phosphatase assay (Section 2.3.2).

2.9.6. Epirubicin accumulation assay on siRNA transfected cells

Cells were seeded and transfected as per section 2.9.3 allowing 3 wells for each condition. 48hrs after transfection cells were trypsinised and re-seeded in triplicate at 2.5×10^5 into 25 cm^2 flasks. An accumulation assay as described in 2.10.1 was then carried out on these cells.

2.10. Epirubicin transport assays

2.10.1. Epirubicin accumulation assays

Cells were seeded at a density of 2.5×10^5 in 25 cm^2 flasks and incubated overnight. Medium was removed and fresh medium containing epirubicin (2 µM) was added. The flasks were then incubated with the drug for various time points up to 2 hours.

2.10.2. Epirubicin efflux assays

Cells were prepared in the same manner as for accumulation assay. Medium was removed, fresh medium containing epirubicin (2 µM) was added and the flasks incubated for 2 hours. At this point (Time 0) medium was removed from flasks and

they were washed with PBS. Medium was then replaced and flasks were incubated for various time points up to 2 hours.

At relevant time points the media was removed from flasks and the flasks washed with PBS. Cells were trypsinised (Section 2.2.1) and counted (Section 2.2.2). Cell pellets were further washed in PBS and frozen at -20˚C.

2.10.3. Epirubicin quantification

Epirubicin quantification was carried out using method previously developed in our laboratory [161].

Table 2.12 List of reagents for epirubicin extraction and quantification

Reagent	Preparation
1M Ammonium Formate Buffer	15.76 g of Formic acid ammonium salt was added to 200 ml of ultrapure (UP) water. The pH was adjusted to 8.5 with concentrated ammonium hydroxide (ammonia). The volume of the solution was brought to 250 ml with more water. The solution was aliquoted into 20 ml stocks and frozen at -20^0C in order to keep it fresh.
33% Silver Nitrate (w/v)	3.3 g of silver nitrate powder was added to a 10 ml universal. U.H.P water was then added to the 10 ml mark. The universal was covered in tin foil, as it is light sensitive and kept frozen at -20^0C.
Mobile Phase	720 µl of formic acid was added to 720 ml of UP water. The pH was brought to 3.2 using 1M ammonium formate. 280 ml of acetonitrile was added and the solution was mixed and left to settle and degas for a few hours with the lid tightly closed.

2.10.4. Epirubicin extraction procedure

The frozen pellets of cells were thawed and re-suspended in 200 µl of ultra pure water. The cells were transferred to a polypropylene extraction tube. For the epirubicin standards, 50 µl of blank cells and 200 µl of each epirubicin standard was

added to extraction tubes in triplicate. The usual range of standards used was 5, 25, 50, 100, 250 and 500 ng/ml.

To both samples and standards, 20 µl of silver nitrate solution, 100 µl of daunorubicin internal standard, 700 µl of ice-cold isopropanol, 100 µl of 1M ammonium formate buffer (pH 8.5) and 1400 µl of chloroform were added.

The tubes were mixed on a blood mixer (Stuart scientific, UK) for 5 minutes. Following centrifugation at 2750xg for 5 minutes, the liquid clarified to two separate layers. The bottom organic layer contained the drug. 1.1 ml of the bottom layer from each tube was removed using a glass pasteur pipette to a conical bottomed glass LC autosampler vial (Chromacol). Samples were evaporated to dryness using Genevac EZ-2 (Ipswich, UK) evaporator. Each sample was reconstituted in 40 µl mobile phase. A system standard containing 2 µg/ml concentration of internal standard and epirubicin and a blank containing mobile phase were also made up.

2.10.5. LC-MS analysis of epirubicin

Chromatographic separation was achieved using a Prodigy reverse phase column (ODS3 100A, 150 X 2.0 mm, 5 micron), (Phenomenex, UK). The mobile phase was made up as in table 2.10 and used at a flow rate of 0.2ml/min. The column temperature was maintained at 45ºC and the temperature of the autosampler was maintained at 4ºC. The complete chromatographic run time of each sample was 15min, which separated epirubicin and daunorubicin from each other with retention times of 3.5 and 9.1 minutes respectively.

The mass spectrometer was operated using an ESI source in the positive ion detection mode. The ionisation temperature was 300^0C, gas flow rate was 10L/min and nebulizer pressure was 50psi. Nitrogen was used as both the ionisation source gas and the collision cell gas.

Analysis was performed using MRM mode with the following transitions: m/z 544→m/z 397 and 86 for epirubicin, and m/z 528→m/z 363 and 321 for daunorubicin.

2.10.6. LC-MS data analysis

Quantification was based on the integrated peak area as determined by the Masshunter Quantification Analysis software which quantitates the peak areas of the MRM transitions of each analyte. A peak area ratio was generated by expressing the

peak area of analyte as a fraction of the peak area from the internal standard. A regression standard curve was generated using a log log plot. The log of peak area ratio was substituted into the equation of the line and the cell counts obtained during the assay were then used to express the result as ng of drug per million cells.

2.11. Lapatinib quantification

Lapatinib quantification was carried out using a method previously developed in our laboratory (Sandra Roche, currently in press).

2.11.1. Lapatinib extraction procedure

The frozen pellets of cells were thawed and transferred to a polypropylene extraction tube. For the lapatinib standards, 100 µl of blank cells and 100 µl of each lapatinib standard was added to extraction tubes in triplicate. The range of standards used was 1 - 2,000 ng/ml.

To both samples and standards 100 µl of dasatinib (500ng/ml) internal standard, 200 µl of 1M ammonium formate buffer (pH 3.5) and 1.6 ml of *tert*-Butyl Methyl Ether (*t*-BME)/Acetonitrile (ACN) 3/1 (v/v) were added. The tubes were mixed on a blood mixer for 15 minutes. The samples were then centrifuged at 2750xg for 5 minutes. The organic layer containing the drug was removed with a glass pasteur pipette and 1.1 ml of the solvent was transferred to a conical bottomed glass LC autosampler vial (Chromacol). Samples were evaporated to dryness using Genevac EZ-2 (Ipswich, UK) evaporator. The samples were reconstituted in 40µL of acetonitrile with 20µl injected automatically by the autosampler. A system standard containing 100ng/ml concentration of internal standard and lapatinib and a blank containing mobile phase were also made up.

2.11.2. LC-MS analysis of lapatinib

Chromatographic separation was achieved using a Hyperclone BDS C18 column (150mm×2.0mm i.d., 3µm) with a SecurityGuard C18 guard column (4mm×3.0mm i.d.) both from Phenomenex, UK. A mixture of acetonitrile–10mM ammonium formate pH 4 (54:46, v/v) was used as mobile phase at a flow rate of 0.2ml/min. The column temperature was maintained at 20^0C and the temperature of the autosampler was maintained 4^0C. The complete chromatographic run time of each sample was

10min, which separated dasatinib and lapatinib from each other with retention times of 2.3 and 5.1 minutes respectively. Peaks were quantified using Agilent Masshunter Software.

The mass spectrometer was operated using an ESI source in the positive ion detection mode. The ionisation temperature was 350^0C, gas flow rate was 11L/min and nebulizer pressure was 50psi. Nitrogen was used as both the ionisation source gas and the collision cell gas. Analysis was performed using MRM mode with the following transitions: m/z 581→m/z 365 for lapatinib, and m/z 488→m/z 231 and 4021 for dasatinib, with a dwell time of 200ms. Data analysis was carried out as in 2.10.3.

2.12. Membrane proteomics

2.12.1. Cell preparation

Nine 75 cm^2 flasks were seeded with approx 5 x 10^4 cells and allowed to grow until 70-80% confluent (5 days) to generate sufficient sample for membrane protein extraction. The medium was removed and flasks washed with PBS. 1 ml of PBS was added to each flask and cell scrapers used to gently scrap cells from bottom of flasks. The cell suspension was centrifuged at 1,000xg for 5 minutes. The resulting pellet was washed in PBS, transferred to an eppendorf and centrifuged again at 1,000xg for 5 minutes. The wet cell pellet was then stored at -80ºC.

2.12.2. Complex membrane protein extraction

The membrane proteins were extracted using the ReadyPrep™ Protein Extraction Kit (Membrane II), (Bio-Rad, 163-2084). The Lysis Buffer and Membrane Protein Concentrating Reagent supplied in the kit were resuspended in mass spectrometry-grade water according to instructions provided. Both reagents were chilled on ice for 10–15 min before proceeding.

To 200mg of wet cell pellet 1ml of the Lysis Buffer was added on ice. The suspension was then sonicated with an ultrasonic probe to disrupt the cells and fragment the genomic DNA. This was done in 30 second bursts, typically 3–4 times and the sample was chilled on ice between each ultrasonic treatment. The sample was

then centrifuged for 10 min at approx 3,000 x g at 4°C to pellet insoluble material and unbroken cells.

The supernatant was removed and diluted directly into a beaker containing 60 ml of the ice-cold Membrane Protein Concentrating Reagent. The suspension was stirred slowly on ice for 60 min. Following this, the sample was transferred to ultracentrifuge tubes and centrifuged (SW-28 rotor) at 100,000 x g for 60 min at 4°C to pellet the membranes and membrane proteins. The supernatant was carefully decanted and discarded. Each pellet was then washed with 3 ml of cold Lysis Buffer and left on ice for 1–2 min before decanting. This wash step was repeated once.

2.12.3. Complex membrane protein digestion

The isolated membrane sample of interest from 2.12.2, were dispersed using 40µl of 50 mM NH_4HCO_3 pH 7.9 in a 1.5 ml microfuge tube. 60µl of methanol to make a final 60% v/v was added to sample. The sample was sonicated for 1 minute and vortexed for 2 minutes to solubilise the membrane proteins. This was carried out five times. Tubes were then incubated in a water bath at 90ºC for 5 minutes to denature proteins and transferred to ice cold water. Proteins were digested in the same tube and solubilising buffer and 6 µl trypsin (Promega, V528A) was added before incubating the sample at 37 °C overnight.

After incubation, the resulting digestate was centrifuged for 5 minutes at 15,000xg and supernatant stored at -80ºC. The pellet was resuspended in 60% methanol, sonicated for 1 minute and then vortex for 2 minutes. Five to ten cycles are usually sufficient to achieve solubilisation. 4 µl of trypsin (promega, V528A) was added and left for 4-5 hrs at 37 °C. The sample was then centrifuged for 5 min at 15,000 x g and pooled with the supernatant that was at -80ºC. The combined supernatants were dried using a speed-vac (MAXI dry plus) and resuspended in 0.1% TFA. This was then briefly sonicated, vortexed and centrifuged for 2 min at 15,000 x g. The resulting supernatant was then ready for mass spec analysis and can be stored at -80ºC until ready to analyse.

2.12.4. Mass spectrometry analysis

Tryptic digests were analyzed using the Ettan MDLC (GE Healthcare), which is a combination of an autosampler, HPLC, and 4-valve plumbing system in one instrument allowing for automated online LC/LC-MS/MS. The plumbing set-up on

the MDLC was in the “Online Salt Step” configuration, (see Ettan MDLC manual), except that the analytical columns were removed from the “column switching valve” and were replaced with a single nano-RPC column (Zorbax 300SB C18 0.075mm x 100mm, Agilent Technologies). The sample flow path leads from the autosampler to the first dimension column, which consisted of a 50x0.3mm 5u BioBasic SCX Kappa capillary column. During loading, the flow through is collected on one of two trap columns (Zorbax 300SB C18, 0.3mm x 5mm). Ultimately, elution buffer is delivered from the autosampler over the first dimension column and eluted peptides are collected on the second trap column, while buffer goes to waste. Peptides bound to each trap column can then be eluted using a reversed phase gradient over the trap column and analytical column. After sample loading and elution, the above procedure was repeated prior to subsequent sample loading.

MDLC buffers used for HPLC included Buffer A (0.1% formic acid) and Buffer B (98% acetonitrile and 0.1% formic acid). The MDLC method used for all multidimensional chromatography consisted of five steps. The first step loads a digested sample (10 µl) onto the first dimension SCX column via the autosampler with the flow through going to Trap Column 1. A five-salt step was performed using 0, 10mM, 25 mM, 50 mM, 100 mM, and 500 mM ammonium acetate. At each step, a salt plug was loaded onto the SCX column for peptide elution. Peptide fractions were then captured by the RPC trap column for pre-concentration and desalting. The mobile phases A and B were 0% and 98% ACN containing 0.1% FA, respectively. Flow rates used in the MDLC separations were as follows: 10 µl/min for loading of sample, wash buffer, and elution buffers onto the first dimension column, 15 µl/min for desalting (using Buffer A) of Trap columns after previously mentioned steps, 150 µl/min for the reversed phase gradient (due to split-flow within the MDLC and length of column, flow rate out of the analytical column tip was ~300 nl/min). The MDLC was interfaced with an LTQ_XL with ETD ion trap mass spectrometer (Thermo Electron) as described above. Data-dependent MS/MS (MS2) acquisition with a combination of CID and ETD was coupled with the above MDLC analyses. BioWorks software was utilised for data analysis. BioWorks uses the SEQUEST protein search algorithm, which automatically identifies proteins by comparing experimental tandem mass spectrometry (MS/MS) data with standard protein and DNA databases. It can analyse a single spectrum or an entire LC/MS/MS data set containing spectra from a mixture of proteins. The ‘cross-correlation’ identification

algorithm within SEQUEST extracts information and correctly identifies proteins even at low concentrations.

2.13. Statistical analysis

Analysis of the difference of comparisons, as well as untreated versus siRNA treated mean invasion counts, apoptosis and percentage survival calculated, were performed using a student t-test (two-tailed with unequal variance), on Microsoft Excel. The student t-test was employed as it establishes whether the means of two groups are significantly different from each other.

*, A p value of ≤ 0.05 was deemed significant
**, A p value ≤ 0.01 was deemed more significant
***, A p value ≤ 0.005 was deemed highly significant

The term "synergy" used when describing combination assays findings refers to a toxic effect greater than anticipated from summating the effect from each agent alone.

2.14. Experimental replication

Where possible, experiments were carried out in experimental triplicate. Biological replication refers to the complete experimental repetition of an assay and hence measures the full biological variation of the experimental phenomenon being measured. Technical replication refers to repeated quantification of a specific assay (or biological sample) and hence measures the variation associated with the measurement alone.

Chapter 3 Results

3.1 Effect of lapatinib in lung cancer cell models

Lapatinib is a potent anti-cancer agent approved for use in metastatic breast cancer [99]. It has been shown to have alternative cellular activity in addition to HER-2 and EGFR kinase inhibition and so it is possible that lapatinib may have uses outside its current realm. Lapatinib can interact with, and inhibit, transmembrane drug transporters, therefore potentially antagonising the phenomenon of multidrug resistance [45, 109, 110]. This body of work investigated the uses of lapatinib as a therapy in lung cancer and also examined its effects on several important drug transporters.

Two different paired resistant lung cancer cell models were chosen to examine the activities of lapatinib. The resistant models were, A549 and its resistant variant, A549-T, and DLKP and its resistant variant, DLKP-A. Additional work was carried out in the breast cell line SKBR3 as it is sensitive to lapatinib and in the lung cell line, H1299-T, as it has a similar resistance profile to A549-T.

3.1.1. Chemotherapy toxicity profile in chosen cell lines

DLKP is a squamous lung cell line which was established from a lymph node biopsy of a 52 year old male. DLKP-A, is a drug-selected variant of DLKP which was developed by exposure to increasing concentrations of adriamycin (doxorubicin). P-glycoprotein was shown to be over-expressed in the resistant cell line [159]. The adenomcarcinoma, A549, was pulse-selected with clinically relevant levels of the chemotherapy drug paclitaxel, to generate the resistant variant, A549-T [157].

Sensitivity to a panel of chemotherapy drugs (epirubicin, doxorubicin, paclitaxel, docetaxel, vinblastine and vincristine) and the tyrosine kinase inhibitor lapatinib was determined in these cell lines by analysing their IC50 values (table 3.1.1.1). The IC50 is the concentration required to kill 50% of cells. Toxicity profiles demonstrated an increased resistance to a variety of chemotherapy drugs in the drug-selected resistant cell lines DLKP-A and A549-T compared with their respective parent cell lines, DLKP and A549.

DLKP-A exhibited the greatest fold resistance over its parent, with A549-T having a more modest fold resistance compared with its parent cell line. Significant resistance was seen in DLKP-A to adriamycin, epirubicin, paclitaxel, docetaxel, vinblastine and vincristine. Of the drugs tested in A549-T, paclitaxel was the only agent that it was significantly resistant to compared with A549. As work was also carried out in the breast cell line SKBR3 and the resistant lung cell line H1299T, IC50 values were also obtained in these cell lines for several drugs. Lapatinib exhibited a similar toxicity profile in the entire panel of lung cell lines used, whereas it is significantly more toxic in the breast cell line SKBR3. IC50 values were not obtained if no further work was carried out with a drug in a particular cell line.

Toxicity profiles in DLKP, DLKP-A, A549, A549-T and SKBR3

Drug	DLKP	DLKP-A	A549	A549-T	SKBR3	H1299T
Lapatinib (μM)	4.2 +/- 0.05	3.6 +/- 0.4	4.8 +/- 0.2	4.9 +/- 0.7	23.3 +/- 5 (nM)	4.2 +/- 0.4
Epirubicin (nM)	9.6 +/- 0.8	1.9 +/- 0.1 (μM)	17.8 +/- 1	18.3 +/- 3	8.7 +/- 1.6	ND
Adriamycin (nM)	24 +/- 2	4.9 +/- 0.3 (μM)	ND	ND	ND	ND
Taxol (nM)	1.2 +/- 0.5	310 +/- 25	2.9 +/- 0.8	9.4 +/- 1.5	1.6 +/- 0.3	21 +/- 6
Taxotere (nM)	0.15 +/- 0.04	38 +/- 3	ND	1 +/- 0.2	N/D	ND
Vinblastine (nM)	0.6 +/- 0.02	76 +/- 10	0.65 +/- 0.1	0. 8 +/- 0.2	0.6 +/- 0.05	ND
Vincristine (nM)	0.91 +/- 0.1	629 +/- 160	ND	ND	ND	ND

Table 3.1.1.1 IC50 values determined from 7-day proliferation assays. Results are expressed as IC50 +/- SD, n = 3. ND, not determined indicates IC50 values which were not done.

3.1.2. Activity of lapatinib in combination therapy toxicity assays

Lapatinib has been shown to have therapeutic use in combination with cytotoxic drugs [127, 130]. The toxicity of lapatinib in combination with a panel of traditional chemotherapy drugs was assessed in DLKP, DLKP-A, A549 and A549-T cell lines. Co-treatment with lapatinib greatly sensitised the resistant cells to chemotherapy drugs. Synergistic toxicity was observed with lapatinib when combined with P-gp substrate drugs epirubicin, paclitaxel, docetaxel and vinblastine in DLKP-A and A549-T (figures 3.1.2.1 – 3.1.2.9). This synergy was statistically significant in all cases at one or more chemotherapy drug concentration with the exception of epirubicin in A549-T although this is likely due to the large standard deviations observed with this result. No synergy was observed in DLKP-A with the non-P-gp substrate drug, 5-fluorouracil. While a trend in decreased survival was evident with combinations of lapatinib with epirubicin or taxol in the parent cell line DLKP this was not statistically significant (figures 3.1.2.10-3.1.2.11). Combinations with vinblastine exhibited only additive toxicity in DLKP (figure 3.1.2.12). In the sensitive parent cell line A549 no synergistic toxicity was observed with lapatinib in combination with taxol or vinblastine, while a slight decrease in survival was observed with epirubicin (figures 3.1.2.13 – 3.1.2.15). As lapatinib is dissolved in DMSO, a 0.1% solution (same volume as highest lapatinib concentration) was used as a control. Statistics was carried out on all data with significant results displayed.

Proliferation assay in DLKP-A

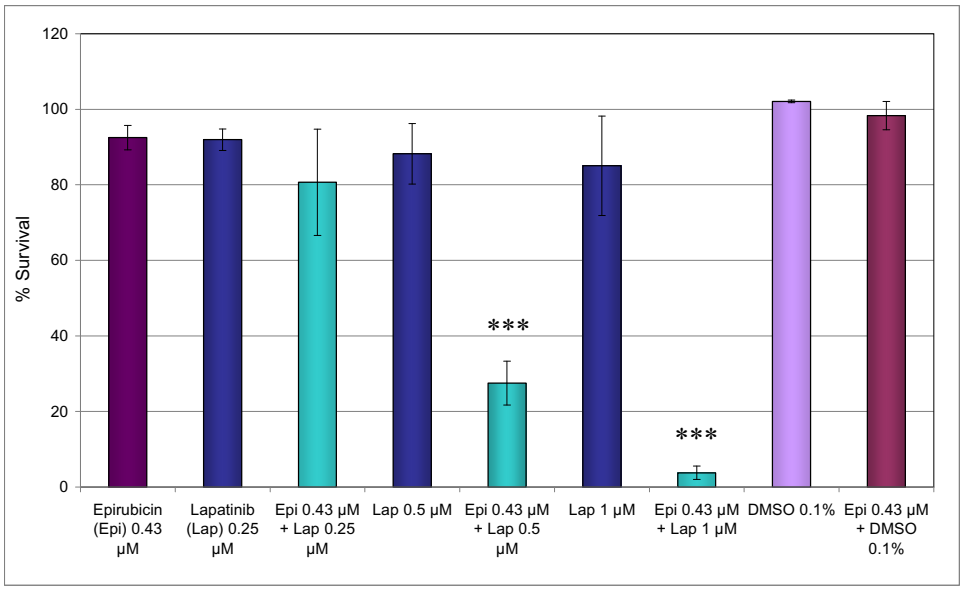

Figure 3.1.2.1 % cell survival in DLKP-A as determined by acid phosphatase assay in response to a six day treatment of lapatinib in combination with epirubicin. Data are mean +/- SD of triplicate experiments. *** significant, P<0.005 compared with epirubicin alone.

Proliferation assay in DLKP-A

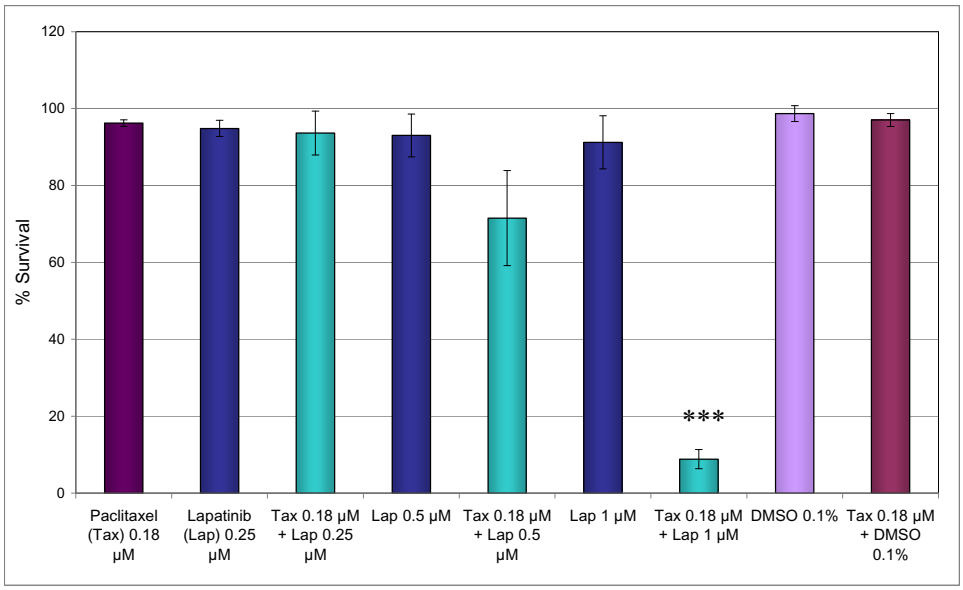

Figure 3.1.2.2 % cell survival in DLKP-A as determined by acid phosphatase assay in response to a six day treatment of lapatinib in combination with paclitaxel. Data are mean +/- SD of triplicate experiments. *** significant, P<0.005 compared with paclitaxel alone.

Proliferation assay in DLKP-A

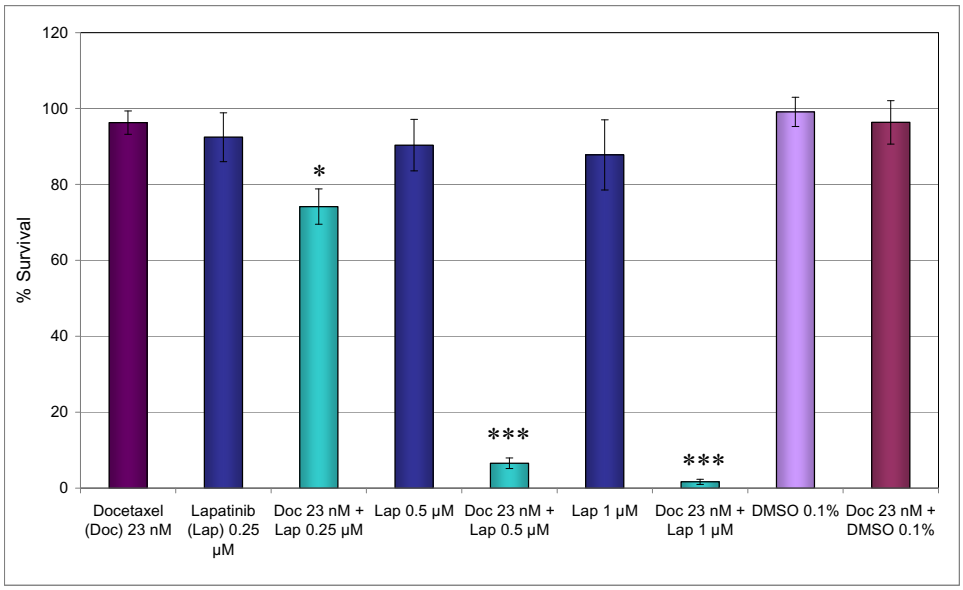

Figure 3.1.2.3 % cell survival in DLKP-A as determined by acid phosphatase assay in response to a six day treatment of lapatinib in combination with docetaxel. Data are mean +/- SD of triplicate experiments. *,*** significant, $P<0.05$, $P<0.005$ compared with docetaxel alone.

Proliferation assay in DLKP-A

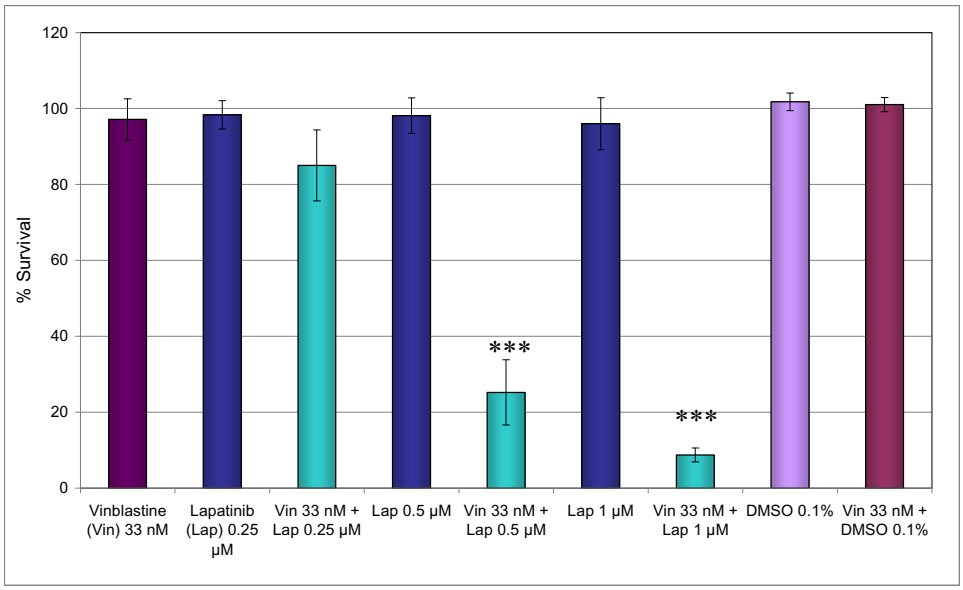

Figure 3.1.2.4 % cell survival in DLKP-A as determined by acid phosphatase assay in response to a six day treatment of lapatinib in combination with vinblastine. Data are mean +/- SD of triplicate experiments. *** significant, P<0.005 compared with vinblastine alone.

Proliferation assay in DLKP-A

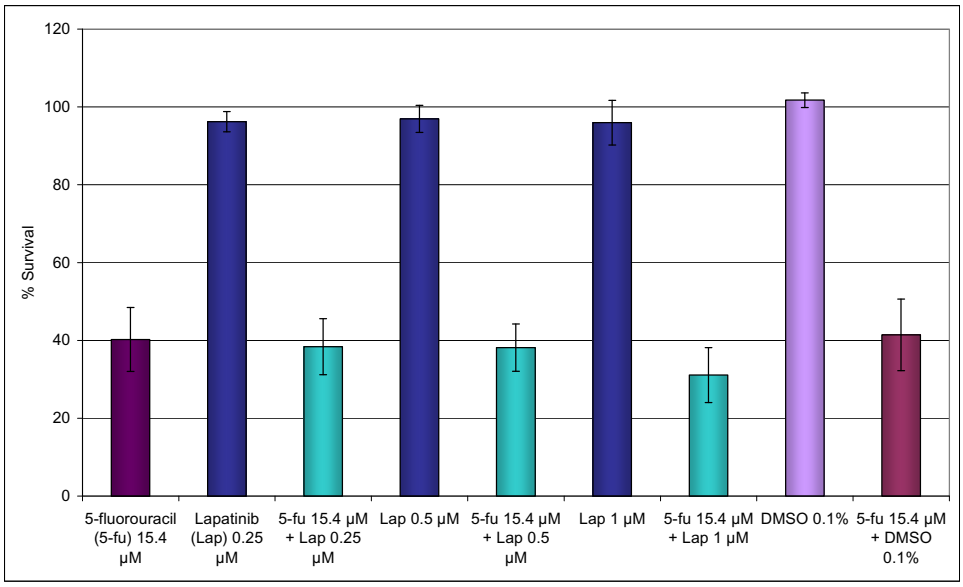

Figure 3.1.2.5 % cell survival in DLKP-A as determined by acid phosphatase assay in response to a six day treatment of lapatinib in combination with 5-fluoruracil. Data are mean +/- SD of triplicate experiments.

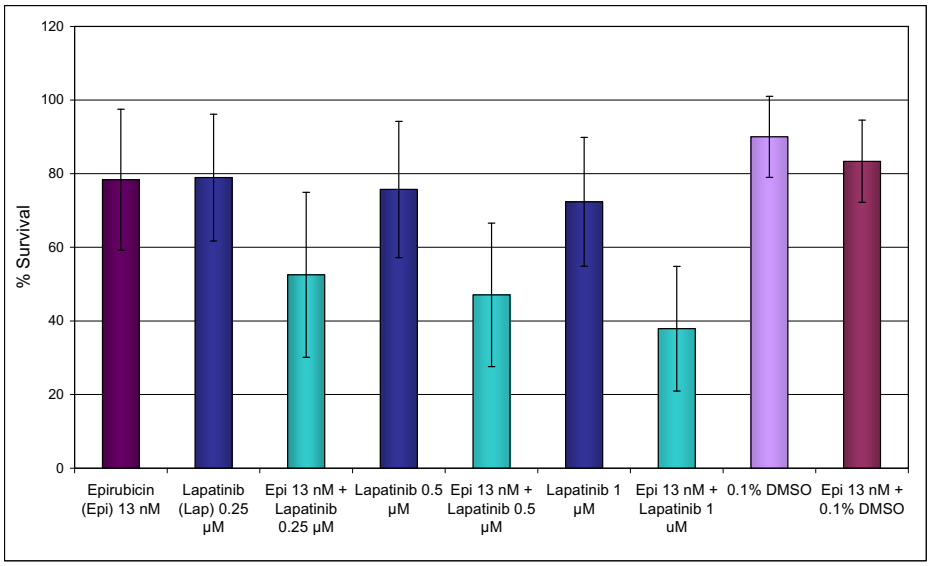

Figure 3.1.2.6 % cell survival in A549-T as determined by acid phosphatase assay in response to a six day treatment of lapatinib in combination with epirubicin. Data are mean +/- SD of triplicate experiments.

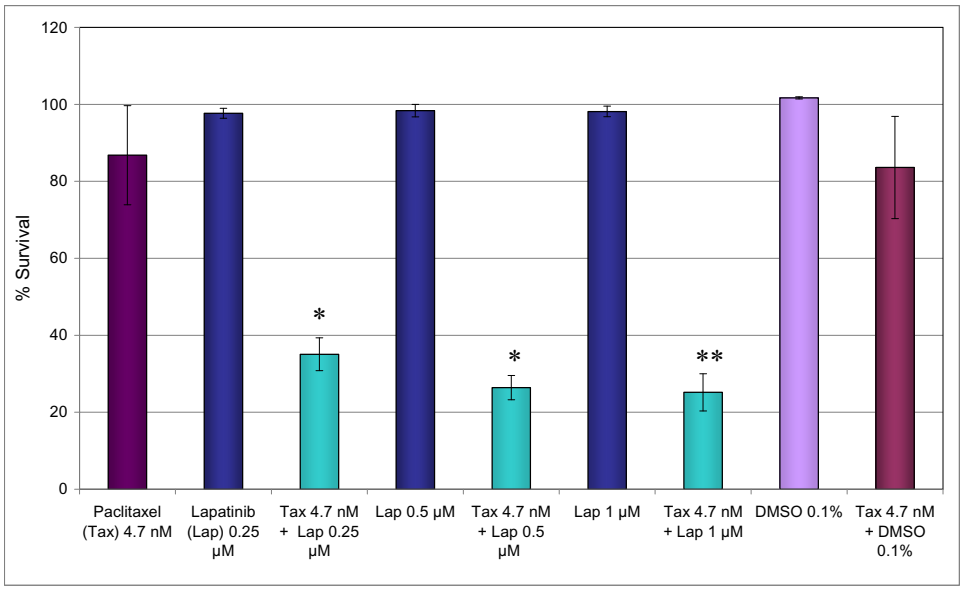

Figure 3.1.2.7 % cell survival in A549-T as determined by acid phosphatase assay in response to a six day treatment of lapatinib in combination with paclitaxel. Data are mean +/- SD of triplicate experiments. *,** significant, $P<0.05$, $P<0.01$ compared with paclitaxel alone.

Proliferation assay in A549-T

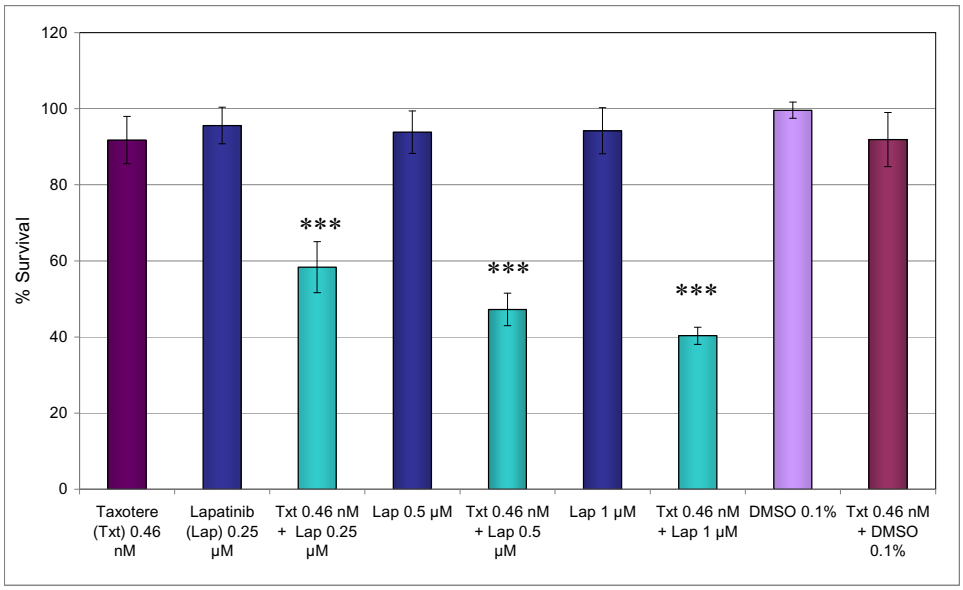

Figure 3.1.2.8 % cell survival in A549-T as determined by acid phosphatase assay in response to a six day treatment of lapatinib in combination with docetaxel. Data are mean +/- SD of triplicate experiments. *** significant, P<0.005 compared with taxotere alone.

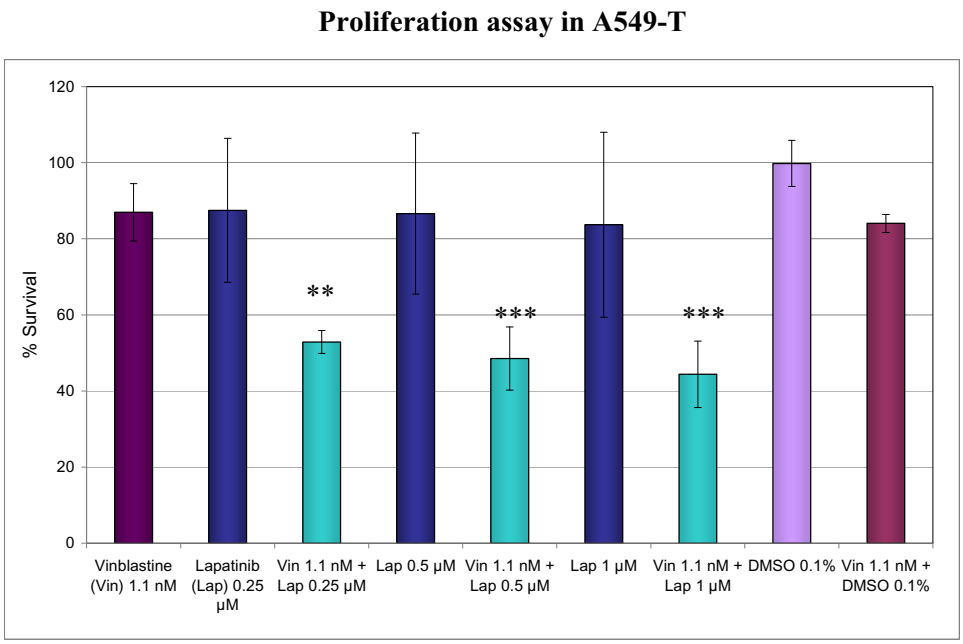

Figure 3.1.2.9 % cell survival in A549-T as determined by acid phosphatase assay in response to a six day treatment of lapatinib in combination with vinblastine. Data are mean +/- SD of triplicate experiments. **,*** significant, P<0.01, P<0.005 compared with vinblastine alone.

Proliferation assay in DLKP

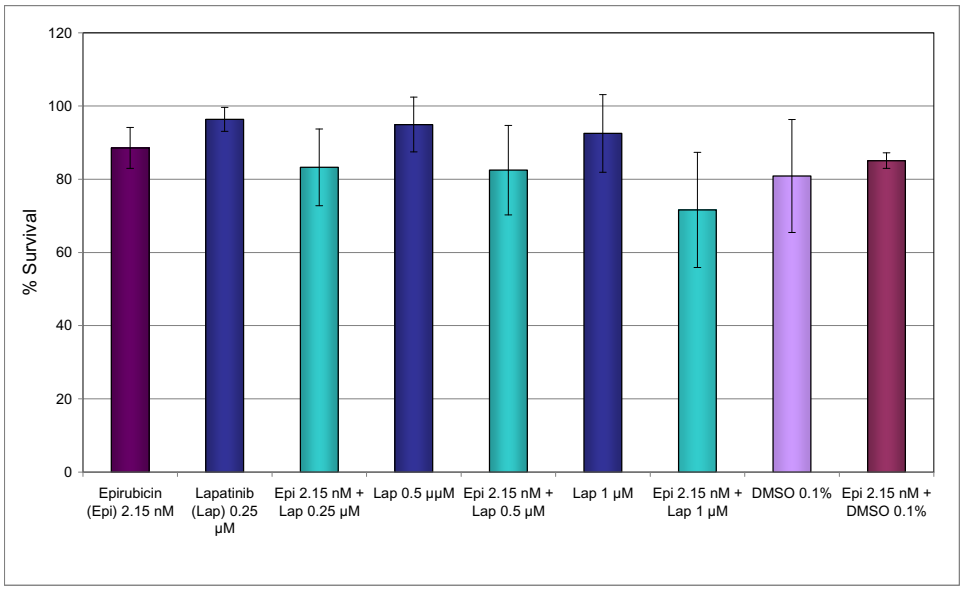

Figure 3.1.2.10 % cell survival in DLKP as determined by acid phosphatase assay in response to a six day treatment of lapatinib in combination with epirubicin. Data are mean +/- SD of triplicate experiments.

Proliferation assay in DLKP

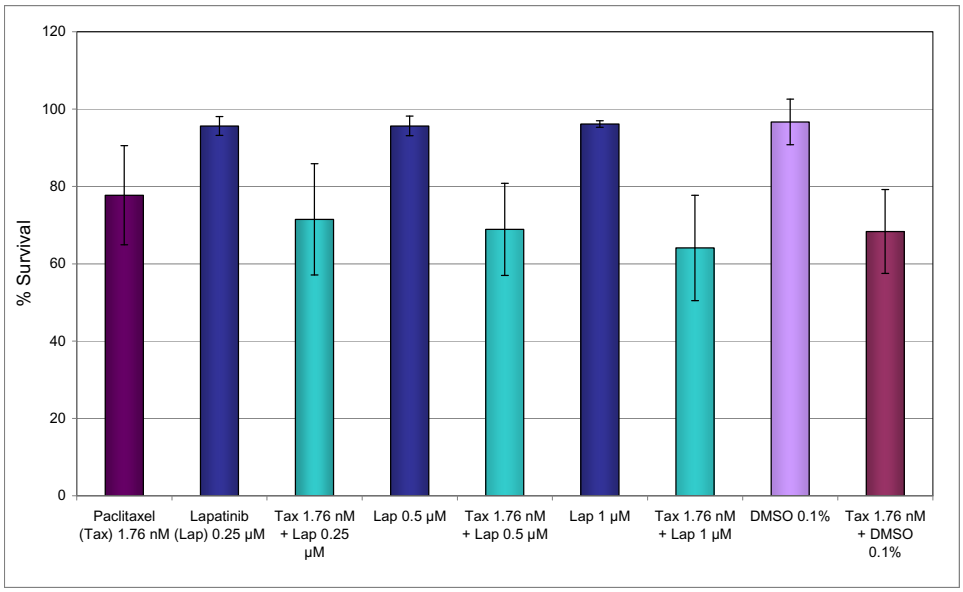

Figure 3.1.2.11 % cell survival in DLKP as determined by acid phosphatase assay in response to a six day treatment of lapatinib in combination with paclitaxel. Data are mean +/- SD of triplicate experiments.

Proliferation assay in DLKP

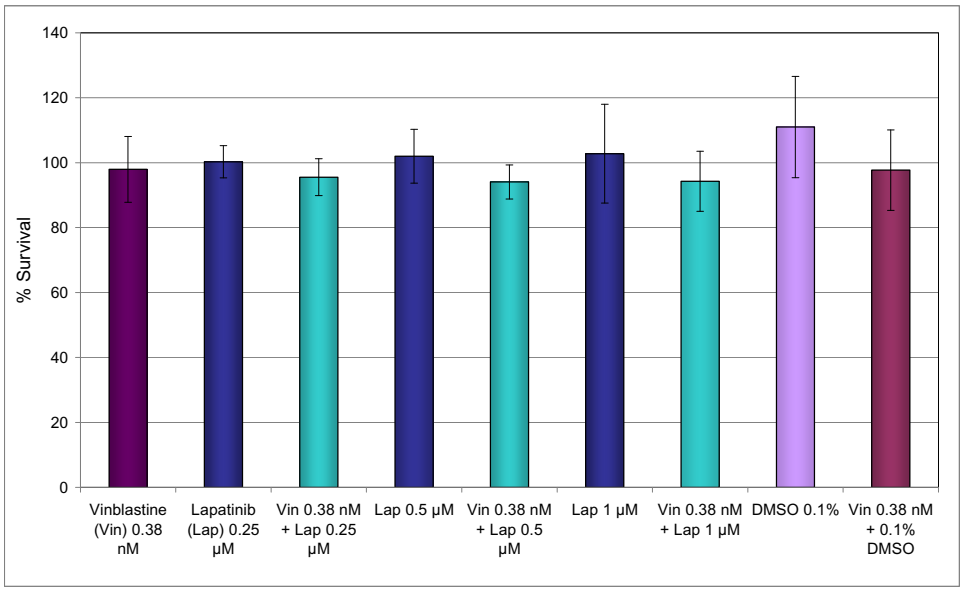

Figure 3.1.2.12 % cell survival in DLKP as determined by acid phosphatase assay in response to a six day treatment of lapatinib in combination with vinblastine. Data are mean +/- SD of triplicate experiments.

Proliferation assay in A549

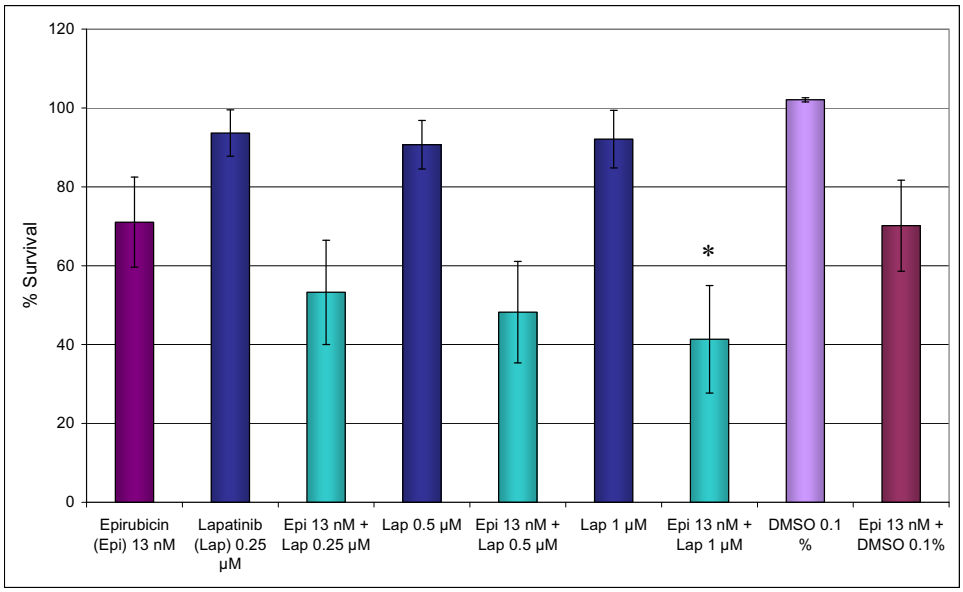

Figure 3.1.2.13 % cell survival in A549 as determined by acid phosphatase assay in response to a six day treatment of lapatinib in combination with epirubicin. Data are mean +/- SD of triplicate experiments. * significant, $P<0.05$ compared with epirubicin control.

Proliferation assay in A549

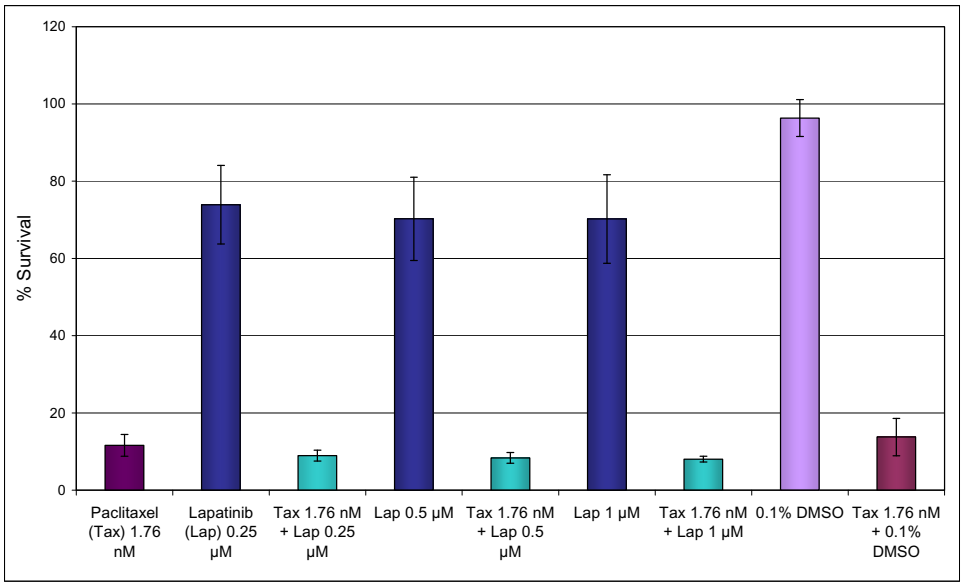

Figure 3.1.2.14 % cell survival in A549 as determined by acid phosphatase assay in response to a six day treatment of lapatinib in combination with paclitaxel. Data are mean +/- SD of triplicate experiments.

Proliferation assay in A549

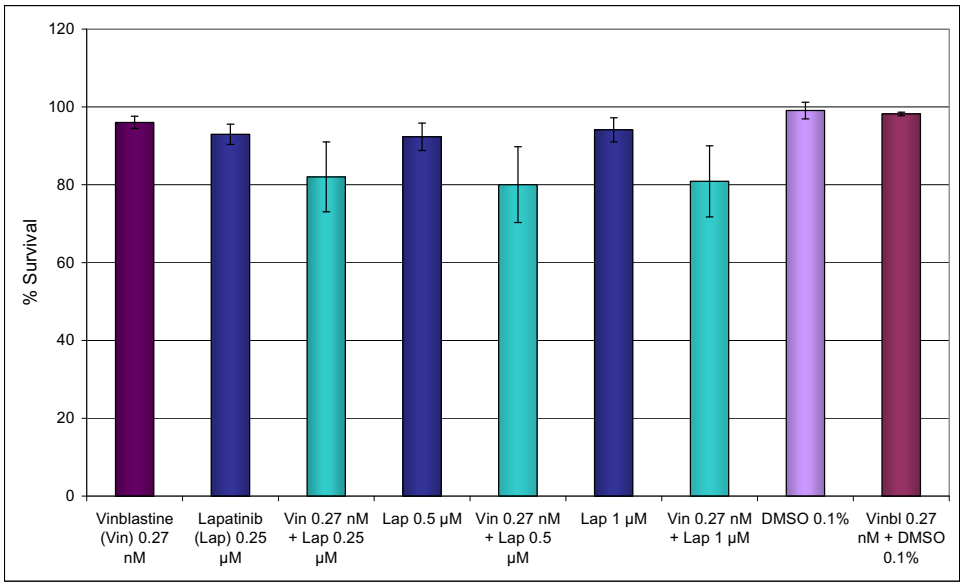

Figure 3.1.2.15 % cell survival in A549 as determined by acid phosphatase assay in response to a six day treatment of lapatinib in combination with vinblastine. Data are mean +/- SD of triplicate experiments.

3.1.3. Apoptotic response to combination therapy

As the acid phosphatase assay determines cell proliferation over a period of time, it is difficult to ascertain if decreased cell count at the end of assay is due to cytostatic or cytotoxic effects. In order to address this, apoptosis, as determined by TUNEL assay, was assessed in DLKP-A and A549-T cells treated with combinations of lapatinib with various chemotherapy agents. The Guava® TUNEL assay determines mid- to late- stage apoptosis when DNA fragmentation is occurring in cells. The DNA degradation generates DNA strands with exposed 3'-hydroxyl ends and terminal deoxynucleotidyl transferase (TdT) catalyzes the incorporation of bromo-deoxyuridine (BrdU) residues into the fragmenting nuclear DNA at the 3'-hydroxyl ends by nicked end labeling. A TRITC-conjugated anti-BrdU antibody can then label the 3'-hydroxyl ends for detection by a Guava System. [162]. In DLKP-A, combinations of lapatinib with paclitaxel, docetaxel or vinblastine resulted in increased apoptosis compared with either agent alone (figure 3.1.3.1). The difference in apoptosis was significant in the case of docetaxel. The trend was also seen with lapatinib and vinblastine, paclitaxel or docetaxel in A549-T, although the increase was not as pronounced (figure 3.1.3.1). Large standard deviations evident in these results are likely due to reagent constraints and the inability to repeat a further time. The results follow a trend and so are likely to be representative.

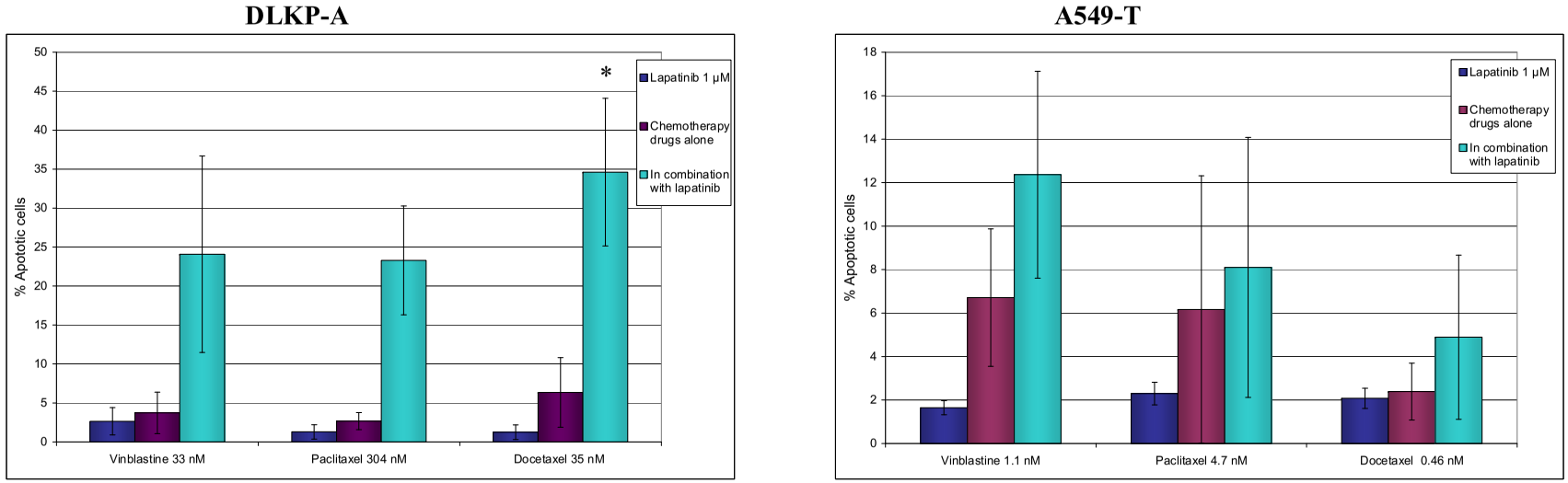

Figure 3.1.3.1 Apoptosis levels as determined by TUNEL staining in DLKP-A and A549-T in response to 72 hour drug treatments of lapatinib in combination with vinblastine, paclitaxel and docetaxel. Data are mean +/- SD of triplicate experiments. * significant, $P<0.05$ compared with chemotherapy drug alone.

3.1.4. Transporter expression in panel of cell lines

ABC drug transporter proteins have been found to be over-expressed in a number of cancers [30, 34, 163] and this generally correlates with increased drug resistance [163, 164]. Expression levels of the drug transporters P-gp, MRP1 and BCRP were determined in the parental and resistant lung cell lines. This was undertaken in order to determine base protein levels for the panel of cell lines. A549-T was shown to express P-gp as seen in figure 3.1.4.1, whereas its parent cell line, A549, had no detectable level of P-gp. DLKP-A cells express large amounts of P-gp and again no P-gp protein expression was detected in its parent, DLKP. MRP1 expression was observed in both A549 and A549-T with the greater expression in the parental variant (figure 3.1.4.1). Neither DLKP nor DLKP-A appeared to express the MRP1 transporter. BCRP was only detected at a low level in A549-T (figure 3.1.4.1).

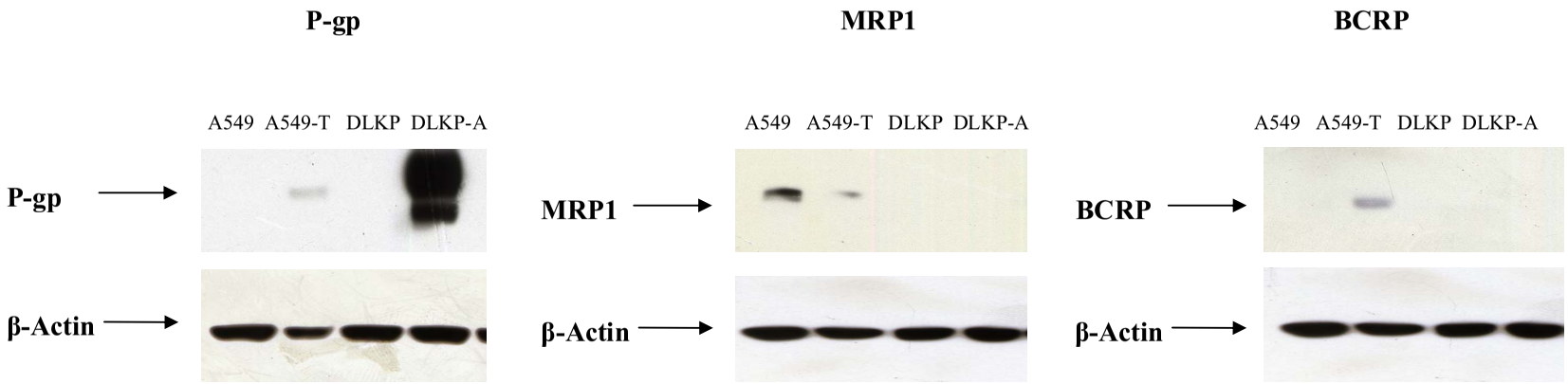

Figure 3.1.4.1 Western blot showing levels of P-gp, MRP1 and BCRP in the parental lung cell lines A459 and DLKP and their resistant variants, A549-T and DLKP-A.

3.1.5. Effect of lapatinib on drug transporter expression

As mentioned previously, lapatinib has been shown to interact with and inhibit P-gp [109, 110]. The synergy observed in the combination assays in P-gp expressing cell lines DLKP-A and A549-T would support these findings. Initial findings from a previous study in our laboratory suggest lapatinib has the ability to alter the expression levels of P-gp [165]. This potential element of lapatinib behaviour has not been reported previously, and so the effect of varying levels of lapatinib on P-pg and MRP1 expression was investigated.

Lapatinib treatments of 2.5, 5 and 10 μM for 24 hrs in A549-T cells caused an increase in P-gp protein levels compared with the untreated control. Densitometric analysis indicated a greater than 3-fold increase in P-gp expression in response to the 2.5 μM lapatinib treatment, which was maintained with 5 μM lapatinib treatment; although the P-gp levels measured in response to 10 μM lapatinib treatment were comparable to control levels (figure 3.1.5.1). Similar lapatinib-induced changes in P-gp expression were observed with 48 and 72 hour treatments of 2.5 μM, 5 μM and 10 μM lapatinib. Densitometric analysis showed the 48 hour 2.5 μM lapatinib treatment caused a similar 3-fold increase in P-gp expression and this level reduced to a 1.5-fold increase with the two higher concentrations (5 μM and 10 μM) (figure 3.1.5.2). The increase in P-gp levels following 72 hour 2.5 μM and 5 μM lapatinib treatments was in the region of 1.8-fold with the 10 μM treatment again exhibiting comparable levels to the control, as determined by densitometry. As lapatinib is dissolved in DMSO, a control for this was also used. Although the P-gp level in cells treated with DMSO altered slightly it was comparable to the control in most cases. The effect of lapatinib on P-gp expression in the sensitive cell line SKBR3 was also determined; however, as can be seen in figure 3.1.5.4, no P-gp protein was detected in this cell line and its expression was not induced with lapatinib.

To examine the dose dependency of the increase in P-gp in A549-T, P-gp levels were assessed in this cell line following 48 hour treatments with a concentration range of 0.1, 0.25, 0.5, 1, 2.5 and 10 μM lapatinib. An increase in P-gp expression was evident from as low as 0.25 μM lapatinib, as can be seen in figure 3.1.5.5. By way of validation a 48 hour lapatinib (2.5 μM, 5 μM and 10 μM) treatment was also carried out in the multi- drug resistant lung cell line H1299-T. P-gp levels detected following

incubation with lapatinib in this cell line showed a similar trend as seen in A549-T as P-gp levels increased compared with control (figure 3.1.5.6).

MRP1 levels were also assessed following treatment with 2.5, 5 and 10 μM lapatinib. In this case the level of drug pump was seen to decrease with lapatinib exposure as shown in figure 3.1.5.7. This decrease in P-gp expression was up to 5-fold with the highest concentration of lapatinib. The effect of lapatinib on P-gp and MRP1 levels was also determined in the non-resistant parent cell line A549. As no detectable levels of P-gp were found in A549, it was investigated if lapatinib treatments had the ability to induce P-gp expression in the parent cell line. As shown in figure 3.1.5.8, lapatinib did not induce P-gp expression in A549. It was sought to establish if lapatinib had a similar effect on MRP1 in A549 as observed in A549-T. Figure 3.1.5.9 shows a reduction in MRP1 level with lapatinib treatments comparable to that observed in A549-T. Again a DMSO control was included and did not prove to greatly alter MRP1 level. All densitometry analysis is normalised to corresponding β-actin control.

P-gp expression in A549-T

(a)

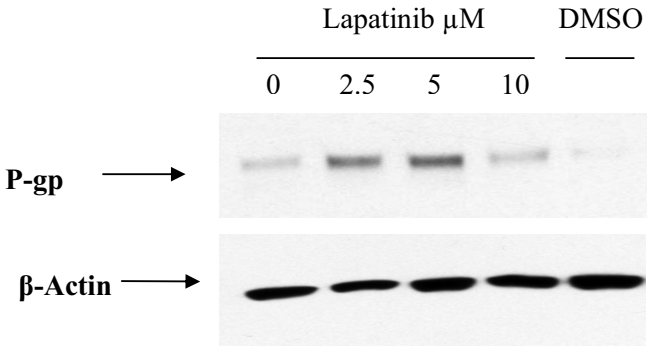

(b)

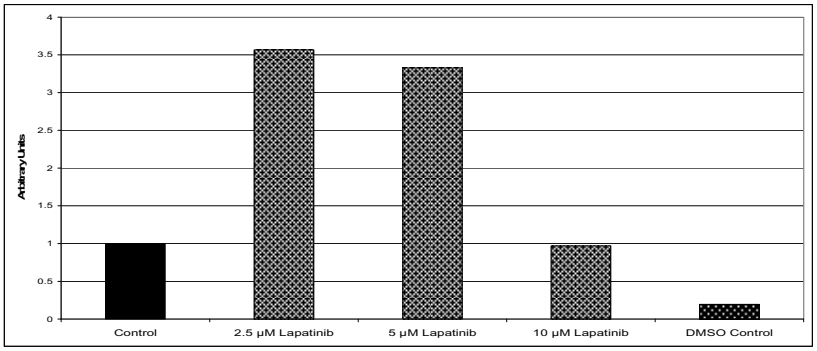

Figure 3.1.5.1 (a) Western blot of P-gp expression with (b) densitometry following 24 hour 2.5 μM, 5 μM and 10 μM lapatinib treatments in A549-T. Control was A549-T cells incubated with growth medium for 24 hours. A DMSO control containing the same quantity of DMSO as in highest lapatinib concentration was included. Western blot was carried out in duplicate and densitometry is of a representative blot.

P-gp expression in A549-T

(a)

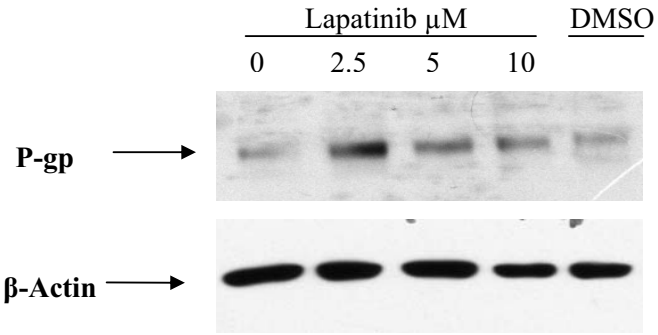

(b)

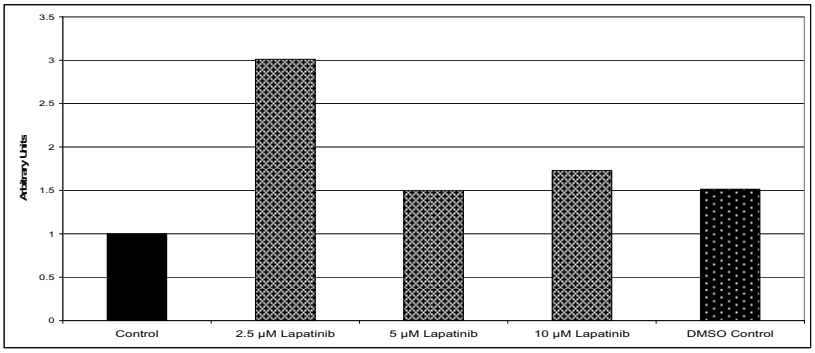

Figure 3.1.5.2 (a) Western blot of P-gp expression with (b) densitometry following 48 hour 2.5 µM, 5 µM and 10 µM lapatinib treatments in A549-T. Control was A549-T cells incubated with growth medium for 48 hours. A DMSO control containing the same quantity of DMSO as in highest lapatinib concentration was included. Western blot was carried out in duplicate and densitometry is of a representative blot.

P-gp expression in A549-T

(a)

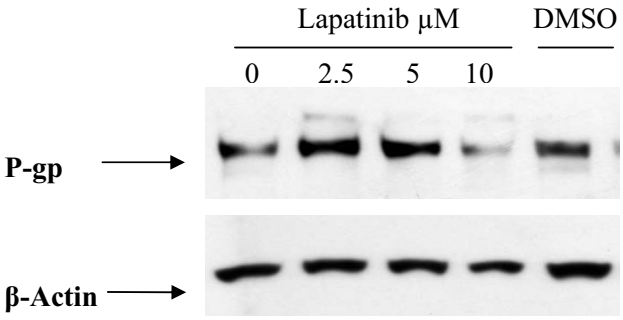

(b)

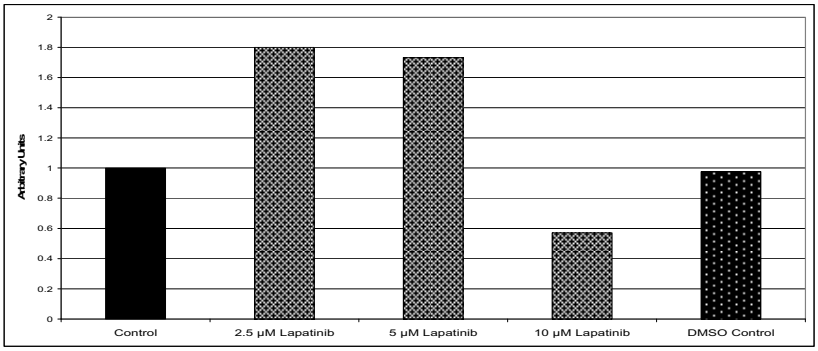

Figure 3.1.5.3 (a) Western blot of P-gp expression with (b) densitometry following 72 hour 2.5 μM, 5 μM and 10 μM lapatinib treatments in A549-T. Control was A549-T cells incubated with growth medium for 72 hours. A DMSO control containing the same quantity of DMSO as in highest lapatinib concentration was included.

P-gp expression in SKBR3

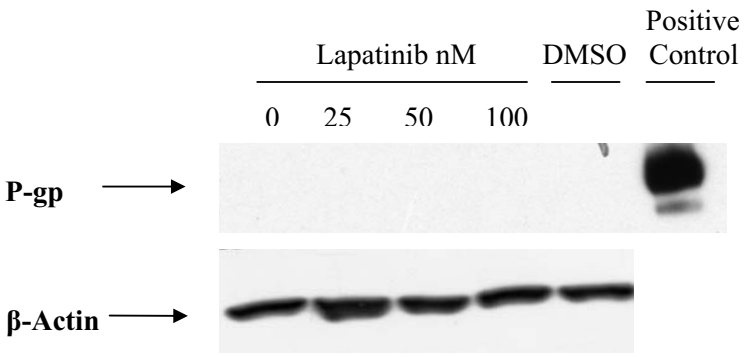

Figure 3.1.5.4 Western blot of P-gp expression following 48 hour 25 nM, 50 nM and 100 nM lapatinib treatments in SKBR3. Control was SKBR3 cells incubated with growth medium for 48 hours. A DMSO control containing the same quantity of DMSO as in highest lapatinib concentration was included.

P-gp expression in A549-T

(a)

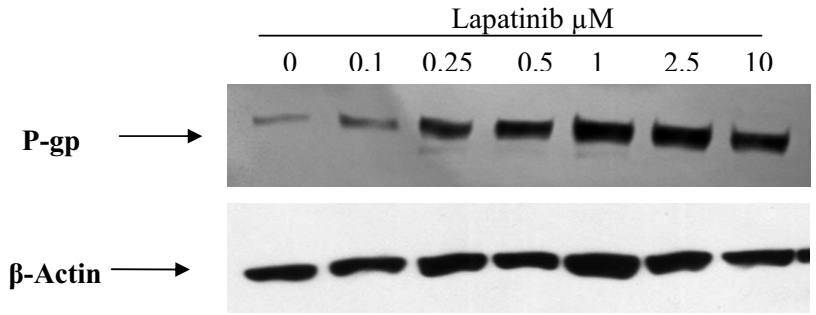

(b)

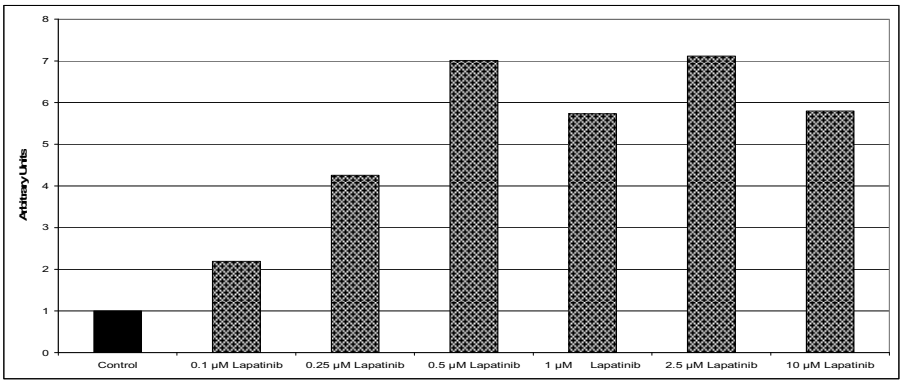

Figure 3.1.5.5 (a) Western blot of P-gp expression with (b) densitometry following 48 hour 0.1 μM, 0.25 μM, 0.5 μM, 1 μM, 2.5 μM, and 10 μM lapatinib treatments in A549-T. Control was A549-T cells incubated with growth medium for 48 hours. Western blot was carried out in duplicate.

P-gp expression in H1299-T

(a)

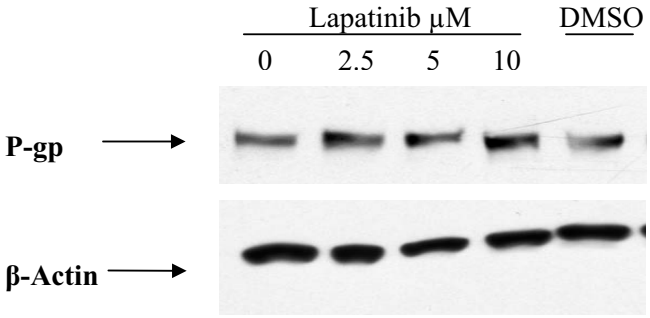

(b)

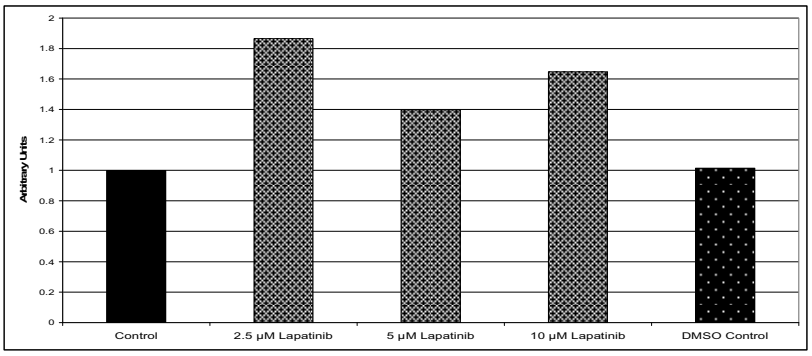

Figure 3.1.5.6 (a) Western blot of P-gp expression with (b) densitometry following 48 hour 2.5 µM, 5 µM and 10 µM lapatinib treatments in H1299-T. Control was H1299-T cells incubated with growth medium for 48 hours. A DMSO control containing the same quantity of DMSO as in highest lapatinib concentration was included. Western blot was carried out in duplicate and densitometry is of a representative blot.

MRP1 expression in A549-T

(a)

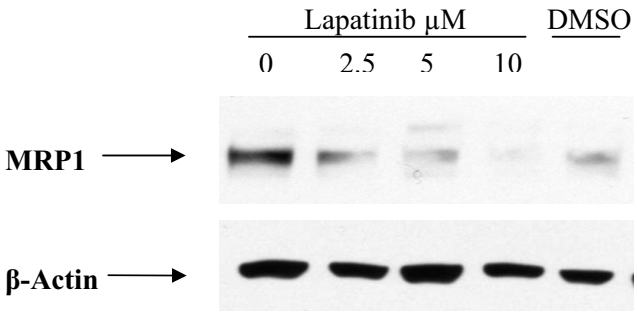

(b)

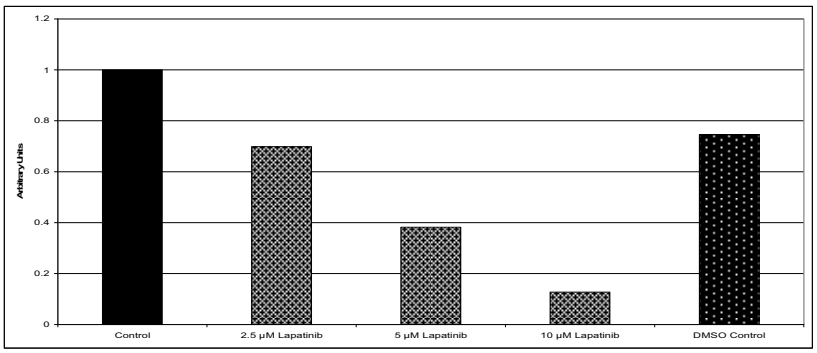

Figure 3.1.5.7 (a) Western blot of MRP1 expression with (b) densitometry following 48 hour 2.5 µM, 5 µM and 10 µM lapatinib treatments in A549-T. Control was A549-T cells incubated with growth medium for 48 hours. A DMSO control containing the same quantity of DMSO as in highest lapatinib concentration was included. Western blot was carried out in duplicate and densitometry is of a representative blot.

P-gp expression in A549

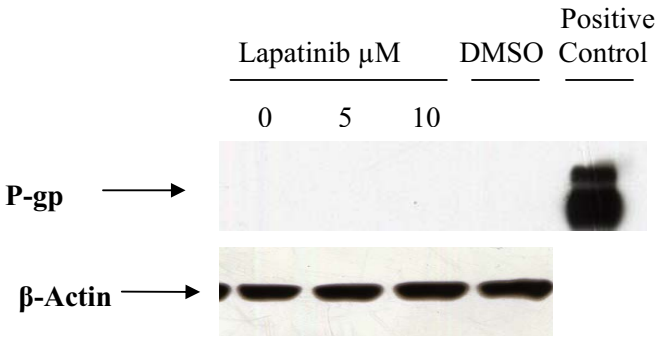

Figure 3.1.5.8 Western blot of P-gp expression following 48 hour 5 μM and 10 μM lapatinib treatments in A549. Control was A549 cells incubated with growth medium for 48 hours. A DMSO control containing the same quantity of DMSO as in highest lapatinib concentration was included.

MRP1 expression in A549

(a)

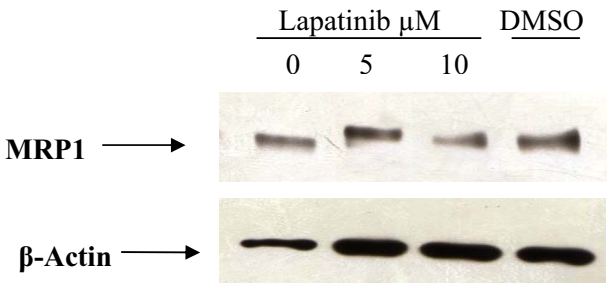

(b)

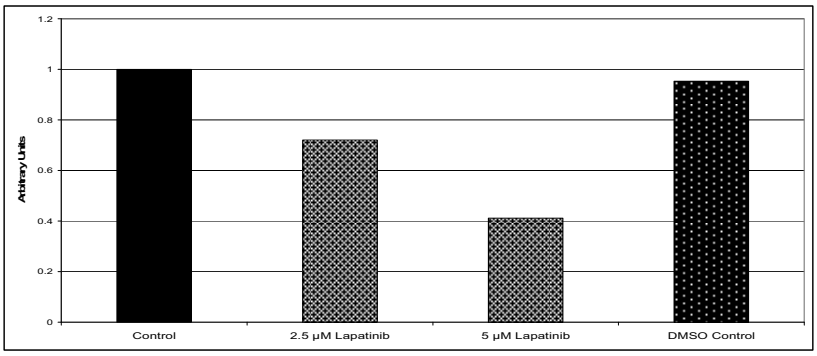

Figure 3.1.5.9 (a) Western blot of MRP1 expression with (b) densitometry following 48 hour 5 µM and 10 µM lapatinib treatments in A549. Control was A549 cells incubated with growth medium for 48 hours. A DMSO control containing the same quantity of DMSO as in highest lapatinib concentration was included. Western blot was carried out in duplicate and densitometry is of a representative blot.

3.1.6. Effect of EGF on drug transporter expression

Lapatinib antagonises the actions of the growth factor receptors due to its inhibition of their kinase domain. EGF on the other hand, is the endogenous ligand and agonist for several growth factor receptors and so it was also examined for its effect on drug pump expression. Incubation in the presence of EGF at varying concentrations decreased the expression of P-gp and MRP1 (figures 3.1.6.1, 3.1.6.2, 3.1.6.3 and 3.1.6.5) compared with the control which in this case was serum free media. However, there was one exception to this, as the 48 hour 10 ng/ml EGF treatment appeared to increase P-gp expression in A549-T. A 2-fold decrease was observed in P-gp expression with 24 and 72 hour EGF treatments, and in MRP1 expression with 48 hours EGF treatment. The lower concentration of 2 ng/ml EGF was also analysed for effect on P-gp level and figure 3.1.6.4 indicates EGF was active at decreasing P-gp protein expression at this concentration.

P-gp expression in A549-T

(a)

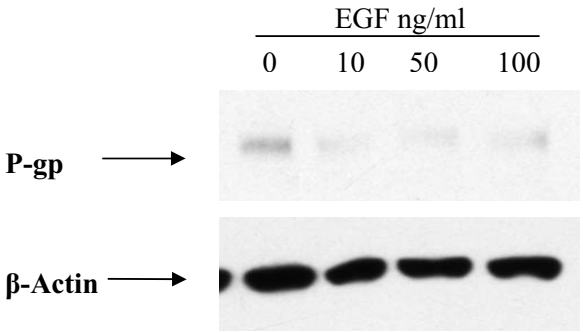

(b)

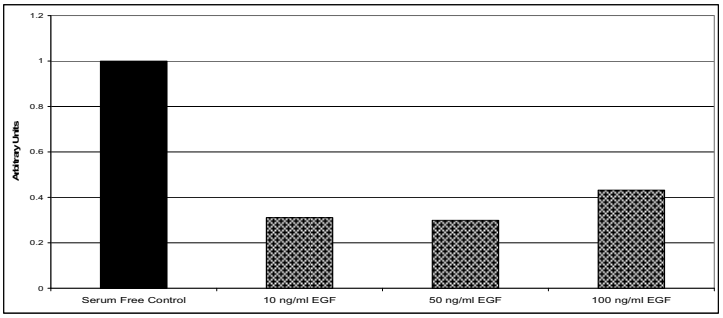

Figure 3.1.6.1 (a) Western blot of P-gp expression with (b) densitometry following 24 hour 10 ng/ml, 50 ng/ml and 100 ng/ml EGF treatments in A549-T. EGF treatments were in serum-free growth medium and control was A549-T cells incubated with serum-free growth medium for 24 hours. Western blot was carried out in duplicate and densitometry is of a representative blot.

P-gp expression in A549-T

(a)

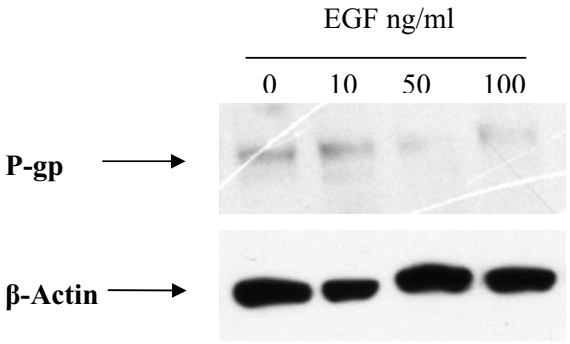

(b)

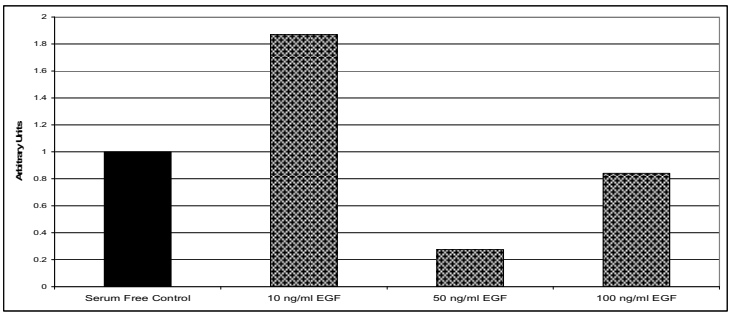

Figure 3.1.6.2 (a) Western blot of P-gp expression with (b) densitometry following 48 hour 10, 50 and 100 ng/ml EGF treatments in A549-T. EGF treatments were in serum-free growth medium and control was A549-T cells incubated with serum-free growth medium for 48 hours. Western blot was carried out in duplicate and densitometry is of a representative blot.

P-gp expression in A549-T

(a)

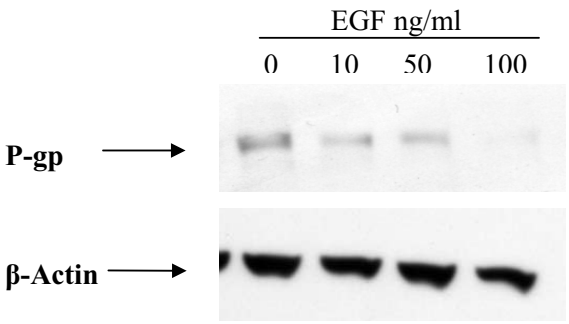

(b)

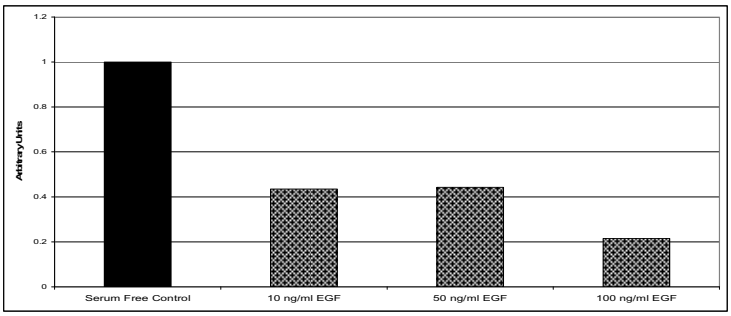

Figure 3.1.6.3 (a) Western blot of P-gp expression with (b) densitometry following 72 hour 10, 50 and 100 ng/ml EGF treatments in A549-T. EGF treatments were in serum-free growth medium and control was A549-T cells incubated with serum-free growth medium for 72 hours.

P-gp expression in A549-T

(a)

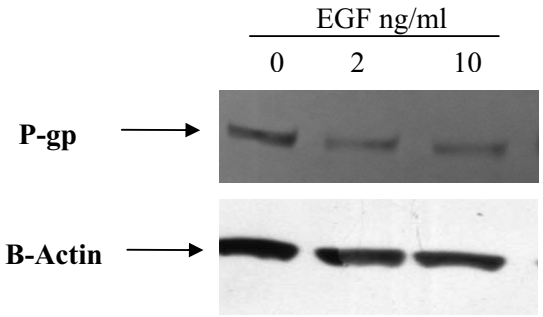

(b)

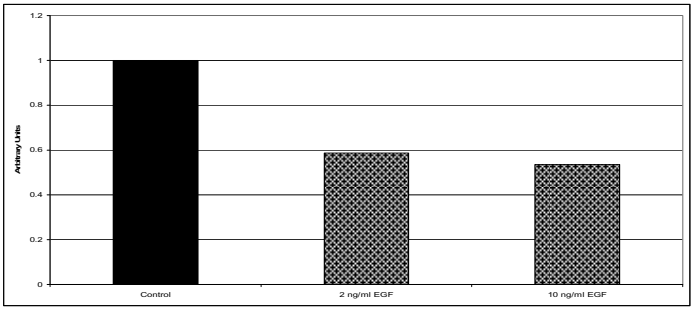

Figure 3.1.6.4 (a) Western blot of P-gp expression with (b) densitometry following 48 hour 2 ng/ml and 10 ng/ml EGF treatments in A549-T. EGF treatments were in serum-free growth medium and control was A549-T cells incubated with serum-free growth medium for 48 hours.

MRP1 expression in A549-T

(a)

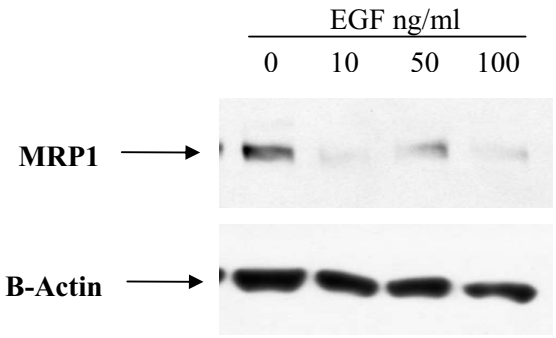

(b)

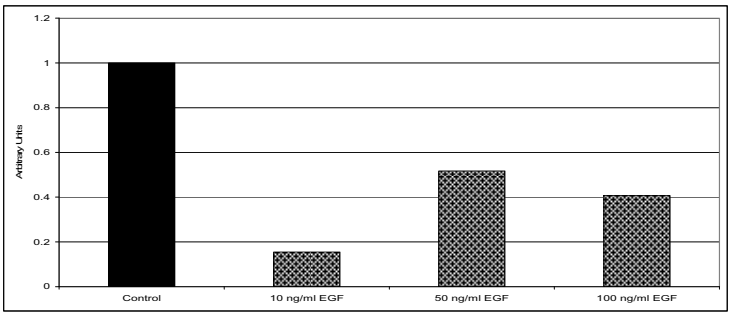

Figure 3.1.6.5 (a) Western blot of MRP1 expression with (b) densitometry following 48 hour 10 ng/ml, 50 ng/ml and 100 ng/ml EGF treatments in A549-T. EGF treatments were in serum-free growth medium and control was A549-T cells incubated with serum-free growth medium for 48 hours. Western blot was carried out in duplicate and densitometry is of a representative blot.

3.1.7. Effect of lapatinib and EGF on P-gp and MRP1 mRNA expression

From section 3.1.5 it can be seen that lapatinib treatment led to an increase in expression of the drug transporter P-gp and a decrease in expression of MRP1. In many cases where drugs induce an increase in P-gp expression, it is as a result of an increase in gene transcription and so an increase in the mRNA expression level accompanies this [166]. To investigate if this was the case following lapatinib treatment, RT-PCR analysis was carried to observe changes in ABCB1 (P-gp) and ABCC1 (MRP1) mRNA levels in A549-T cells following 24 hour treatments with 2.5 μM and 5μM lapatinib. Again as the lapatinib was dissolved in DMSO a control for this was included. 24 hour EGF treatments were also examined to see if they had any effect on P-gp and MRP1 mRNA level. The 2.5 μM lapatinib treatment which effected protein levels of the drug transporters did not have any major effect on P-gp or MRP1 mRNA level as shown in figure 3.1.7.1, while analysis of the densitometric data showed that the 5μM treatment did appear to have an effect on mRNA levels of both P-gp and MRP1. No substantial changes were observed in P-gp or MRP1 mRNA levels in response to EGF treatments either.

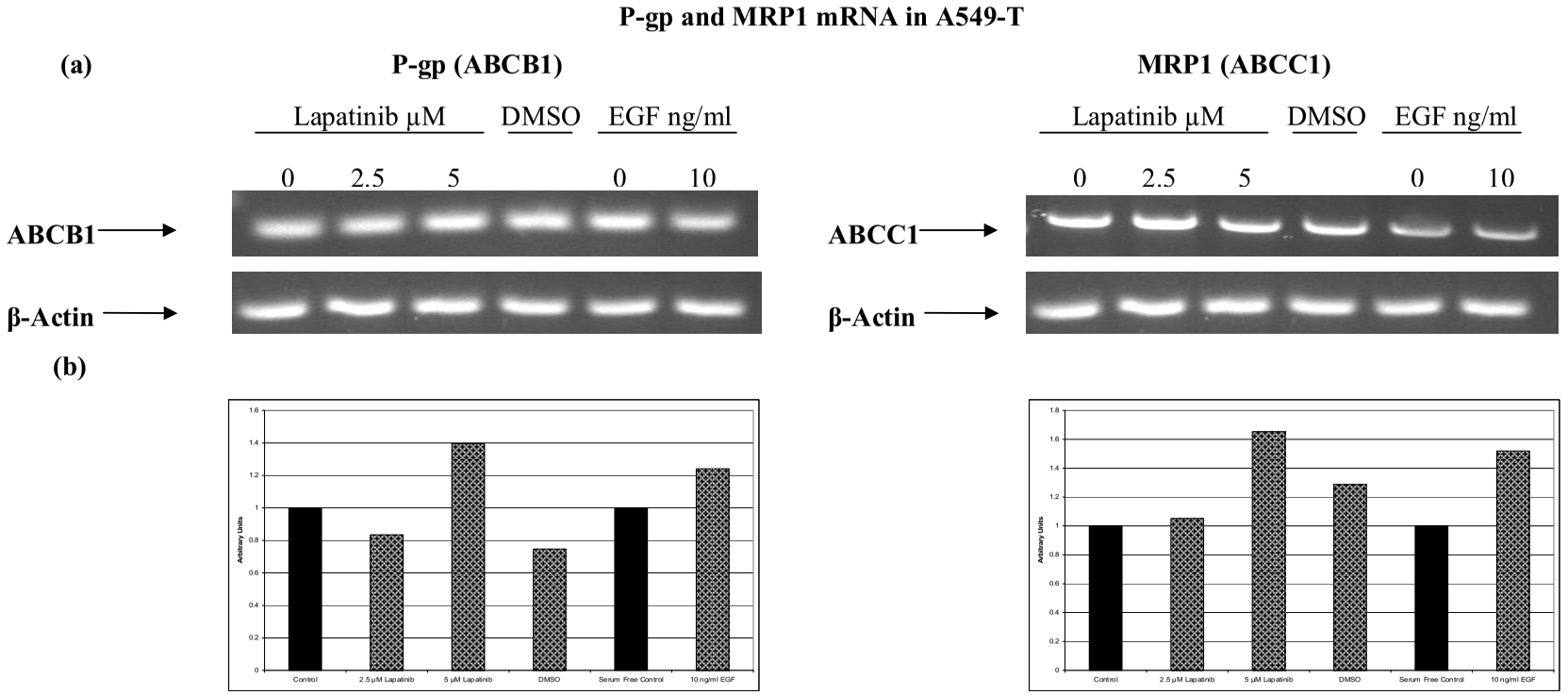

Figure 3.1.7.1 (a) RT-PCR mRNA analysis of P-gp (ABCB1) and MRP1 (ABCC1) mRNA expression (b) with densitometry in A549-T following 24 hour 2.5 µM and 5 µM lapatinib and 10 ng/ml EGF treatments. Control for lapatinib treated samples was A549-T incubated with growth medium for 24 hours. A DMSO control containing the same quantity of DMSO as in highest lapatinib concentration was included. EGF treatments were in serum-free growth medium and control was A549-T cells incubated with serum-free growth medium for 24 hours.

3.1.8. Effect of lapatinib treatments on total and phosphorylated EGFR and HER-2

As EGFR and HER-2 are the targets for lapatinib, its effect on their total and phosphorylated levels was also determined. This was examined in A549-T, SKBR3 and H1299-T cells. Lapatinib treatments in A549-T resulted in a slight reduction in total EGFR whereas, in SKBR3 (a lower concentration), a slight increase in total EGFR was observed (figure 3.1.8.1 and 3.1.8.2). Changes in total EGFR were observed in H1299-T, with a decrease after 12 hours and an increase after 24 hours induced by lapatinib, as seen in figure 3.1.8.3. In the case of phosphorylated EGFR no major change was observed with 12 and 24 hour lapatinib treatments in A549-T whereas after 48 hour treatments there was an increase in levels compared with control (figure 3.1.8.4). Although an increase in phosphorylated EGFR was also observed in SKBR3 after both 12 and 24 hour lapatinib treatments and in H1299-T after 24 hour treatments, it must be noted that the standard errors were very large (figures 3.1.8.5 and 3.1.8.6).

Total HER-2 levels increased in response to 48 hour 2.5 μM lapatinib treatments in A549-T (figure 3.1.8.7). This trend was also evident in SKBR3 at all time points, however, again standard errors overlapped (figure 3.1.8.8). Lapatinib also induced an increase in phosphorylated HER-2 in both A549-T and SKBR3 as shown in figures 3.1.8.9 and 3.1.8.10. It is of importance to note that the DMSO controls included appeared to have an effect in altering the protein levels in some cases, rendering these particular results somewhat inconclusive. Statistics were not carried out as only duplicate data was available.

EGFR expression in A549-T

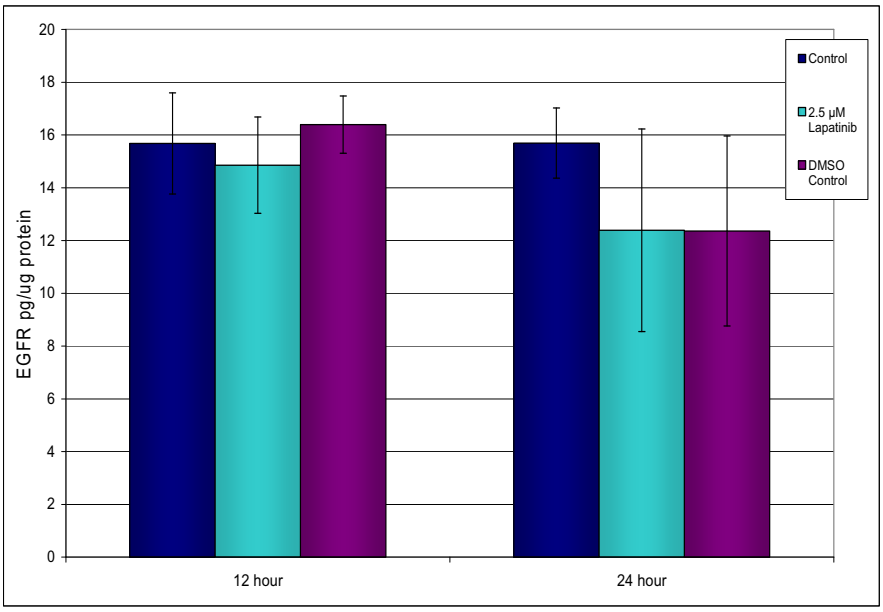

Figure 3.1.8.1 ELISA of total EGFR expression in A549-T, following 12 and 24 hour 2.5 µM lapatinib treatments. Control for lapatinib treated samples was A549-T incubated with growth medium for 12 and 24 hours. A DMSO control containing the same quantity of DMSO as in highest lapatinib concentration was included. Experiments were performed in duplicate on biological duplicates and data represents the mean +/- range.

EGFR expression in SKBR3

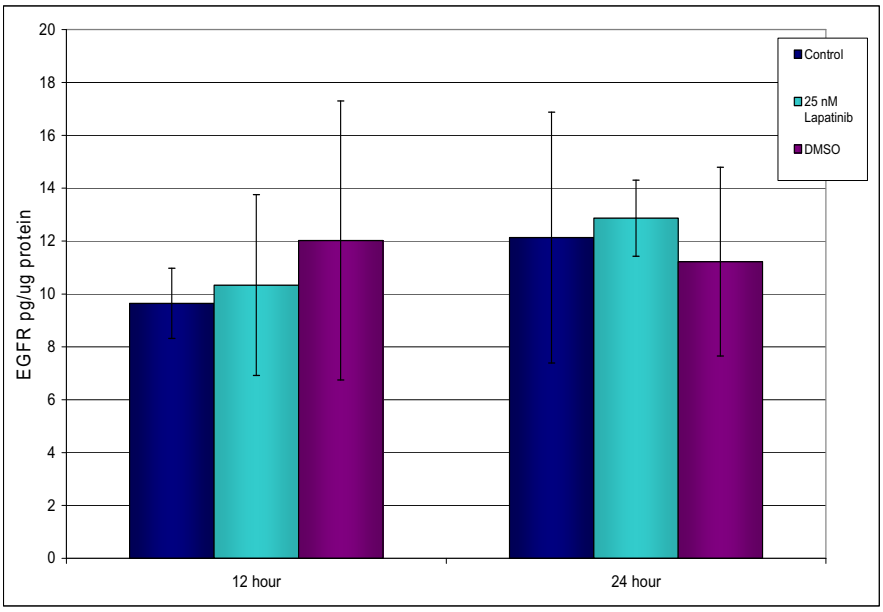

Figure 3.1.8.2 ELISA of total EGFR expression in SKBR3, following 12 and 24 hour 25 nM lapatinib treatments. Control for lapatinib treated samples was SKBR3 incubated with growth medium for 12 and 24 hours. A DMSO control containing the same quantity of DMSO as in highest lapatinib concentration was included. Experiments were performed in duplicate on biological duplicates and data represents the mean +/- range.

EGFR expression in H1299-T

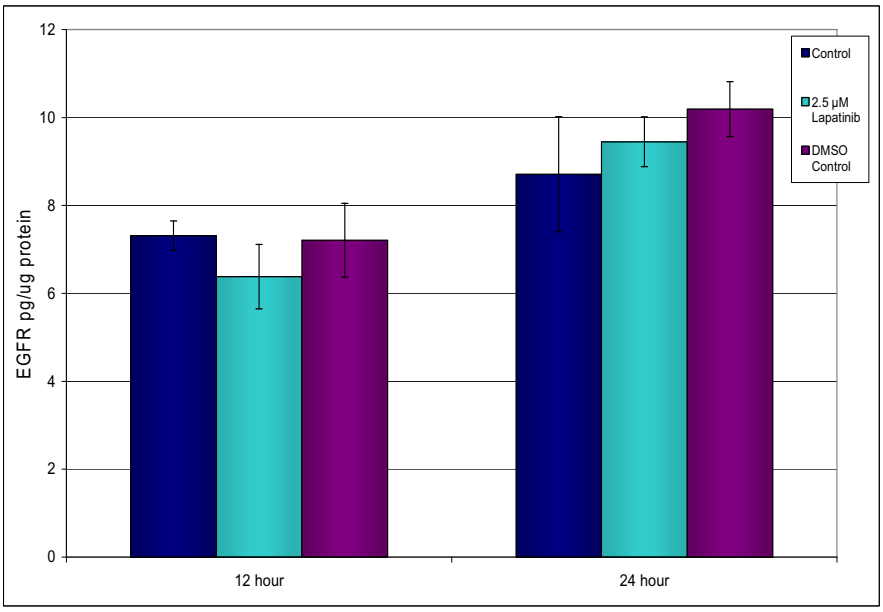

Figure 3.1.8.3 ELISA of total EGFR expression in H1299-T, following 12 and 24 hour 2.5 µM lapatinib treatments. Control for lapatinib treated samples was H1299-T incubated with growth medium for 12 and 24 hours. A DMSO control containing the same quantity of DMSO as in highest lapatinib concentration was included. Experiments were performed in duplicate on biological duplicates and data represents the mean +/- range.

Phosphorylated EGFR expression in A549-T

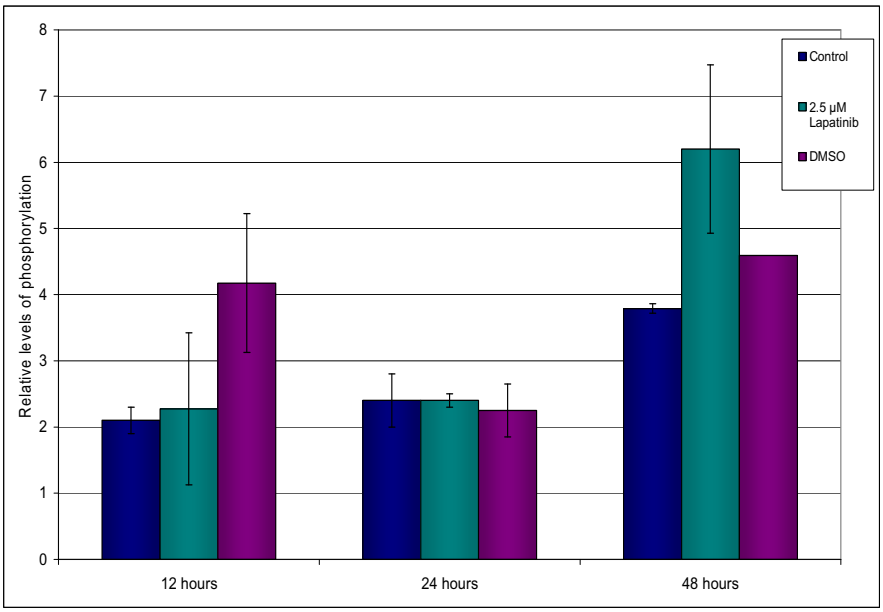

Figure 3.1.8.4 ELISA of phosphorylated EGFR expression in A549-T, following 12, 24 and 48 hour 2.5 µM lapatinib treatments. Units were expressed in terms of a quantified control. Control for lapatinib treated samples was A549-T incubated with growth medium for 12, 24 and 48 hours. A DMSO control containing the same quantity of DMSO as in highest lapatinib concentration was included. Experiments were performed in duplicate on separate samples and data represents the mean +/- range.

Phosphorylated EGFR expression in SKBR3

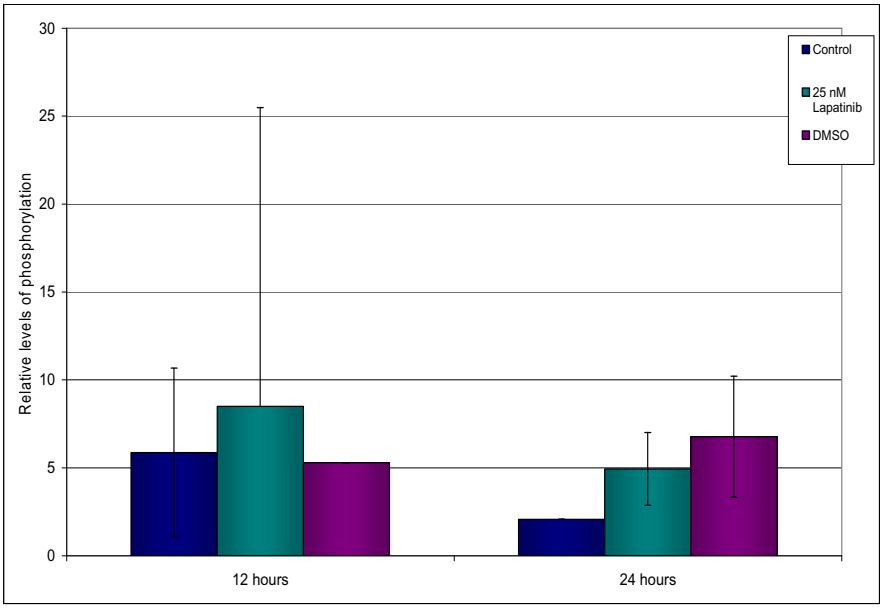

Figure 3.1.8.5 ELISA of phosphorylated EGFR expression in SKBR3, following 12 and 24 hour 2.5 µM lapatinib treatments. Units are arbitrary and were expressed in terms of a quantified control. Control for lapatinib treated samples was SKBR3 incubated with growth medium for 12 and 24 hours. A DMSO control containing the same quantity of DMSO as in highest lapatinib concentration was included. Experiments were performed in duplicate and data represents the mean +/- range.

Phosphorylated EGFR expression in H1299-T

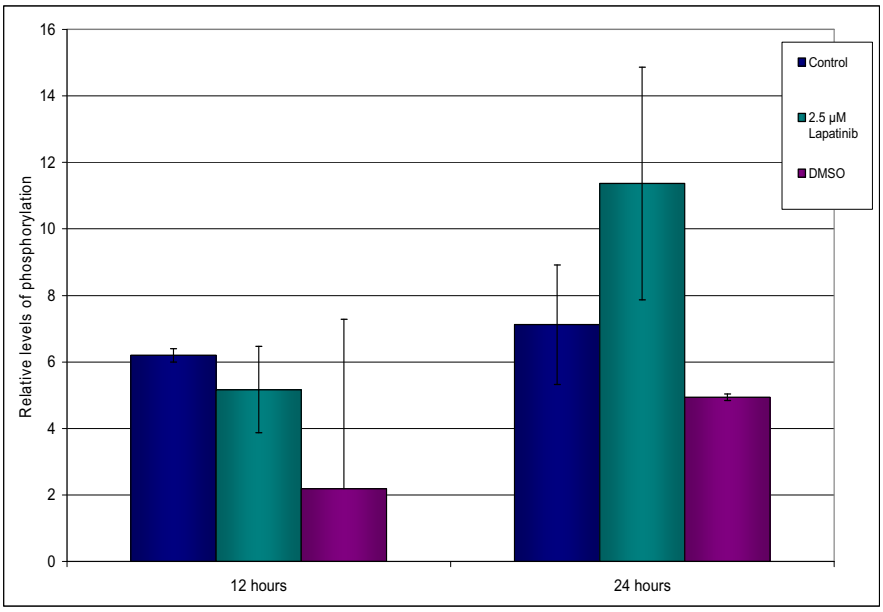

Figure 3.1.8.6 ELISA of phosphorylated EGFR expression in H1299-T, following 12 and 24 hour 2.5 µM lapatinib treatments. Units are arbitrary and were expressed in terms of a quantified control. Control for lapatinib treated samples was H1299-T incubated with growth medium for 12 and 24 hours. A DMSO control containing the same quantity of DMSO as in highest lapatinib concentration was included. Experiments were performed in duplicate and data represents the mean +/- range.

HER-2 expression in A549-T

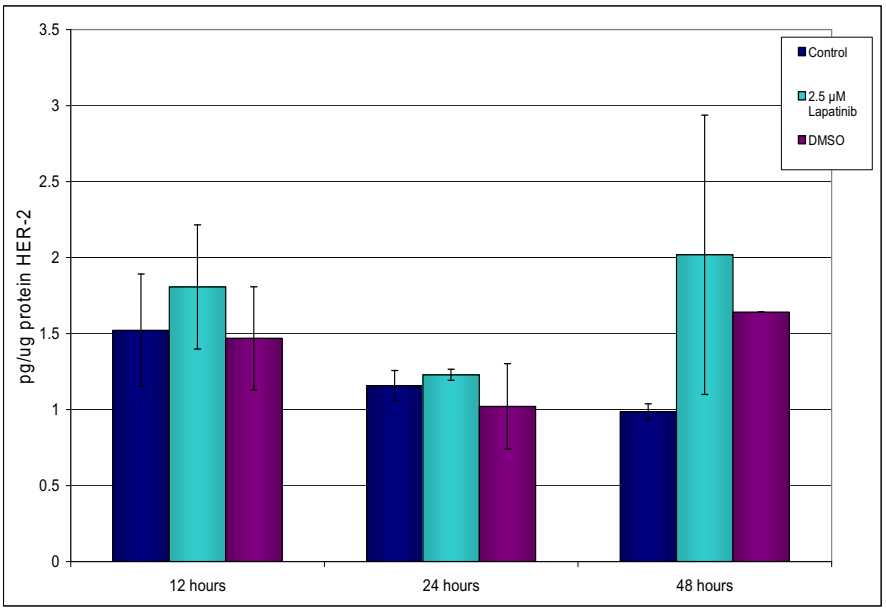

Figure 3.1.8.7 ELISA of total HER-2 expression in A549-T, following 12, 24 and 48 hour 2.5 µM lapatinib treatments. Control for lapatinib treated samples was A549-T incubated with growth medium for 12 and 24 hours. A DMSO control containing the same quantity of DMSO as in highest lapatinib concentration was included. Experiments were performed in duplicate on separate samples and data represents the mean +/- range.

HER-2 expression in SKBR3

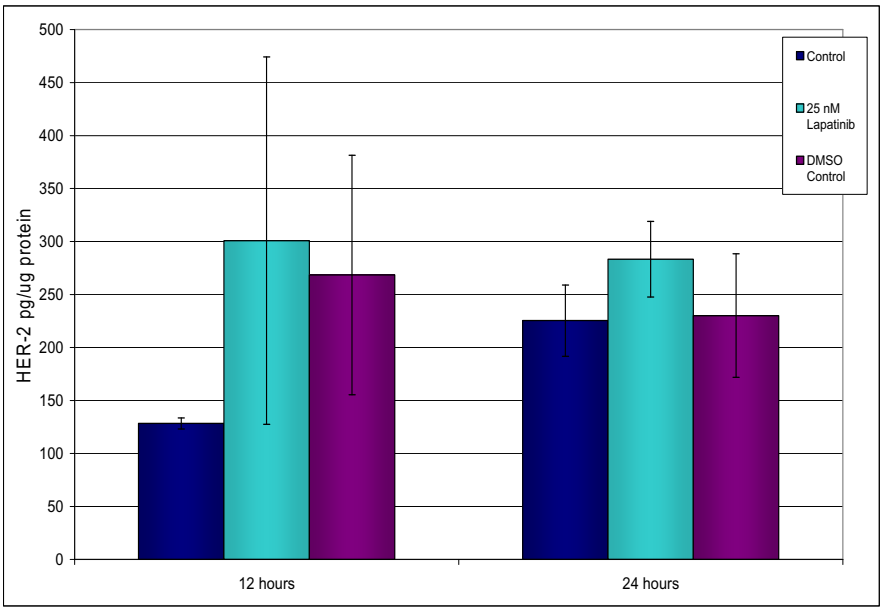

Figure 3.1.8.8 ELISA of total HER-2 expression in SKBR3, following 12 and 24 hour 2.5 μM lapatinib treatments. Control for lapatinib treated samples was SKBR3 incubated with growth medium for 12 and 24 hours. A DMSO control containing the same quantity of DMSO as in highest lapatinib concentration was included. Experiments were performed in duplicate on separate samples and data represents the mean +/- range.

Phosphorylated HER-2 expression in A549-T

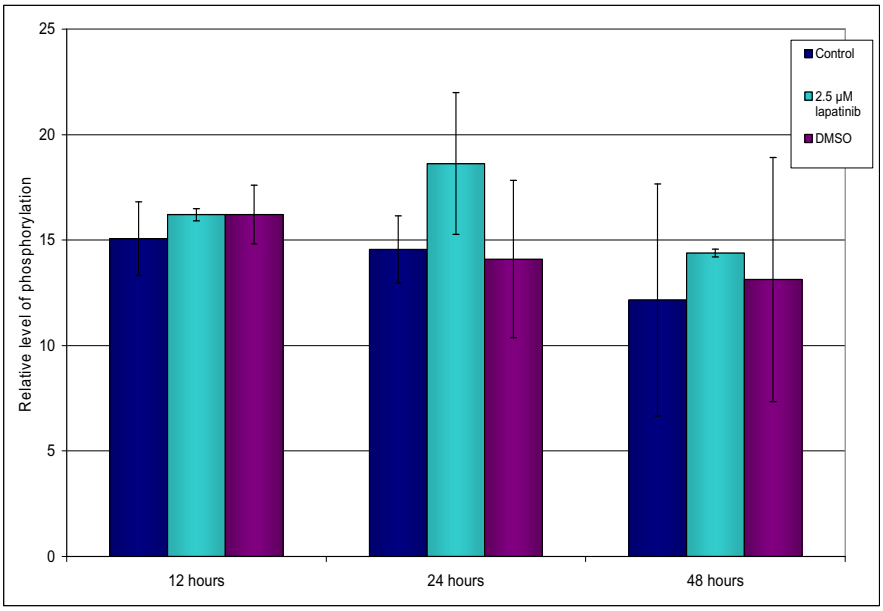

Figure 3.1.8.9 ELISA of phosphorylated HER-2 expression in A549-T, following 12, 24 and 48 hour 2.5 µM lapatinib treatments. Units are arbitrary and were expressed in terms of a quantified control. Control for lapatinib treated samples was A549-T incubated with growth medium for 12, 24 and 48 hours. A DMSO control containing the same quantity of DMSO as in highest lapatinib concentration was included. Experiments were performed in duplicate on separate samples and data represents the mean +/- range.

Phosphorylated HER-2 expression in SKBR3

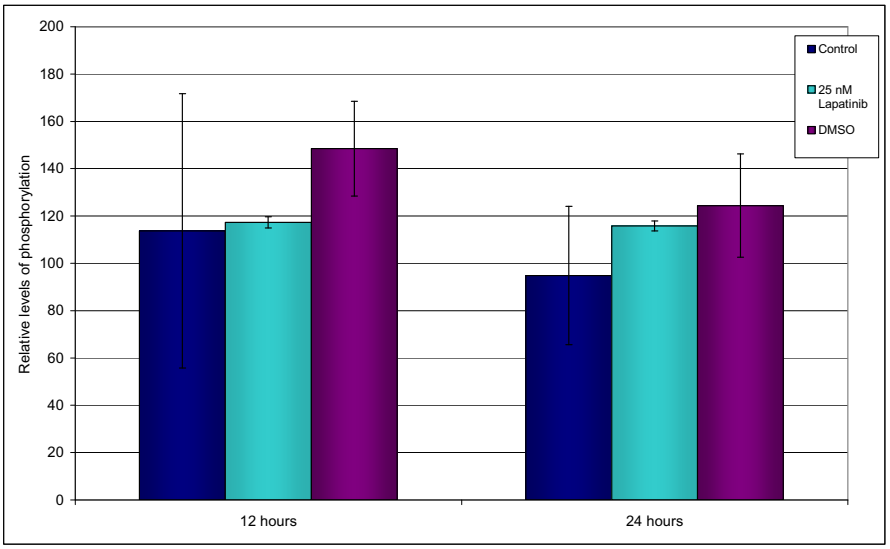

Figure 3.1.8.10 ELISA of phosphorylated HER-2 expression in SKBR3, following 12 and 24 hour 2.5 μM lapatinib treatments. Units are arbitrary and were expressed in terms of a quantified control. Control for lapatinib treated samples was SKBR3 incubated with growth medium for 12 and 24 hours. A DMSO control containing the same quantity of DMSO as in highest lapatinib concentration was included. Experiments were performed in duplicate on separate samples and data represents the mean +/- range.

3.1.9. Effect of EGF treatments on total and phosphorylated EGFR and HER-2

EGF treatments were analysed for their effects on the growth factor receptor total and phosphorylated levels. A reduction in total EGFR level was observed following 12 and 24 hour EGF treatments in A549-T as shown in figure 3.1.9.1. A downward trend was also observed in SKBR3 (figure 3.1.9.2). Due to large standard errors results cannot be drawn from phosphorylated EGFR in response to EGF treatment in A549-T or SKBR3 (figures 3.1.9.3 and 3.1.9.4).

The trend in HER-2 expression was downward in A549-T from 24 hours and in SKBR3 after 12 hours treatment with lapatinib, however, large standard errors were present (figure 3.1.9.5 and 3.1.9.6). Little change was observed in phosphorylated HER-2 in response to lapatinib (figure 3.1.9.7 and 3.1.9.8). Statistics were not carried out as data only available in duplicate.

EGFR expression in A549-T

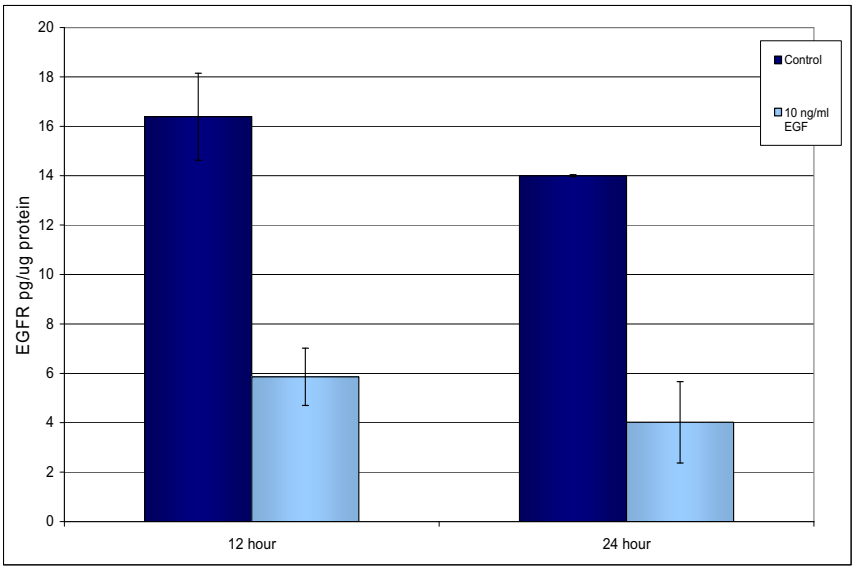

Figure 3.1.9.1 ELISA of total EGFR expression in A549-T, following 12 and 24 hour 10 ng/ml EGF treatments. EGF treatments were in serum-free medium and control was A549-T incubated with serum-free growth medium for 12 and 24 hours. Experiments were performed in duplicate on biological duplicates and data represents the mean +/- range.

EGFR expression in SKBR3

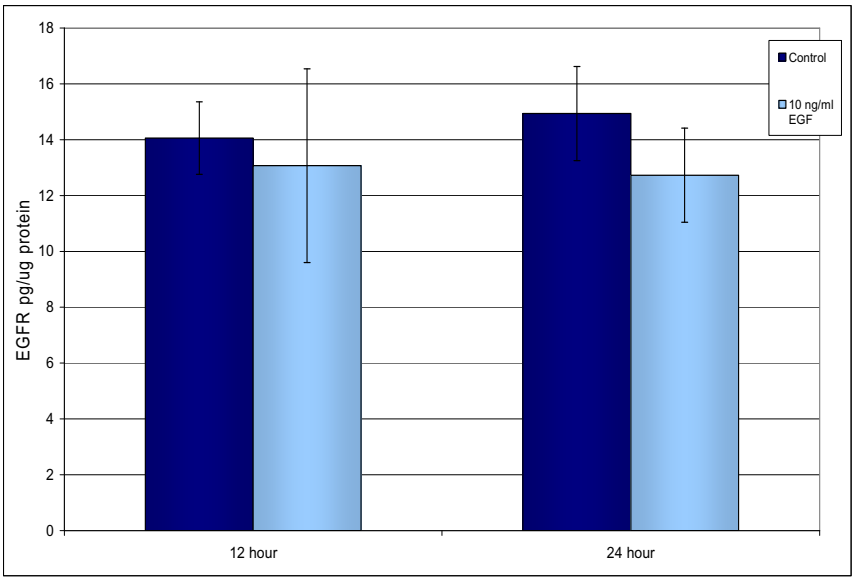

Figure 3.1.9.2 ELISA of total EGFR expression in SKBR3, following 12 and 24 hour 10 ng/ml EGF treatments. EGF treatments were in serum-free medium and control was SKBR3 incubated with serum-free growth medium for 12 and 24 hours. Experiments were performed in duplicate on biological duplicates and data represents the mean +/- range.

Phosphorylated EGFR expression in A549-T

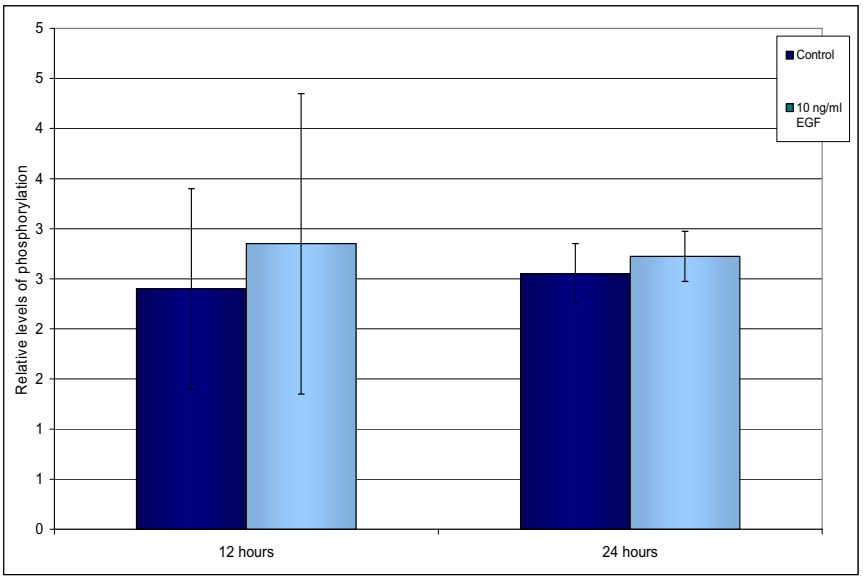

Figure 3.1.9.3 ELISA of phosphorylated EGFR expression in A549-T, following 12 and 24 hour 10 ng/ml EGF treatments. Units were expressed in terms of a quantified control. EGF treatments were in serum-free medium and control was A549-T incubated with serum-free growth medium for 12 and 24 hours. Experiments were performed in duplicate and data represents the mean +/- range.

Phosphorylated EGFR expression in SKBR3

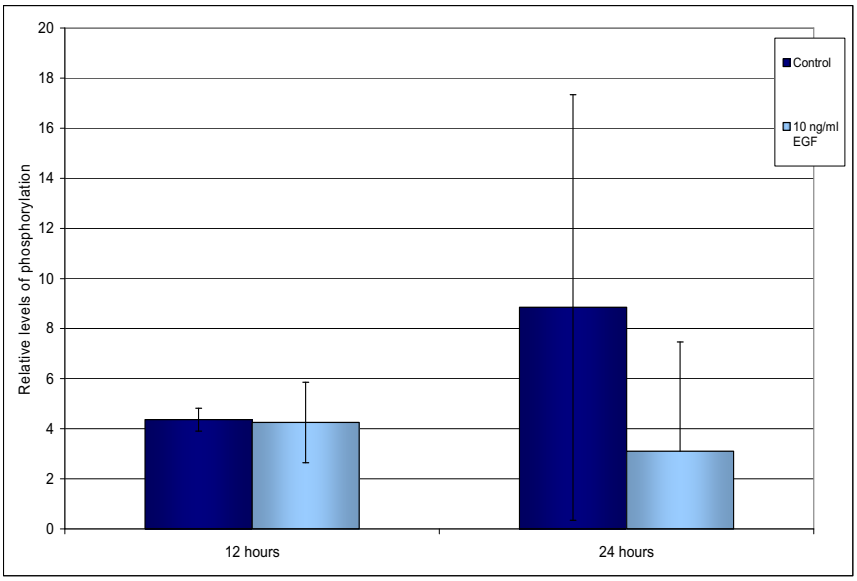

Figure 3.1.9.4 ELISA of phosphorylated EGFR expression in SKBR3, following 12 and 24 hour 10 ng/ml EGF treatments. Units were expressed in terms of a quantified control. EGF treatments were in serum-free medium and control was SKBR3 incubated with serum-free growth medium for 12 and 24 hours. Experiments were performed in duplicate and data represents the mean +/- range.

HER-2 expression in A549-T

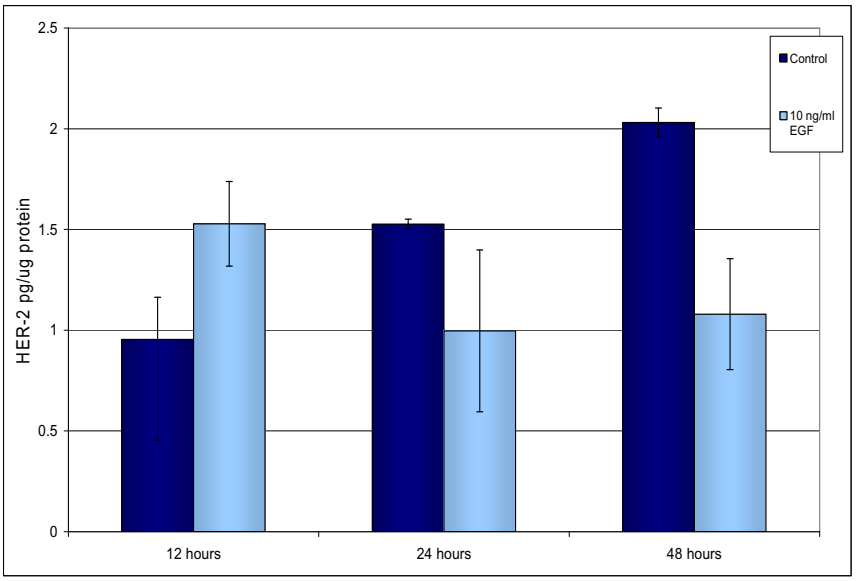

Figure 3.1.9.5 ELISA of total HER-2 expression in A549-T, following 12, 24 and 48 hour 10 ng/ml EGF treatments. EGF treatments were in serum-free medium and control was A549-T incubated with serum-free growth medium for 12, 24 and 48 hours. Experiments were performed in duplicate on biological duplicates and data represents the mean +/- range.

HER-2 expression in SKBR3

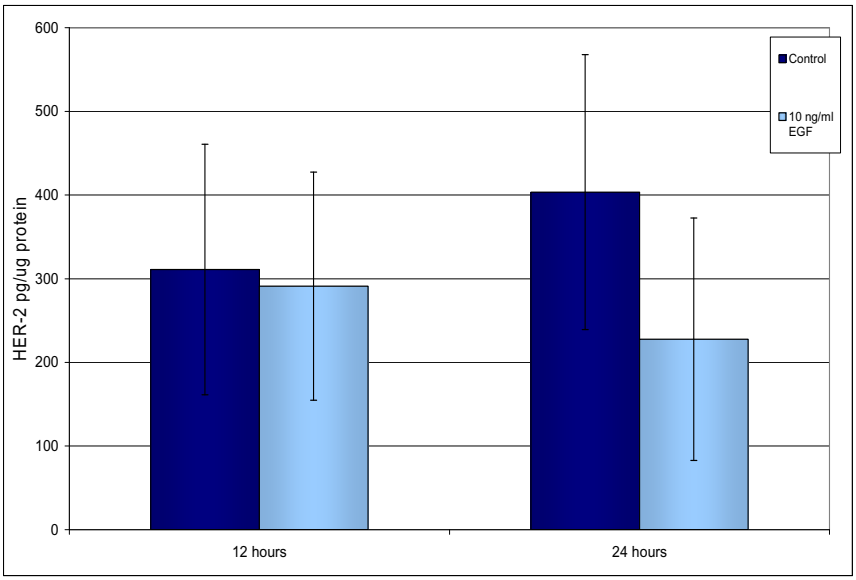

Figure 3.1.9.6 ELISA of total HER-2 expression in SKBR3, following 12 and 24 hour 10 ng/ml EGF treatments. Units are arbitrary and were expressed in terms of a quantified control. EGF treatments were in serum-free medium and control was SKBR3 incubated with serum-free growth medium for 12 and 24 hours. Experiments were performed in duplicate on biological duplicates and data represents the mean +/- range.

Phosphorylated HER-2 expression in A549-T

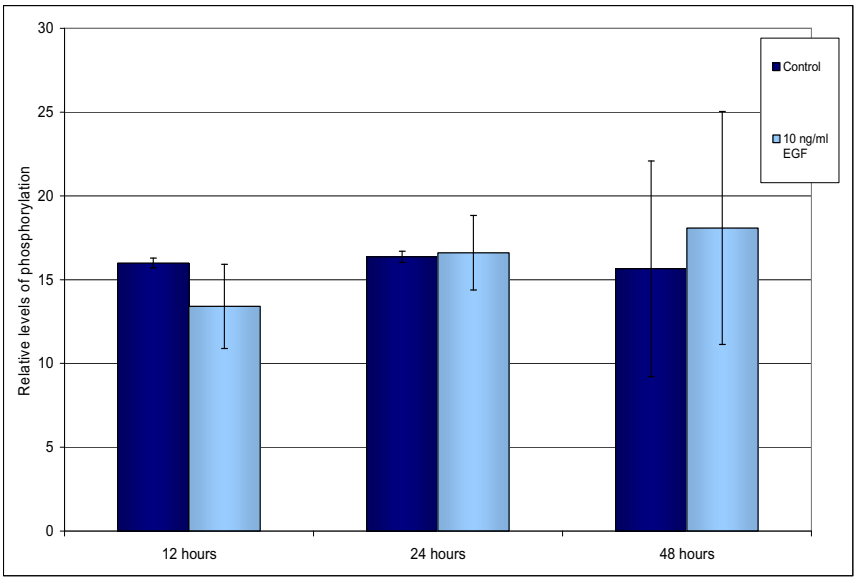

Figure 3.1.9.7 ELISA of phosphorylated HER-2 expression in A549-T, following 12, 24 and 48 hour 10 ng/ml EGF treatments. Units were expressed in terms of a quantified control. EGF treatments were in serum-free medium and control was A549-T incubated with serum-free growth medium for 12, 24 and 48 hours. Experiments were performed in duplicate on biological duplicates and data represents the mean +/- range.

Phosphorylated HER-2 expression in SKBR3

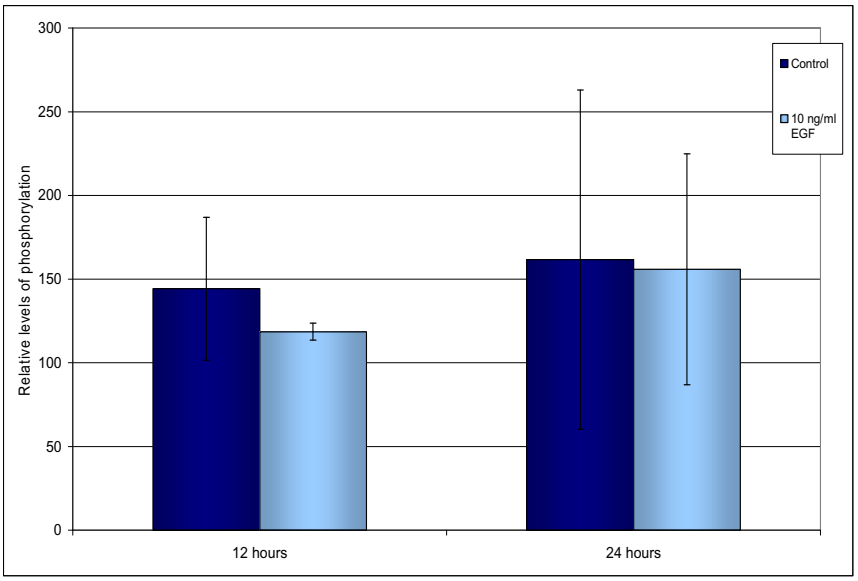

Figure 3.1.9.8 ELISA of phosphorylated HER-2 expression in SKBR3, following 12 and 24 hour 10 ng/ml EGF treatments. Units were expressed in terms of a quantified control. EGF treatments were in serum-free medium and control was SKBR3 incubated with serum-free growth medium for 12 and 24 hours. Experiments were performed in duplicate on biological duplicates and data represents the mean +/- range.

3.1.10. Persistence of lapatinib-induced increase in P-gp expression

Further assays were carried out in order to establish if the increase in P-gp protein expression caused by lapatinib was of a transient or more persistent nature. A549-T cells were treated for 48 hours with 2.5 μM and 5 μM lapatinib, following which the drug was removed and replaced with growth medium. Protein samples were taken and analysed for P-gp expression at various time points after lapatinib removal. A similar assay was also set up with 1 μM lapatinib treatments. In both of these assays P-gp remained up regulated up to 120 hours following P-gp removal as seen in figures 3.1.10.1 and 3.1.10.2. A clear increase in lapatinib was observed in response to 2.5 μM and 5 μM treatments at 24, 48, 72 and 120 hours with the exception of the 5 μM treatment at 72 hours. Increased P-gp expression also remained constant at 24, 96 and 120 hours following the removal of 1 μM lapatinib. This would indicate the effect lapatinib is having on P-gp expression is not transient.

Levels of lapatinib in the A549-T cells were also quantified by mass spectrometry at the various time points following the removal of 1μM treatments, in order to evaluate if lapatinib was remaining in the cells and therefore continuing to cause the increase in P-gp expression by presence alone. Figure 3.1.10.3 shows how the levels of lapatinib were below 500 ng per million cells 120 hours following the removal of a 48 hour 1 μM lapatinib treatment in the A549-T cells. It is difficult, however, to translate this to a concentration and decipher if this level is biologically active in these cells.

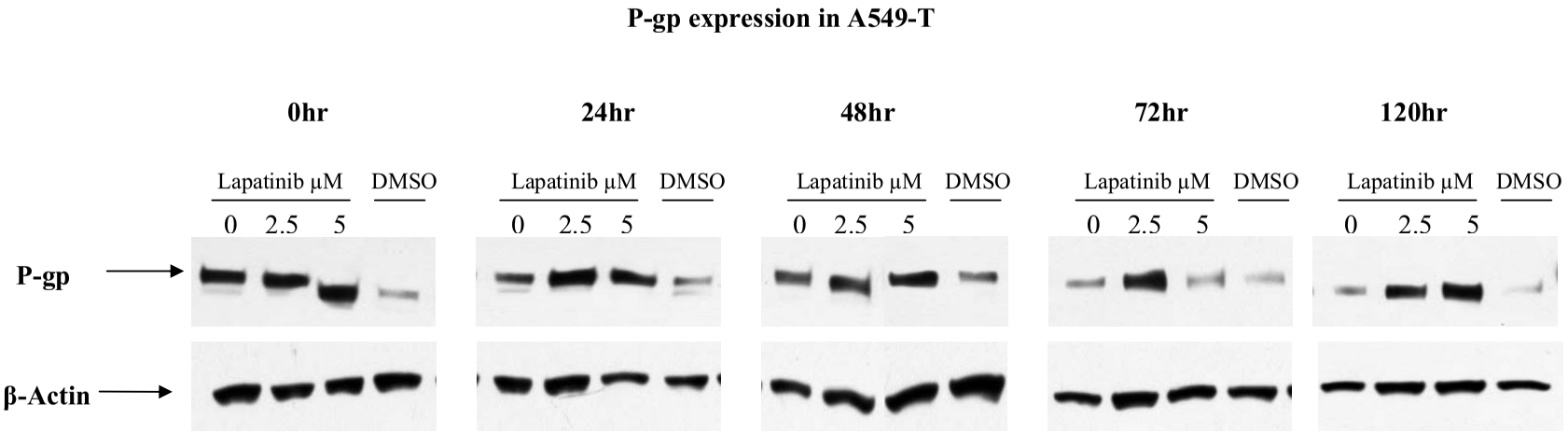

Figure 3.1.10.1 Western blot of P-gp expression subsequent to 48 hours exposure to 2.5 µM and 5 µM lapatinib in A549-T. 0hrs represents the time at which the lapatinib was removed from A549-T and P-gp expression was analysed at 24, 48, 72 and 120 hours after this point. Control was A549-T cells incubated with growth medium for each respective time point hours. A DMSO control containing the same quantity of DMSO as in highest lapatinib concentration was included.

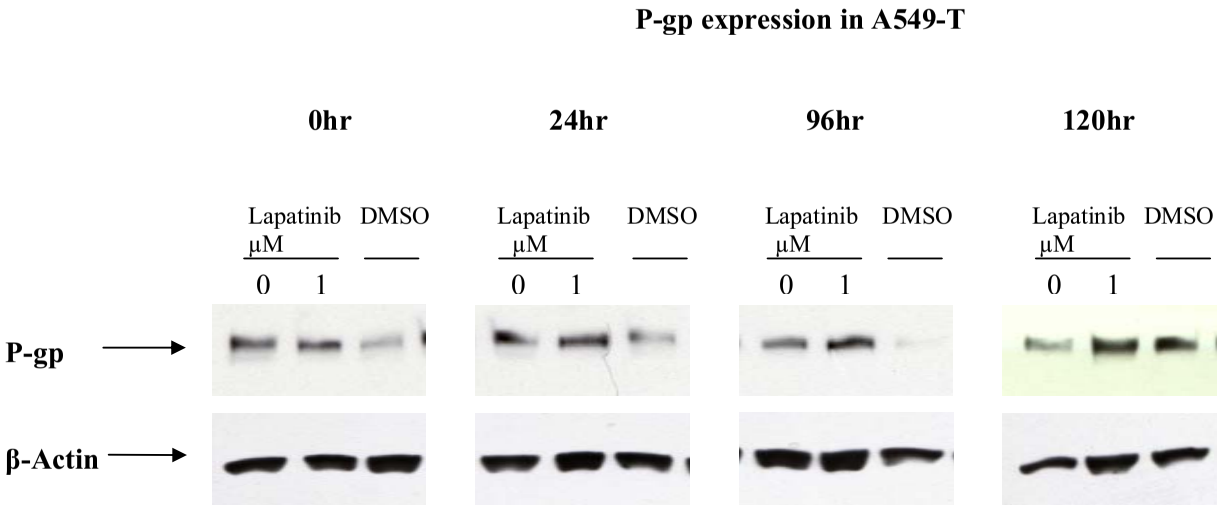

Figure 3.1.10.2 Western blot of P-gp expression subsequent to 48 hours exposure to 1 µM lapatinib in A549-T. 0hrs represents the time at which the lapatinib was removed from A549-T and P-gp expression was analysed at 24, 96 and 120 hours after this point. Control was A549-T cells incubated with growth medium for each respective time point hours. A DMSO control containing the same quantity of DMSO as in highest lapatinib concentration was included.

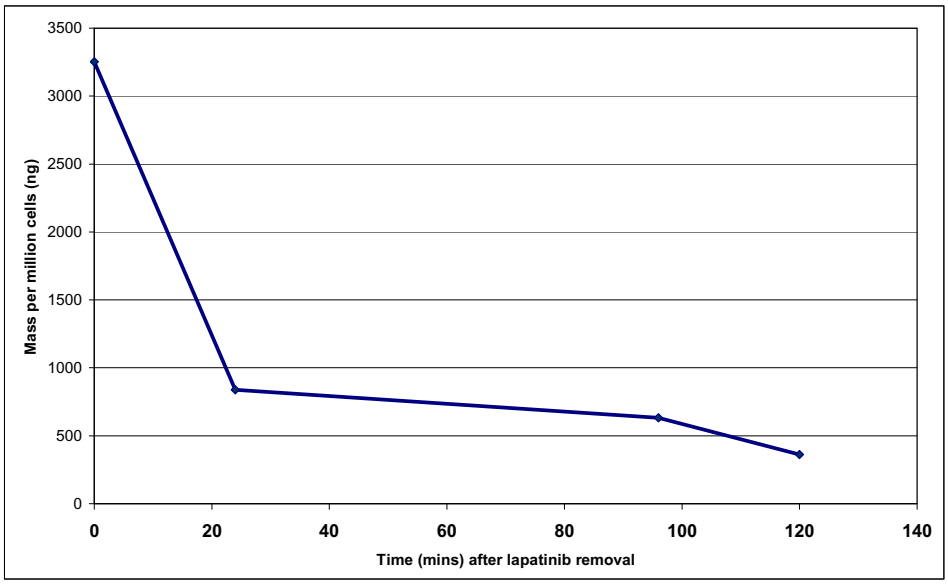

Figure 3.1.10.3 Lapatinib quantification in A549-T subsequent to 48 hour exposure to 1 μM lapatinib. 0 hours represents the time at which lapatinib was removed and samples were analysed at 24, 96 and 120 hours after this. The quantification was carried out using an LC-MS method on single samples.

3.1.11. Effect of lapatinib-induced increase and EGF-induced decrease of P-gp expression on chemotherapy accumulation and efflux

The increased expression of P-gp induced by lapatinib has the potential to have a negative impact on chemotherapy drug sensitivity. This was investigated firstly by carrying out accumulation and efflux assays. Epirubicin accumulation and efflux was determined in the A549-T cells, following a 48 hour treatment with 2.5 μM lapatinib. Epirubicin was quantified using an LCMS method. The accumulation data show a decrease in accumulation in epirubicin after 120 mins in the cells treated with lapatinib (figure 3.1.11.1). No great difference in epirubicin efflux was observed in lapatinib-treated cells compared with control and after 120 minutes the quantity of drug in the cells across all conditions was of a similar level (figure 3.1.11.2). To examine if any effect was observed in a cell line with a greater expression of P-gp, an efflux assay was carried out in DLKP-A. Again, although there was a difference in initial accumulation, after 120 minutes the levels of epirubicin were similar in the lapatinib treated DLKP-A cells as in control (figure 3.1.11.3). Following the same logic, the decrease in expression of P-gp observed with EGF might result in a decreased efflux of chemotherapy drugs. This was analysed in DLKP-A, and results demonstrated that the 50ng/ml EGF treatment had little bearing on the efflux of epirubicin as shown in figure 3.1.11.4.

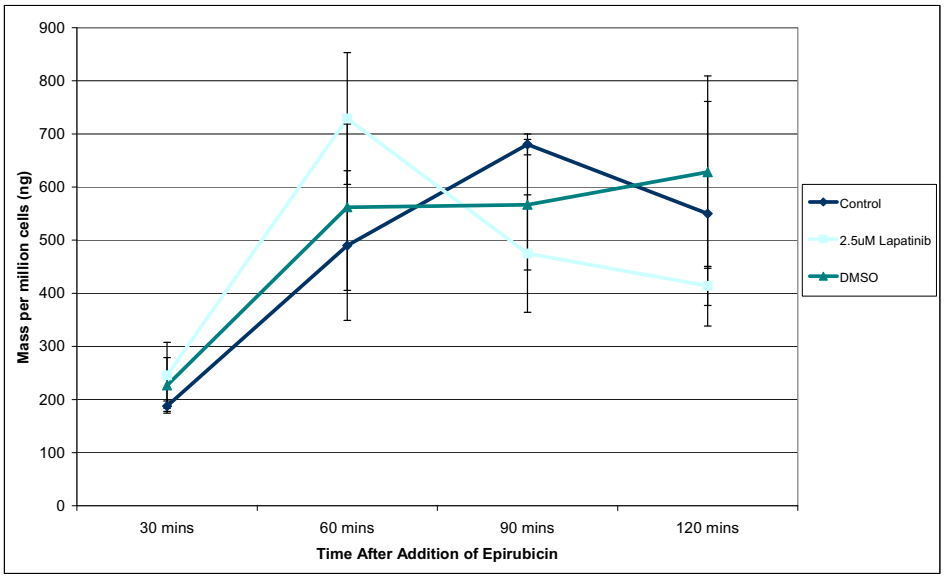

Figure 3.1.11.1 Epirubicin accumulation in A549-T cells following 48 hour treatment with 2.5 μM lapatinib. A549-T cells were incubated with 2 μM epirubicin and samples were analysed at 30, 60, 90 and 120 minutes for epirubicin accumulation. A DMSO control containing the same quantity of DMSO as in highest lapatinib concentration was included. Data are mean +/- SD of triplicate experiments.

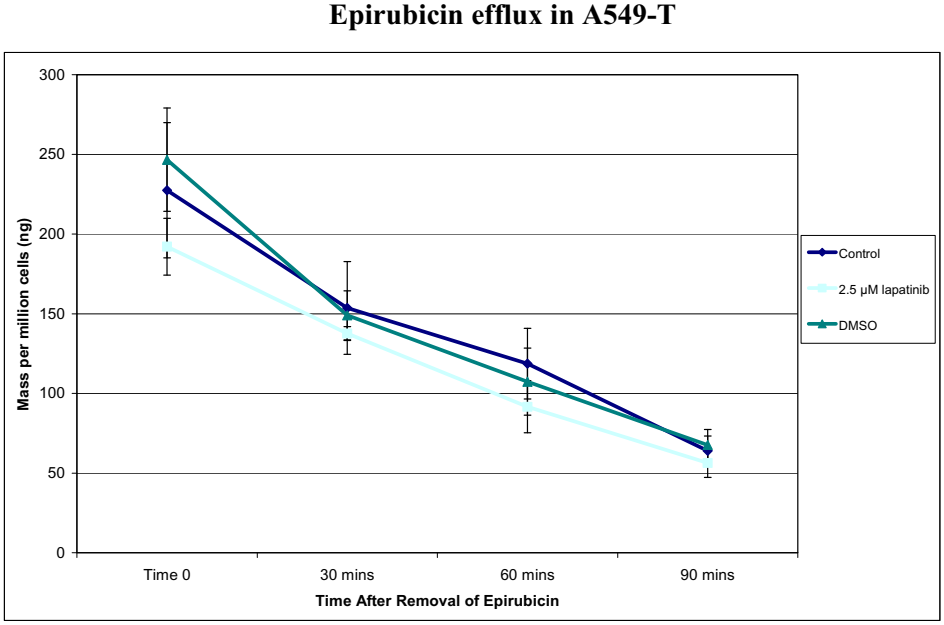

Figure 3.1.11.2 Epirubicin efflux in A549-T cells following 48 hour treatment with 2.5 µM lapatinib. A549-T cells were incubated with 2 µM epirubicin for 2 hours at which time drug was removed. Samples were analysed at 30, 60, 90 and 120 minutes after removal of drug for epirubicin efflux. A DMSO control containing the same quantity of DMSO as in highest lapatinib concentration was included. Data are mean +/- SD of triplicate experiments.

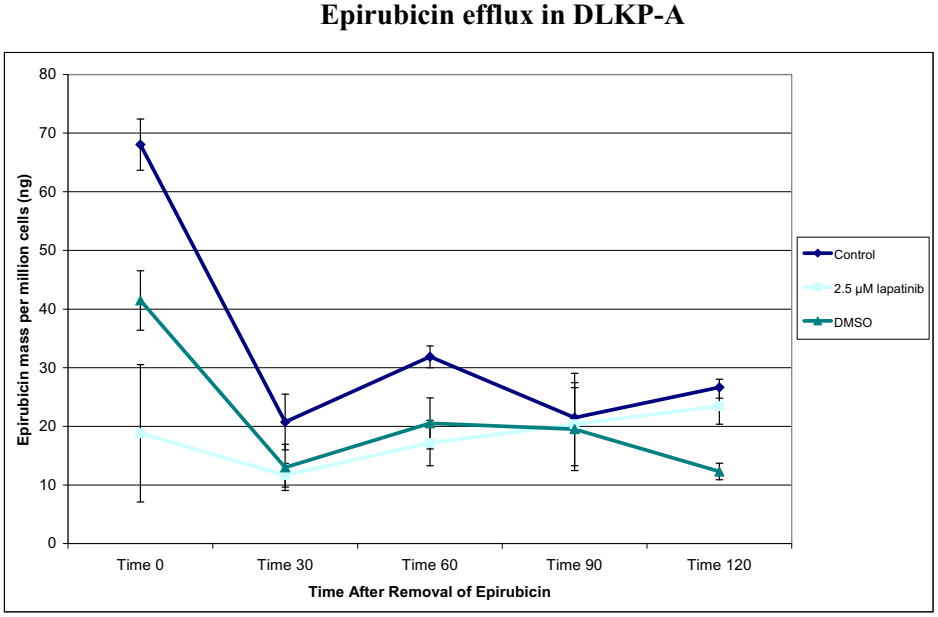

Figure 3.1.11.3 Epirubicin efflux in DLKP-A cells following 48 hour treatment with 2.5 µM lapatinib. DLKP-A cells were incubated with 2 µM epirubicin for 2 hours at which time drug was removed. Samples were analysed at 30, 60, 90 and 120 minutes after removal of drug for epirubicin efflux. A DMSO control containing the same quantity of DMSO as in highest lapatinib concentration was included. Data are mean +/- SD of triplicate experiments.

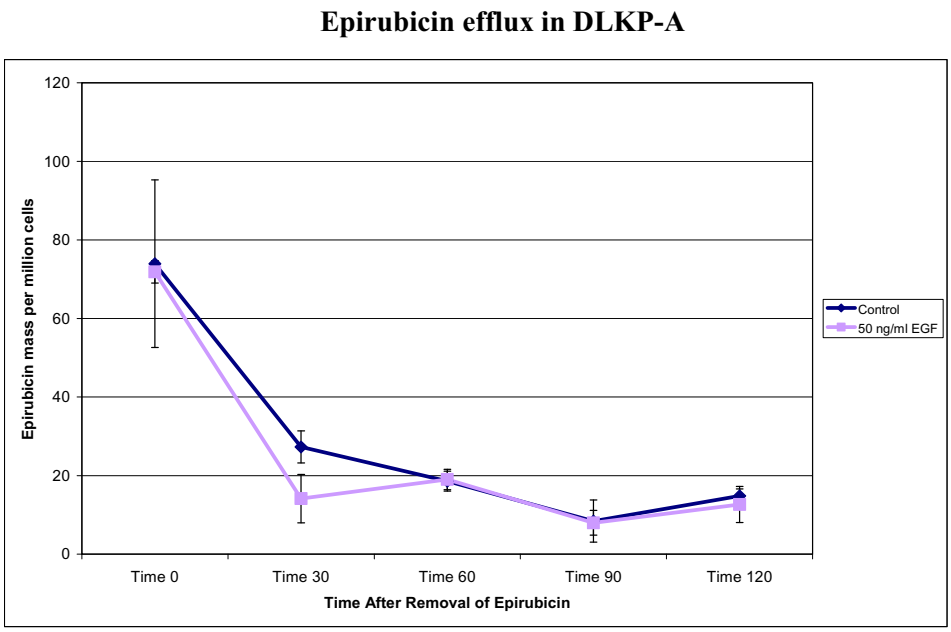

Figure 3.1.11.4 Epirubicin efflux in DLKP-A cells following 48 hour treatment with 50 ng/ml EGF. DLKP-A cells were incubated with 2 μM epirubicin for 2 hours at which time drug was removed. Samples were analysed at 30, 60, 90 and 120 minutes after removal of drug for epirubicin efflux. A DMSO control containing the same quantity of DMSO as in highest lapatinib concentration was included. Data are mean +/- SD of triplicate experiments.

3.1.12. Effect of lapatinib-induced increase and EGF-induced decrease in P-gp expression on chemotherapy sensitivity

To examine if the increased P-gp expression observed in response to lapatinib affected chemotherapy drug sensitivity, toxicity assays were carried out in A549-T. Cells were treated for 48 hours with 2.5 μM lapatinib after which a 72 hour toxicity assay was carried with either, paclitaxel, docetaxel or the non-P-gp substrate drug, 5-fluorouracil. No major change in sensitivity was observed in these toxicity assays. A decrease in survival was observed in lapatinib pre-treated cells, however, this also occurred in the control and so the effect was classed as additive (figure 3.1.12.1 – 3.1.12.3). To further investigate this additional toxicity assays were carried out under slightly different conditions.

In order to reduce the chances of residual lapatinib, from the pre-treatment, having an effect on the cell drug sensitivity, the concentration of lapatinib used was reduced to 1 μM and a washout period of 24 hours was included in the assay. A combination of the chemotherapy drug with 1 μM lapatinib was also carried out alongside the pre-treatments so that a direct comparison could be made between pre- and co-treatments with lapatinib. These results again showed that pre-treatment with lapatinib had no negative impact on chemotherapy drug sensitivity with paclitaxel and epirubicin showing an additive effect on toxicity (figure 3.1.12.4 – 3.1.12.5). The results also showed that co-treatment achieved synergistic toxicity in line with earlier data.

EGF treatments were shown to decrease levels of the drug pumps P-gp and MRP1 in A549-T and so toxicity assays investigating the effect of this reduction on chemotherapy drug sensitivity were also carried out. The EGF treatments indicate a downward trend in toxicity to paclitaxel and docetaxel in the A549-T (figures 3.1.12.6 – 3.1.12.9).

Proliferation assay in A549-T

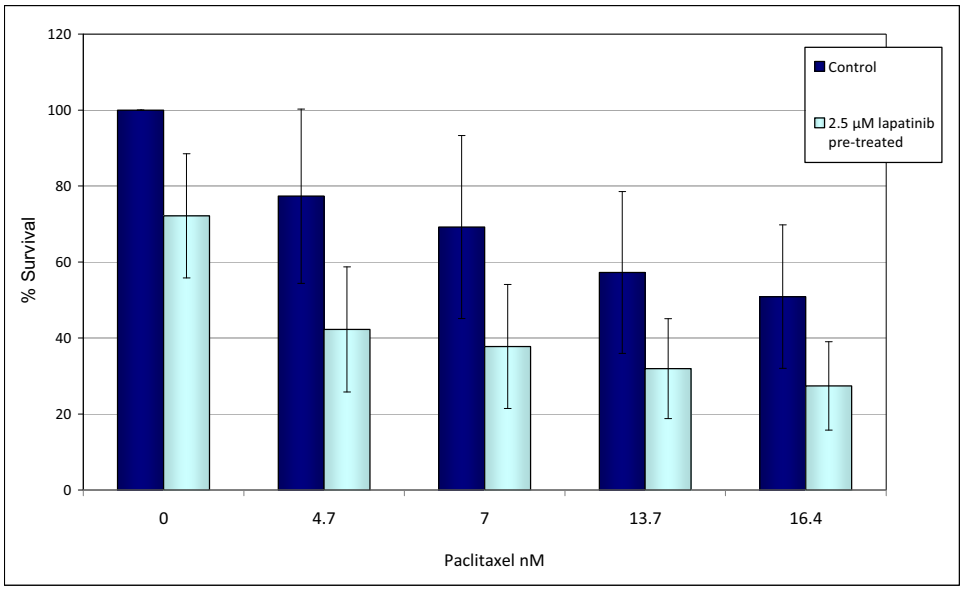

Figure 3.1.12.1 % cell survival in A549-T as determined by acid phosphatase assay in response to a three day treatment of paclitaxel in lapatinib pre-treated A549-T cells. The pre-treated cells were exposed to 2.5 µM lapatinib for 48 hours. Data are mean +/- SD of triplicate experiments.

Proliferation assay in A549-T

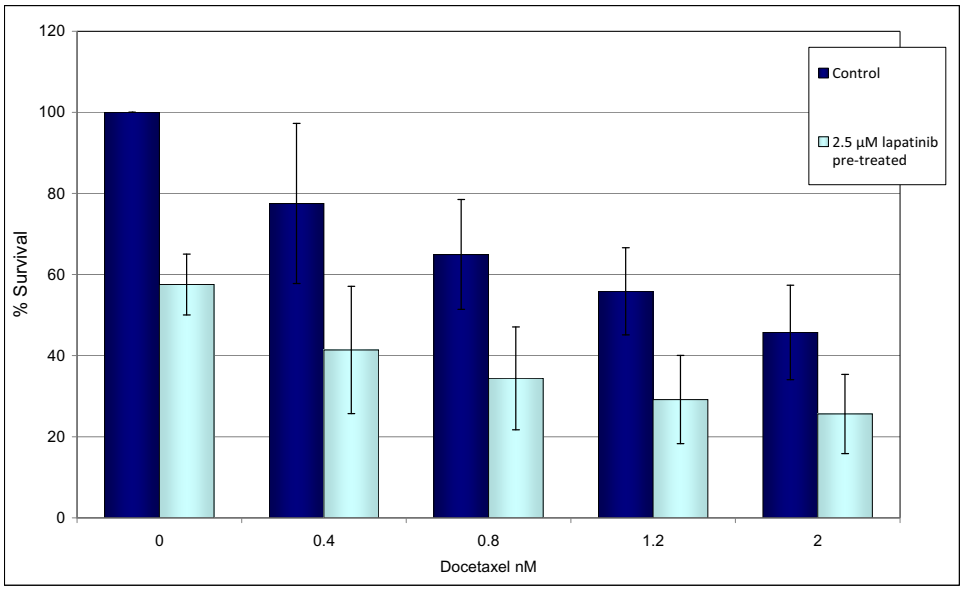

Figure 3.1.12.2 % cell survival in A549-T as determined by acid phosphatase assay in response to a three day treatment of docetaxel in lapatinib pre-treated A549-T cells. The pre-treated cells were exposed to 2.5 µM lapatinib for 48 hours. Data are mean +/- SD of triplicate experiments.

Proliferation assay in A549-T

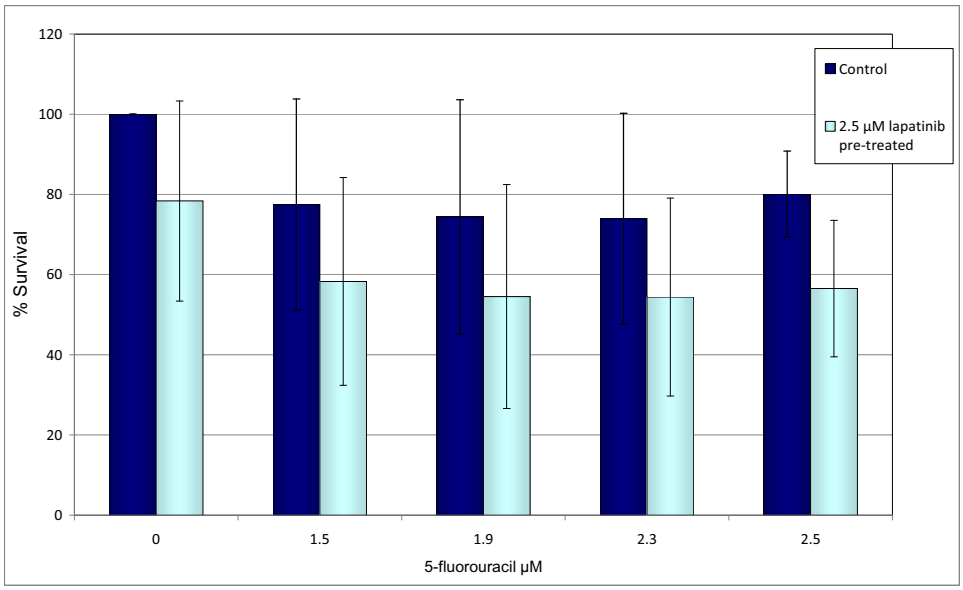

Figure 3.1.12.3 % cell survival in A549-T as determined by acid phosphatase assay in response to a three day treatment of 5-fluorouracil in lapatinib pre-treated A549-T cells. The pre-treated cells were exposed to 2.5 µM lapatinib for 48 hours. Data are mean +/- SD of triplicate experiments.

Proliferation assay in A549-T

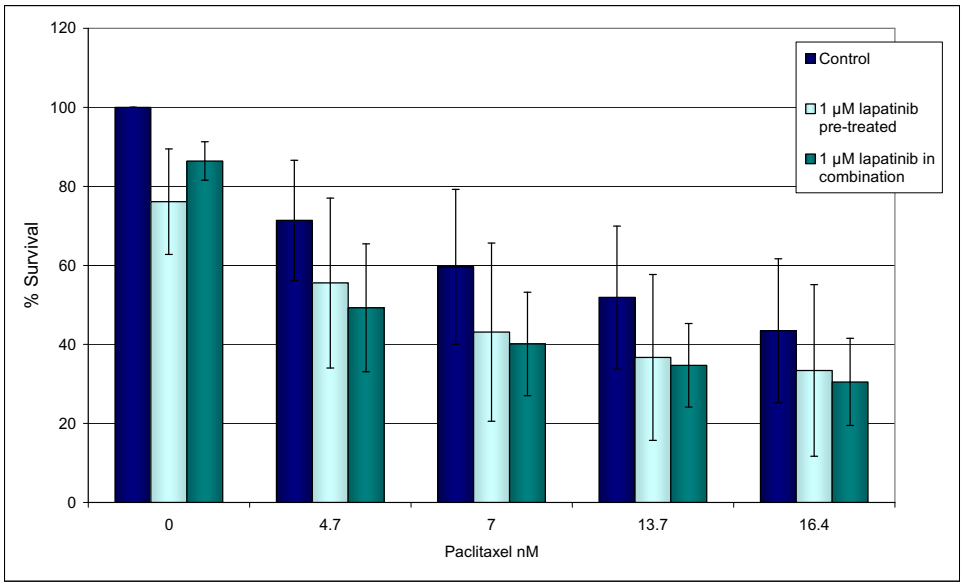

Figure 3.1.12.4 % cell survival in A549-T as determined by acid phosphatase assay in response to a three day treatment of paclitaxel either, in lapatinib pre-treated A549-T cells or in combination with 1 μM lapatinib in A549-T. The pre-treated cells were exposed to 1 μM lapatinib for 48 hours and a 24 hour washout period is allowed before chemotherapy drug is added. Data are mean +/- SD of triplicate experiments.

Proliferation assay in A549-T

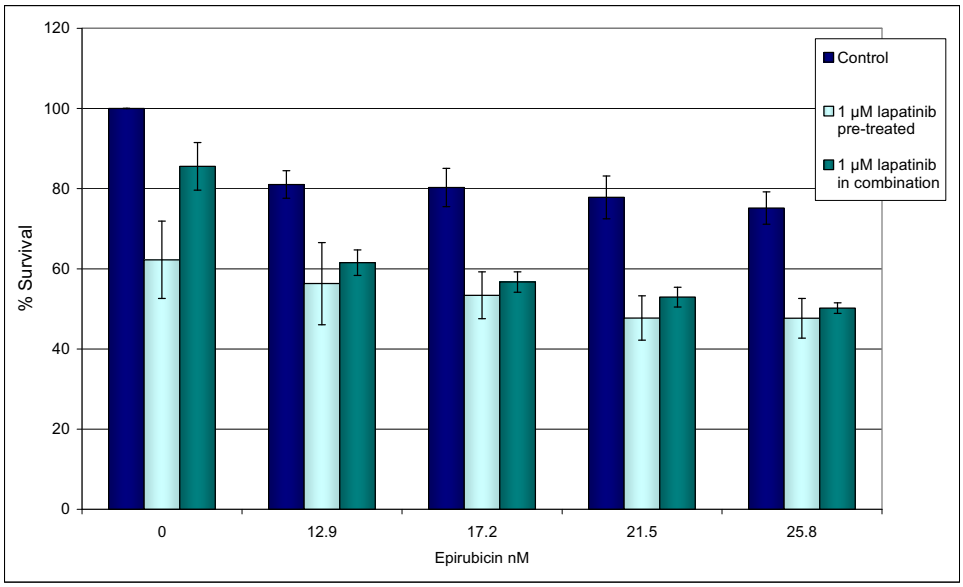

Figure 3.1.12.5 % cell survival in A549-T as determined by acid phosphatase assay in response to a three day treatment of epirubicin, either, in lapatinib pre-treated A549-T cells or in combination with 1 μM lapatinib in A549-T. The pre-treated cells were exposed to 1 μM lapatinib for 48 hours and a 24 hour washout period is allowed before chemotherapy drug is added. Data are mean +/- SD of triplicate experiments.

Proliferation assay in A549-T

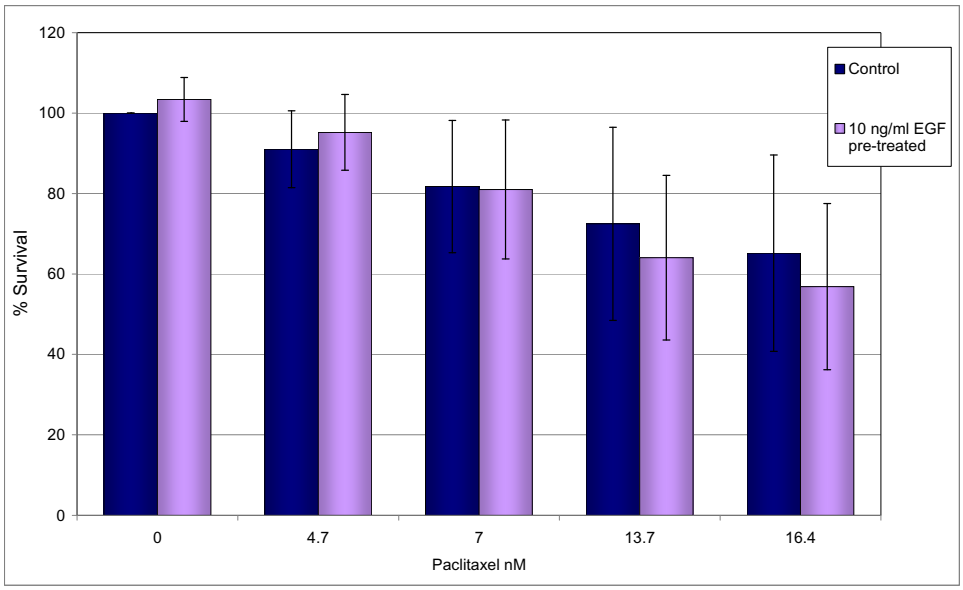

Figure 3.1.12.6 % cell survival in A549-T as determined by acid phosphatase assay in response to a three day treatment of 5-fluorouracil in EGF pre-treated A549-T cells. The pre-treated cells were exposed to 10 ng/ml EGF for 48 hours. Data are mean +/- SD of triplicate experiments.

Proliferation assay in A549-T

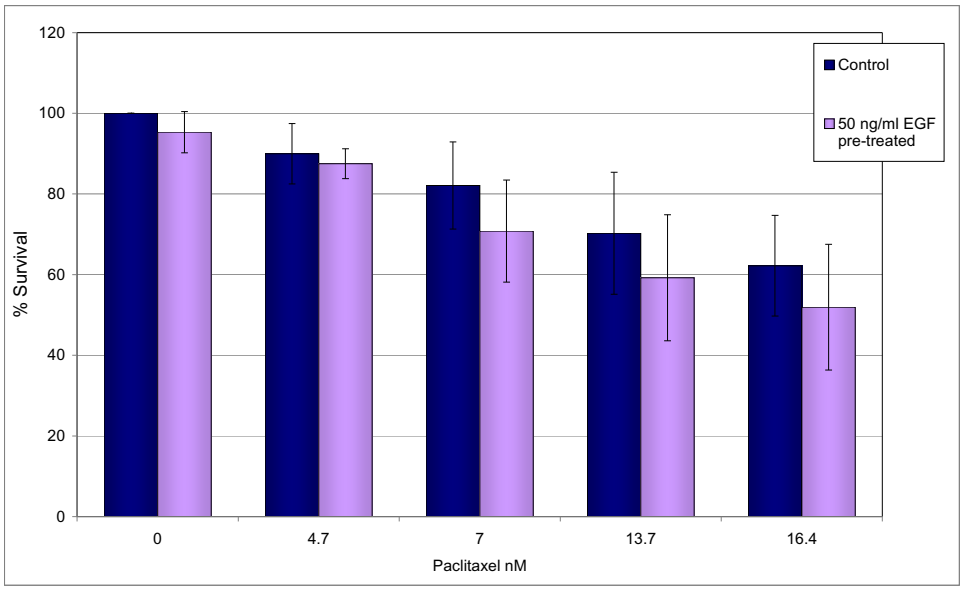

Figure 3.1.12.7 % cell survival in A549-T as determined by acid phosphatase assay in response to a three day treatment of paclitaxel in EGF pre-treated A549-T cells. The pre-treated cells were exposed to 50 ng/ml EGF for 48 hours. Data are mean +/- SD of triplicate experiments.

Proliferation assay in A549-T

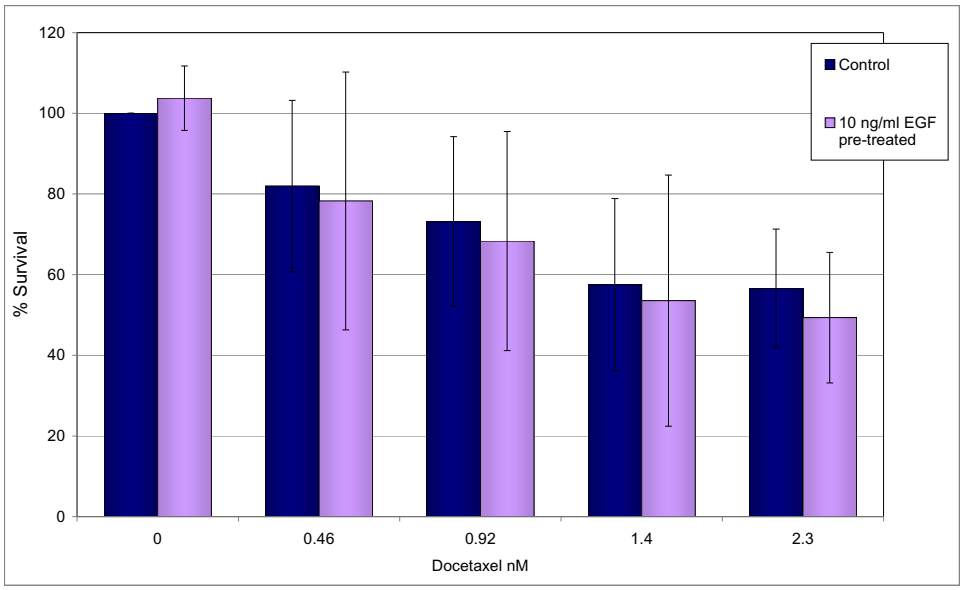

Figure 3.1.12.8 % cell survival in A549-T as determined by acid phosphatase assay in response to a three day treatment of docetaxel in EGF pre-treated A549-T cells. The pre-treated cells were exposed to 10 ng/ml EGF for 48 hours. Data are mean +/- SD of triplicate experiments.

Proliferation assay in A549-T

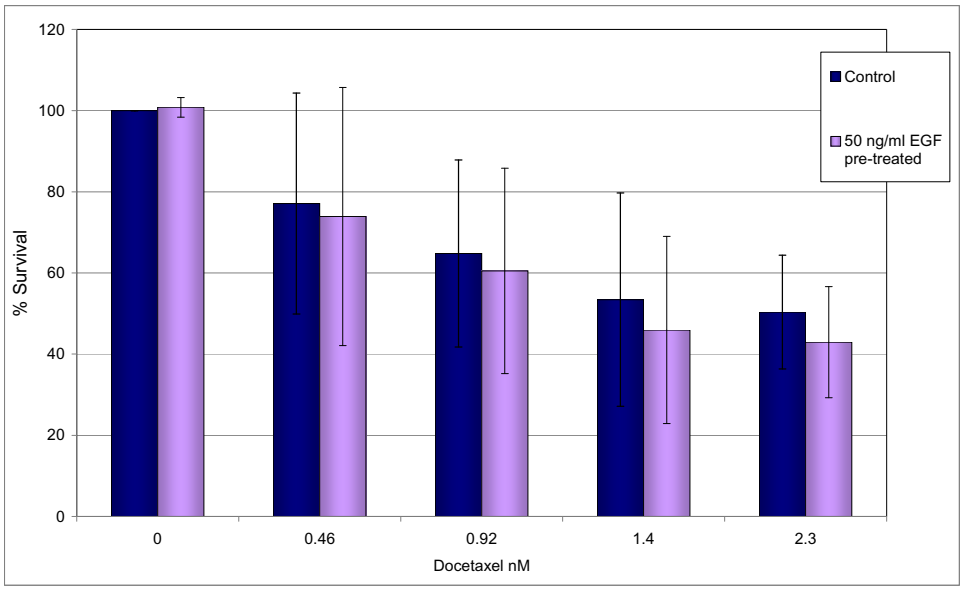

Figure 3.1.12.9 % cell survival in A549-T as determined by acid phosphatase assay in response to a three day treatment of docetaxel in EGF pre-treated A549-T cells. The pre-treated cells were exposed to 50 ng/ml EGF for 48 hours. Data are mean +/- SD of triplicate experiments.

3.1.13. Investigating the nature of lapatinib induction of P-gp expression

The data from section 3.1.9 indicate that the up-regulated P-gp may have no toxicological consequences. Further experiments were therefore carried out to check that the increased expression was a real phenomenon. The effect of lapatinib treatment on P-gp expression when added to A549-T cell lysates was determined. As can be seen in figure 3.1.13.1 no change in P-gp levels were observed across all of the time points and conditions. An early time course of 2.5 μM treatments was carried out and results are shown in figure 3.1.13.2. This was to determine if the increase in P-gp expression compared with control was observed at a time unreasonable to the process of protein turnover. An increase is observed at 8 hours and to a lesser extent at 12 hours, however, the largest increase was seen at 24 hours. Protein synthesis and degradation is substantially reduced at 4º C and so the activity of lapatinib on P-gp expression was examined at this temperature compared with controls at 37º C [167]. An increase in P-gp expression compared with control was observed in response to 2.5 μM lapatinib as expected at 37º C but not at 4º C (figure 3.1.13.3).

P-gp expression in A549-T

(a)

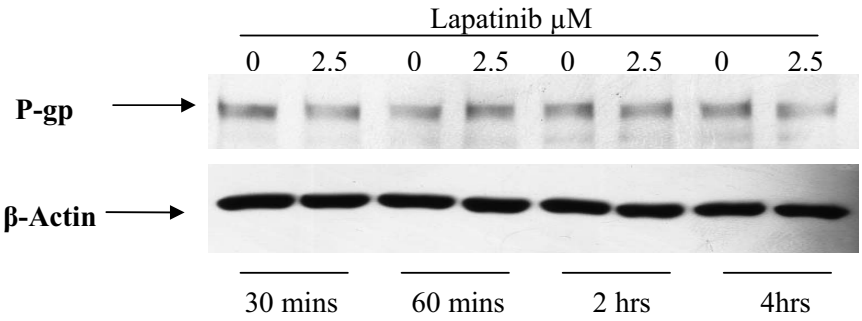

(b)

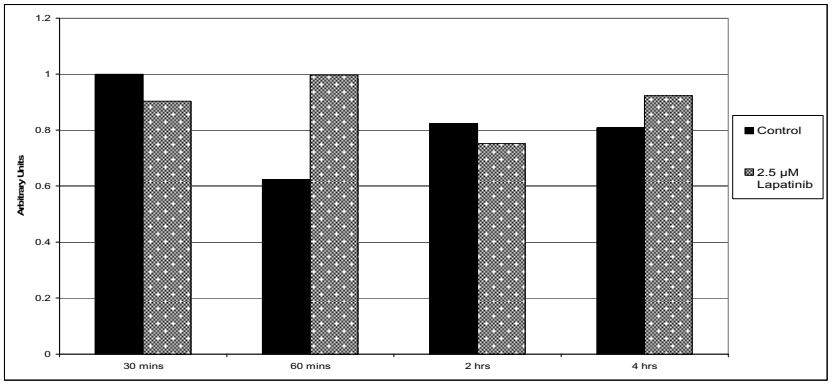

Figure 3.1.13.1 (a) Western blot of P-gp expression with (b) densitometry following treatments with 2.5 μM lapatinib in A549-T cell lysates. The lysates which were on ice during treatment were frozen to -80ºC at 30 minutes, 60 minutes, 2 hours and 4 hours to terminate treatment. Controls were A549-T cell lysates, allowed to sit on ice for the corresponding duration to the lapatinib samples.

P-gp expression in A549-T

(a)

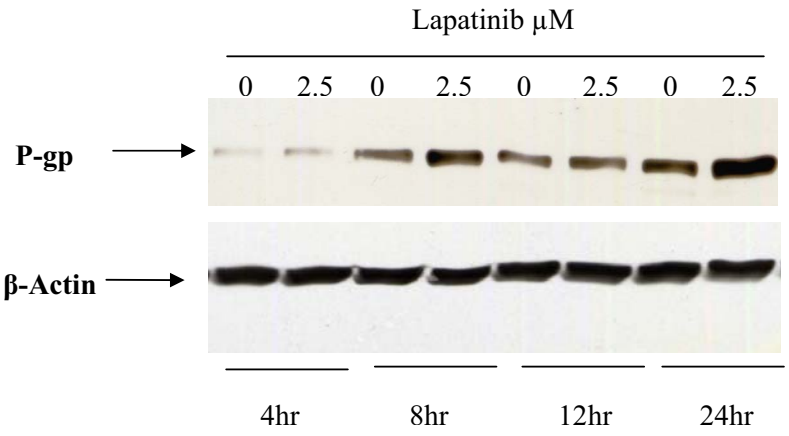

(b)

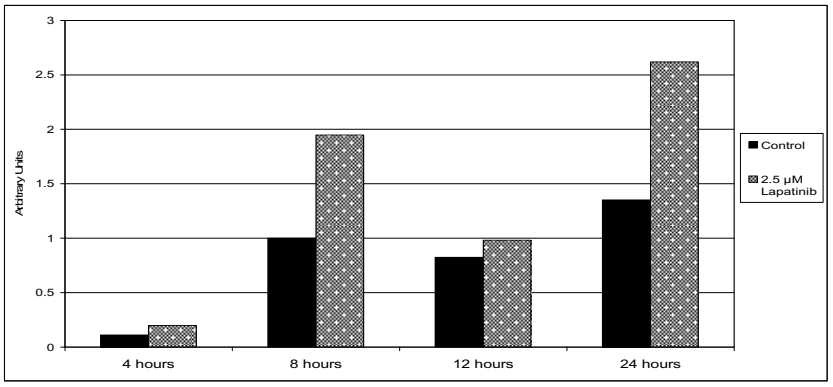

Figure 3.1.13.2 (a) Western blot of P-gp expression with (b) densitometry following 4, 8, 12 and 24 hours treatments with 2.5 μM lapatinib in A549-T. Control was A549-T cells incubated with growth medium for each time point.

P-gp expression in A549-T

(a)

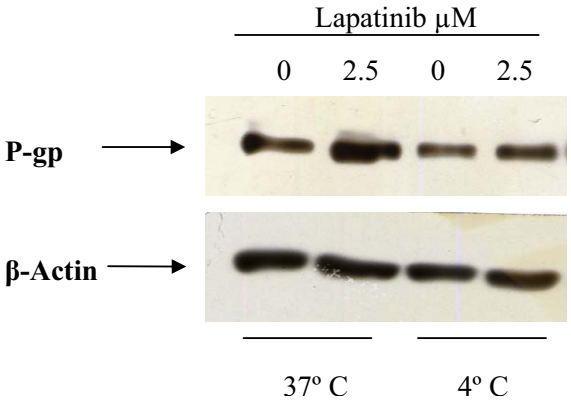

(b)

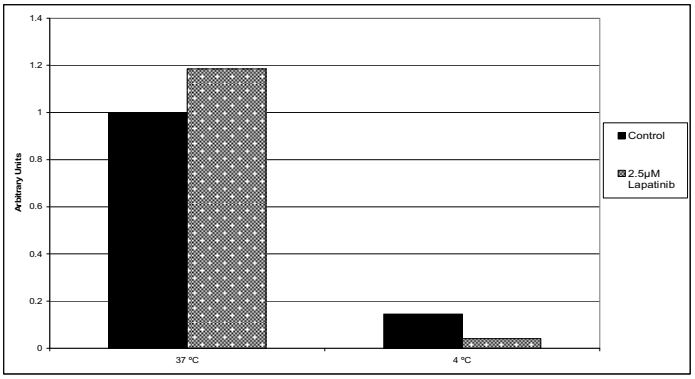

Figure 3.1.13.3 (a) Western blot of P-gp expression with (b) densitometry following 24 hours treatments of 2.5 μM lapatinib in A549-T incubated at 4ºC and 37 ºC. Control was A549-T cells incubated with growth medium at 4 ºC and 37 ºC.

3.1.14. Examination of the mechanism involved in lapatinib-induced increase in P-gp protein

RT-PCR analysis demonstrated little change in ABCB1 levels with lapatinib treatment, indicating the lapatinib effect on P-gp expression is post-translational. Western blot analysis examined P-gp expression, following co-treatment with lapatinib and either the protein synthesis inhibitor cycloheximide or degradation inhibitor bortezomib [168, 169]. Figure 3.1.14.1 illustrates how bortezomib treatment alone caused an increase in P-gp level and the co-treatment with lapatinib and bortezomib resulted in an even greater increase in the P-gp expression. Cycloheximide treatment did not alter the P-gp protein level and the co-treatment with lapatinib and cycloheximide abolished the increase in P-gp observed with lapatinib treatment alone as shown in figure 3.1.14.2.

Experiments were carried out to investigate if the lapatinib-induced increase and EGF-induced decrease of P-gp expression were dependent on growth factor receptor signalling. Previously it was determined in section 3.1.5 that lapatinib starts to induce P-gp expression from concentrations of 0.25 μM and EGF exerts its effects from 2ng/ml. In this section it was established if the increase in P-gp seen with this lapatinib concentration coincided with an increase or decrease in downstream signalling intermediates in the EGFR/HER-2 signalling pathway. Western blots were carried out to determine AKT and MAPK expression following lapatinib and EGF treatments. Lapatinib treatments caused little alteration in AKT expression with the exception of the 10 μM concentration which induced a 1.4-fold increase as determined by densitometry (figure 3.1.14.4). Alterations were observed in MAPK levels with lapatinib, however, the trend was not consistent with the P-gp protein expression increase observed. An increase in MAPK was observed with 0.1 μM, 0.25 μM, 1 μM and 10 μM, with no changes observed at 0.5 μM and 2.5 μM lapatinib (figure 3.1.14.5). Phosphorylated AKT appeared to be up-regulated by lapatinib treatment; however, similarly this did not correlate to the changes observed in P-gp protein levels (3.1.14.7). Phosphorylated MAPK was not detected in any of the A549-T samples. 10 ng/ml EGF treatments resulted in a decreased expression of both AKT and MAPK, however, no change in either of these proteins was observed at 2 ng/ml. Levels of phosphorylated AKT, in addition to phosphorylated MAPK, were not detected in any of the EGF treated samples.

P-gp expression in A549-T

(a)

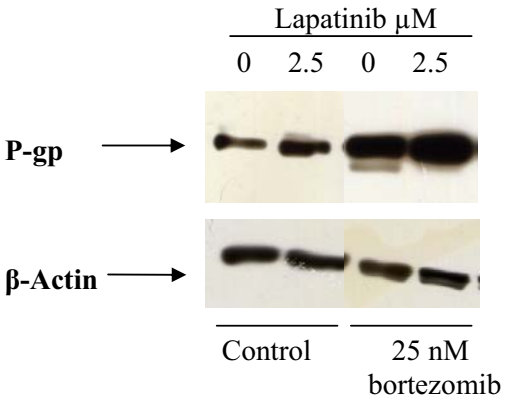

(b)

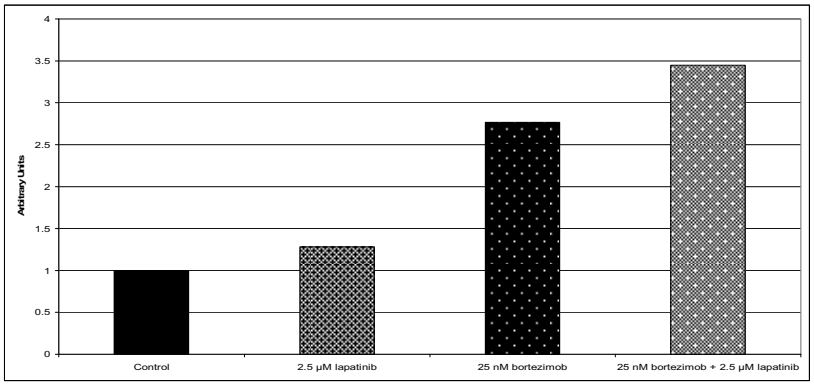

Figure 3.1.14.1 (a) Western blot of P-gp expression with (b) densitometry following 24 hour 2.5 µM lapatinib treatments in A549-T with and without 25nM bortezomib. Control was A549-T cells incubated with growth medium for 24 hours. A bortezomib control of A549-T cells incubated with 25nM bortezomib for 24 hours was also included.

P-gp expression in A549-T

(a)

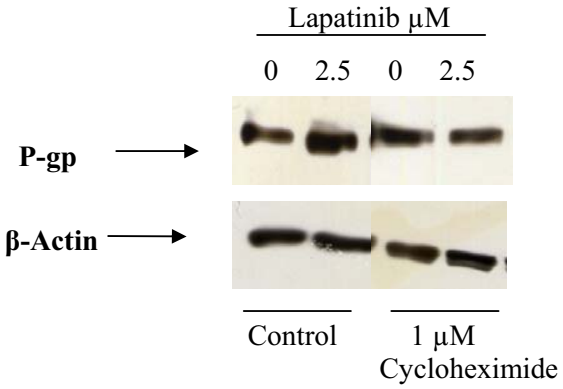

(b)

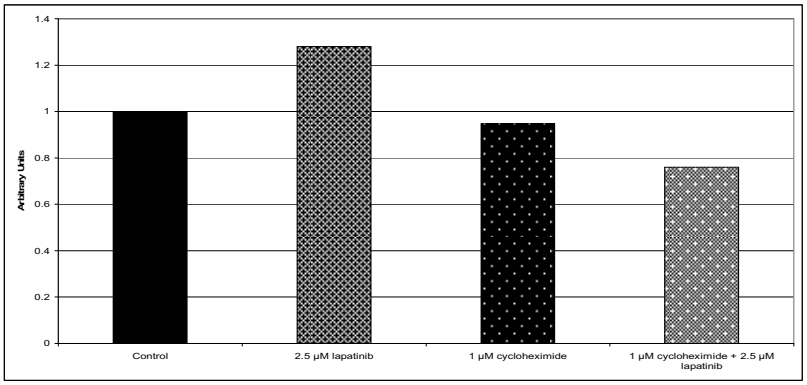

Figure 3.1.14.2 (a) Western blot of P-gp expression with (b) densitometry following 24 hour 2.5 µM lapatinib treatments in A549-T with and without 1 µM cycloheximide. Control was A549-T cells incubated with growth medium for 24 hours. A cycloheximide control of A549-T cells incubated with 1 µM cycloheximide for 24 hours was also included.

AKT expression in A549-T

(a)

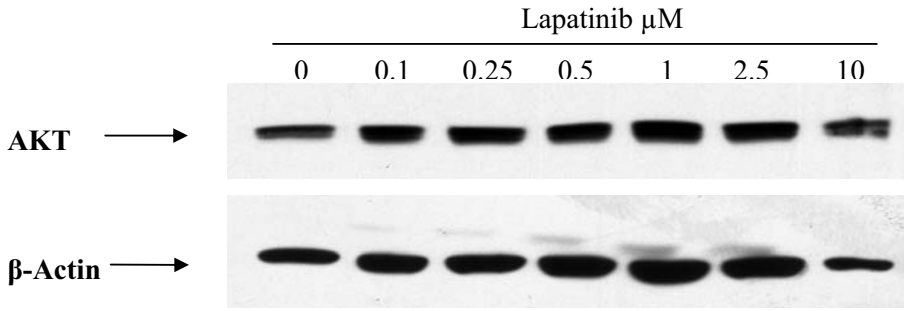

(b)

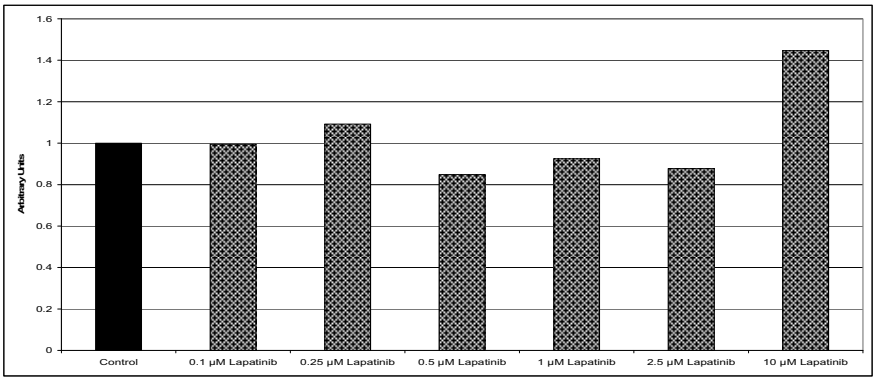

Figure 3.1.14.3 (a) Western blot of AKT expression with (b) densitometry following 48 hour 0.1 μM, 0.25 μM, 0.5 μM, 1 μM, 2.5 μM and 10 μM lapatinib treatments in A549-T. Control was A549-T cells incubated with growth medium for 48 hours.

AKT expression in A549-T

(a)

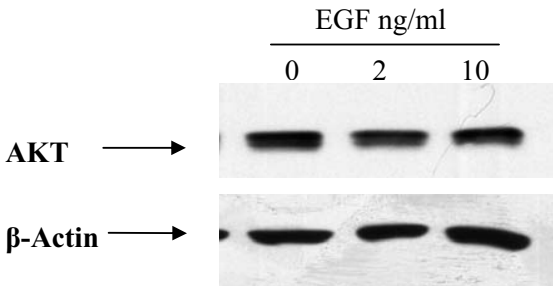

(b)

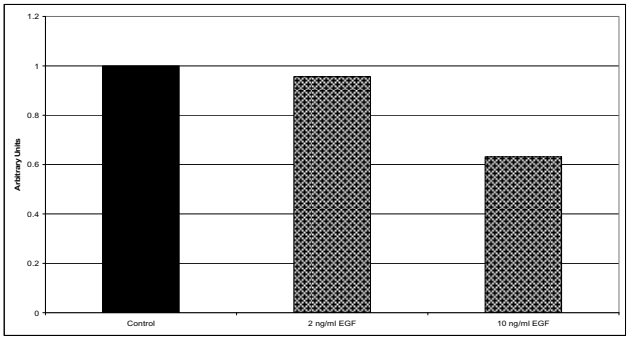

Figure 3.1.14.4 (a) Western blot of AKT expression with (b) densitometry following 48 hour 2 ng/ml and 10 ng/ml EGF treatments in A549-T. EGF treatments were in serum-free growth medium and control was A549-T cells incubated with serum-free growth medium for 48 hours.

MAPK expression in A549-T

(a)

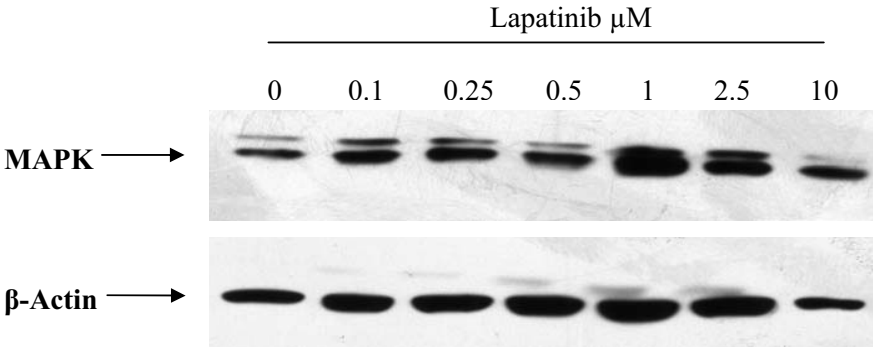

(b)

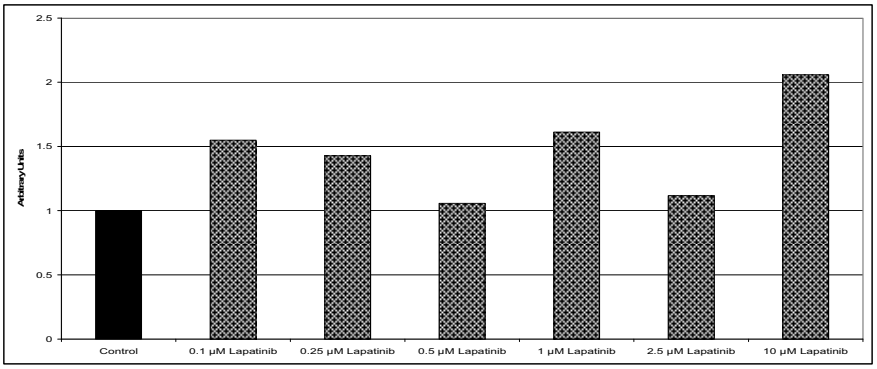

Figure 3.1.14.5 (a) Western blot of MAPK expression with (b) densitometry following 48 hour 0.1 μM, 0.25 μM, 0.5 μM, 1 μM, 2.5 μM and 10 μM lapatinib treatments in A549-T. Control was A549-T cells incubated with growth medium for 48 hours.

MAPK expression in A549-T

(a)

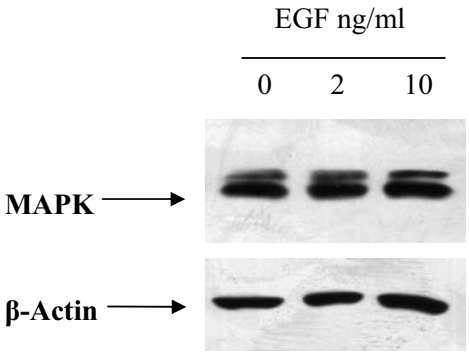

(b)

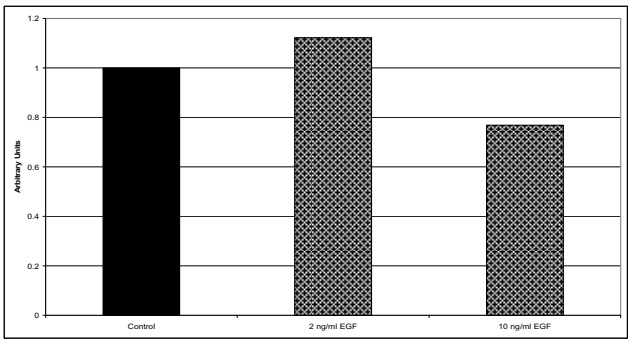

Figure 3.1.14.6 (a) Western blot of AKT expression with (b) densitometry following 48 hour 2 ng/ml and 10 ng/ml EGF treatments in A549-T. EGF treatments were in serum-free growth medium and control was A549-T cells incubated with serum-free growth medium for 48 hours.

Phosphorylated AKT expression in A549-T

(a)

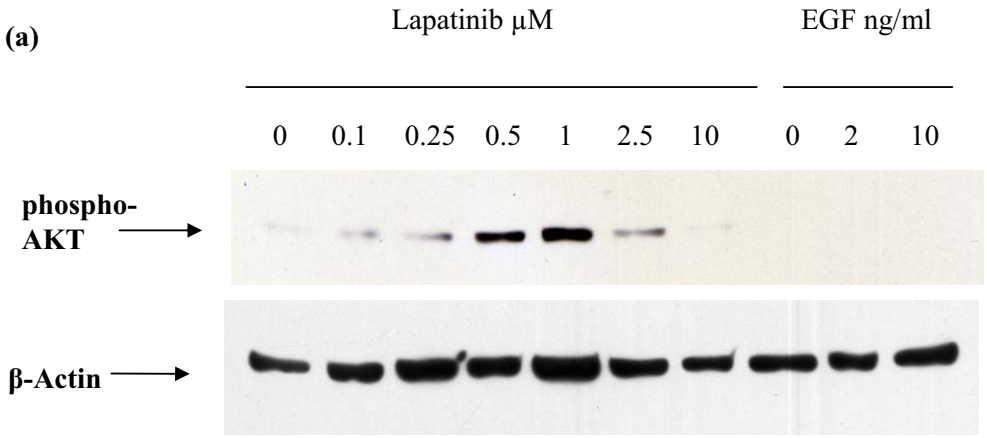

(b)

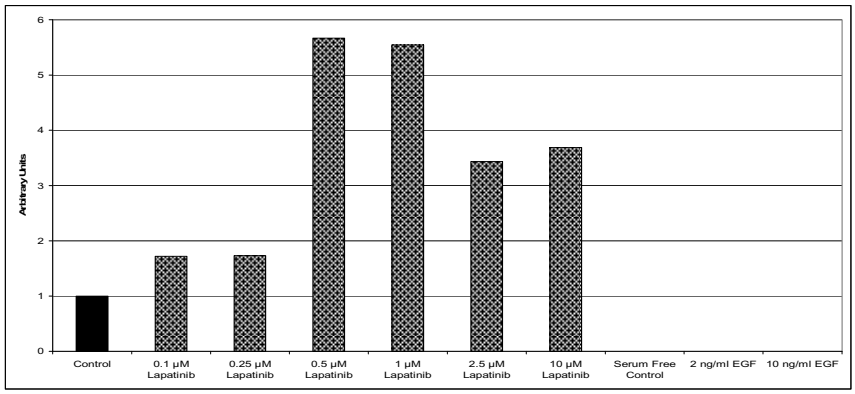

Figure 3.1.14.7 Western blot of phosphorylated AKT expression following 48 hour 0.1 µM, 0.25 µM, 0.5 µM, 1 µM, 2.5 µM and 10 µM lapatinib and 2 ng/ml and 10 ng/ml EGF treatments in A549-T. Control for lapatinib treatments was A549-T cells incubated with growth medium for 48 hours. EGF treatments were in serum-free growth medium and control was A549-T cells incubated with serum-free growth medium for 72 hours.

Phosphorylated MAPK expression in A549-T

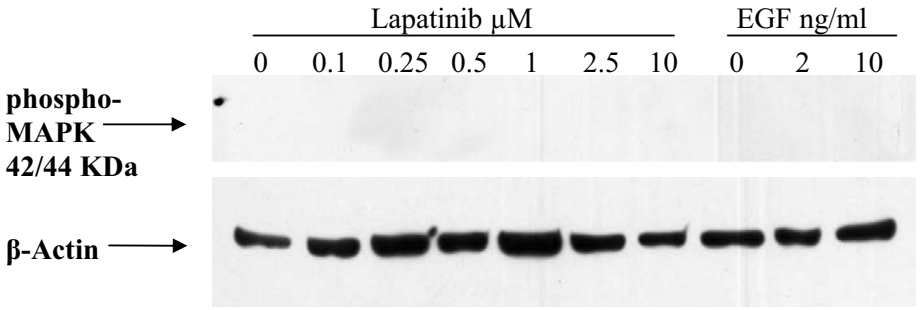

Figure 3.1.14.8 Western blot of phosphorylated MAPK expression following 48 hour 0.1 µM, 0.25 µM, 0.5 µM, 1 µM, 2.5 µM and 10 µM lapatinib and 2 ng/ml and 10 ng/ml EGF treatments in A549-T. Control for lapatinib treatments was A549-T cells incubated with growth medium for 48 hours. EGF treatments were in serum-free growth medium and control was A549-T cells incubated with serum-free growth medium for 48 hours.

3.2. Use of siRNA gene silencing techniques to investigate targets with potential roles in drug resistance

SiRNA-mediated RNA interference is a useful technique which can be employed to explore the contribution of certain proteins to the phenomenon of multidrug resistance. P-gp has been shown to be up regulated in the resistant lung cell lines DLKP-A and A549-T (figure 3.1.4.1) and so siRNA-induced alterations in the expression of P-gp were used to develop and test the applicability of this technology.

3.2.1. SiRNA transfection coupled with toxicity and accumulation assays

Toxicity and accumulation assays were coupled with siRNA transfection techniques in order to examine the effects of knocking down certain genes and reducing associated protein expression on chemotherapy sensitivity and accumulation. Firstly, a Western blot was carried out to confirm that the P-gp siRNAs being used were, in fact, reducing the expression of P-gp present in the cells. A reduced amount of the protein was observed with both siRNAs and this is shown in figure 3.2.1.1. Toxicity assays were then carried out on cells in which P-gp expression was silenced.

When P-gp was silenced in A549-T cells, an increase in sensitivity to paclitaxel was observed at the higher concentration and to epirubicin across all concentrations (figure 3.2.1.2 and 3.2.1.3), however, this increase was not statistically significant. In DLKP-A, a significant increase in toxicity with paclitaxel and epirubicin was observed in the cells transfected with P-gp siRNA as shown in figures 3.2.1.4 and 3.2.1.5. The paclitaxel treatment exhibited greater toxicity in the P-gp knocked down DLKP-A cells than was observed with epirubicin. Elacridar, which is a potent inhibitor of P-gp, was included in these toxicity assays as a control for total P-gp inhibition [41].

It would be expected that knocking down P-gp expression should increase the amount of P-gp substrate drugs in the cells. SiRNA techniques were coupled with an accumulation assay in order to investigate this. An assay measuring epirubicin accumulation 72 hours after P-gp knockdown in DLKP-A cells was carried out to address this. This accumulation data from DLKP-A cells transfected with P-gp siRNA showed a great increase in epirubicin level compared with control cells transfected with scrambled siRNA (figure 3.2.1.6). This was particularly evident

from the P-gp siRNA 1 and so further analysis carried out utilises this particular siRNA.

Western blot of P-gp in DLKP-A

(a)

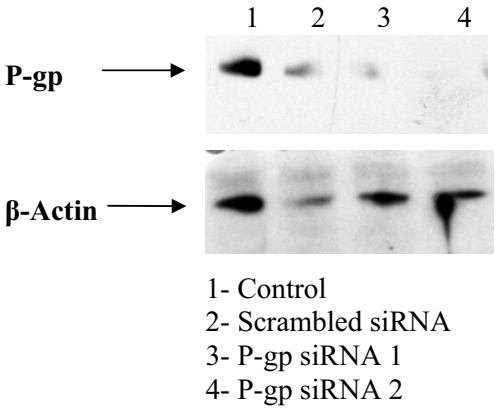

(b)

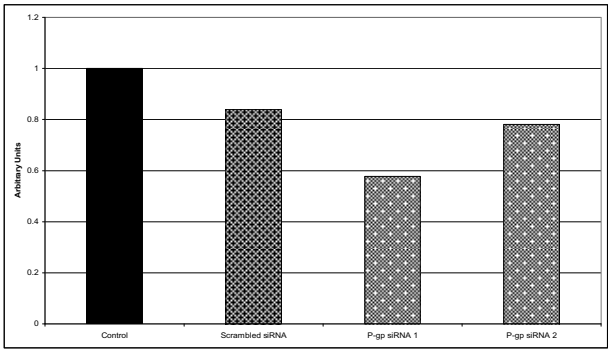

Figure 3.2.1.1 (a) Western blot of P-gp expression with (b) densitometry 72 hours after transfection with P-gp siRNA in DLKP-A. Scrambled siRNA was included as control.

Proliferation assay in A549-T

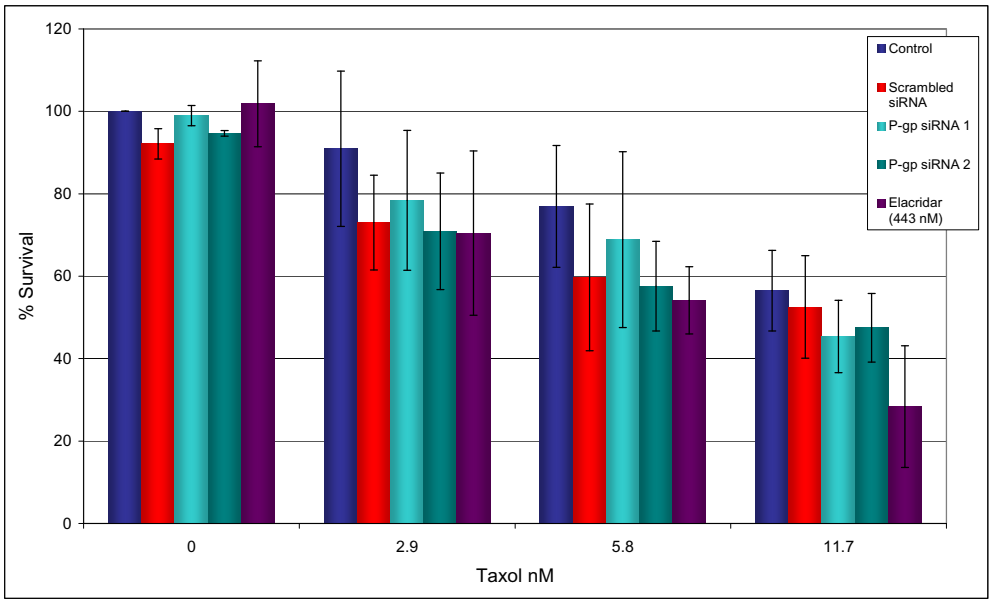

Figure 3.2.1.2 Paclitaxel toxicity as determined by acid phosphatase assay in A549-T cells transfected with P-gp siRNA. Data are mean +/- SD of triplicate experiments.

Proliferation assay in A549-T

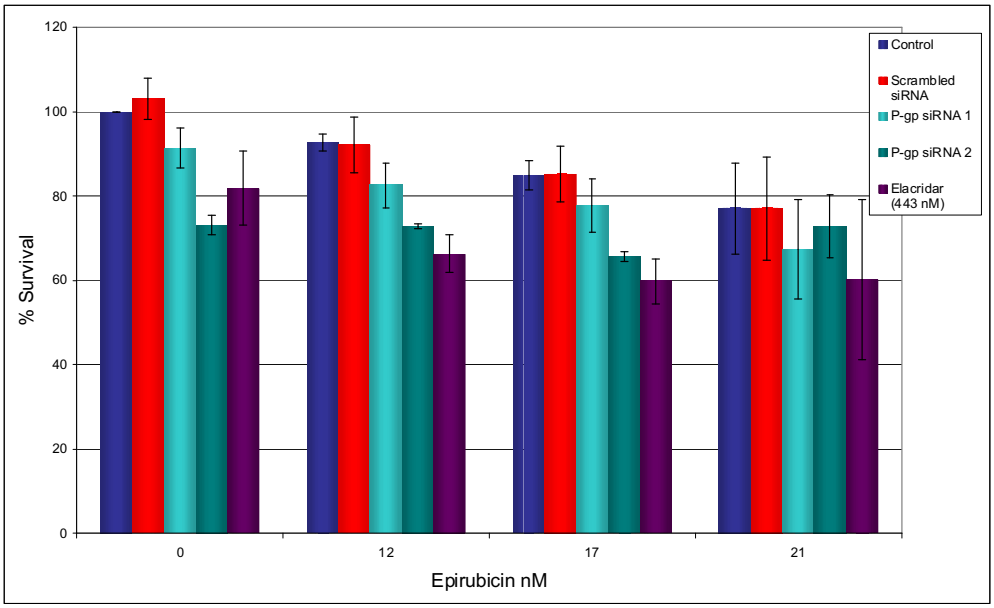

Figure 3.2.1.3 Epirubicin toxicity as determined by acid phosphatase assay in A549-T cells transfected with P-gp siRNA. Data are mean +/- SD of triplicate experiments.

Proliferation assay in DLKP-A

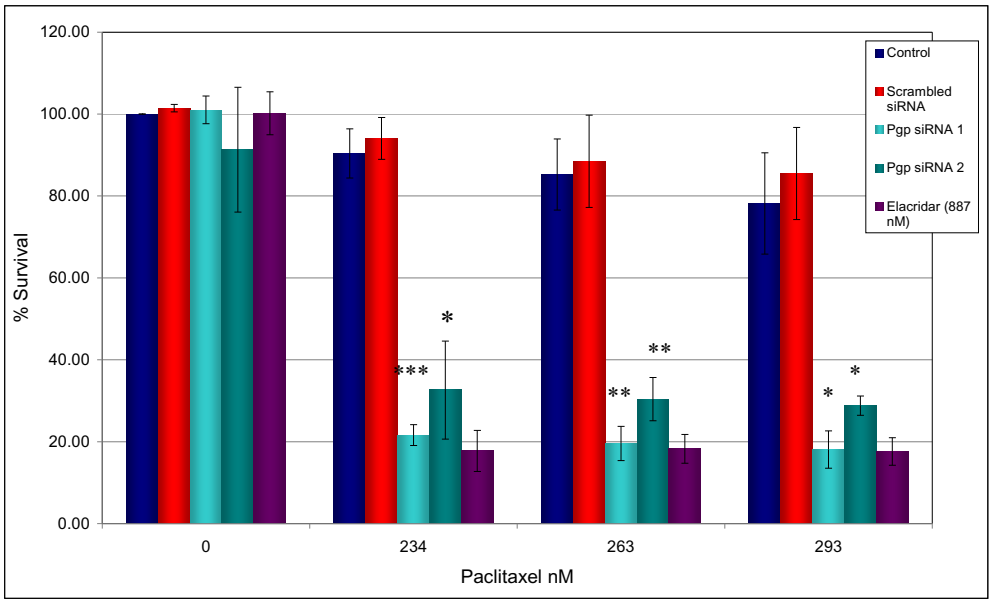

Figure 3.2.1.4 Paclitaxel toxicity as determined by acid phosphatase assay in DLKP-A cells transfected with P-gp siRNA. Data are mean +/- SD of triplicate experiments. *, **, *** significant P<0.05, <0.01, <0.005 compared with control.

Proliferation assay in DLKP-A

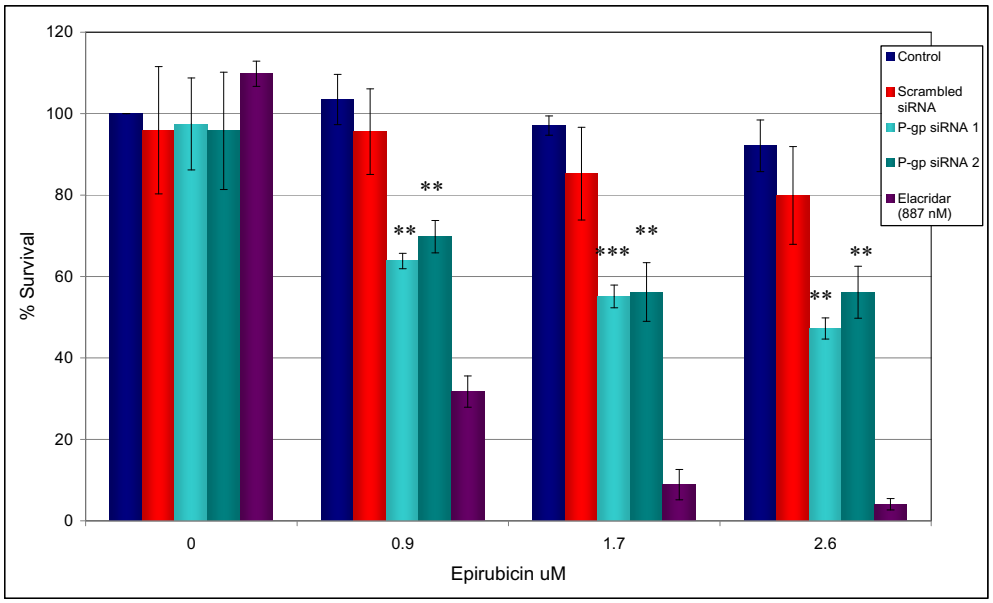

Figure 3.2.1.5 Epirubicin toxicity as determined by acid phosphatase assay in DLKP-A cells transfected with P-gp siRNA. Data are mean +/- SD of triplicate experiments. *,**,*** significant P<0.05, <0.01, <0.005 compared with control.

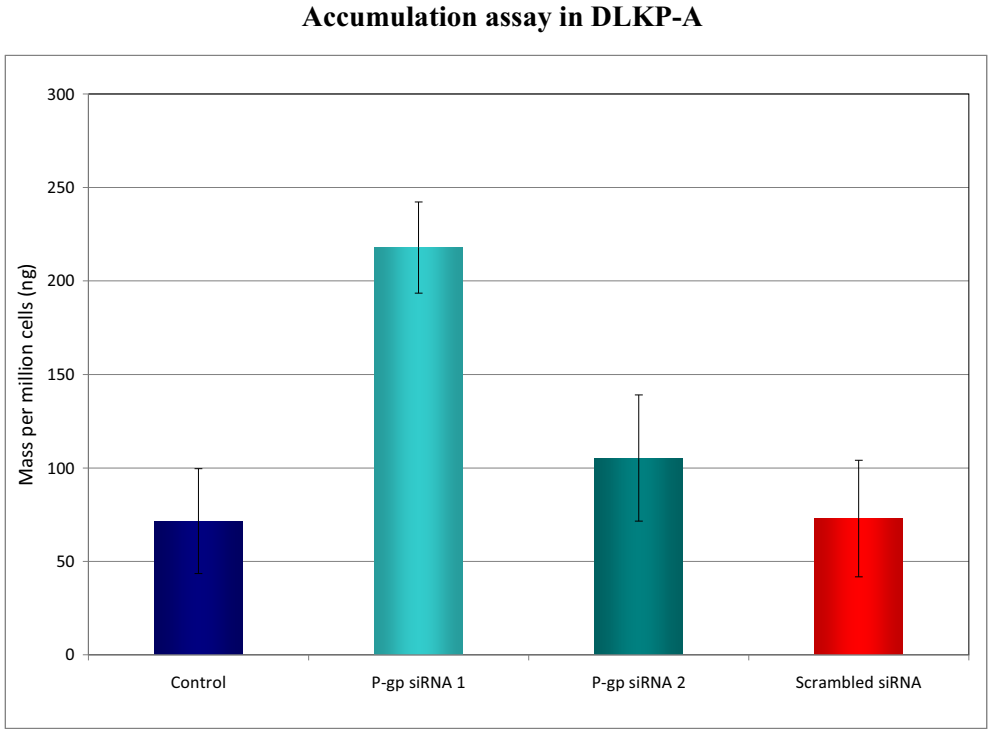

Figure 3.2.1.6 Epirubicin accumulation in DLKP-A cells over two hours, transfected with P-gp siRNA as determined from quantification by mass spectrometry. Assay was carried out in triplicate flasks on duplicate days and data are mean +/- SD.

3.2.2. SiRNA transfection of targets in A549-T and A549

P-gp appears to account for a large proportion of the resistance in the resistant lung cell lines tested, in particular DLKP-A. However, other mechanisms may also have a potential role in this chemotherapy drug resistance and these were investigated as outlined in the next two sections. Targets were chosen from analysis of transcriptomic experiments on resistant cell lines carried out previously in our laboratory [49]. This work generated a list of differentially expressed genes in resistant cell lines, including A549-T and H1299-T, compared with their respective parental cell lines, from which a few targets were chosen. Inhibitor of DNA binding 3, ID3 and Crystallin-zeta were shown to have a higher expression and Cysteine-rich protein 1, a lower expression in resistant cell lines compared with parent in these micro-array studies. Toxicity assays were undertaken to investigate if knocking down these targets had any effect on chemotherapy drug sensitivity.

Transfection with ID3 siRNA in A549-T increased sensitivity to paclitaxel but not to a significant degree, as shown in figure 3.2.2.1. This trend was also seen in DLKP-A, but to a greater extent, with significant differences in toxicity observed at all concentrations (figure 3.2.2.2). In both cell lines ID3 siRNA reduced cell survival even with no drug present. Figure 3.2.2.2 (b) displays the same data as in figure 3.2.2.2 (a) but it is graphed to allow all control levels with no chemotherapy drug to equal 100%. This discounts the initial drop in survival seen with ID3 siRNA to determine if the increased toxicity was due to some element of sensitization and not just the initial reduction in survival. This graph does in fact indicate an increase in paclitaxel toxicity in DLKP-A cells transfected with ID3 siRNA.

Transfection of Crystallin-zeta siRNA in A549-T and DLKP-A appeared to moderately sensitize the cells to paclitaxel, and in this case, in the absence of drug, it did not greatly effect cell survival (figure 3.2.2.3 and figure 3.2.2.4). As Cysteine-rich protein 1 (CRIP1) was down regulated in the resistant cell lines, the parent cell line was chosen as the vehicle to examine the effects of CRIP1 siRNA. Transfection of CRIP1 siRNA in A549 had no great effect on the lower paclitaxel concentrations, but at the highest paclitaxel concentration an opposing effect to that expected with a slight increase in paclitaxel toxicity was observed (figure 3.2.2.5).

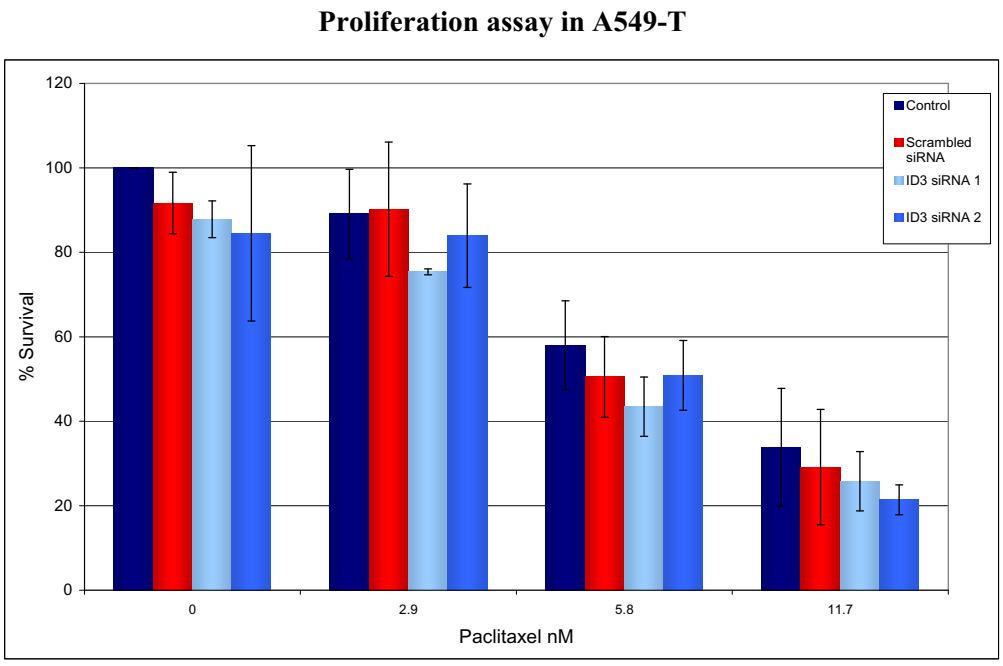

Figure 3.2.2.1 Paclitaxel toxicity as determined by acid phosphatase assay in A549-T cells transfected with ID3 siRNA. Data are mean +/- SD of triplicate experiments.

Proliferation assay in DLKP-A

(a)

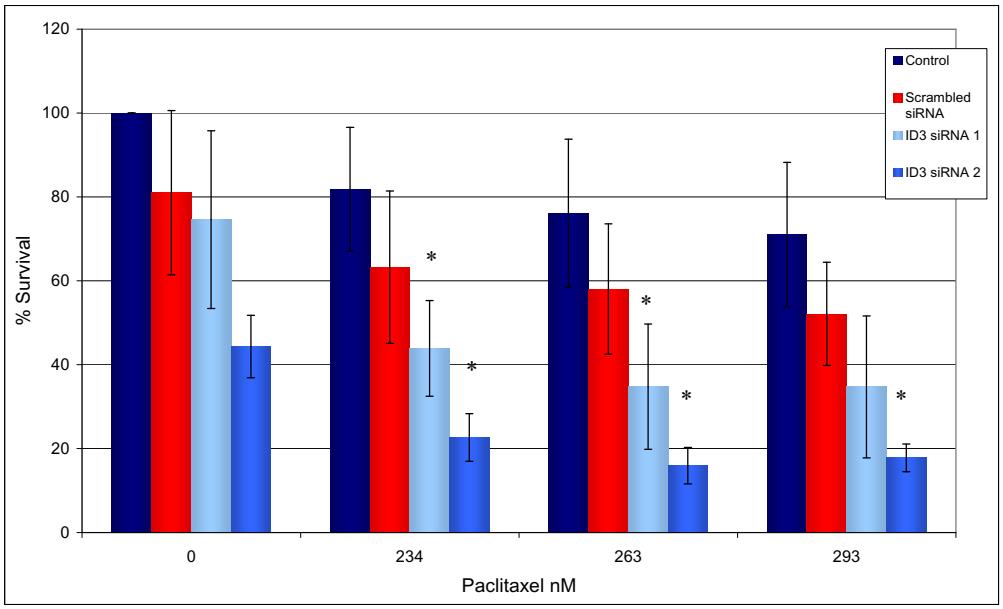

(b)

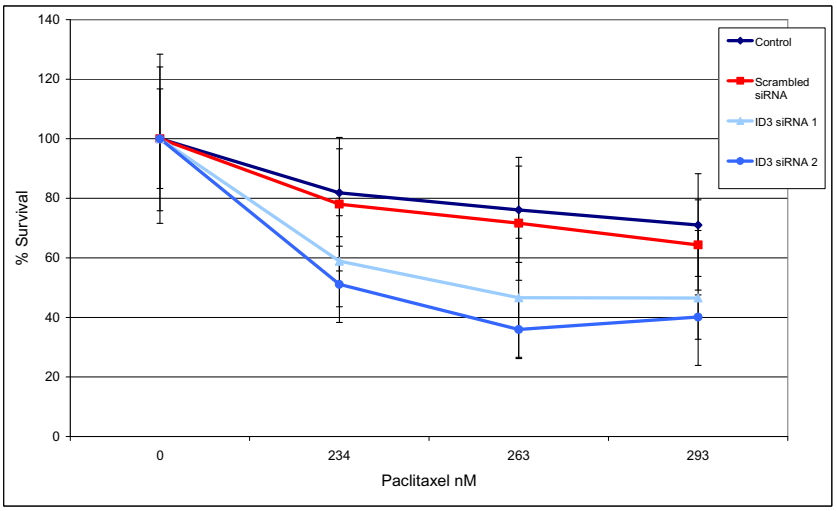

Figure 3.2.2.2 Paclitaxel toxicity as determined by acid phosphatase assay in DLKP-A cells transfected with ID3 siRNA. (a) Expressed in terms of untreated control (b) Expressed in terms of each conditioned control. Data are mean +/- SD of triplicate experiments. * significant $P<0.05$ compared with un-transfected control.

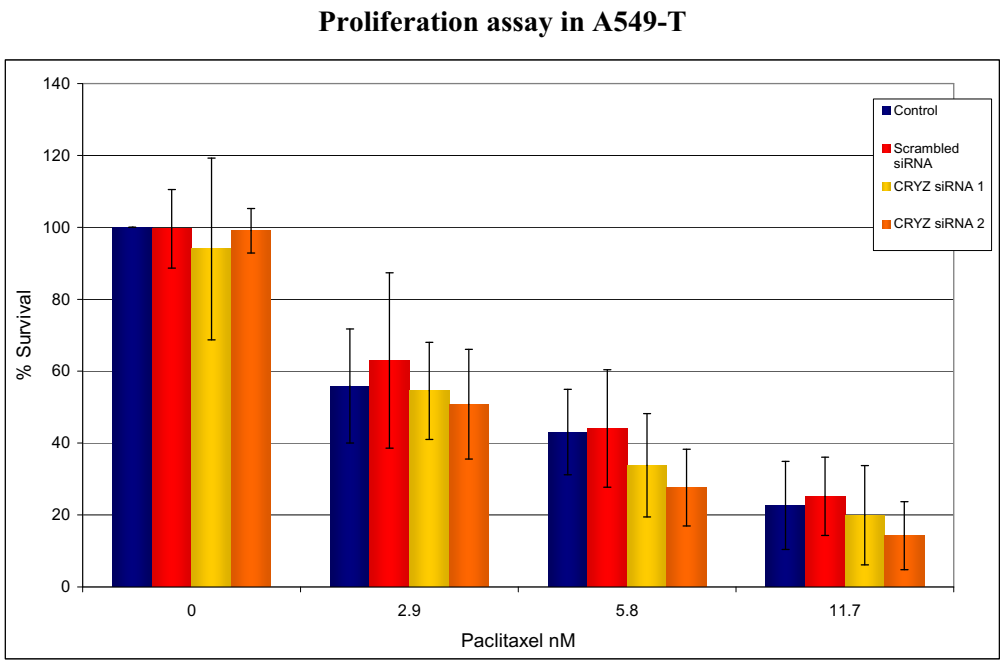

Figure 3.2.2.3 Paclitaxel toxicity as determined by acid phosphatase assay in A549-T cells transfected with CRYZ siRNA. Data are mean +/- SD of triplicate experiments.

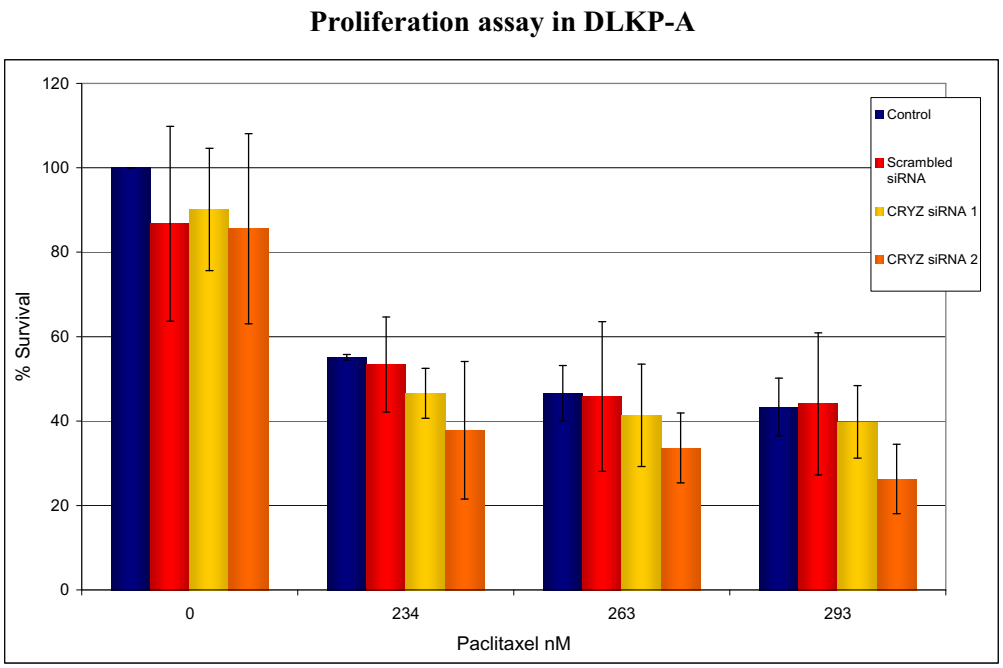

Figure 3.2.2.4 Paclitaxel toxicity as determined by acid phosphatase assay in DLKP-A cells transfected with CRYZ siRNA. Data are mean +/- SD calculated on experiments performed in triplicate.

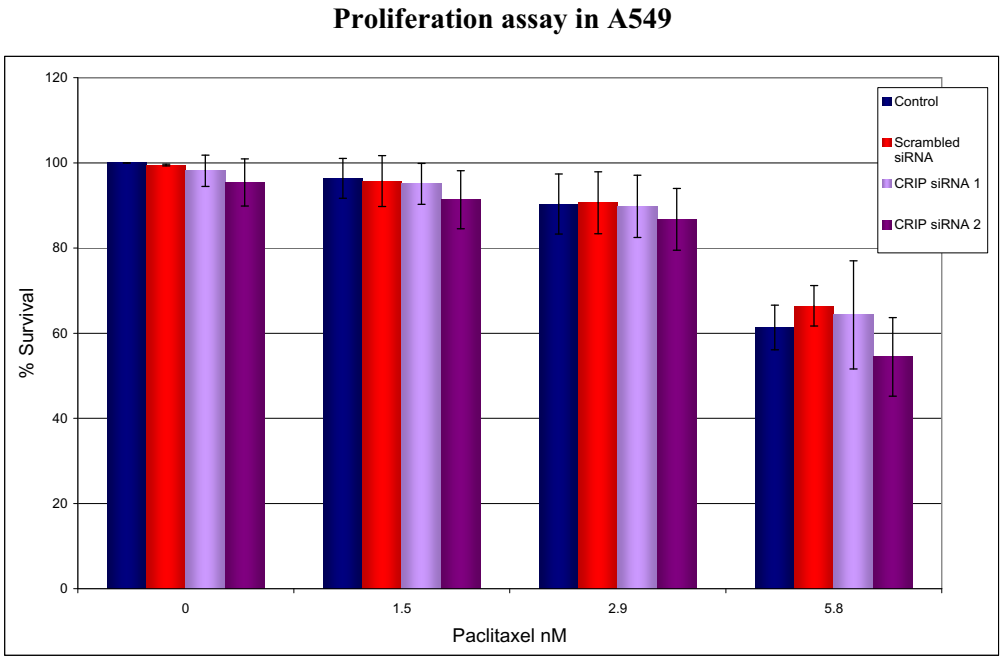

Figure 3.2.2.5 Paclitaxel toxicity as determined by acid phosphatase assay in A549 cells transfected with CRIP1 siRNA. Data are mean +/- SD of duplicate experiments.

3.2.3. Transfection of siRNA for targets of interest with P-gp and subsequent effect on resistance

As P-gp expression appears to generate resistance in A549-T and more so in DLKP-A, it was hypothesised that silencing P-gp as well as the protein of interest might

allow dissection of the individual contribution of the protein of interest to the total resistance phenotype. SiRNAs for the chosen targets were co-transfected with P-gp siRNA in A549-T cells to see if this increased chemotherapy sensitivity compared with knocking P-gp down alone.

Cells were transfected with siRNA for targets of interest and drug treated in the presence of the P-gp inhibitor elacridar. Chemotherapy drugs exhibited a similar level of kill in the cells with target siRNA and elacridar as with elacridar alone. In both A549-T and DLKP-A, transfection with ID3 siRNA with elacridar slightly increases paclitaxel toxicity compared with elacridar alone (figures 3.2.3.2 and 3.2.3.3). It must be noted that the scrambled siRNA control with the elacridar also appeared to show increase toxicity to paclitaxel and so these result should be viewed bearing this in mind. Figure 3.2.3.3 shows that taking the initial decrease in survival caused by transfection with ID3 siRNA out of the equation, no difference existed in sensitivities to paclitaxel between elacridar control and ID3 transfected cells with elacridar. In DLKP-A, co-transfection with both P-gp and ID3 siRNA resulted in a non-significant increase in paclitaxel toxicity, as shown in figure 3.2.3.1.

In A549-T, co-transfection of CRYZ siRNA with P-gp siRNA exhibited a trend towards increased paclitaxel sensitivity although this was not significant degree, whereas an opposing effect was observed in DLKP-A (figures 3.2.3.4 and 3.2.3.5).

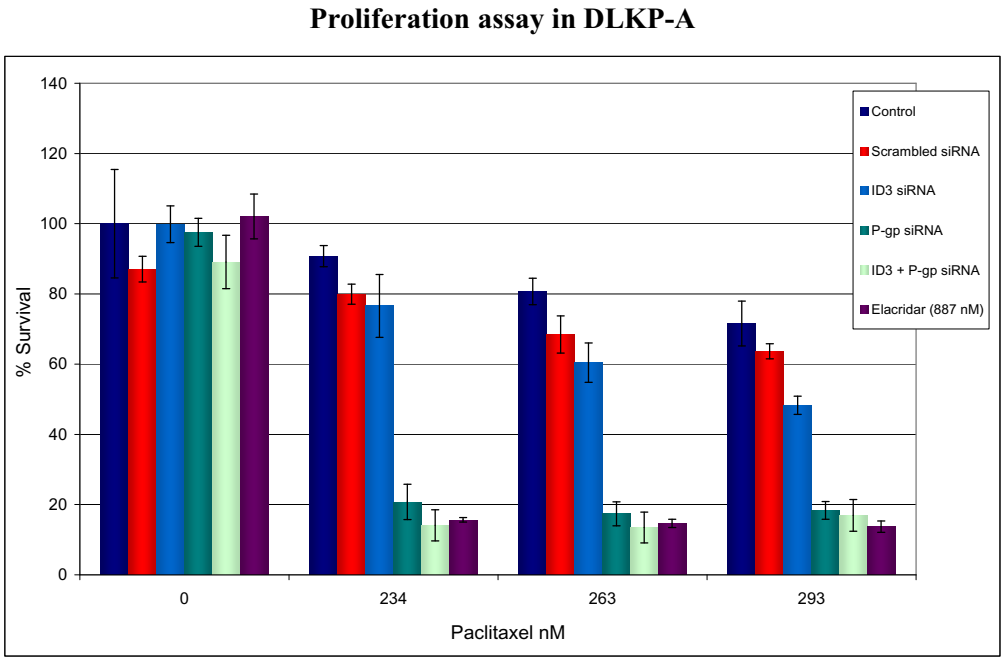

Figure 3.2.3.1 Paclitaxel toxicity as determined by acid phosphatase assay in DLKP-A cells co-transfected with ID3 and P-gp siRNA. Data are mean +/- SD of triplicate experiments.

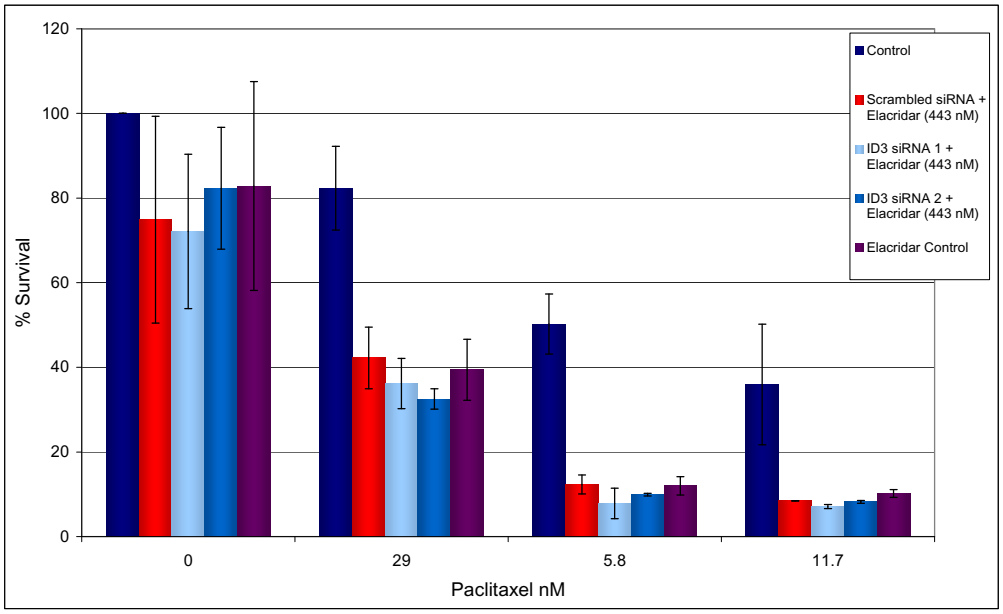

Figure 3.2.3.2 Paclitaxel toxicity as determined by acid phosphatase assay in A549-T cells transfected with ID3 siRNA in the presence of elacridar. Data are mean +/- SD of triplicate experiments.

Proliferation assay in DLKP-A

(a)

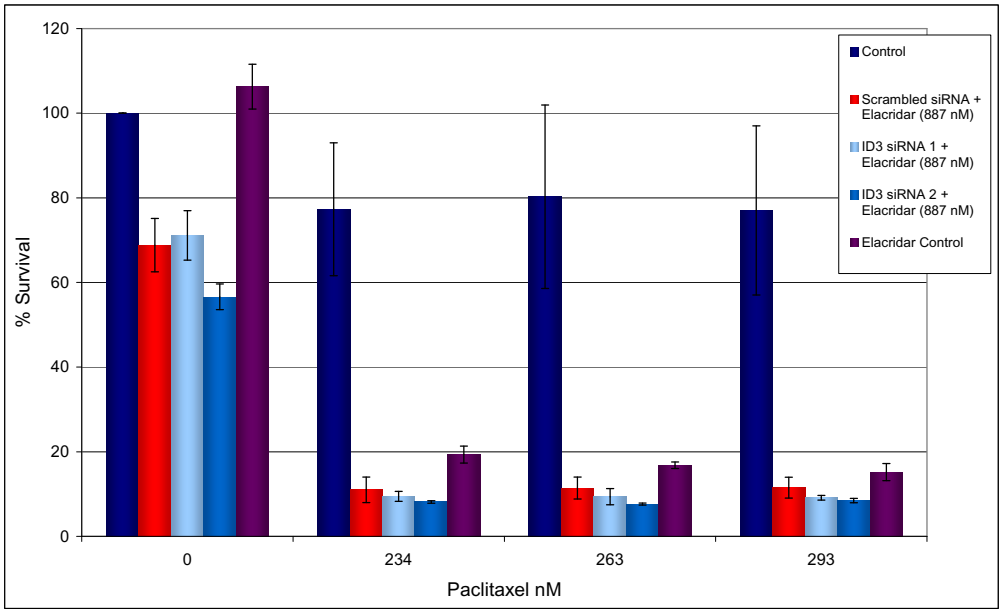

(b)

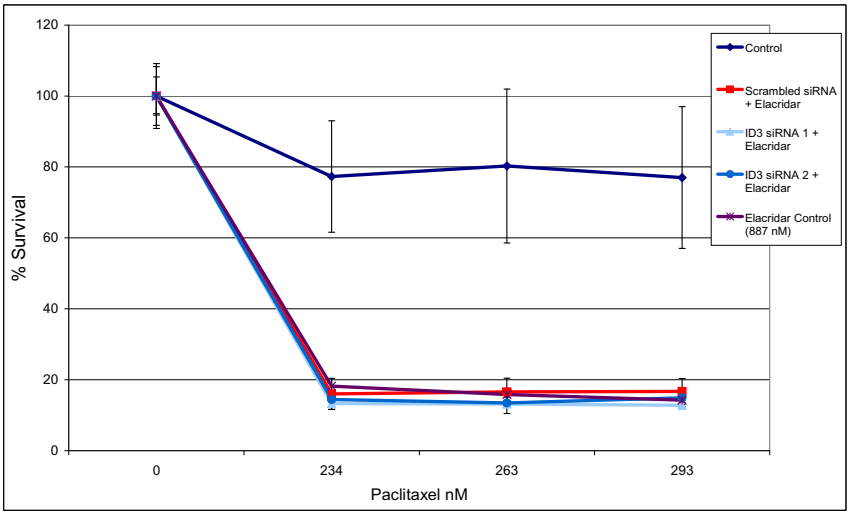

Figure 3.2.3.3 Paclitaxel toxicity as determined by acid phosphatase assay in DLKP-A cells transfected with ID3 siRNA in the presence of elacridar. (a) Expressed in terms of untreated control (b) Expressed in terms of each conditioned control. Data are mean +/- SD of triplicate experiments.

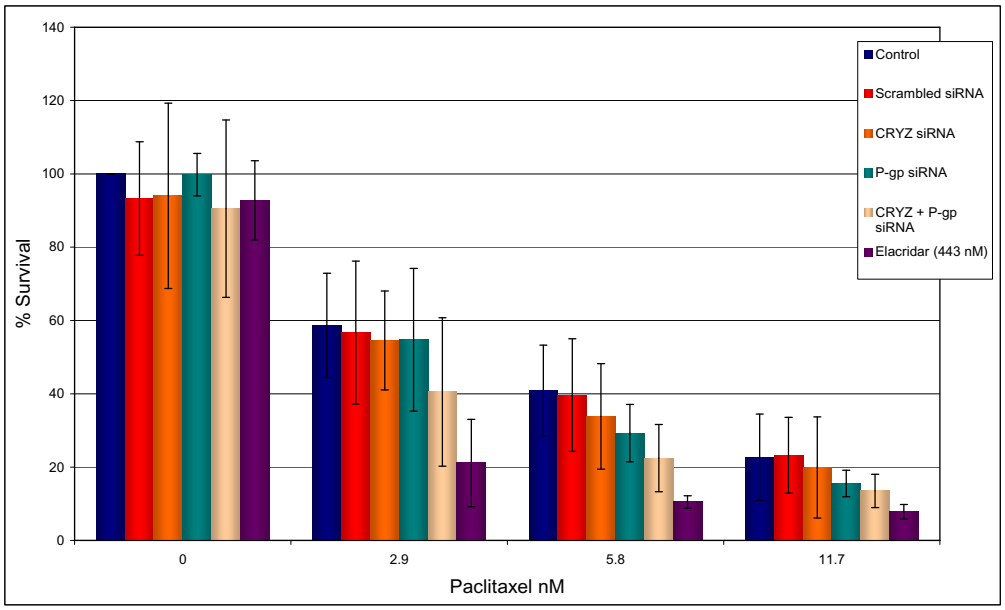

Figure 3.2.3.4 Paclitaxel toxicity as determined by acid phosphatase assay in A549-T cells co-transfected with CRYZ and P-gp siRNA. Data are mean +/- SD of triplicate experiments.

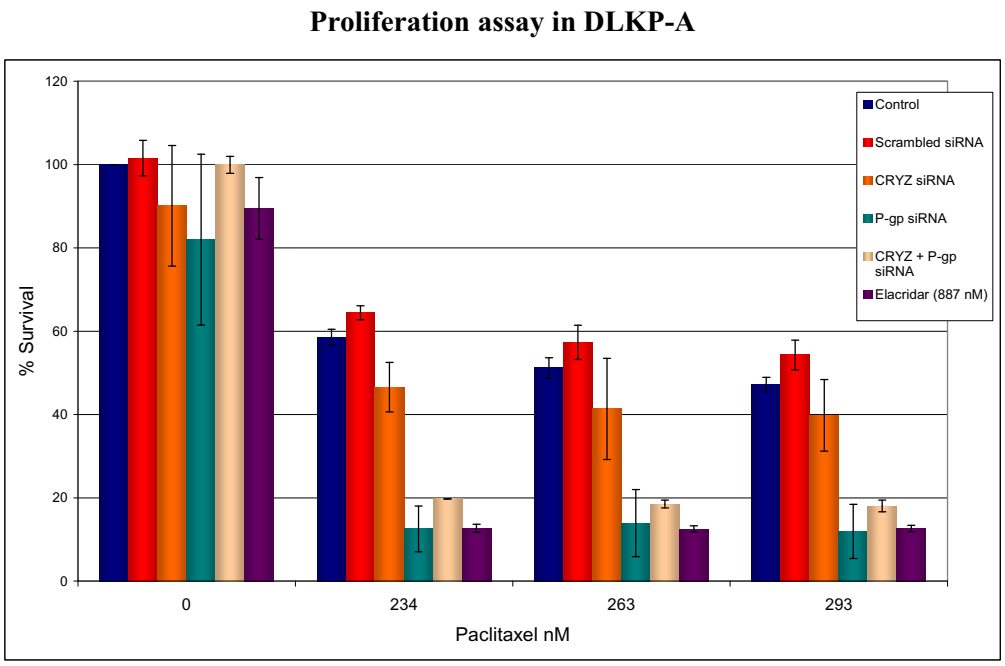

Figure 3.2.3.5 Paclitaxel toxicity as determined by acid phosphatase assay in DLKP-A cells co-transfected with CRYZ and P-gp siRNA. Data are mean +/- SD of triplicate experiments.

3.3. Membrane Protein Analysis

Much of the drug resistance research carried out in this project related to proteins expressed in the cell membrane and involved extensive use of the Western Blot assays. To examine technology which might make such research easier, membrane protein extraction coupled with LC-MS identification was explored. The membrane proteins were isolated and solubilised in an organic solvent as this methodology has been shown to be compatible with LC and provide good conditions for tryptic digestion [141]. Trypsin, which cleaves at arginine and lysine, was the enzyme of choice for digestion of the membrane proteins. Tandem mass spectrometry was chosen and the MS/MS methods utilised were collision-induced dissociation (CID) and electron transfer dissociation (ETD). The database-searching algorithm SEQUEST was then used to identify the isolated membrane proteins. There are inherent challenges with a technique like this. Aside from biological variances, there are a number of areas in which issues may arise when dealing with such a complex sample, namely; separation by LC, detection and analysis by MS and identification by bioinformatics and data analysis. The separation method of multidimensional chromatography was briefly examined for quality and consistency. A quick evaluation of the level and quality of detection from the mass spectrometer was also carried out. The main focus of this body of work was to investigate the impact of statistical parameters employed in the protein identification process. When suitable parameters were determined they were then applied to the remaining samples, allowing comparisons of parent versus resistant cells and treated versus untreated.

This work was carried out on data generated from a sample from the resistant cell line DLKP-A (**DLKP-A 1**) and a re-analysis of this same sample on a different date (technical repeat) (**DLKP-A 2**).

3.3.1. Assessment of liquid chromatography

To achieve a valuable end result, each aspect of this method needs to be performing to an adequate standard. A small representative number of peptides were chosen from 10mM fraction generated using CID from each DLKP-A 1 and DLKP-A 2. The retention times (RT) for these peptides were obtained and compared and the visual aspect of the chromatography also analysed. Table 3.3.1.1 displays data relevant to the six representative peptides chosen. It shows the retention times to be of a reasonable consistency across all peptides from sample 1 to sample 2, with the differences all falling around 1 minute. This indicates the separation technique is robust and reproducible when applied to complex samples of this nature. The quality of the LC was evaluated also. This was done through analyses of chromatograms and mass spectra, corresponding to peptides from MDR1 and ANAX1, from both DLKP-A 1 and DLKP-A 2. Figures 3.3.1.1-3.3.1.4 display; base peak chromatograms, encompassing both MS and MS/MS therefore showing all of the ions within that fraction; an ion extraction of the specific peptide of interest; and the full mass spectrum showing the peptide of interest.

Peptide retention times from DLKP-A 1 and 2

Peptide ID and Sequence	Isotopic Mass $[M+H]^+$	DLKP-A 1 RT (min)	DLKP-A 2 RT (min)	Difference in RT
MDR1 K.SEIDALEMSSNDSR.S	778	33.7	32.4	1.3
GRP78 R.IEIESFYEGEDFSETLTR.A	1083	41.7	40.7	1
ANAX1 K.GLGTDEDTLIEKASR.T	852	46.5	45.6	0.9
LAP2B RIDGPVISESTPIAET	978	44.1	42.9	1.2
LYRIC R.EEAAAVPAAAPD	883	38.8	37.8	1
SCAM1 K.TVQTAAANAAS	718	36.5	35.4	1.1

Table 3.3.1.1 Comparison of retention times (RT) of peptides from proteins identified in the 10mM fraction of DLKP-A 1 and 2.

Peptide of mass 777 from MDR1 identified in DLKP-A 1

(a)

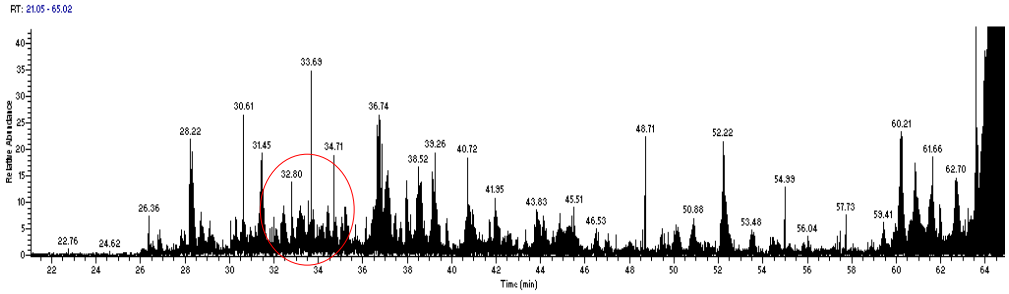

(b)

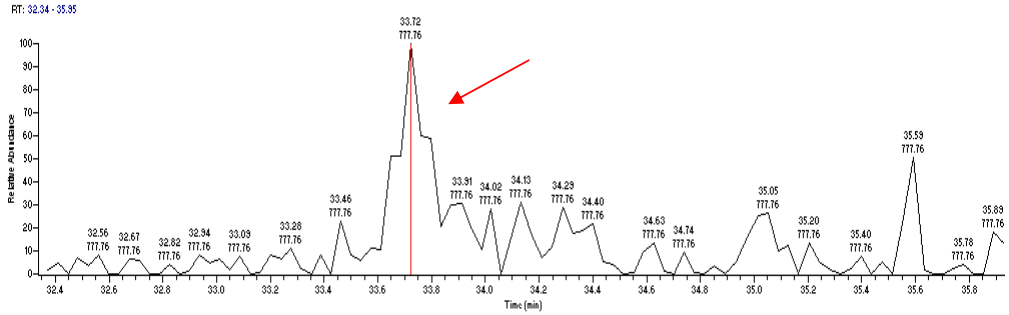

(c)

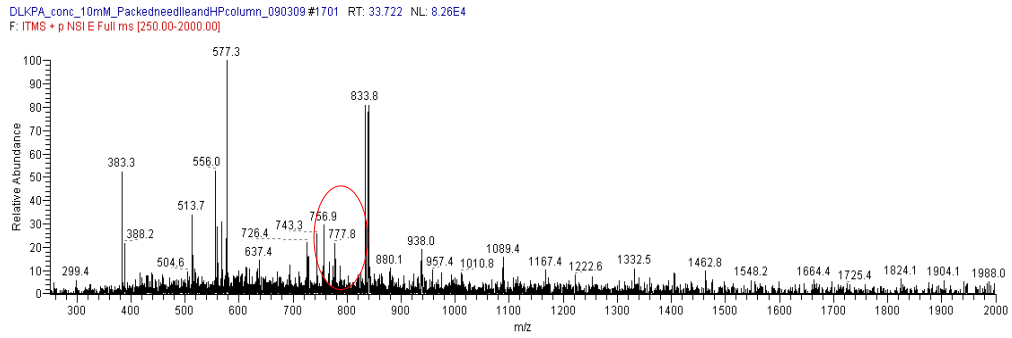

Figure 3.3.1.1 Base peak chromatogram (a), ion extraction (b), and full mass spectrum (c), corresponding to the peptide with mass 778 and retention time of 33.7 minutes, from MDR1 identified in DLKP-A 1. Peptide highlighted in each view.

Peptide of mass 777 from MDR1 identified in DLKP-A 2

(a)

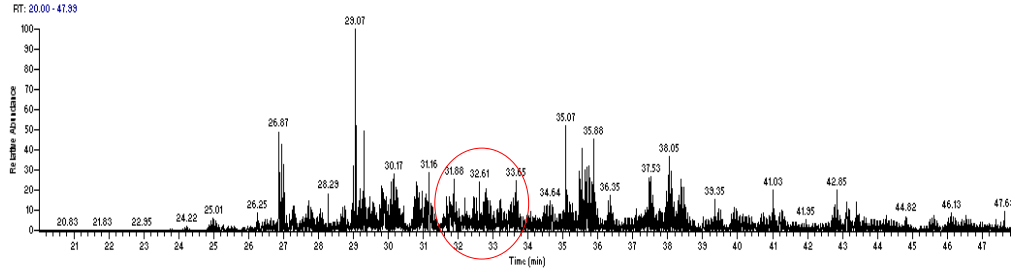

(b)

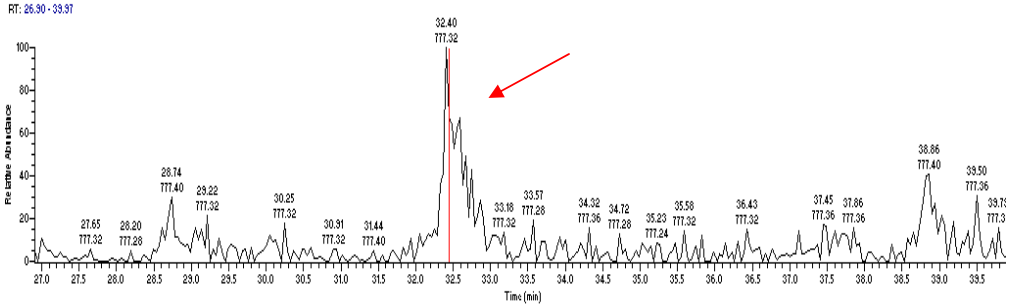

(c)

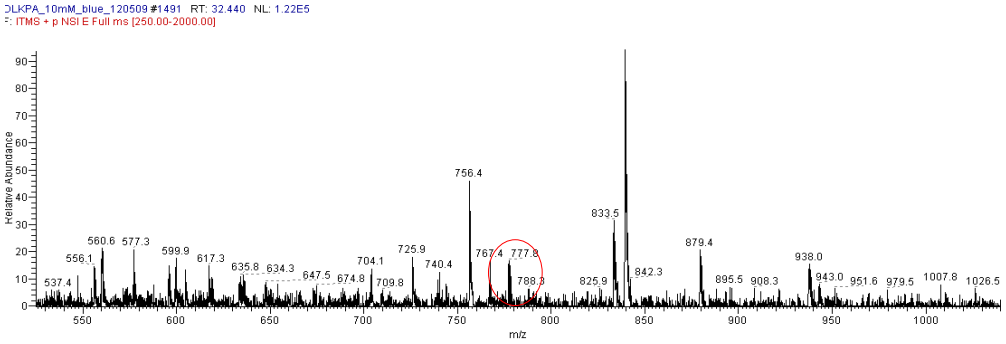

Figure 3.3.1.2 Base peak chromatogram (a), ion extraction (b) and full mass spectrum (c), corresponding to the peptide with mass 777 and retention time of 32.4 minutes, from MDR1 identified in DLKP-A 2. Peptide highlighted in each view.

Peptide of mass 852 from ANAX1 identified in DLKP-A 1

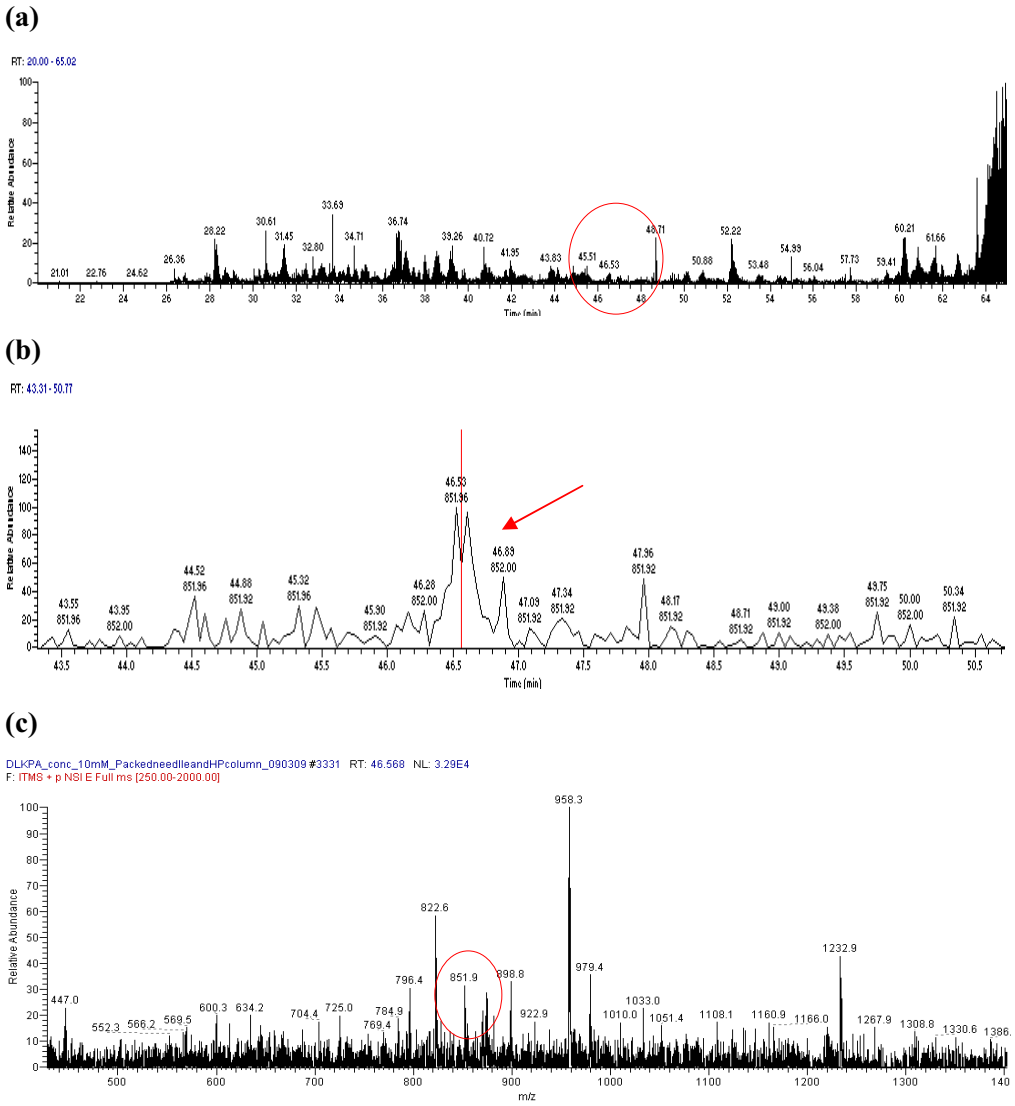

Figure 3.3.1.3 Base peak chromatogram (a), ion extraction (b) and full mass spectrum (c), corresponding to the peptide with mass 852 and retention time of 46.5 minutes, from ANAX1 identified in DLKP-A 1. Peptide highlighted in each view.

Peptide of mass 852 from ANAX1 identified in DLKP-A 2

(a)

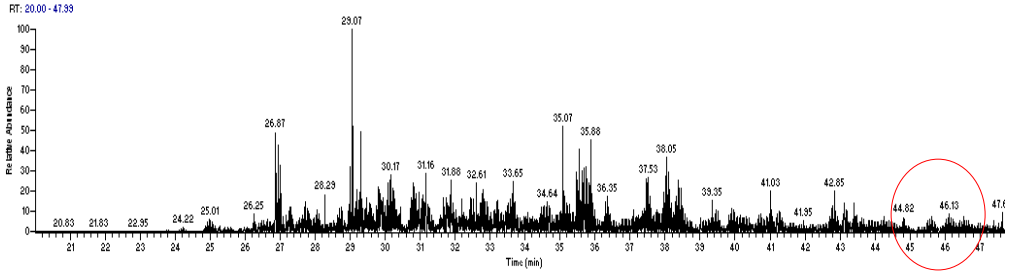

(b)

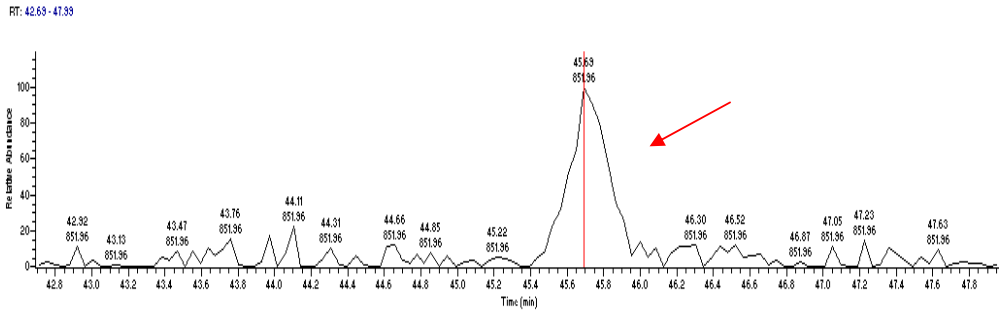

(c)

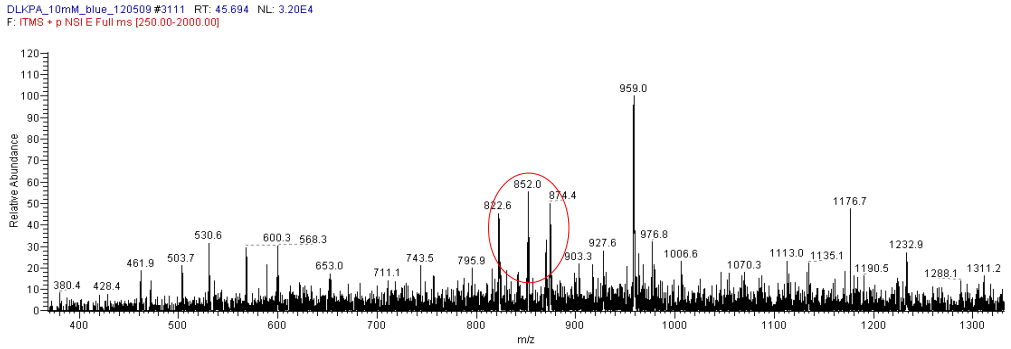

Figure 3.3.1.4 Base peak chromatogram (a), ion extraction (b) and full mass spectrum (c), corresponding to the peptide with mass 852 and retention time of 45.6 minutes, from ANAX1 identified in DLKP-A 2. Peptide highlighted in each view.

3.3.2. Analysis of DLKP-A 1 and 2 tandem mass spectrometry data with standard statistical parameters

The MS identification process is governed largely by statistics, and different parameters can be applied in such analysis so work was carried out to determine the parameters which yielded the 'best' representation of proteins. This was based on protein number, overlap between technical repeats and the quality of the mass spectra. SEQUEST, the database-searching algorithm, uses a cross-correlation (XCorr) function to assess the quality of the match between a tandem mass spectrum and amino acid sequence information from the database. This value represents an absolute measure of spectral quality and closeness of fit to the model spectrum [170].
Initial **standard parameters** for the identification of proteins were selected based on evidence found in the literature. These were then applied to both combined CID and ETD data of the DLKP-A membrane protein sample (DLKP-A 1) and its technical repeat (DLKP-A 2) [171-173]. The criteria consisted of the following conditions:

1) 2 peptides; a minimum of two peptides required for identification
2) Distinct peptides; the two peptides had to be distinct from each other
3) XCorr values of 1.9 for singly charged peptides, 2.2 for doubly charged peptides, 3.0 for triply charged peptides and 3.5 for quadruple charged peptides

Two lists of proteins were generated after the application of these parameters. An outline of the findings is shown in table 3.3.2.1., with a diagrammatic view shown in figure 3.3.2.1. 42% of the total number of identified proteins, were found in both the original sample and the repeat. However, quite a high number of the total combined proteins (41%) were identified in the first sample only, with just 17% found in the repeat sample only.
A number of the proteins identified with lower x-correlation scores were manually validated, in order to assess the quality and stringency of parameters employed. This was done according to criteria similar to that outlined by others [171], whereby the MS/MS spectrum must be of good quality with the fragmented ions showing distinct fragmentation and being observed clearly above baseline noise. There also must be some continuity observed in the b and y (CID) and the c and z (ETD) ion series. All ten proteins which were manually analysed and listed in table 3.3.2.2 were deemed

valid by these criteria and by way of representation mass spectra and ion series data for two of the peptides are shown in figure 3.3.2.1 and 3.3.2.2. Figure 3.3.2.1 displays data representing a peptide with a mass of 2019.5 for N-acetyltransferase 10 which is an activator for up-regulating telomerase activity that was identified in DLKP-A 1 [174]. In figure 3.3.2.2, diagrams representing a peptide with a mass of 973.6 from fatty acid desaturase 1, a component of the plasma membrane that catalyzes the transformation of saturated to monounsaturated fatty acids which was identified in DLKP-A 2 are shown [175].

A list of membrane proteins previously shown to be expressed either by Western blot or 2-D DIGE in DLKP-A was generated from data in this body of work and from other work carried out in this institute [176]. This includes P-gp, the glucose transporters GLUT's 1 and 3, HSP 70 variant 6, lamin B1, aldehyde dehydrogenase 1 (ALDH 1) and annexin A1. The DLKP-A 1 and DLKP-A 2 membrane protein identifications with the above standard parameters were observed for inclusion of these proteins and the results are shown in table 3.3.2.3. P-gp was found in both DLKP-A 1 and 2 as was annexin A1 and GLUT 3. GLUT 1, HSP 70 variant 6 and lamin B1 were found in DLKP-A 1 but not its technical repeat and ALDH A1 was not identified from either set of MS data.

Protein numbers identified in DLKP-A 1 and 2

(a)

Sample	Condition	No. Of Proteins	% Of Total Proteins
DLKP-A 1	Total Proteins	635	
DLKP-A 2	Total Proteins	447	
DLKP-A 1 + DLKP-A 2	Total Proteins	761	
DLKP-A 1 + DLKP-A 2	Commonly Expressed Proteins	321	42 %
DLKP-A 1	In DLKP-A 1 only	314	41 %
DLKP-A 2	In DLKP-A 2 only	126	17 %

(b)

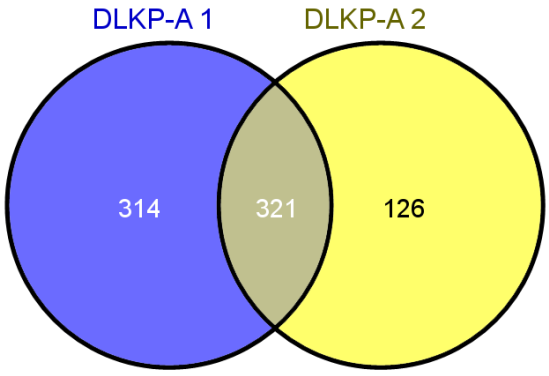

Figure 3.3.2.1 Comparison of numbers of proteins identified in DLKP-A MS samples 1 and 2 with the application of standard parameters in table format (a) or as a Venn diagram (b).

Validated proteins identified in DLKP-A 1 and 2

DLKP-A 1	DLKP-A 2
N-acetyltransferase 10 (NAT10)	Fatty acid desaturase 1 (FADS1)
MAGUK p55 subfamily member 5 (MMP5)	Zinc finger protein 622 (ZN622)
Structural maintenance of chromosome protein 2 (SMC2)	Myosin Va (MYO5A)
Tyrosine-protein kinase transmembrane receptor (ROR2)	A-kinase anchor protein 9 (AKAP9)
Integrin beta-5 (ITB5)	Ubiquitin carboxyl-terminal hydrolase 1 (UBP1)

Table 3.3.2.2 Proteins which were manually validated and deemed acceptable from the identified proteins in DLKP-A 1 and 2 MS samples with the application of standard parameters.

B and y ion series and mass spectrum from peptide in DLKP-A 1

(a)

		MW (Da)				MW (Da)				
AA	A	B	B*	Bo	C	Y	Y*	Yo	Z	
	☐	☑	☐	☐	☐	☑	☐	☐	☐	
N		115.05				-				17
M		246.09				1904.94				16
V		345.16				1773.90				15
D		460.19				1674.83				14
Y		623.25				1559.81				13
H		760.31				1396.74				12
L		873.39				1259.69				11
I		986.48				1146.60				10
M		1117.52				1033.52				9
D		1232.54				902.48				8
M		1363.58				787.45				7
I		1476.67				656.41				6
P		1573.72				543.32				5
A		1644.76				446.27				4
I		1757.84				375.24				3
S		1844.87				262.15				2
R		-				175.12				1

(b)

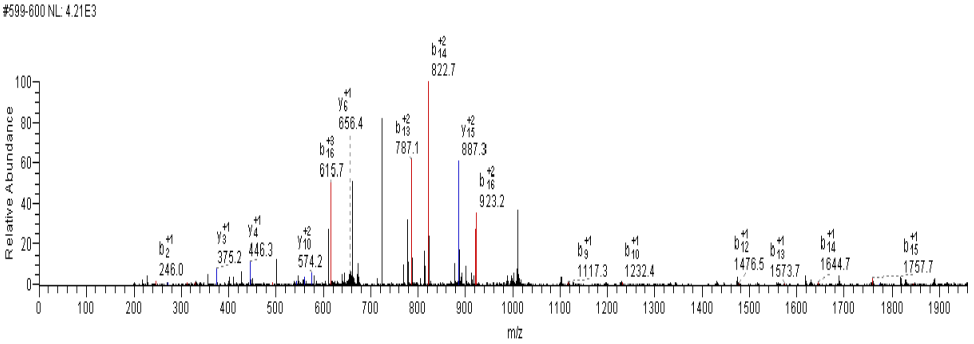

Figure 3.3.2.2 B and y ion series (a), and mass spectrum (b), corresponding to a peptide from N-acetyltransferase 10, identified in DLKP-A 1 with the application of standard parameters.

B and y ion series and mass spectrum from peptide in DLKP-A 2

(a)

		MW (Da)					MW (Da)				
	AA	A	B	B*	Bo	C	Y	Y*	Yo	Z	
		☐	☑	☐	☐	☐	☑	☐	☐	☐	
1	E		130.05				-				8
2	L		243.13				844.50				7
3	R		399.24				731.42				6
4	A		470.27				575.31				5
5	T		571.32				504.28				4
6	V		670.39				403.23				3
7	E		799.43				304.16				2
8	R		-				175.12				1

(b)

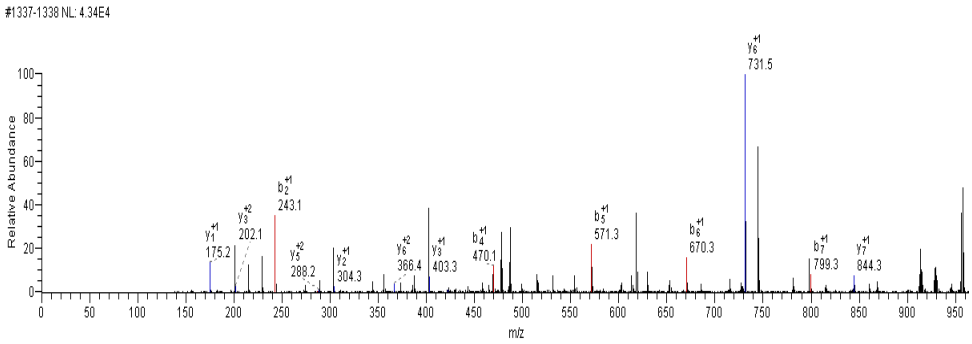

Figure 3.3.2.3 B and y ion series (a), and mass spectrum (b), corresponding to a peptide from fatty acid desaturase 1 (FADS1), identified in DLKP-A 2 with the application of standard parameters.

Proteins identified in DLKP-A 1 and 2

Protein	DLKP-A 1	DLKP-A 2
P-glycoprotein	Yes	Yes
Annexin A1	Yes	Yes
GLUT 1	Yes	No
GLUT 3	Yes	Yes
HSP 70 variant 6	Yes	No
Lamin B1	Yes	No
ALDH A1	No	No

Table 3.3.2.3 The presence of membrane proteins known to be expressed in DLKP-A, in proteins identified in DLKP-A 1 and 2 with the application of standard parameters.

3.3.3. Analysis of DLKP-A tandem MS data with peptide probability applied to CID data

Using the ETD tandem mass spectrometry method enhances our data as it gives better fragmentation of larger peptides and so the combination of CID and ETD enables a greater identification of a wide variety of peptide types [150, 177]. CID data can, however, be analysed slightly differently to ETD data, by including an extra parameter namely the Mascot algorithm. This method incorporates probability-based scoring and is described as advantageous as a simple rule can be used to judge whether a result is significant or not [178]. It was determined if applying this algorithm to CID data was beneficial to protein identifications in our samples. In order to carry out this analysis the ETD MS datasets were subjected to the standard parameters outlined in section 3.3.2, whereas identifications from CID MS datasets were determined by these same initial criteria with the addition of a peptide probability of 0.05.

Table 3.3.3.1 illustrates the findings which resulted in the total number of proteins identified reduced to 432 of which 51% were found in both sample's, 34% in DLKP-A 1 only and 15% in DLKP-A 2 only. The higher percentage of proteins observed in DLKP-A 1 only and lower observed in DLKP-A 2 only are likely to be reflective of the respective higher and lower total proteins identified for each sample. The inclusion of a peptide probability of 0.05 rendered the parameters more stringent and so no manual validation was carried out. The list of membrane proteins known to be expressed in DLKP-A, outlined in section 3.3.2 were again analysed for inclusion in the new membrane protein lists generated (table 3.3.3.2). The results were similar to previous findings with P-gp, annexin A1 and GLUT 3 being identified in both samples, ALDH 1 found in neither and HSP 70 variant 6 only observed in DLKP-A 1. This time, however, GLUT 1 and lamin B1 were not identified in the DLKP-A 1 sample. Although a larger number of the identified proteins over-lapped between samples, a smaller number of total proteins were identified and several more of the proteins known to be expressed in the DLKP-A membrane were not identified in the samples. For this reason this criteria will not be used for future analyses.

Protein numbers identified in DLKP-A 1 and 2

(a)

Sample	Condition	No. Of Proteins	% Of Total Proteins
DLKP-A 1	Total Proteins	367	
DLKP-A 2	Total Proteins	286	
DLKP-A 1 + DLKP-A 2	Total Proteins	432	
DLKP-A 1 + DLKP-A 2	Commonly Expressed Proteins	221	51%
DLKP-A 1	In DLKP-A 1 only	146	34%
DLKP-A 2	In DLKP-A 2 only	65	15%

(b)

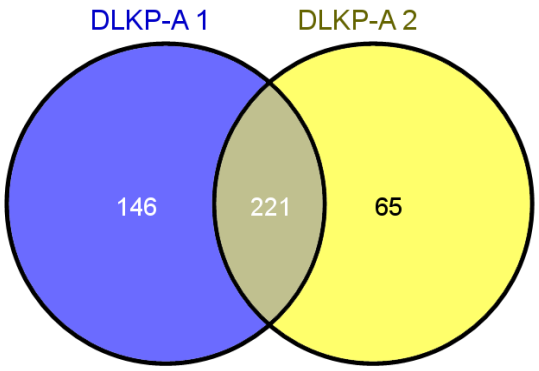

Figure 3.3.3.1 Comparison of numbers proteins identified in DLKP-A MS samples 1 and 2 with the additional application of a peptide probability of 0.05 on CID data, in table format (a) or as a Venn diagram (b).

Proteins identified in DLKP-A 1 and 2

Protein	DLKP-A 1	DLKP-A 2
P-glycoprotein	Yes	Yes
Annexin A1	Yes	Yes
GLUT 1	No	No
GLUT 3	Yes	Yes
HSP 70 variant 6	Yes	No
Lamin B1	No	No
ALDH A1	No	No

Table 3.3.3.3 The presence of membrane proteins known to be expressed in DLKP-A, identified in DLKP-A 1 and 2 with the additional application of a peptide probability of 0.05 on CID data.

3.3.4. Investigating the benefits of using both CID and ETD tandem MS methods

As mentioned previously, ETD adds another dimension to the fragmentation of peptides and subsequent identification of proteins. Where CID is good at fragmenting doubly charged peptides, ETD is superior at fragmenting triply charged peptides [150]. Analysing the data together also has benefits when including the criteria of 2 distinct peptides, as one peptide may be generated from CID with the other from ETD data. Also, the analysis outlined in section 3.3.3 indicated there was no added advantage of analysing the data separately to include a peptide probability of 0.05, as it proved unnecessarily stringent with the overall number of identifications greatly reduced. In this section, a more in depth analysis of the benefits of using both CID and ETD methods and an investigation into the impact of analysing them together was examined.

This work focused on the 50mM fraction from DLKP-A 1, as it was easier to work with a smaller number of proteins and it was representative of all the proteins identified from each fraction. The parameters outlined in section 3.3.2 were used. Firstly, the ETD and CID data was analysed separately. It can be observed from the data, that 38% of the total proteins were identified in both data generated from CID and ETD tandem MS, whereas 51% were found from CID and 11% from ETD (table 3.3.4.1). Thirteen extra proteins were identified with ETD (figure 3.4.1.1).

Next the CID and ETD MS data was pooled before analysis and results from this can be seen in table 3.3.4.2 and figure 3.3.4.2. This generated a higher number of protein identifications (table 3.3.4.2). The 139 proteins identified included all 117 of the proteins found in the previous CID and ETD data which had been analysed separately as well as 22 newly identified as shown in figure 3.3.4.2. The 22 proteins represent 16% of the total number identified which is a large enough proportion to warrant carrying all further analysis containing the criteria of 2 distinct peptides together.

Protein numbers identified in DLKP-A 1 50mM fraction

(a)

Sample	Condition	No. Of Proteins	% Of Total Proteins
CID Only	Total Proteins	104	
ETD Only	Total Proteins	57	
CID Only + ETD Only	Total Proteins	117	
CID Only + ETD Only	Commonly Expressed Proteins	44	38 %
CID Only	In CID only not ETD	60	51 %
ETD Only	In ETD only not CID	13	11 %

(b)

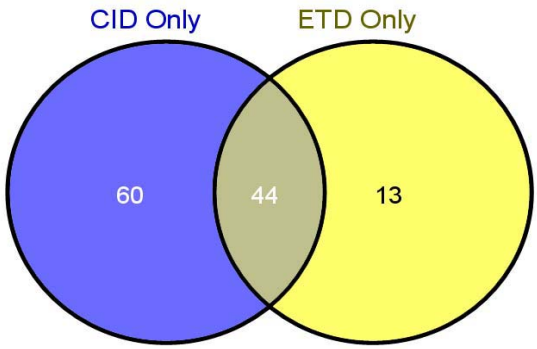

Figure 3.3.4.1 Comparison of numbers proteins identified in DLKP-A 50mM fraction from either CID or ETD tandem MS, in table format (a) or as a venn diagram (b).

Proteins identified in DLKP-A 1 50mM fraction

(a)

Sample	Condition	No. Of Proteins	% Of Total Proteins
CID + ETD Combined Analysis	Total Proteins	139	
ETD + CID Combined Analysis	In ETD + CID Combined Only	22	16%
CID Separate Analysis	In CID only and not in ETD + CID Combined	0	
ETD Separate Analysis	In ETD only and not CID + ETD Combined	0	

(b)

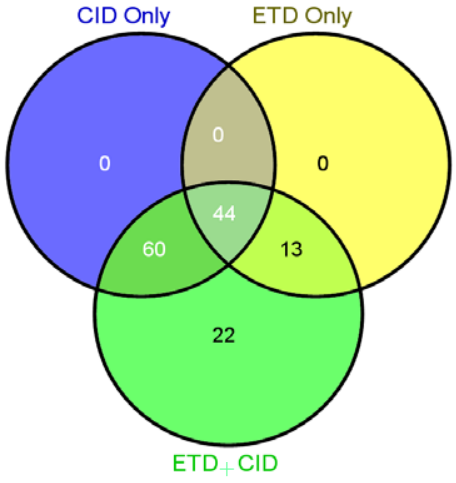

Figure 3.3.4.1 Comparison of numbers proteins identified in DLKP-A 50mM fraction from either CID or ETD tandem MS analysed together or separately, in table format (a) or as a Venn diagram (b).

3.3.5. Analysis of DLKP-A 1 and 2 tandem MS data with less stringent statistics; lower cross-correlation scores

As seen in section 3.3.2, the standard parameters appear to yield protein identifications with a good degree of confidence based on quality of fragmentation and continuity of b and y ion series. This sub-section investigated whether credible protein identifications were missed by the standard parameters set. Analysis was carried out on the combination of ETD and CID data from DLKP-A samples 1 and 2 with new less stringent XCorr scores. Two distinct peptides were still required; however, the cross-correlation scores assigned were lowered to the following; 1.5 for single charge, 1.9 for double charge, 2.5 for triple charge and 3 for quadruple charge.

Applying these parameters had a big impact on the number of proteins identified, with the total number rising to 1755. Although the number of overlapping proteins increased to 455 the % decreased to 26% compared with the standard parameters outlined in section 3.3.2. A large number of proteins were identified from the DLKP-A 2 sample only whereas a much smaller number were found in DLKP-A 1 only (table 3.3.5.1 and figure 3.3.5.1).

Again, five of the proteins with lower XCorr scores from each dataset were manually validated as described in section 3.3.2. Again all the proteins were deemed to be acceptable identifications and a list is shown in table 3.3.5.2. Ion series and mass spectrum data for two representative peptides from the validated proteins are displayed in figures 3.1.5.2 and 3.1.5.3. The zinc finger protein 749, a member of the zinc finger proteins whose functions are of a highly diverse nature and include, protein folding and assembly, DNA recognition and transcriptional activity, was identified in DLKP-A 1 and the b and y ion series and mass spectrum for one of its peptides with a mass of 1681.9 is shown in figure 3.1.5.2 [179]. In figure 3.3.5.3, the b and y ion series and mass spectrum for one of the peptides with a mass of 1662.7 from the tyrosine-protein phosphatase non-receptor type 14 also known as pez, is shown. This protein is involved in the cytoskeleton and cell adhesion and was previously identified in DLKP-A [180].

The identified protein lists were then checked for the presence of the 6 proteins known to be expressed in DLKP-A (section 3.3.2). In this case P-gp, annexin A1, GLUT 1 and 3, HSP 70 variant 6 and lamin B1 were all identified in both DLKP-A 1

and DLKP-A 2 with ALDH 1 being the only protein not identified in either (table 3.3.5.3).

Protein numbers identified in DLKP-A 1 and 2

(a)

Sample	Condition	No. Of Proteins	% Of Total Proteins
DLKP-A 1	Total Proteins	1559	
DLKP-A 2	Total Proteins	651	
DLKP-A 1 + DLKP-A 2	Total Proteins	1755	
DLKP-A 1 + DLKP-A 2	Commonly Expressed Proteins	455	26%
DLKP-A 1	In DLKP-A 1 only	196	11%
DLKP-A 2	In DLKP-A 2 only	1104	63%

(b)

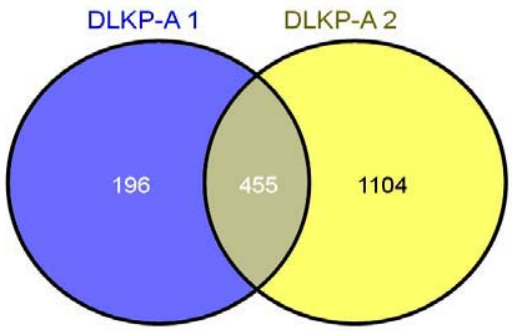

Figure 3.3.5.1 Comparison of numbers of proteins identified in DLKP-A MS samples 1 and 2 with the application of less stringent XCorr scores, in table format (a) or as a Venn diagram (b).

Validated proteins identified in DLKP-A 1 and DLKP-A 2

DLKP-A 1	DLKP-A 2
Zinc finger protein 749 (ZN749)	Tyrosine-protein phosphatase non-receptor type 14 (PTN14)
Ephexin-1 (NGEF)	Microtubule-associated protein 2 (MAP2)
Hydroxyacid oxidase (HAOX1)	Leucine-rich repeat-containing protein 45 (LRC45)
N-acetlygalactosaminyltransferase-like 4 (GLTL4)	Complement receptor type 2 (CR2)
DNA J homolog subfamily C member 11 (DJC11)	R3H domain-containing protein 1 (R3HD1)

Table 3.3.5.2 Proteins which were manually validated and deemed acceptable from the identified proteins in DLKP-A 1 and 2 MS samples with the application of less stringent XCorr scores.

B and y ion series and mass spectrum from peptide in DLKP-A 1

(a)

MW (Da) MW (Da)

	AA	A	B	B*	Bo	C	Y	Y*	Yo	Z	
1	D		116.03				-				13
2	F		263.10				1567.72				12
3	C		423.13				1420.65				11
4	H		560.19				1260.62				10
5	Q		688.25				1123.56				9
6	H		825.31				995.51				8
7	G		882.33				858.45				7
8	L		995.42				801.43				6
9	F		1142.48				688.34				5
10	E		1271.53				541.27				4
11	H		1408.59				412.23				3
12	Q		1536.64				275.17				2
13	K		-				147.11				1

(b)

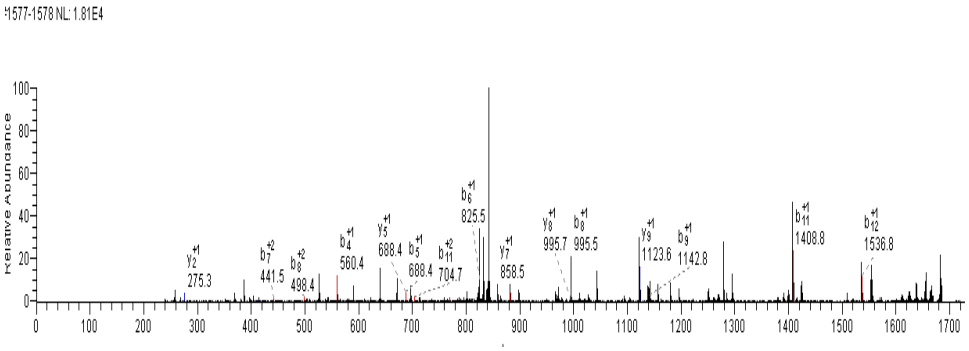

Figure 3.3.5.3 B and y ion series (a), and mass spectrum (b), corresponding to a peptide from zinc finger protein 749 (ZN 749), identified in DLKP-A 1 with the application of less stringent XCorr scores.

B and y ion series and mass spectrum from peptide in DLKP-A 2

(a)

MW (Da) MW (Da)

	AA	A	B	B*	Bo	C	Y	Y*	Yo	Z	
1	A		72.04				-				16
2	N		186.09				1589.79				15
3	G		243.11				1475.75				14
4	I		356.19				1418.73				13
5	F		503.26				1305.64				12
6	S		590.29				1158.57				11
7	T		691.34				1071.54				10
8	A		762.38				970.50				9
9	A		833.42				899.46				8
10	L		946.50				828.42				7
11	P		1043.55				715.34				6
12	E		1172.59				618.28				5
13	N		1286.64				489.24				4
14	A		1357.67				375.20				3
15	E		1486.72				304.16				2
16	R		-				175.12				1

(b)

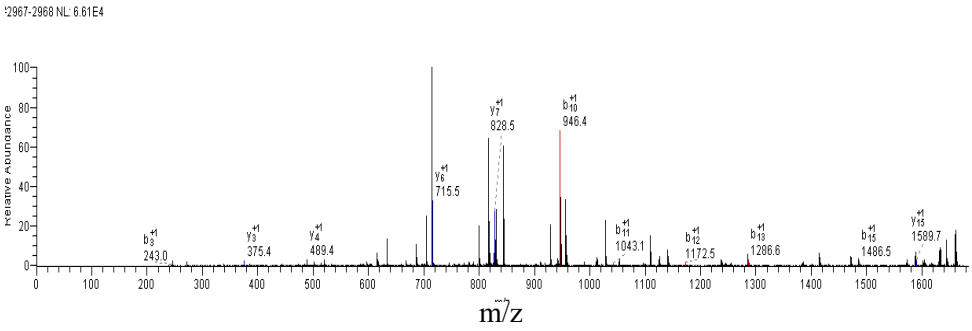

Figure 3.3.5.4 B and y ion series (a), and mass spectrum (b), corresponding to a peptide from tyrosine-protein phosphatase non-receptor type 14 identified in DLKP-A 2 with the application of less stringent XCorr scores.

Proteins identified in DLKP-A 1 and 2

Protein	DLKP-A 1	DLKP-A 2
P-glycoprotein	Yes	Yes
Annexin A1	Yes	Yes
GLUT 1	Yes	Yes
GLUT 3	Yes	Yes
HSP 70 variant 6	Yes	Yes
Lamin B1	Yes	Yes
ALDH A1	No	No

Table 3.3.5.3 The presence of membrane proteins known to be expressed in DLKP-A, identified in DLKP-A 1 and 2 with the application of more stringent XCorr scores.

3.3.6. Analysis of DLKP-A 1 and 2 tandem MS data with less stringent statistics; 1 distinct peptide

In section 3.3.5 less stringent parameters were applied to DLKP-A 1 and 2 MS data by increasing the XCorr scores and therefore accepting more protein identifications. Another aspect of the analysis which had been kept constant was the requirement of 2 distinct peptides for a positive identification. In this reanalysis, the parameters were altered to allow single peptides to be accepted, however, in order address quality control, the XCorr scores were increased to 2 for singly charged, 2.5 for doubly charged, 3.2 for triply charged and 3.5 for quadruple charged peptides.

Table and figure 3.3.5.1 shows how 1420 proteins were identified between both DLKP-A 1 and 2 samples. 40% of these were common to both with 452 (32%) identified in DLKP-A 1 only and 403 (28%) in DLKP-A 2 only.

As previously, ten proteins identified with lower x-correlation scores were validated (figure 3.3.6.2). Of the ten proteins manually analysed there was a lower degree of confidence in the identifications than previously seen, especially when taking into account that a second distinct peptide was not required. C and z, and b and y ion series and mass spectrums for two representative proteins are displayed in figures 3.3.6.2 and 3.3.6.3. The first of these figures shows the c and z ion series and mass spectrum for a peptide with a mass of 1553.57 from the arylsulfatase G protein, identified in DLKP-A 1. This protein hydrolyses sulfate esters in a wide variety of substrates such as glycosaminoglycans, steroid sulfates, or sulfolipids [181]. The second figure shows the b and y ion series and mass spectrum for the peptide of mass 2212.11 from the cadherin-4 protein, which is a transmembrane glycoprotein with roles in proliferation, differentiation and cell transformation, identified in DLKP-A 2 [182].

The proteins identified in DLKP-A 1 and 2 with the criteria of one peptide were checked for inclusion of the list of known membrane proteins expressed in DLKP-A (section 3.3.2). P-gp, annexin A1, GLUT 1 and 3 and HSP 70 variant 6 were identified in both DLKP-A 1 and 2, with lamin B1 and ALDH 1 not found in either DLKP-A 1 or 2 (table 3.3.6.3).

Protein numbers identified in DLKP-A 1 and 2

(a)

Sample	Condition	No. Of Proteins	% Of Total Proteins
DLKP-A 1	Total Proteins	1017	
DLKP-A 2	Total Proteins	968	
DLKP-A 1 + DLKP-A 2	Total Proteins	1420	
DLKP-A 1 + DLKP-A 2	Commonly Expressed Proteins	565	40%
DLKP-A 1	In DLKP-A 1 only	452	32%
DLKP-A 2	In DLKP-A 2 only	403	28%

(b)

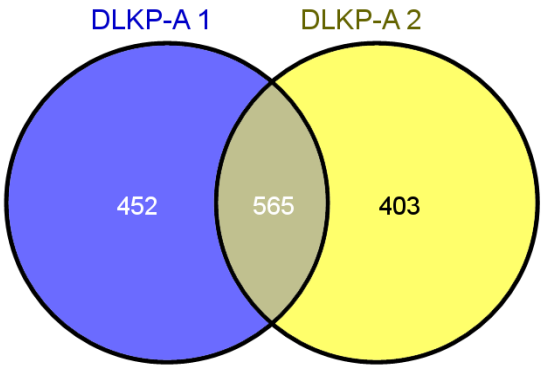

Figure 3.3.6.1 Comparison of numbers of proteins identified in DLKP-A MS samples 1 and 2, with the abolishment of the requirement for 2 distinct peptides, in table format (a) or as a Venn diagram (b).

Validated proteins identified in DLKP-A 1 and DLKP-A 2

DLKP-A 1	DLKP-A 2
Arylsulfatase G (ARSG)	Cadherin-4 (CADH4)
Gamma-taxilin (TXLNG)	Zinc finger protein 292 (ZN292)
Nuclear pore complex protein (Nup205)	S-phase kinase-associated protein 1 (SKP1)
Phosphatidlyinositol-4,5 bisphosphate phosphodiesterase (PLCG2)	Rap guanine nucleotide exchange factor 1 (RPGF1)
Zinc finger B-box domain containing protein 1 (ZBBX)	ALK tyrosine kinase receptor (ALK)

Table 3.3.6.2 Proteins which were manually validated and from the identified proteins in DLKP-A 1 and 2 MS samples with the abolishment of the requirement for 2 distinct peptides.

C and z ion series and mass spectrum from peptide in DLKP-A 1

(a)

						MW (Da)				MW (Da)	
	AA	A	B	B*	Bo	C	Y	Y*	Yo	Z	
1	D					133.06				-	14
2	T					234.11				1423.64	13
3	A					305.15				1322.60	12
4	N					419.19				1251.56	11
5	L					532.27				1137.52	10
6	D					647.30				1024.43	9
7	K					775.39				909.40	8
8	M*					922.43				781.31	7
9	A					993.47				634.27	6
10	S					1080.50				563.24	5
11	E					1209.54				476.20	4
12	G					1266.56				347.16	3
13	M					1397.60				290.14	2
14	R					-				159.10	1

(b)

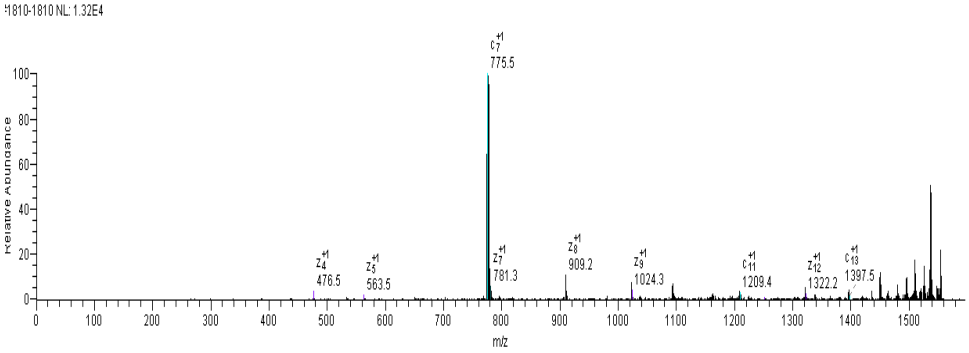

Figure 3.3.6.3 C and z ion series (a), and mass spectrum (b), corresponding to a peptide from arylsulfatase G identified in DLKP-A 1 with the abolishment of the requirement for 2 distinct peptides.

B and y ion series and mass spectrum from peptide in DLKP-A 2

(a)

		MW (Da)					MW (Da)				
	AA	A	B	B*	Bo	C	Y	Y*	Yo	Z	
		☐	☑	☐	☐	☐	☑	☐	☐	☐	
1	V		100.08				-				18
2	E		229.12				2112.99				17
3	N		343.16				1983.95				16
4	P		440.21				1869.91				15
5	I		553.30				1772.85				14
6	D		668.32				1659.77				13
7	L		781.41				1544.74				12
8	Y		944.47				1431.66				11
9	I		1057.56				1268.59				10
10	Y		1220.62				1155.51				9
11	V		1319.69				992.45				8
12	I		1432.77				893.38				7
13	D		1547.80				780.29				6
14	M*		1694.83				665.27				5
15	N		1808.88				518.23				4
16	D		1923.90				404.19				3
17	N		2037.95				289.16				2
18	R		-				175.12				1

(b)

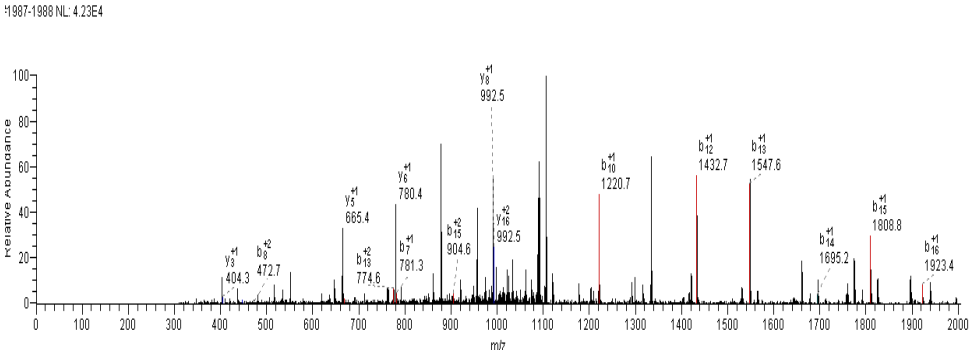

Figure 3.3.6.3 B and y ion series (a), and mass spectrum (b), corresponding to a peptide from cadherin-4 identified in DLKP-A 2 with the abolishment of the requirement for 2 distinct peptides.

Proteins identified in DLKP-A 1 and 2

Protein	DLKP-A 1	DLKP-A 2
P-glycoprotein	Yes	Yes
Annexin A1	Yes	Yes
GLUT 1	Yes	Yes
GLUT 3	Yes	Yes
HSP 70 variant 6	Yes	Yes
Lamin B1	No	No
ALDH A1	No	No

Table 3.3.6.3 The presence of membrane proteins known to be expressed in DLKP-A, identified in DLKP-A 1 and 2 with the abolishment of the requirement for 2 distinct peptides.

3.3.7. Assessment of mass spectrometry

The mass spectrometry data also provided a challenge when analysing a sample with such complexity. The repetition of identified proteins between DLKP-A sample 1 and its technical repeat was disappointing. Section 3.3.1 outlines the various aspects associated with liquid chromatography and it was determined to be of adequate quality, indicating that some issues may lie with the MS. This section aims to investigate this. Two proteins that were considered to be strong identifications in one DLKP-A sample and not identified in the other were chosen. These proteins were ADAM 10, identified in DLKP-A 2 and not in DLKP-A 1 and MRP1, identified in DLKP-A 1 and not DLKP-A 2.

Figure 3.3.7.1 and 3.3.7.2 show the mass spectra and b and y or c and z ion series for two peptides with isotopic masses of 449 and 419 from the ADAM 10 protein and indicate the excellent quality of the fragmentation and continuity with the ion series. A closer look was taken at the peptide of mass 420 from ADAM 10 with a retention time of 29.6 minutes, identified by ETD in the 500 mM fraction in DLKP-A 2 and an extraction of its ion and full MS is shown in figure 3.3.7.3. The mass spectrum from the corresponding fraction and area in DLKP-A 1 was then analysed for a peptide of this mass. Figure 3.3.7.4 shows from the ion extraction and full MS, a peak was generated for a peptide of this mass at a similar retention time of 30.5 min in DLKP-A 1. After this full MS, MS/MS was carried out on peptides with masses of 528.6 and 666.9 and when full MS was carried out the next time, the peptide of interest with mass 419.9 could no longer be seen as shown in figure 3.3.7.5.

A similar analysis was carried out for the MRP1 protein which was identified in DLKP-A 1 and not 2. Figures 3.3.7.6 and 3.3.7.7 show the quality of two of the peptides of masses 440.6 and 748.8 that lead to the identification of MRP1 in DLKP-A 1. The peptide of mass 440.6 with a retention time of 25.7, found in the 100mM ETD fraction of DLKP-A 1 was further analysed and the extracted ion and full MS corresponding to this peptide are displayed in figure 3.3.7.8. The equivalent fraction in DLPK-A 2 was scanned for peptides of this mass. Figure 3.3.7.9 shows the extracted ion and full MS corresponding to a peptide with the same mass that has a similar retention time as the 440.6 peptide for MRP1 in DLKP-A 2. The next full MS is shown in figure 3.3.7.10, and the peptide can no longer be seen.

B and y ion series and mass spectrum from peptide in DLKP-A 2

(a)

MW (Da) MW (Da)

	AA	A	B	B*	Bo	C	Y	Y*	Yo	Z	
1	R		157.11				-				11
2	P		254.16				1188.65				10
3	P		351.21				1091.60				9
4	Q		479.27				994.54				8
5	P		576.33				866.48				7
6	I		689.41				769.43				6
7	Q		817.47				656.35				5
8	Q		945.53				528.29				4
9	P		1042.58				400.23				3
10	Q		1170.64				303.18				2
11	R		-				175.12				1

(b)

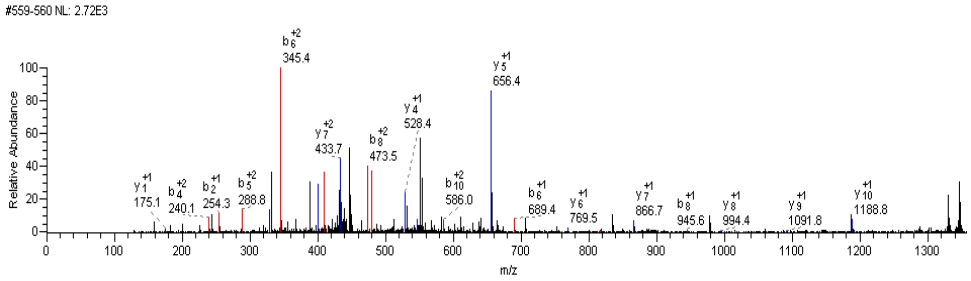

Figure 3.3.7.1 B and y ion series (a) and mass spectrum (b) corresponding to peptide of mass 449 for the ADAM 10 protein identified in DLKP-A 2.

C and z ion series and mass spectrum from peptide in DLKP-A 2

(a)

MW (Da) MW (Da)

	AA	A	B	B*	Bo	C	Y	Y*	Yo	Z	
1	L					131.12				-	12
2	P					228.17				1128.69	11
3	P					325.22				1031.64	10
4	P					422.28				934.58	9
5	K					550.37				837.53	8
6	P					647.42				709.44	7
7	L					760.51				612.38	6
8	P					857.56				499.30	5
9	G					914.58				402.25	4
10	T					1015.63				345.23	3
11	L					1128.71				244.18	2
12	K					-				131.09	1

(b)

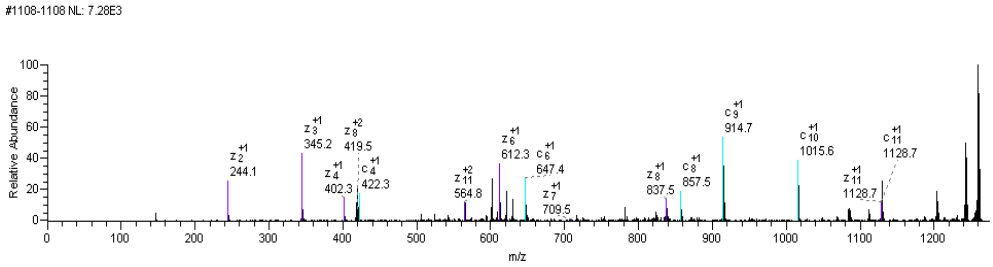

Figure 3.3.7.2 C and z ion series (a) and mass spectrum (b) corresponding to peptide of mass 420 for the ADAM 10 protein identified in DLKP-A 2.

Ion extraction and full MS from peptide in DLKP-A 2

(a)

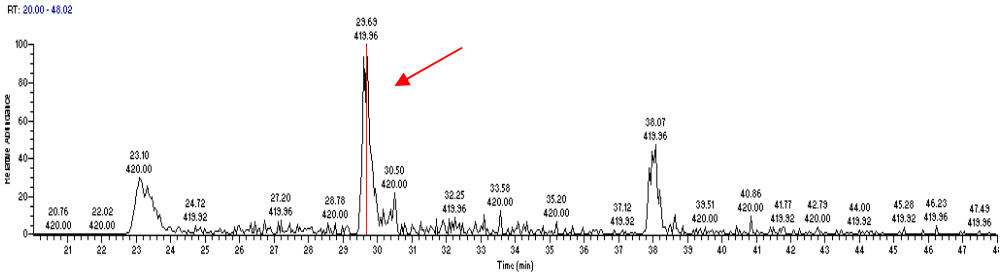

(b)

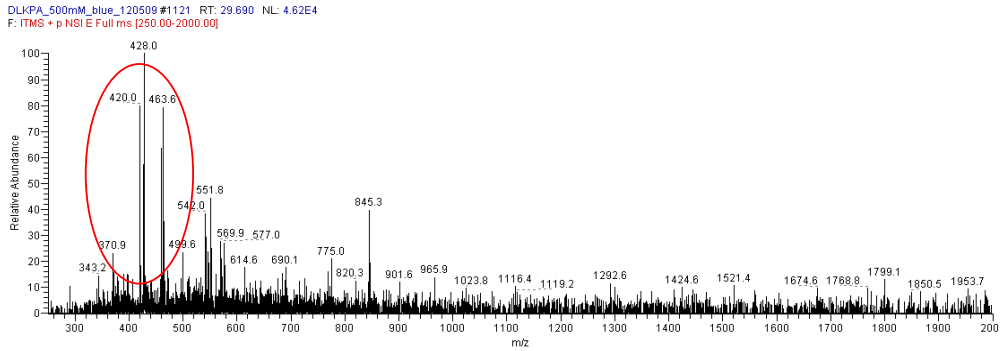

Figure 3.3.7.3 Ion extraction (a) and full mass spectrum (b) corresponding to peptide of mass 419 from ADAM 10 identified in DLKP-A 2. Peptide highlighted in each view.

Ion extraction and full MS from DLKP-A 1

(a)

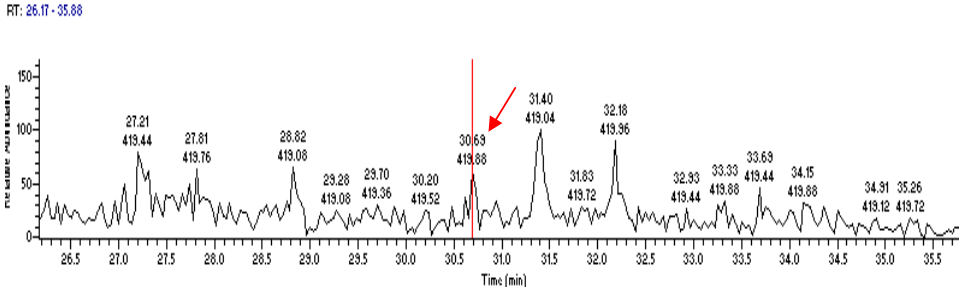

(b)

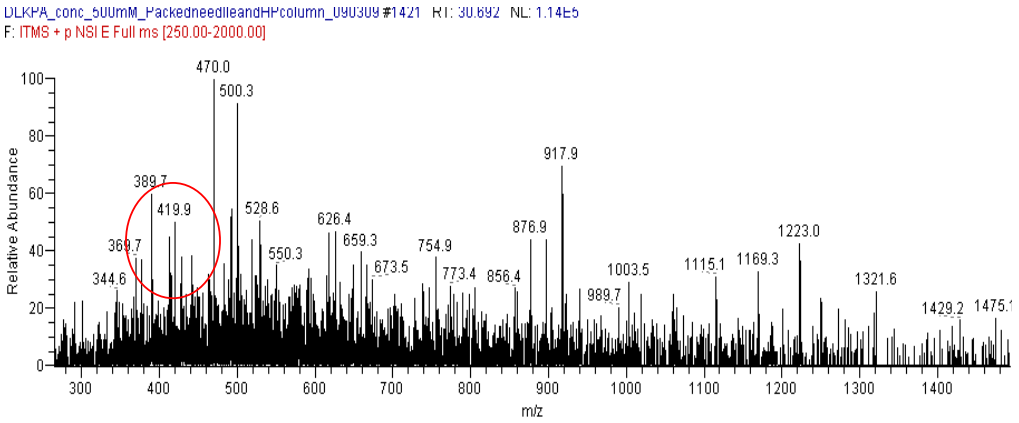

Figure 3.3.7.4 Ion extraction (a) and full mass spectrum (b) corresponding to same area in 500 mM fraction in DLKP-A 1 where peptide of mass 419 from ADAM 10 was identified in DLKP-A 2. Peptide highlighted in each view.

Full MS from DLKP-A 1

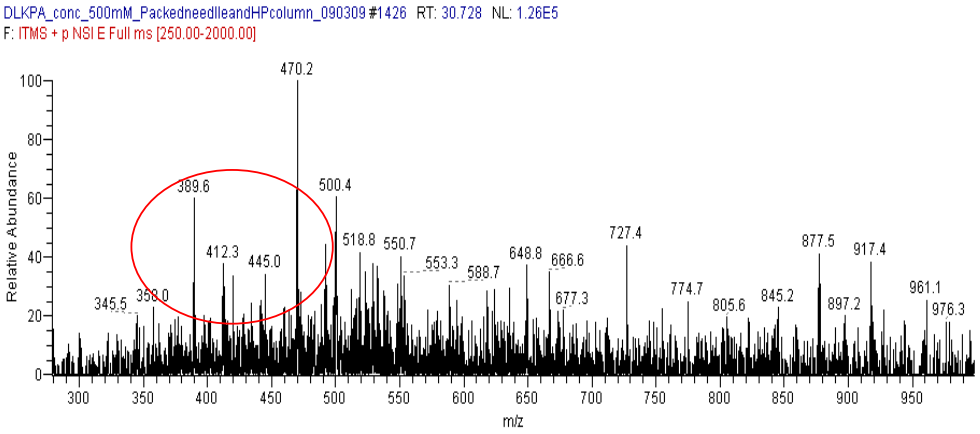

Figure 3.3.7.5 Full mass spectrum from 500mM fraction in DLKP-A 1 directly following the full MS in which the peptide of mass 420 was identified in DLKP-A 1. This peptide can no longer be seen and the area in which it would be expected is highlighted.

C and z ion series and mass spectrum from peptide in DLKP-A 1

(a)

MW (Da) MW (Da)

	AA	A	B	B*	Bo	C	Y	Y*	Yo	Z	
1	V					117.10				-	12
2	V					216.17				1203.61	11
3	Y					379.23				1104.54	10
4	S					466.27				941.48	9
5	S					553.30				854.45	8
6	K					681.39				767.42	7
7	D					796.42				639.32	6
8	P					893.47				524.30	5
9	A					964.51				427.24	4
10	Q					1092.57				356.21	3
11	P					1189.62				228.15	2
12	K					-				131.09	1

(b)

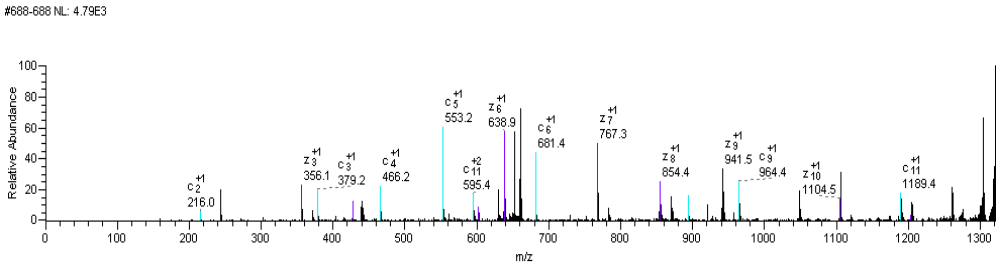

Figure 3.3.7.6 C and z ion series (a) and mass spectrum (b) corresponding to peptide of mass 440.6 for the MRP1 protein identified in DLKP-A 1.

B and y ion series and mass spectrum from peptide in DLKP-A 1

(a)

		MW (Da)				MW (Da)				
1	I		114.09				-			13
2	S		201.12				1383.66			12
3	E		330.17				1296.63			11
4	M		461.21				1167.58			10
5	G		518.23				1036.54			9
6	S		605.26				979.52			8
7	Y		768.32				892.49			7
8	Q		896.38				729.43			6
9	E		1025.42				601.37			5
10	L		1138.51				472.32			4
11	L		1251.59				359.24			3
12	A		1322.63				246.16			2
13	R		-				175.12			1

(b)

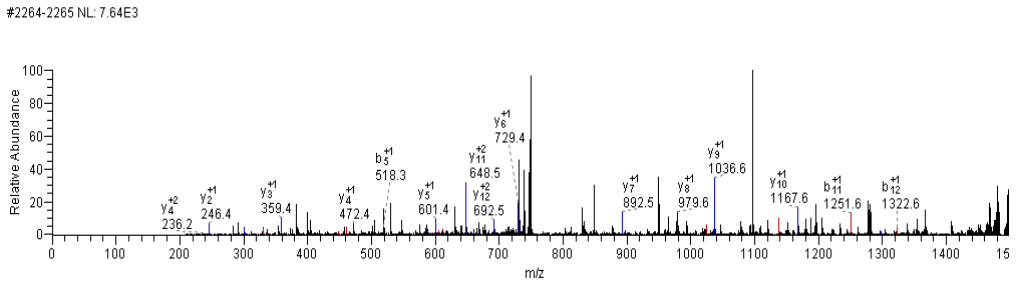

Figure 3.3.7.7 B and y ion series (a) and mass spectrum (b) corresponding to peptide of mass 748.8 for the MRP1 protein identified in DLKP-A 1.

Ion extraction and full MS from peptide in DLKP-A 1

(a)

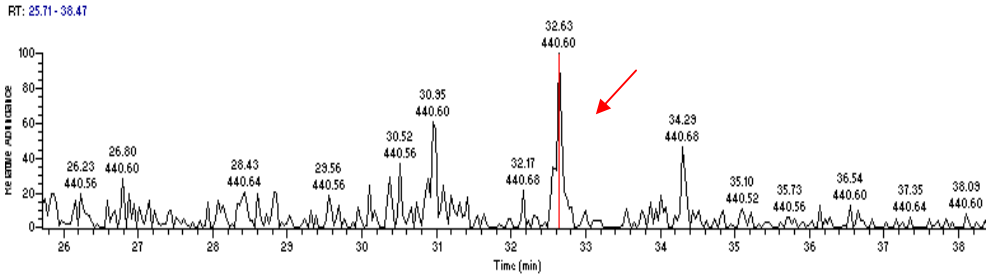

(b)

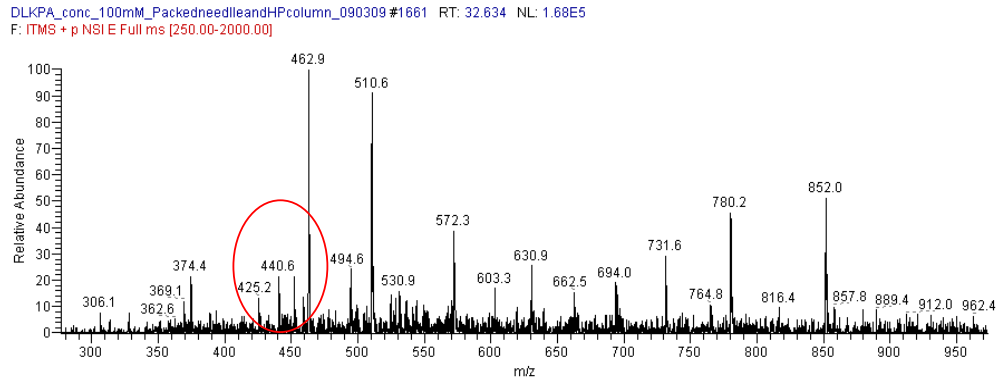

Figure 3.3.7.8 Ion extraction (a) and full mass spectrum (b) corresponding to peptide of mass 440.6 from MRP1 identified in DLKP-A 1. Peptide is highlighted in each view.

Ion extraction and full MS from DLKP-A 2

(a)

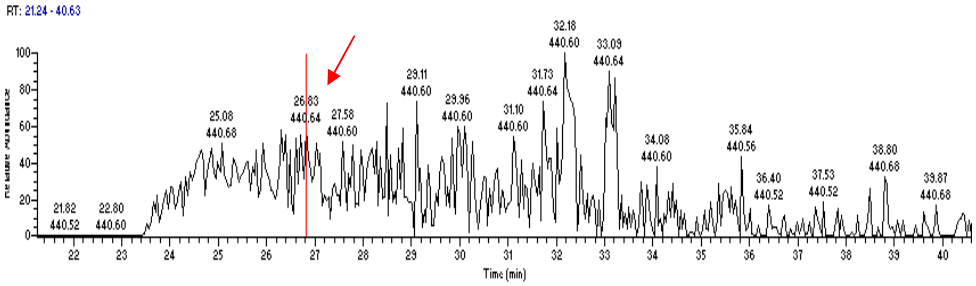

(b)

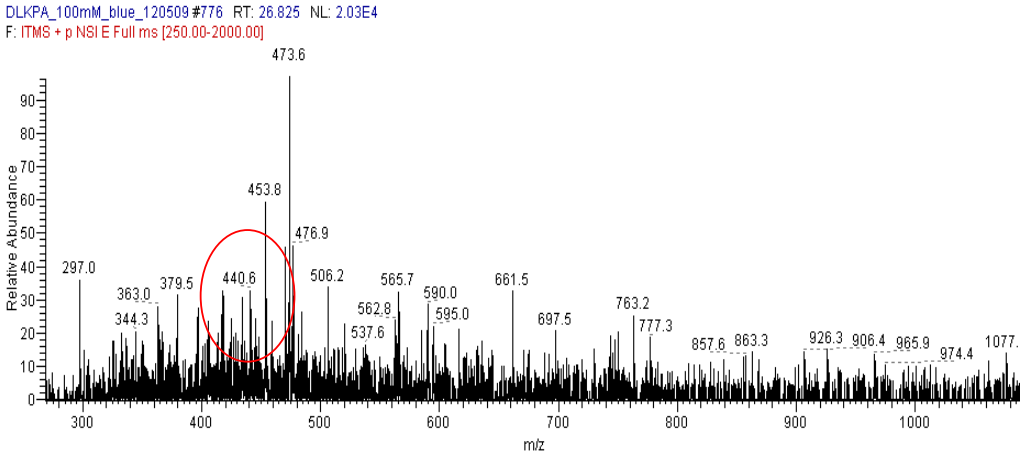

Figure 3.3.7.9 Ion extraction (a) and full mass spectrum (b) corresponding to same area in 100 mM ETD fraction in DLKP-A 2 where peptide of mass 440.6 from MRP1 was identified in DLKP-A 1. Peptide is highlighted in each view.

Full MS from DLKP-A 2

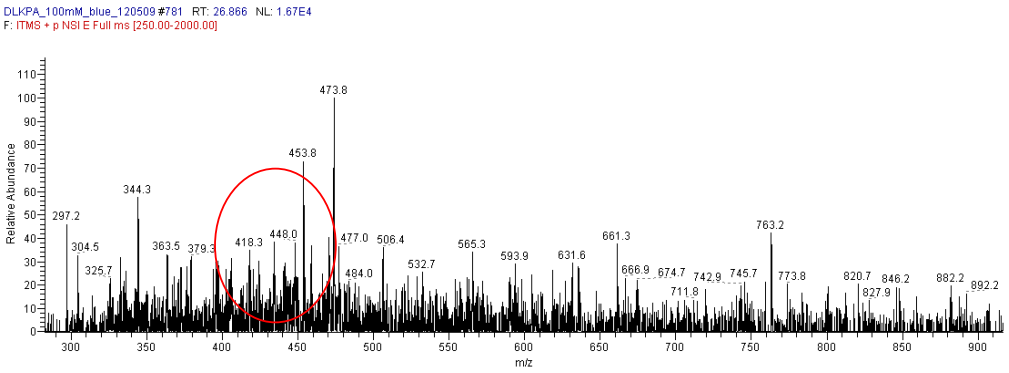

Figure 3.3.7.10 Full mass spectrum from 100mM ETD fraction in DLKP-A 1, directly following the full MS in which the peptide of mass 420 was identified in DLKP-A 1. This peptide can no longer be seen and the area in which it would be expected is highlighted.

3.3.8. Analysis of DLKP tandem MS data

Based on the findings outlined in sections 3.3.2 – 3.3.6, the most suitable parameters to identify membrane proteins from MS data were determined to be those employed in section 3.3.4. This was due to a large number of proteins identified with good quality mass spectrometry observed in the validated proteins and the inclusion of five out of the six proteins from the list of known membrane proteins to be expressed in DLKP-A.

Membrane protein isolation was also carried out on a DLKP cell preparation and it was subjected to 2D LC MS and analysed with the most suitable parameters (section 3.3.5). A technical repeat was also carried out of this sample and so analysis was carried out on that also (DLKP 2).

In total, for DLKP 1 and 2 2444 proteins were identified. 775 proteins which represented 32% of the total proteins were identified in both sample 1 and 2, with 1081 found in DLKP 1 only and 588 in DLKP 2 only (table 3.3.8.1 and figure 3.3.8.1)

Protein numbers in DLKP 1 and 2

(a)

Sample	Condition	No. Of Proteins	% Of Total Proteins
DLKP 1	Total Proteins	1856	
DLKP 2	Total Proteins	1363	
DLKP 1 + DLKP 2	Total Proteins	2444	
DLKP 1 + DLKP 2	Commonly Expressed Proteins	775	32%
DLKP 1	In DLKP 1 only	1081	44%
DLKP 2	In DLKP 2 only	588	24%

(b)

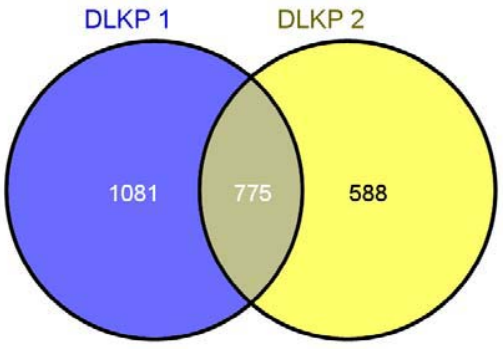

Figure 3.3.8.1 Comparison of numbers of proteins identified in DLKP MS samples 1 and 2 with the application of the parameters in section 3.3.5, in table format (a) or as a Venn diagram (b).

3.3.9. Differentially detected membrane proteins in parent DLKP and resistant variant DLKP-A

A comparison was made between proteins found in the parent cell line DLKP and its resistant variant DLKP-A, so as to potentially determine proteins with a role in drug resistance. In order to determine proteins which were differentially identified, proteins that were common to the original DLKP and DLKP-A samples (1) and their repeats (2) were compared.

590 proteins were observed to be differentially detected with 455 identified in DLKP and not in DLKP-A and 135 identified in DLKP-A and not DLKP (table 3.3.9.1 and figure 3.3.9.1). Multidrug resistant proteins 1 (P-gp) and 3, which are known to have a role in resistance were identified in the resistant variant but not the parent [183]. Other proteins which may have a role in resistance were also identified and outlined in table 3.3.9.2.

Protein numbers in DLKP and DLKP-A

(a)

Sample	Condition	No. Of Proteins	% Of Total Proteins
DLKP	Total Proteins	775	
DLKP-A	Total Proteins	455	
DLKP + DLKP-A	Total Proteins	910	
DLKP + DLKP-A	Commonly Expressed Proteins	320	35%
DLKP	In DLKP only	455	50%
DLKP-A	In DLKP-A only	135	15%

(b)

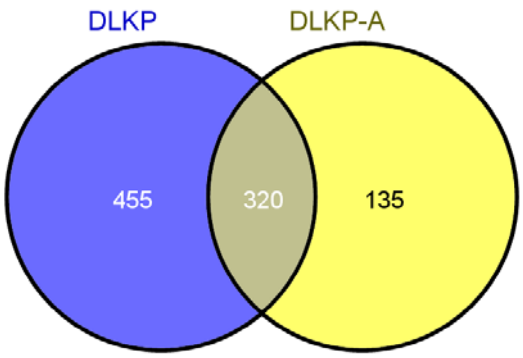

Figure 3.3.9.1 Comparison of numbers of proteins identified in DLKP and its resistant variant DLKP-A MS sample with the application of the parameters in section 3.3.5, in table format (a) or as a Venn diagram (b).

Differentially detected proteins in resistant DLKP-A

Proteins identified in DLKP-A but absent from DLKP	
Protein	**Function**
P-glycoprotein (MDR1)	Transport
Multidrug resistant protein 3 (MDR3)	Transport
Heat shock protein 70 (HSP71)	Stress response
Lamin B1	Cytoskeleton
Vimentin	Cytoskeleton
Cadherin 2	Signalling/Adhesion
Integrin beta-4	Cytoskeleton

Table 3.3.9.2 List of possible resistance-related proteins identified in DLKP-A and not its sensitive parent cell line, DLKP.

3.3.10. Differentially detected membrane proteins in parent A549 and resistant variant A549-T

Membrane proteins were also isolated from cell preparations of A549 and A549-T and these were analysed as above. As in section 3.3.8 proteins identified in the parent cell line A549 were compared with those identified in its resistant variant A549-T. 35% of the total identifications were found in both A549 and its resistant variant A549T. Proteins which were identified in A549-T and not A549 and have a potential role in resistance add up to 979 (table and figure 3.3.10.1). Four proteins of interest were found to be differentially detected between A549-T and A549 are outlined in table 3.3.10.2.

Protein numbers identified in A549 and A549-T

(a)

Sample	Condition	No. Of Proteins	% Of Total Proteins
A549	Total Proteins	1969	
A549-T	Total Proteins	2003	
A549 + A549-T	Total Proteins	2848	
A549 + A549-T	Commonly Expressed Proteins	1024	35%
A549	In A549 only	945	32%
A549-T	In A549-T only	979	33%

(b)

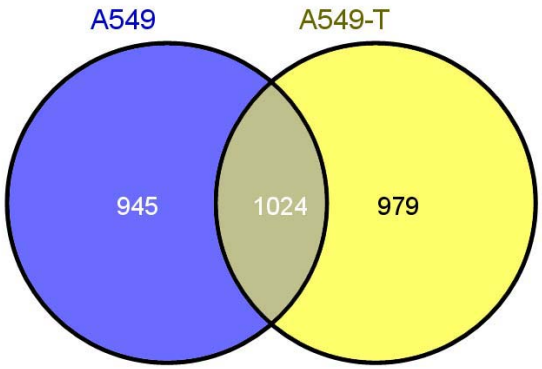

Figure 3.3.10.1 Comparison of numbers of proteins identified in A549 and its resistant variant A549-T MS sample with the application of the parameters in section 3.3.5, in table format (a) or as a Venn diagram (b).

Differentially detected proteins in resistant A549-T

Proteins identified in A549-T but absent from A549	
Protein	**Function**
ABCA3	Transport
ABCB5	Transport
ADAM-17	Stress response
ATP7B	Transport

Table 3.3.10.2 List of possible resistance-related proteins identified in A549-T and not its sensitive parent cell line, A549.

3.3.11. Comparison of proteins expressed only in resistant DLKP-A and A549-T

In section 3.3.10 and 3.3.11, lists of proteins detected in DLKP-A only and A549-T only compared with their parent cell lines DLKP and A549, respectively, were established. It was of interest to see if any of the proteins potentially associated with resistance were commonly expressed in these two very different resistant cell lines. 18 proteins were common to both resistant cell lines, indicating these proteins may have a robust role in resistance, regardless of the how the resistance is developed (table 3.3.11.1 and figure 3.3.11.1). Two of the 18 proteins commonly identified were interesting and they are outlined in table 3.3.11.2.

Protein numbers identified in DLKP-A and A549-T

(a)

Sample	Condition	No. Of Proteins	% Of Total Proteins
DLKP-A	Total Proteins	134	
A549-T	Total Proteins	978	
DLKP-A + A549-T	Total Proteins	1095	
DLKP-A + A549-T	Commonly Expressed Proteins	18	2%
DLKP-A	In DLKP-A only	116	11%
A549-T	In A549-T only	961	87%

(b)

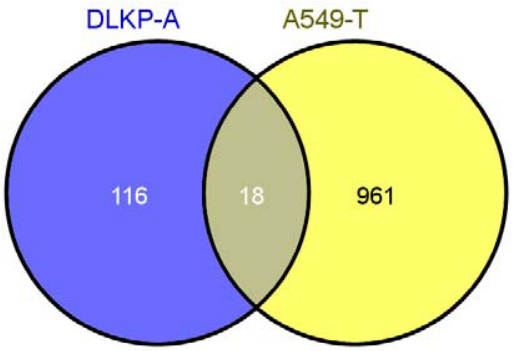

Figure 3.3.11.1 Comparison of numbers of proteins identified in the resistant DLKP-A and A549-T only compared with parental cell lines, MS samples with the application of the parameters in section 3.3.5, in table format (a) or as a Venn diagram (b).

Differentially detected proteins in resistant DLKP-A and A549-T

Proteins identified in A549-T and DLKP-A but absent from A549 and DLKP	
Protein	**Function**
Coxsackievirus and adenovirus receptor	Signalling
Integrin beta-4	Cytoskeleton

Table 3.3.11.2 List of possible resistance-related proteins identified in DLKP-A and A549-T and not their sensitive parent cell lines, DLKP and A549.

3.3.12. Differentially detected membrane proteins in A549-T and A549-T treated with lapatinib

In section 3.1 it was shown how lapatinib had the ability to alter levels of some of the membrane proteins. In order to investigate this using membrane proteomics, membrane proteins were also isolated from A549-T cells that had been treated for 48 hours with 2.5 μM lapatinib. This time point and concentration of lapatinib were chosen as a clear change in P-gp and MRP1 proteins were observed at these conditions as outlined in section 3.1.

It can be observed from table 3.3.12.1 and figure 3.3.12.1 that of the 2926 proteins identified 1924 were differentially identified, with 963 found only in A549-T and 923 found only in A549-T treated with lapatinib. Table 3.3.12.2 outlines three of the interesting proteins identified in the lapatinib treated A549-T sample.

Protein numbers identified in A549-T and A549-T lapatinib treated

(a)

Sample	Condition	No. Of Proteins	% Of Total Proteins
A549-T	Total Proteins	2003	
A549-T + L	Total Proteins	1963	
A549-T + A549-T + L	Total Proteins	2926	
A549-T + A549-T + L	Commonly Expressed Proteins	1040	35%
A549-T	In A549-T only	963	33%
A549-T + L	In A549-T + L only	923	32%

(b)

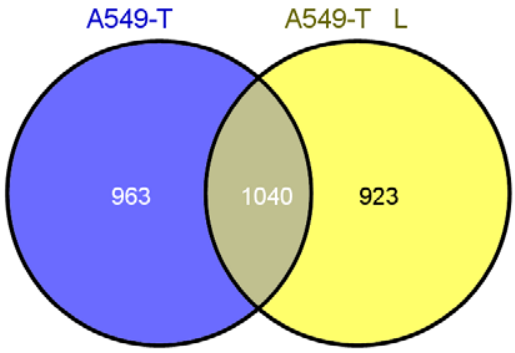

Figure 3.3.12.1 Comparison of numbers of proteins identified in A549-T and A549-T lapatinib treated, MS samples with the application of the parameters in section 3.3.5, in table format (a) or as a Venn diagram (b)

Differentially detected proteins in lapatinib treated A549-T

Proteins identified in lapatinib treated A549-T but absent from untreated A549-T	
Protein	**Function**
ABCC3 (MRP3)	Transport
ABCA5	Transport
Calrecticulin	Stress response

Table 3.3.12.2 List of proteins of interest identified in A549-T treated with lapatinib and not in untreated A549-T.

Chapter 4 Discussion

The work carried out in this thesis aimed to increase our understanding of various aspects of multidrug resistance, using the following approaches:

1. Investigating the role of lapatinib in multidrug resistant cell lines and further examining its modulatory effects on drug transporter pumps.
2. Determining the involvement of proteins of interest in multi-drug resistance using siRNA mediated knock-down.
3. Utilising and optimising a proteomic method to successfully identify membrane proteins involved in multidrug resistance.

4.1. The role and effects of lapatinib in drug resistant cancers

The following body of work utilised two different paired models of lung cancer resistance in order to evaluate the potential therapeutic contribution of lapatinib in resistant cancers and the potential effects of such treatments. Multidrug resistance, characterised by an increase in drug efflux ATP binding cassette transporters, remains a challenge in many current cancer therapies. Strategies to overcome multidrug resistance are therefore currently sought after [184]. Targeted therapies aimed at more cancer-specific pathways are being developed in order to address issues of toxicity associated with current less specific chemotherapy drugs. One group of targeted agents namely, the tyrosine kinase inhibitors, appear to have the qualities of a double edged sword, in that they may be able to tackle both issues of resistance and toxicity [103, 108, 185]. Lapatinib, a recently approved EGFR and HER-2 tyrosine kinase inhibitor, has shown much promise in its clinically approved use in combination with capecitabine in patients with advanced metastatic breast cancer. It has proved a more potent *in vitro* inhibitor of kinase activity compared with previously developed gefitinib and erlotinib which only inhibit the tyrosine kinase domain of EGFR and so it is likely that it may have a role outside of its current approved use [89, 186, 187]. There has been some investigation into lapatinib anti-tumour actions outside of breast cancer and the evidence to date indicates some clear activity in bladder, gastric and ovarian carcinomas as well as in NSCLC [127, 188-190]. As outlined previously, lapatinib has the ability to modulate and inhibit P-glycoprotein (P-gp) functions [108, 109]. This thesis focuses on establishing if it has other resistance modulatory activity.

4.1.1. Lapatinib as a potential therapy in resistant lung cancer

The lung cell lines chosen to carry out these studies, DLKP-A and A549-T, represent good models of multidrug resistance, having 300-fold and 5-fold resistance respectively to adriamycin (doxorubicin) and taxol (paclitaxel). They both display cross resistance to a number of other chemotherapy drugs and over-express the drug efflux transporter P-gp, thereby attempting to mirror the phenomenon of resistance found in the clinic [34]. As mentioned in the results section, DLKP is a cell line established from a lymph node biopsy of a 52 year old male diagnosed with a poorly differentiated squamous cell carcinoma of the lung. DLKP-A is a drug-selected variant generated from exposure of DLKP cells to increasing concentrations of doxorubicin. DLKP-A demonstrated a 254-fold resistant to adriamycin, as well as displaying cross-resistance to VP-16, VM-26, colchicine, vincristine and cisplatin due to significant P-gp over-expression [159]. The adenocarcinoma cell line, A549, was pulse-selected with clinically relevant levels of the chemotherapeutic, paclitaxel, to generate the resistant variant A549-T. In this case, the selected cell line displayed a more modest resistance to taxol and cross-resistance to VP-16, vincristine, carboplatin and doxorubicin is also evident with a moderate over-expression of P-gp [49, 109, 157]. The initial establishment of IC50 values in this project found the fold differences in resistance to doxorubicin in DLKP-A, and to paclitaxel in A549-T to be 204 and 3, respectively. Of note, the reduced resistance from 300-fold to 204-fold in DLKP-A and 5-fold to 3-fold in A549-T is likely to be due to instability of resistance over time.

Although several targeted therapies have proved successful in the clinic, it is unlikely in the near future that they will completely replace chemotherapy drugs. Despite the toxicity profile associated with chemotherapy agents, they remain a successful treatment, and so it is more likely that targeted agents will more generally be employed in combination with these more traditional drugs. In this project it was sought to establish if lapatinib could add synergistically, to the toxic effects of a panel of chemotherapy drugs in our two paired MDR cell models. Lapatinib proved successful in both resistant cell lines, DLKP-A and A549-T, enhancing the cytotoxic actions of a variety of chemotherapy agents (epirubicin, paclitaxel, docetaxel and vinblastine) (figure 3.1.2.1-3.1.2.9). The large decrease in cell survival, associated

with the addition of lapatinib in DLKP-A and A549-T was significant in all cases with the exception of epirubicin in A549-T. A considerable decrease in cell survival was observed with the combination of lapatinib and epirubicin in A549-T, and the lack of significance was most likely owed to the larger standard deviations associated with this data. These larger standard deviations are more than likely associated with experimental error related to chemotherapy drug concentrations which is not all that uncommon with the very toxic drugs. This increased toxicity proved concentration-dependent on the part of lapatinib with 1μM of the TKI producing the most pronounced effect on cell survival. A decrease in survival were observed in DLKP and A549 with the addition of lapatinib to epirubicin or paclitaxel and epirubicin or vinblastine, respectively (figure 3.1.2.10-3.1.2.14), although this was not significant. Although in some cases it was an additive effect, synergy was observed with epirubicin and vinblastine in A549 and epirubicin and paclitaxel in DLKP. The increase in toxicity in these non-P-gp over-expressing cell lines was, considerably less than that observed in DLKP-A and A549-T. One of the major cellular features, distinguishing the resistant from the parent cell lines is the over-expression of P-gp, and so it is conceivable that this contributes to the differences in toxicity observed with lapatinib combinations.

Based on literature evidence, it is hypothesised that the synergistic toxic actions of lapatinib with the chemotherapy drugs, is due to its P-gp-inhibitory activity, thereby allowing more of the chemotherapy drug to accumulate [109]. This is a very plausible explanation, as the same level of synergy was not observed in the parental cell lines as in their resistant P-gp over-expressing counterparts. Apoptosis levels in the DLKP-A and A549-T cells, increased with the addition of lapatinib which is consistent with an increased accumulation of cytotoxic drug in the cells. In support of this also, the addition of lapatinib in combination with the non-P-gp substrate chemotherapy agent, 5-fluorouracil, in DLKP-A produced no increase in toxicity. The synergistic toxicity seen in the parent cell lines with lapatinib combinations, were unanticipated and would suggest an alternative mechanism for the synergistic behaviour of the TKI. It is unlikely to be associated with EGFR or HER-2 signalling, as these cell lines express relatively low levels of these growth factor receptors [109]. Lapatinib may be affecting another element of the transport of these drugs, but the mechanism as yet remains unknown.

The increased toxicity observed with lapatinib-P-gp substrate combinations, in the P-gp over-expressing cell lines, is consistent with other findings in the literature whereby, lapatinib has been shown to enhance the accumulation of chemotherapy agents in drug-resistant P-gp-expressing cell lines [108, 109]. These findings demonstrate a potential use for lapatinib in the clinic outside its approved use in HER-2-over-expressing metastatic breast cancer. DLKP-A and A549-T cell lines have relatively low levels of EGFR and HER-2, the primary targets for lapatinib [109]. It may therefore have a role as a P-gp modulating agent, and be given in combination with chemotherapy agents in patients with advanced cancers, so as to decrease the clearance of chemotherapy drugs. Unlike other P-gp inhibitors which have been developed, lapatinib has been established to have an acceptable toxicity profile. However, it is important to note, greater accumulation of chemotherapy drugs might occur in all P-gp over-expressing tissues in the body as a result of this, and may increase toxicity in these normal tissues. High P-gp expression is found in the biliary canaliculi of the liver, the proximal tubules of the kidneys, and the small intestine, colon, and adrenal cortex [191, 192]. A report by Sikic *et al.,* (1997), summed up some of the potential toxicities associated with reduced P-gp activities in these tissues. They indicated gastrointestinal toxicity was not an issue with P-gp inhibition. No additional toxicity on the central nervous system was reported in clinical trials despite it being observed in MDR-knockout mice [193]. A reduction in the amount of drug administered may balance out any of the potential toxicities. Several, more recent, clinical trials investigating the efficacy of lapatinib with chemotherapy drugs have indicated increased toxicity not to be major problem and combinations have proved tolerable. Phase I/II trials of lapatinib with various chemotherapy agents such as topotecan, docetaxel and paclitaxel indicated favourable results, with the combinations being well tolerated [125, 129, 130, 194].

4.1.2. Lapatinib-induced alterations in drug transporter expression

It is clear that lapatinib can interact with and inhibit the energy-dependent pumping mechanism of P-gp [109, 110]. Preliminary results in our laboratory showed that lapatinib has the ability to increase P-gp protein levels [165]. The ability of the drug to interact with the P-gp protein in this way is unusual, and in effect it is having somewhat conflicting actions; up-regulation of the protein might be anticipated to increase resistance through the efflux of substrate drugs, although, it has the ability to

inhibit this proteins' efflux mechanism. Ultimately due to the ability of P-gp to confer multidrug resistance, this could have devastating effects in the clinic. This project therefore, sought to examine the nature of this lapatinib-induced alteration in drug transporter level and any potential impact it may have on treatment.
In A549-T, lapatinib treatment did in fact; induce an increase in P-gp expression. This was determined to be in a dose-dependent manner and was induced with concentrations of lapatinib as low as 0.1 μM. These findings were robust, with an increase in P-gp observed across a variety of time points (24, 48 and 72 hours). By way of validation, the effect of lapatinib on P-gp expression was also analysed in H1299-T, a cell line with moderate P-gp over-expression, and an increase in the drug transporter expression was also observed (section 3.1.5).

MRP1 is another well established drug transporter with a role in mediating MDR, therefore alterations in its levels were also examined following lapatinib treatment. Of interest and perhaps somewhat unexpected, lapatinib treatment had an opposing effect on MRP1 expression than that seen on P-gp levels. Treatment with lapatinib in A549-T cells, at various time points and concentrations, resulted in a decrease in MRP1 expression as shown in section 3.1.5. MRP1 levels were also analysed in the parent cell line, A549, and they were also decreased with lapatinib treatment. At this point it should be noted that BCRP expression was also analysed for expression changes with lapatinib, however, no detectable levels were observed in control samples and so no conclusive results were obtained. To our knowledge lapatinib has not previously been shown to alter levels of this drug transporter, and so these novel findings warranted further work to investigate the potential mechanism and any further implications of this protein alteration.

The induction of P-glycoprotein and other drug transporters is largely governed by a small number of nuclear hormone receptors, called 'xenosensors' [166]. The pregnane X receptor (PXR) and constitutive androstane receptor (CAR) are two transcription factors which detect xenobiotics and stimulate genes encoding proteins involved in their detoxification and elimination [195]. In order to establish if lapatinib may be exerting its actions on P-gp protein level through these 'xenosensors', P-gp mRNA levels were determined in response to lapatinib. RT-PCR analysis carried out, indicated no corresponding change in mRNA levels of the drug

transporter P-gp and so the increase in protein level is likely to be a post transcriptional effect and not due to transcriptional activity from PXR or CAR receptor (figure 3.1.7.1 and 3.1.7.2). In support of this, lapatinib could not induce the expression of P-gp in A549 which had no detectable levels of the protein initially. These findings suggest its actions are occurring at the protein level and its does not have the ability to drive transcription of the ABCB1 gene.

The MRP1 alteration in expression did not occur at a transcriptional level either, as RT-PCR results indicate no lapatinib-induced change in ABCC1 mRNA levels. As lapatinib had an opposing effect on MRP1 levels to P-gp, it is possible that the effect on MRP1 levels is directly as a result of alterations in P-gp levels. There is evidence to suggest that mechanisms of resistance conferred by the drug transporters are linked. Liver cells exposed to the toxic insult of endotoxin exhibited an increase in MRP1 and MDR1b whereas a marked decrease in MRP2 was observed [196]. In a doxorubicin resistant lung cell line, the over-expression of P-gp was accompanied with a decrease in expression of BCRP when in a drug free state [197]. A relationship between P-gp and MRP1 has also been reported. In AML cell lines, lower concentrations of doxorubicin-induced MRP expression but higher concentrations resulted in an over-expression of P-gp. Across a number of AML (Acute Myeloid Leukaemia) cell lines this research also showed that increasing P-gp expression decreased amounts of MRP, suggesting P-gp can negatively regulate MRP expression [198]. It may therefore be possible that altered expression of one ABC transporter may be compensated by another, in this case up-regulation of P-gp resulting in down-regulation of MRP1.

As P-gp appears to be the primary mediator of MDR in the resistant lung cell models chosen for this study, further work was carried out to investigate the nature of the P-gp increase. Of great interest, the increase in P-gp induced by this TKI was sustained up to 120 hours following removal of lapatinib (section 3.1.10). There is however, a level of uncertainty with these conclusions as quantification studies showed residual levels of lapatinib were present at 120 hours after its removal. It is difficult to determine if lapatinib was active in the cells at these concentrations and if so whether it had an effect on P-gp or if the increased protein is of a sustained nature.

The residual nature of the increased expression of P-gp seemed unusual and further investigations were carried out to gain a greater insight into the nature of the

lapatinib-induced increase in this protein level and to determine if a real increase being observed. The addition of lapatinib to A549-T cell lysates, had no effect on P-gp protein level, indicating normal cellular functions are necessary for the process. Protein synthesis and degradation are greatly reduced in animal cells at temperatures of 4ºC and so the lapatinib effect in A549-T cells was compared at this temperature and normal 37 ºC incubation [167]. Treatment of the A549-T cells with lapatinib for 24 hours at 4ºC had no effect on P-gp level whereas the control at 37ºC displayed the expected increase in P-gp (figure 3.1.13.3). These findings indicate the increase in P-gp observed with lapatinib treatment is reliant on the basic cellular functions of protein synthesis and degradation.

From the above, it was deduced that the changes in the expression level of P-gp by lapatinib are post-translational. Protein levels are maintained in the cell through a balance of *de novo* protein synthesis and protein degradation. To examine if the lapatinib actions observed on the P-gp protein are due to alterations in protein turnover, observations in protein level of the transporter pump were made in the presence of cycloheximide and bortezomib (figure 3.1.14.1 and 3.1.14.2). The protein synthesis inhibitor cycloheximide has been shown to reduce the levels of total P-gp present in cells [168]. Cycloheximide treatment alone had little effect on P-gp levels in the A549-T cells. The lapatinib-induced increase in P-gp expression observed in control cells was abolished in the presence of cycloheximide; implying lapatinib is exerting its effects on P-gp protein level through increased P-gp protein synthesis. Bortezomib, a proteasome inhibitor, prevents protein degradation by inhibiting the proteolysis of long lived proteins [169]. Bortezomib treatment in A549-T cells resulted in an increased level of P-gp and the addition of lapatinib to these treatments led to an even greater increase in P-gp. This indicates P-gp degradation is mediated through the proteasomal pathway which is consistent with previous literature evidence [199]. Agents that modulate and antagonise P-gp activity, such as nifedipine and cyclosporin A have previously been reported to have the ability to increase this transporters protein level [200, 201]. However, these increases were accompanied with increased mdr1 mRNA which is not observed with the lapatinib-induced increase in P-gp in A549-T, indicating a different mechanism of induction.

Although, the results suggest the increase in P-gp observed with lapatinib treatment is due to an increase in protein synthesis, it does not rule out the possibility that

lapatinib may also have an effect on the degradation of the protein. Ubiquitination is a process which plays a great part in the regulation of protein turnover [199]. P-gp stability has been shown to be regulated by this process. In its steady state, this drug pump is located in the plasma membrane and after time it is subjected to endocytosis and recycling. Transfection with wild-type ubiquitin resulted in an increased level of ubiquitinated P-gp which was accompanied by a reciprocal decrease in P-gp. Proteasome inhibitors can also contribute to decreased activity as they prevent the maturation of P-gp and its localisation in the plasma membrane [199]. The epidermal growth factor receptors have also been shown to be regulated by the ubiquitination pathway [202]. A recent paper investigated if lapatinib could affect ubiquitination of HER-2. Scaltriti *et al* (2009) transiently expressed hemaglutinin (HA)-tagged ubiquitin in MCF-7HER-2 cells and examined HER-2 ubiquitination in the presence of lapatinib. This showed levels of ubiquitinated HER-2 to be barely present when the cells were treated with lapatinib. They also examined the HER-2 protein turnover rate and showed that lapatinib caused a marked reduction in receptor degradation. This was accompanied by a substantial accumulation of inactive HER-2 receptors at the cytoplasmic membrane [203]. Although there is no direct evidence as yet to support this, a possible hypothesis to explain the increase in P-gp levels could be that lapatinib has a similar action on this transmembrane drug transporter protein as the transmembrane growth factor receptor HER-2. It is also conceivable that EGFR signalling is linked to P-gp regulation in some way and this is discussed further in section 4.1.4.

4.1.3. EGF-induced alterations in drug transporter expression

Lapatinib antagonises the EGFR and HER-2 receptors and it was of interest to determine if an agonist for these receptors could also alter P-gp levels. EGF, an EGFR and HER-2 ligand, was analysed for its ability to alter P-gp and MRP1 expression. EGF has been shown to interact with the P-gp protein and alter its phosphorylation [80]. A report by Wartenberg *et al.* (2001) showed that treatment with this growth factor can down-regulate P-gp expression in a process that may be mediated by reactive oxygen species. They suggest that the expression of P-gp may be associated with cell quiescence and can be down-regulated by mitogenic stimulation [204]. Of note, this could explain the altered levels in P-gp observed between different control A549-T cells, throughout all Western blots, which may

have had fresh medium at varying time points. The findings in this thesis are consistent with this evidence, as EGF treatment in A549-T cells had an opposing effect to lapatinib, resulting in a decreased P-gp expression (section 3.1.6). This was also determined to be a robust change in protein level, and was observed from concentration of 2 ng/ml across a variety of time points with the shortest being 24 hours. To put this in perspective, the circulating serum concentrations of EGF is approximately 700 pg/ml [205]. The effect on P-gp protein levels was considerable, with EGF treatments resulting in levels of P-gp that were barely detectable in some cases. The EGF effect on MRP1 levels was comparable to that observed with P-gp, whereby the growth factor receptor induced a decreased expression of the protein. Similar to that of the lapatinib, the alterations in P-gp and MRP1 levels were not observed at the mRNA level and changes were determined to be post-translational (figure 3.1.7.1 and 3.1.7.2).

4.1.4. Potential link between EGFR signalling and P-gp

As both lapatinib and EGF had opposing effects on P-gp expression in the A549-T cells, it would seem possible that their actions are mediated by EGFR signalling and there is a link between the EGFR and P-gp. Many cell lines over-express both of these membrane proteins. A study carried out in actinomycin D-resistant Chinese hamster lung cells, first introduced the idea of crosstalk between the EGFR and P-gp, whereby by EGF treatment resulted in a significant reduction in P-gp phosphorylation in these cells [206]. EGF was later shown to have the ability to regulate the phosphorylation and hence the activity of P-gp in a human MDR breast cell line (MCF-7/AdrR) and this is likely to be mediated by phospholipase C (PLC) [80]. Evidence suggests a link between signalling from the phosphatidylinositol 3-kinase/Akt pathway and P-gp, with inhibition of phosphorylated AKT expression resulting in the down-regulation of P-gp expression in gastric cancer cells [207]. We therefore examined (section 3.1.14) if the lapatinib- or EGF- induced effect on P-gp expression was associated with altered EGFR or HER-2 signalling. A549-T cells, which were shown to express increased levels of P-gp when treated with certain concentrations of lapatinib, were analysed for changes in the two main downstream EGFR/HER-2 signalling molecules, MAPK and AKT. Slight variances were observed in MAPK levels; however, these did not correspond to the changes seen in P-gp expression. AKT and MAPK levels decreased slightly in response to 10 ng/ml

EGF, but very little change was observed with 2 ng/ml EGF treatment, a concentration which down-regulated of P-gp. Phosphorylated levels of these signalling molecules were also analysed. Phosphorylated MAPK was not detected in any of the samples examined. Phosphorylated AKT showed varying levels in response to lapatinib treatment but again these did not directly correspond to changes observed in P-gp expression. These results indicate clearly that the lapatinib-induced increase or EGF-induced decrease of P-gp expression is not related to signalling from the epidermal growth factor receptors EGFR and HER-2 through MAPK or AKT.

4.1.5. Changes in EGFR and HER-2 expression

As outlined above, lapatinib has the ability to alter the levels of the transmembrane drug transporter proteins. It has also been reported that lapatinib can increase HER-2 levels and the tyrosine kinase inhibitor, AG1478, has been shown to have the ability to increase inactive EGFR levels [203, 208]. It was therefore of interest to determine if lapatinib could alter the expression levels of its target transmembrane growth factor receptor proteins EGFR and HER-2 in the cell models used in this thesis. EGF was analysed for its ability to induce a change in EGFR and HER-2 levels. The phosphorylated levels of these target proteins were also examined for change. Analysis was also carried out in H1299-T, a resistant lung cell line generated in the same fashion as A549-T, however, both of these lung cell lines are not considered as being sensitive to lapatinib and so the lapatinib-sensitive breast cell line SKBR3 was also observed for changes in EGFR and HER-2 levels following lapatinib treatment (section 3.1.8).

Firstly, it is of importance to note, the two resistant lung cell lines expressed reasonably low levels of EGFR and HER-2 receptors. SKBR3 exhibited similar levels of EGFR but had much higher levels of HER-2. Relatively few changes in total levels of EGFR were observed over various time points with lapatinib or EGF treatments. This was not the case with total HER-2 levels, which were up-regulated to varying degrees in A549-T and SKBR3 after treatment with lapatinib. This finding supports evidence in the literature, whereby lapatinib was shown to cause a marked accumulation of inactive HER-2 receptors in MCF7-HER-2, through alterations of the ubiquitination process [203].

It would be expected that a reduction in phosphorylation of these growth factor receptors would be observed with lapatinib as it blocks the tyrosine kinase domain

and autophosphorylation of the receptors [96]. However, the opposite effect was observed in phosphorylated EGFR in A549-T and H1299-T following 48 and 24 hour lapatinib treatments respectively. These phosphorylation results may not be so surprising due to the relatively small amounts of growth factor receptors and the nature of sensitivity of these cell lines to lapatinib. The changes are also minor in nature and it must also be noted several points had reasonably large deviations. Statistics were not performed as data was only available in duplicate.

An increase in phosphorylated HER-2 levels was observed after 24 hour lapatinib treatment in A549-T, although this was small in nature, with no change seen in SKBR3. No substantial changes were observed in phosphorylated EGFR with lapatinib treatment in SKBR3 and experimental error was considerable so it was difficult to draw any conclusions.

Ligand binding and activation of epidermal growth factor receptors is followed rapidly by internalisation of the receptor-ligand complex and evidence suggests that receptor dimerisation is vital for this process [209]. The internalised receptors either undergo lysosomal degradation or recycling back to the cell surface and so the regulation of growth factor receptor expression does appear to be somewhat complex [209]. A considerable reduction in total EGFR levels was observed in A549-T with EGF treatment. EGF treatment in SKBR3 also led to a decrease in EGFR, but to a much lesser extent. Although not observed across all of the time points, this was also the general trend seen with total HER-2 expression as a result of EGF treatment. These results are consistent with evidence in the literature, with EGF proving to negatively regulate the expression of the growth factor receptors. This ligand has been previously shown to reduce the expression of HER-2 protein without altering mRNA levels in the breast tumour cell lines T47D and ZR75.1 [210]. One study demonstrated that prostate cancer cells with EGF stimulation caused an increase in EGFR mRNA and *de novo* EGFR protein synthesis; however, overall it led to a significant decrease in total EGFR. In these cells, EGF treatment was also associated with a decrease in the EGFR protein half-life and therefore stability. This indicates that although this growth factor induces mRNA and an increase in the rate of EGFR protein synthesis, its induction of protein degradation ultimately leads to reduced expression at the cell surface [211]. An earlier report, in fact, demonstrated that under normal conditions, EGF receptors were diffusely distributed along the cell

surface and upon the addition of EGF a rapid internalisation of the receptor-ligand occurred. This EGF-EGFR complex was transported internally to lysosomes where the receptor was degraded [212].

4.1.6. Implications of modifications in P-gp expression

It has been well established that increased P-gp expression leads to a decreased accumulation of a wide variety of cancer drugs across many cell lines, ultimately reducing substrate drug efficacy [213-216]. This can result in treatment failure, ultimately causing problems in the clinic. It was therefore important to establish if the lapatinib-induced increase in P-gp levels seen in A549-T interfered with chemotherapy toxicity. This was examined with accumulation, efflux and toxicity assays (section 3.1.11). Lapatinib treatments proved to have no major negative effect on the accumulation or efflux of epirubicin in A549-T. Although initial volumes differed slightly, after 120 minutes in each assay, drug levels were the same in the lapatinib treated cells as that seen in the control. Epirubicin efflux was also analysed in the greater P-gp expressing cell line DLKP-A. A lower amount of drug was observed in the lapatinib-treated cells, after 120 minutes of epirubicin accumulation. However, efflux data demonstrated similar levels of epirubicin across all conditions after 120 minutes, indicating that over time any possible differences in P-gp levels in the A549-T cells has little impact intracellular drug levels over time.

Lapatinib pre-treatment in A549-T resulted in an additive toxicity with paclitaxel and docetaxel treatments, thereby displaying no negative effects on chemotherapy sensitivity. Further analysis was carried out to directly compare pre- and co-treatment of lapatinib and in this instance a 24 hour wash out period was included to attempt to remove remnants of lapatinib. This direct comparison of pre-treatment and co-treatment with lapatinib in A549-T cells indicated little difference in toxic response, however, lapatinib pre-treatment caused a substantial reduction in cell survival prior to chemotherapy. The combination therapy is likely to be the better treatment option in order to take advantage of possible extra toxicity with synergistic interaction.

As this assay involves a pre-treatment it is a challenge to remove all molecules of lapatinib and to be sure if this is achieved. It is therefore important to view these findings with an air of caution, as although no immediate impact on chemotherapy drug sensitivity was observed, if small active levels of lapatinib are present, this in

turn could be inhibiting the effects of the increased P-gp protein. It is possible that the increased P-gp expression seen with lapatinib treatment compared with controls is of a non-functional nature. Immature core-glycosylated P-gp that is prevented from travelling to the cell surface is inactive and so would have no effects on drug sensitivity. However, it is unlikely that this is the case here as lapatinib is a substrate, and the presence of a substrate drug was shown to induce the transporter to adopt its mature conformation and undergo trafficking to the cell surface where it exhibited drug-stimulated ATPase activity [217]. From the findings carried out in this thesis it is difficult to ascertain if P-gp protein up-regulated in response to lapatinib is fully functional. Regardless of these initial results, indicating no negative implications with the increased drug transporter expression, it is possible the increase in P-gp may have longer term implications that are not seen here which may warrant further study.

The consequences of the EGF effect on P-gp expression were also analysed. Epirubicin efflux would be expected to be reduced and a greater accumulation of the drug seen. However, this was not the case, although an initial difference was observed after 30 minutes, the levels of drug were the same after 2 hours. In toxicity assays EGF treatments only slightly sensitized the A549-T cells to paclitaxel and docetaxel. The observed effect was small and as the taxanes primarily act on cells in the G_2 and M phase of the cell cycle, it seems possible the EGF is pushing more cells into this phase and the decreased cell survival is not due to reduced P-gp [22]. EGF has been shown to stimulate the phosphorylation of P-gp and enhance its transport activity. If this is happening here, it would suggest the small amount of P-gp in the cells may be working harder and so in effect cancelling out the expected consequences of reduced P-gp expression [80].

Lapatinib seems promising as an agent in the treatment of resistant lung cancer in the role as a P-gp modulator, although cytotoxic drug concentrations will have to be taken into consideration to counteract potential toxicity. The observation that lapatinib can induce an increase in P-gp expression is novel and requires further study to fully investigate what exactly is happening in the cell. Although it did not increase resistance in our models, this alteration may have long term clinical implications and so it would be important to address these with future work. As a relatively new drug on the market it is important that it remains the focus of

continuing research. This study indicated probable expansions for its use while also highlighting potential problematic activity.

4.2. SiRNA techniques and multidrug resistance

As explained previously, the cell lines used in this thesis represent good *in vitro* models of multidrug resistance, and so siRNA techniques were utilised in order to examine, more closely, proteins which may be contributing to the resistant phenotype. SiRNAs which mediate RNA interference, involving the double-stranded RNA silencing of homologous genes, are a valuable and useful technique when studying multidrug resistance. Previous work in our laboratory highlighted proteins with roles in the development of paclitaxel resistance through microarray studies [49]. In this thesis several of these proteins were chosen for further study in the resistant cell lines A549-T and DLKP-A. The siRNAs were primarily coupled with toxicity assays, with the protein of interests' effects on drug sensitivity ultimately being analysed. This technique was also coupled with drug accumulation assays and so the effects of gene silencing on drug transport can be analysed in the cell.

4.2.1. Knocking down of ABCB1 in DLKP-A and A549-T

The drug transporter protein P-gp has already proved to have an important role in drug resistance and was up-regulated along with the other proteins of interest in the paclitaxel resistant cell lines, and so it was the first focus of this work [49]. Western blots confirmed the knockdown of P-gp protein in the DLKP-A cells (figure 3.2.1). Silencing of ABCB1 with siRNA rendered DLKP-A cells significantly more sensitive to paclitaxel and epirubicin (figure 3.2.1.4 and 3.2.1.5). The increased toxicity in siRNA-transfected cells, observed with paclitaxel was comparable to that achieved with elacridar, a potent P-gp inhibitor [218]. These results are as expected as P-gp has been shown to be up-regulated in these resistant cells and paclitaxel and epirubicin are substrates for this transmembrane pump [219, 220]. Such a substantial effect, however, was not observed in the resistant cell line A549-T (figure 3.2.1.2 and 3.2.1.3). Knocking down P-gp expression resulted in a reduced increase in sensitivity in A549-T to paclitaxel, nonetheless the trend does remain. High standard deviations were an issue in these assays and these were likely due to experimental error relating to chemotherapy drug concentrations. The physical consistency of paclitaxel, can make it difficult to measure consistently accurately. Although not significant, a trend towards an increase in sensitivity was observed to epirubicin, in A549-T cells transfected with P-gp siRNA. It is not surprising that the silencing of P-gp in A549-T

did not have the same effect as in DLKP-A as their relative P-gp levels differ greatly with substantially more P-gp being expressed in DLKP-A. These results were expected, as silencing P-gp expression leading to decreased function, allows more drug to accumulate in the cells, thereby increasing their toxic effects. A study in colon cancer cells, showed the siRNA mediated knockdown of P-gp increased the cytotoxicity associated with adriamycin and vincristine [221]. Daunorubicin sensitivity was restored in leukaemia cells which were transfected with P-gp siRNA [222]. The findings observed here are also consistent with the literature, whereby inhibition of P-gp function led to increased toxicity associated with paclitaxel and epirubicin [45, 109].

The employment of siRNA transfection with other techniques is extremely useful in cancer studies. In order to establish the effect of P-gp knockdown on drug transport, siRNA mediated gene knockdown was coupled with an accumulation assay. 72 hours following siRNA treatment of DLKP-A cells, an accumulation assay was carried out and epirubicin levels quantified (figure 3.2.1.6). This method proved very successful and epirubicin levels were significantly increased in the cells treated with ABCB1 siRNA. These results are very encouraging, as due to the substantial levels of P-gp in DLKP-A, it was difficult to predict if the P-gp siRNA would be powerful enough in having an impact on epirubicin accumulation. Previous studies have shown knockdown of P-gp expression through siRNA, reduced intracellular accumulation of daunorubicin in leukaemia cells [222]. Consistent with these findings are results from another study carried out in MCF-7/Adr whereby paclitaxel accumulation was significantly enhanced in cells transfected with P-gp siRNA [223]. This method should be suitable for investigating the accumulation of drugs with the silencing of other drug transporters and could also be applied to the determination of substrates for the pumps. This result also served to further validate the ABCB1 siRNAs being used.

4.2.2. The role of proteins identified from microarrays in resistance

As mentioned previously (section 1.3.1), three genes were chosen from analysis of micro-array data of genes associated with the development of paclitaxel resistance [49]. These particular genes were chosen as their expression was altered in three resistant lung cancer cell lines compared with sensitive parental cell lines. Two of

these genes, Inhibitor of DNA binding 3 (ID3) and Crystallin, zeta (CRYZ) were up-regulated in three paclitaxel resistant lung cell lines, A549-T, H1299-T and H460-T. Cysteine-rich protein 1 (CRIP1) the third gene, was down-regulated in these same cell lines. ID3 was 1.3, 2.7 and 2.3 fold up-regulated in resistant cells compared with A549, H1299 and H460, respectively. In the same three resistant cells lines CRYZ was up-regulated 1.6, 1.5 and 1.2, respectively. CRIP1 on the other hand was down-regulated 2.6, 30.9 and 3.4 fold in A549-T, H1299-T and H460-T, compared with parental cells, respectively. Although these genes were chosen from data from the A549/A549-T cell lines, transfections were also carried out in DLKP-A to determine if expressed, their possible contributions to resistance in a different model of resistance. In order to establish if ID3 or CRYZ have direct roles in resistance, cells were transfected with their corresponding siRNAs and analysed for sensitivity to the chemotherapeutic, paclitaxel. CRIP1 was down-regulated in the resistant cell lines, and so A549 cells were transfected with siRNA corresponding to it and paclitaxel sensitivity determined.

A small increase in toxicity with paclitaxel was observed in A549-T cells transfected with inhibitor of DNA binding 3 (ID3) siRNA (figure 3.2.2.1). This protein has previously been shown to be up-regulated in small cell lung cancer tissue [224]. The ID proteins neutralize the transcriptional activity of basic helix-loop-helix (bHLH) proteins, negatively regulating differentiation and promoting proliferation [225]. This would explain the decreased cell survival observed in A549-T cells transfected with ID3 siRNA in the absence of paclitaxel. A similar result was observed in DLKP-A cells, however, considerably higher toxicity was observed with ID3 siRNA in these cells, with approximately 40% survival observed in the absence of paclitaxel. In the presence of paclitaxel an increased toxicity was observed in the DLKP-A cells transfected with ID3 siRNA compared with control (figure 3.2.2.2). It is important not to disregard the effect the ID3 siRNA transfection alone is having on the cells. This effect renders the results difficult to analyse, and causes difficulties in ascertaining if there is a synergistic or additive effect on paclitaxel sensitivity. The results were graphed allowing all control conditions with no chemotherapy drug to equal 100%, and from this data it would certainly appear that the ID3 siRNA is playing some role in re-sensitising the cells to paclitaxel. To investigate this further and examine if the P-gp-mediated resistance was masking a more subtle mechanism

of resistance, elacridar, the potent P-gp inhibitor, and P-gp siRNA was used in combination with ID3 siRNA and chemotherapy sensitivity analysed (figure 3.2.3.2 and 3.2.3.3). In A549-T, there was no siginificant difference in paclitaxel toxicity between the cells transfected with ID3 siRNA in the presence of elacridar and those treated with elacridar alone. In DLKP-A on the other hand, there was a significant difference in paclitaxel toxicity with the two higher concentrations in ID3 siRNA transfected cells with elacridar and those with elacridar alone. However, again the transfection with ID3 siRNA in the absence of paclitaxel gave rise to a large decrease in cell survival compared with elacridar control. When graphed allowing all of the controls to equal 100% it was shown that there was no added increase in sensitivity to paclitaxel in the ID3 siRNA transfected cells with elacridar compared with elacridar only. Co-transfection of ID3 and P-gp siRNA in DLKP-A was consistent with the elacridar data as no added sensitization was observed with the ID3 siRNA (figure 3.2.3.1).

The transfection of ID3 siRNA did appear to slightly re-sensitize the cells to paclitaxel in DLKP-A, suggesting that it plays a small part in resistance in this cell line. In A549-T, the same effect was not observed and so this protein does not therefore appear to have a direct role in resistance in this cell line but may be contributing in a small way by driving proliferation in the face of toxic insult. Also of note, this gene exhibited a modest 1.3 fold up-regulated in this resistant cell line and so perhaps this is why no great effect was observed with ID3 siRNA transfection. There is no evidence in the literature to suggest a role for ID3 in resistance, however, this work suggests a minor role, secondary to P-gp in our DLKP-A model and it is conceivable that it is contributing to the cells defence by promoting growth. The role of ID proteins in the cell is a complex and cell specific one and so it is difficult to hypothesis what is happening in the resistant cells [226].

Although a slight increase in paclitaxel toxicity was observed in A549-T cells transfected with Crystallin-zeta (CRYZ) siRNA, it was not of significance (figure 3.2.3.4). A greater increase in paclitaxel sensitivity was observed in DLKP-A (figure 3.2.3.5). As above, co-transfection of CRYZ siRNA with P-gp siRNA was carried out. The small increase in paclitaxel toxicity, observed with transfection of both CRYZ and P-gp resulted in A549-T is to be interpreted with caution as the error bars overlapped (figure 3.2.3.6). The opposite trend is observed in DLKP-A, but to no

significant level (figure 3.2.3.7). This protein is a NADPH-dependent quinone reductase and can repair oxidative damage in cells [53]. The role of this protein is still unclear but it is thought to have trans-acting activities that can regulate the turn-over of certain mRNAs [227]. The results here indicate it is unlikely to have a direct contribution to chemotherapy resistance.

Cysteine-rich protein 1 (CRIP1) was down-regulated in the resistant cell lines compared with parental cell lines and so A549 was transfected with siRNA in this case to ascertain the potential role of CRIP 1 in resistance. It would be expected that transfection with siRNA against Cysteine-rich protein 1 in A549, might mimic resistance seen in A549-T if this protein has a role in the resistance. However, it was not observed in this cell line and down-regulation of this LIM/double zinc finger protein family member is unlikely to contribute to resistance in this model (figure 3.2.2.5).

The body of work produced mixed data with regards to resistance mechanisms in our lung cancer models. Drug resistance is unlikely to be caused by one factor and so these genes still may prove to be important in drug resistance. SiRNA mediated gene knockdown coupled with toxicity assays does not provide enough information to fully examine this. Further work with ID3 may reveal an definite role for it in some mechanisms of resistance, however, P-gp proved to be the main mediator of resistance in these models, in particular in DLKP-A. However, it does indicate the great potential for the use of siRNA mediated gene knockdown together with toxicity and transport assays. Using siRNA together with toxicity assays gives an efficient indication of the contribution of a protein to chemotherapy resistance in a cell line. The coupling of siRNA P-gp knockdown with accumulation and efflux assays revealed much information about the transport of chemotherapy drugs in our cell line. This could be expanded further to investigate a range of transport or transport related proteins and various drugs. These are simple but effective techniques and this section of work highlighted their effectiveness.

4.3. Membrane proteomics and multidrug resistance

As mentioned previously, a large portion of the research in this project focused on membrane proteins, such as the drug transporters and growth factor receptors, and was reliant on the technique of Western blotting. Despite being a very powerful technique, Western blotting is hugely dependent on the quality of the antibody and remains a semi-quantitative low through-put technique. Proteomics, and more specifically membrane proteomics, may be utilised to provide an alternative to this technique. Studying membrane proteins is, however, problematic in itself due to the hydrophobic nature and size of these proteins.

As part of this thesis an initial examination of a chosen membrane proteomic method involving membrane protein isolation, organic solvent solubilisation and tryptic digestion followed by multidimensional liquid chromatography coupled to tandem mass spectrometry, was carried out to see if this was in fact a useful technique in analysing membrane proteins. It is anticipated that in time this method could be used in conjunction with a quantitative method and provide an alternative reliable technique to Western blotting with the added advantage of being able to analyse greater numbers of proteins.

4.3.1. Development of membrane proteomic method

Membrane proteins are problematic to analyse by mass spectrometry due to their hydrophobic nature which makes them difficult to solubilise. Detergents which are commonly used for solubilisation can suppress ionisation and affect the performance of liquid chromatography. Organic solvents have proved to be a possible alternative to these detergents [135, 139, 141]. Membrane proteins solubilise well in organic solvents and also these solvents can be readily removed after protein digestion [135, 139, 141]. Trypsin, the enzyme of choice, which cleaves exclusively after arginine and lysine, has also been reported to remain functional in solutions of up to 65% methanol and there have been reports suggesting an increase in protein digestion in organic solvents [228, 229]. For these reasons, organic solvent solubilisation followed by tryptic digestion was employed to allow LC-MS based protein identification in this project.

The appropriate separation strategy was then identified. 2-D PAGE has limited application for membrane proteins as its does not resolve these proteins well, leaving them under-represented in research using this method [135]. Liquid chromatography has proved very useful in the separation of more problematic membrane proteins subsequent to digestion and so this was chosen for the separation technique. Multidimensional LC (MDLC) combines two or more types of LC, thereby subjecting each part of the sample to two different separation dimensions. This substantially increases the peak capacity and thus the resolving power. The peak capacity refers to a measure of the maximum number of components that can be resolved during a single chromatographic analysis and should be significantly larger than the number of sample constituents. Highly complex mixtures require methods with increased resolving power for separation. Due to this increase in peak capacity and resolving power MDLC results in better fractionation of the peptides before being analysed by the mass spectrometer [142, 230]. It is therefore more capable of separating complex samples and so an MDLC system coupling the first dimensional strong cation exchange (SCX) chromatography with the second dimensional reverse phase (RP) liquid chromatography (LC) was employed in this work.

The MDLC method was then coupled with tandem mass spectrometry (MS/MS). MS/MS, which involves peptide ion fragmentation with subsequent m/z measurement, is a capable method in the identification of large numbers of proteins. Parent ions, which are generated as the mass spectrometer records the mass/charge (m/z) of each peptide ion (MS^1), are selected for further fragmentation to obtain sequence information (MS^2) [231, 232]. There are several fragmentation methods which can be employed for MS^2. Collision induced dissociation (CID) is a well established and successful fragmentation method. It yields an increase in the number of precursor ions that fragment in the reaction region and also the number of fragmentation paths. Electron transfer dissociation (ETD) is a relatively new method of fragmentation but has proved a very robust method and has been shown to out-perform CID with peptides of charge states more than 2. ETD fragments peptides through the transferring of electrons from radical anions to protonated peptides. In our method it was decided to use both CID and ETD modes of fragmentation as literature has shown benefits of employing both of these methods together to achieve better fragmentation of a wider variety of peptide types [150, 233].

Due to the complexity of the mixtures to be analysed, there are inherent challenges with this LC-MS technique and this body of work set out to address these to varying degrees. Taking the biological side out of the equation, there are three major components to this method; separation by liquid chromatography, detection by mass spectrometry and identification of proteins by software and data analysis. Challenges lie with all of these aspects, in terms of separation, detection and analysis. The ability of the multidimensional liquid chromatography method employed to separate peptides was assessed. The capabilities of the mass spectrometer to detect ions from separated and fragmented peptides were also examined. A more in depth examination was carried out of the data analysis and the impact of different statistical filters. It is hoped this body of work will give a clear indication if this membrane protein analysis is sufficient for dealing with complex membrane protein samples, and address some important issues with the three main components contributing to this method.

4.3.2. Assessment of liquid chromatography

Good peptide separation is vital for the LC-MS and so the MDLC method used was analysed for this. The MDLC separation method, which utilised strong cation exchange chromatography coupled with reverse phase chromatography, proved to be reproducible between samples run on different days, indicating reasonable levels of consistency with the method. The retention times, of six peptides chosen at random in order to assess chromatography, all only differed by approximately a minute from DLKP-A 1 (first sample analysed) and DLKP-A 2 (technical repeat) (table 3.3.1.1). This separation technique is therefore quite reliable and reproducible. The quality of separation from the liquid chromatography was also analysed. Clear peaks were evident for each ion investigated, and the peak width was around 20/30 seconds for these peaks, indicating a nice distinct peak with good intensity (figure 3.3.1.1-3.3.1.4). This data showed the liquid chromatography separation of the samples to be satisfactory and any issues are most likely due to mass spectrometry or data analysis.

4.3.3. Assessment of data analysis and statistical filters

Both the resistant DLKP-A and its parent DLKP samples were analysed on a second occasion, thus generating technical repeat data. Membrane proteins isolated from A549, A549-T and A549-T-lapatinib treated cells, were also analysed. This

membrane proteomic method proved successful in that large quantities of proteins were identified. The identifications were made by employing the use of the SEQUEST and Mascot algorithms. SEQUEST employs the use of a cross-correlation (XCorr) function to assess the quality of the match between a tandem mass spectrum and amino acid sequence information from the database [170]. The Mascot algorithm is a multiple alignment system for protein sequences based on three-way dynamic programming and is probability based [178, 234]. Due to the complex nature of the samples, it was difficult to assign statistical parameters governing the protein identification process. One of the main purposes of this particular body of work was to investigate and identify appropriate statistical settings yielding the best representation of protein identifications. All of this work was carried out on the first DLKP-A (DLKP-A 1) sample run and its technical repeat (DLKP-A 2).

4.3.3.1. The determination of suitable parameters

Firstly, a 'standard' set of statistical parameters (settings/filters) were selected from researching the literature. These were based on cross-correlation (XCorr) scores that were chosen based on their acceptance to yield true identifications in published literature. The XCorr function assesses the quality of the match between a tandem mass spectrum and the amino acid sequence from a database, and in this instance were chosen to be 1.9 for singly charged, 2.2 for doubly charged, 3.0 for triply charged and 3.5 for quadruple charged [170]. The standard filter also included the requirement of at least two distinct peptides being recognised for any given protein identified. These were applied to the combined CID and ETD datasets from the DLKP-A membrane protein preparation (DLKP-A 1) and its technical repeat DLKP-A 2. The resulting protein lists were then critically analysed through examination of; protein number and overlap between samples, peptide quality and the identification of several membrane proteins previously shown to be expressed in this cell line (section 3.3.2). The list of proteins previously shown to be expressed in DLKP-A were identified using 2D-DIGE or in the case of P-gp Western blot [176].

This standard filter yielded a good number of protein identifications from DLKP-A 1 and 2, 635 and 447 respectively. The quality of peptide fragmentation was good, as determined by clear distinct peaks with good continuity of b and y and c and z ion series. However, the number of proteins commonly expressed between DLKP-A 1 and 2 were a disappointing 42% and only three out of the seven membrane proteins

known to be expressed in DLKP-A were identified in both datasets. It is unclear as to why less than half the proteins were commonly expressed between the first run sample and its technical repeat or why the number of proteins known to be expressed was so low, although as the liquid chromatography was shown to be of good quality it is likely this is due to the detection by the mass spectrum. To further analyse the contribution of the governing statistics on protein identifications a number of changes were applied to these standard filters and again protein lists critically analysed like above.

4.3.3.2. Benefits of analysing ETD and CID data together

As explained, the tandem mass spectrometry method employed for these samples included fragmentation from both ETD and CID. When CID is used in isolation, the resulting data is analysed with an extra parameter, namely the Mascot algorithm of peptide probability. This provides an extra level of stringency, while allowing looser XCorr scores to be applied and so it would further reduce the amount of potential false positives. However, maintaining continuity across ETD and CID data presents disadvantages with Mascot, as the same XCorr scores and filters should be applied to both. This could render the CID data unnecessarily stringent with peptide probability and would lead to the loss of some true protein identifications. The other issue with analysing the data separately is regarding the minimum requirement of two distinct peptides. If this parameter is in place and the data is analysed together, a protein may be identified based on one peptide from ETD and one from CID. However, if they are analysed separately, all of the single peptide protein identifications in ETD with a matching single peptide protein identification in CID, or vice versa will be lost. This point was proved when a loss of 16% of protein identifications was observed when separate analysis of ETD and CID datasets took place. Therefore, it was concluded from this section of work that the use of both CID and ETD methods of fragmentation greatly improves the number of protein identifications. Evidence in the literature supports this, suggesting the use of both CID in conjunction with ETD to be most beneficial, as they complement each other and significantly improve yield of proteins identified [150, 151, 235]. In addition, although the parameter of peptide probability is useful when analysing CID data, it was determined of greater benefit to analyse the CID and ETD data together (section 3.3.3 and 3.3.4).

4.3.3.3. Impact of reducing cross-correlation scores

The next step taken was to address the stringency of the 'standard' XCorr scores (section 3.3.5). As four out of the seven membrane proteins which were known to be expressed in DLKP-A, were not identified using the first standard set of parameters, false negatives were highlighted as an issue. The impact of lowering the XCorr scores was analysed. The XCorr scores were set to 1.5 for singly charged, 1.9 for doubly charged, 2.5 for triply charged and 3 for quadruple charged and the minimum requirement for two distinct peptides remained. As expected, this yielded far greater numbers of proteins. Surprisingly though 1559 proteins were identified from DLKP-A 1's sample with only 651 from DLKP-A 2. This was not consistent with all the previous filters where the protein numbers were reasonably similar and no explanation was found for this discrepancy. Despite this, the validation of several proteins which just made the cut in terms of XCorr scores, determined them to be of acceptable quality. Of great encouragement, both sets of identifications included six out of the seven membrane proteins known to be expressed in this cell line. Disappointingly, only a 26% overlap in proteins was observed between DLKP-A 1 and 2 samples, although it is felt that the difference in protein identifications to begin with, contributed to this small number.

There are certain drawbacks with these particular criteria; however, they did yield the best representation of proteins while maintaining quality and keeping the number of false positives and false negatives low. These parameters appear to achieve a balance between quality and number which is the required outcome for identifications.

4.3.3.4. Impact of abolishment of requirement for two distinct peptides

One parameter which remained constant throughout the above investigations was the minimum requirement for two distinct peptides for protein identification. The impact of abolishing this requirement was analysed (section 3.3.6). In order to maintain a certain level of stringency, the XCorr scores were increased to 2 for singly charged, 2.5 for doubly, 3.2 for triply and 3.5 for quadruple charged. A large number of proteins were identified with these parameters. Although on whole, most of the peptides chosen for closer analysis were validated as true identifications, a number of the peptides were not as convincing. In these cases, the lack of security of having a second peptide was far from ideal, leaving the possibility of too many false positives in the list of identified proteins. It is also widely accepted that proteins identified

from a single peptide are dubious identifications and are discouraged, as reported in a published article regarding the rules governing protein identifications by mass spectrometry [236]. In keeping with this, the requirement of two distinct peptides was maintained.

A balance needs to be achieved between the number of proteins identified and the quality of the protein identifications, in particular with samples of such complexity. False positives, whereby proteins not present in the sample are identified, and false negatives, whereby proteins present in the sample are not detected, lead to misrepresentation of data. It is imperative that a minimum amount of false positive and false negative identifications are made. This section determined the filter with slightly less stringent XCorr scores of 1.5, 1.9, 2.5 and 3 and the requirement of two distinct peptides to provide a good balance between protein number and potential false positives or negatives and was chosen to apply to other samples analysed.

As a repeat was carried out on the exact same sample, no biological variances come in to play and it was purely the LC-MS side of the method that was being tested for reproducibility. Along with the DLKP-A samples a DLKP sample was also run initially and again at a later date. Based on the criteria chosen, the reproducibility as determined by commonly expressed proteins was 26% and 32% in DLKP-A and DLKP, respectively. This was disappointing as although the outcomes were of an unpredictable nature, it would have been expected that with no biological variances involved that a much higher overlap of commonly expressed proteins would have been observed. Firstly, it is important to note there was a two month gap between the analysis of the first and second samples. The samples were stored at the correct temperature of -80ºC and so this would not have been expected to have too much impact but nonetheless slight alterations in the mass spectrometer may account for a small portion of the inconsistency.

Section 4.3.1 has already addressed the issue of chromatography and the data verified this to be consistent. The data analysis clearly has a large bearing on protein identifications, however, the levels of reproducibility never reached higher than 51% and so it would appear the main issue lies with the mass spectrometry and this is dealt with in more detail in the next section.

4.3.4. Assessment of mass spectrometry in complex protein identification

The mass spectrometry analysis appears to be the most limiting of the three components to the method, which is not so surprising due to the extremely complex nature of the sample. It is hypothesised that the low overlap in proteins identified from DLKP-A sample 1 and 2 may be due to the mass spectrometer having too much data to handle at any given time leading to proteins being missed in one or other of the samples. Issues with the mass spectrometry were examined to a small degree by choosing a number of proteins that were expressed in DLKP-A 1 and not 2 and *vice versa* and taking a closer look at the chromatography and mass spectrums to see why they have not appeared in their alternative sample. Two proteins with strong identifications were chosen in order to carry out this analysis (section 3.3.7).

This analysis implicated the mass spectrometry as the weakest link in this method. Two peptides for the proteins, ADAM 10 and MRP1 identified in DLKP-A 2 and DLKP-A 1, respectively were shown to be true identifications based on mass spectra and continuity in their b and y or c and z ion series. One peptide from each ADAM 10 and MRP1 was further examined, and their isotopic mass, retention time and what fraction they were in, were determined. The mass spectrum from the corresponding sample, in which each protein was not identified, was analysed around the appropriate retention time for a peptide of the same mass. In the case of ADAM 10, a clear peak corresponding to a peptide with the same mass was observed in the full MS with a retention time differing in approximately one minute, which is consistent with previous data examining the retention times. However, following this full MS, the fragmentation by CID and ETD was carried out on two peptides with different masses. In the next full mass spectrum, the peptide of interest was no longer visible. The very same sequence of events was observed for the MRP1 peptide, although it must be noted that the chromatogram of the ion extraction did not show a distinct peak and so the quality of chromatography may have contributed in this case. These findings indicate that, the sample is too complex for the mass spectrometer. Too many peptide ions were present at any given time and the mass spectrometer was unable to process them all.

The chromatography method involved five-step salt solutions to generate fractions of peptides. An increased number of salt steps may give the peptides a better chance to

elute distinctly and also lead to the creation of potentially smaller fractions which in turn may help with the MS. However, there is a danger that with a longer salt gradient, that peak definition can be lost. Digestion with chymotrypsin in combination with trypsin could also be investigated to see if it produces more peptides, ultimately giving the mass spectrometry a greater chance to detect a number of peptides for a given protein. This is a less specific enzyme but effectively cleaves bonds made up of amino acids with aromatic or large hydrophobic side chains thus enabling the generation of more hydrophobic peptides [135]. Another approach to improve detection by the mass spectrometry could involve the employment of dynamic exclusion lists, that contain molecular masses of already fragmented peptides in association with a fixed or flexible retention time window, whereby peptides are excluded in replicate analysis of a sample leading to a greater number of unique peptide identifications in replicate runs [237, 238].

4.3.5. Potentially differentially expressed proteins in parent and resistant cell lines

Although, further work is required to optimise this method, samples which were run were analysed for differences in protein expression between parent and resistant cell lines. Some observations of proteins identified in the resistant variants are discussed below. It is important to bear in mind, no validation was carried out and so extensive investigations on the lists of proteins were not performed.

Proteins which were commonly identified in DLKP-A samples 1 and 2 and DLKP samples 1 and 2 were compared against each other. 320 (35%) of the total 910 proteins were expressed in both parent (DLKP) and resistant (DLKP-A) cell lines. 135 proteins were found in DLKP-A only. This is valuable data and may identify proteins with a role in chemotherapy drug resistance. It is promising that many proteins identified which have known roles in resistance were found to be expressed in DLKP-A only and several of these are discussed here. More repeats would be necessary before an in depth analysis of the data could be done, with the potential for identifying novel proteins with roles in multidrug resistance.

Consistent with earlier data in this thesis (figure 3.1.4.1), P-gp (MDR1) was present only in the resistant DLKP-A cell line. Not surprisingly, MDR3 or multidrug

resistant protein 3, which is often over-expressed with MDR1 and has itself a minor role in resistance, was identified in DLKP-A and not DLKP [239, 240]. Also identified in the resistant variant only was HSP71, a member of the heat shock protein 70 family of chaperone proteins which has been shown to be expressed in cancer cells in response to stress including anti-cancer agents. This chaperone, has protective properties in the cell, allowing survival in normally lethal conditions and hence this protein has a role in chemotherapy resistance [241]. Lamin B1, a cytoskeletal protein which has been previously shown to be expressed in chemotherapy resistant cell lines, was found to be expressed in DLKP-A but not in the sensitive parent. It is thought that the up-regulation of Lamin B1 may contribute to resistance by inhibiting or delaying the onset of apoptosis [176, 242]. Another protein, found in the resistant variant, DLKP-A, and not in its parent was integrin beta-4. Evidence suggests it also contributes to resistance to chemotherapy agents as it promotes stable interactions between cells and so has a role in the evasion of apoptosis [243-246]. Vimentin and cadherin 2, also found in the resistant DLKP-A and not DLKP, are associated with epithelial to mesenchymal transitions (EMT), a process which has an established role in resistance to chemotherapeutics. EMT refers to the altering of a cells epithelial phenotype to one of a mesenchymal nature which results in cancer cells adapting an enhanced survival status [247-249].
Confirmation and validation by Western blot would of course strengthen these findings, although due to time constraints this was not carried out. However, the results do indicate the huge potential for this technique in the study of membrane proteins involved in the highly complex and important process of drug resistance.

A549 and A549-T membrane protein samples were also analysed in the same manner and compared for differences in protein expression. These samples were only analysed once and so greater numbers of proteins were compared yielding a greater number of differences. However, several proteins involved in, and some with established roles in resistance were identified in the resistant variant A549-T only.

The members of the ABC transporter family ABCA3 and ABCB5 were found exclusively in A549-T. Although ABCA3 is not said to confer ‘classical’ MDR, nonetheless, evidence suggests a role in resistance and an association with poor response has been demonstrated in AML [183]. Blocking the activity of ABCB5, has

been shown to reverse resistance to doxorubicin in melanoma cells due to increased accumulation of the drug [250]. Filamin A, a cytoskeletal protein which has been shown to be up-regulated in other resistant models, was identified in A549-T cell line only [251, 252]. The ADAM family of proteins are involved in regulating cell phenotype via their effects on cell adhesion, migration, proteolysis and signalling. Altered expression of members of this family has been implicated in cancer progression. ADAM-17, which was found in A549-T, is required for generation of the active forms of EGFR ligands, and so its expression may have been triggered to enforce a protective role and promote cell growth in the face of toxic insult [253, 254]. The copper transporter ATP7B was identified in A549-T and not its parent. This protein has been shown to confer resistance to platinum-containing agents. As A549-T displays cross resistance to carboplatin and to a lesser extent cisplatin, this is a interesting result and suggests the resistance to these agents could be mediated through ATP7B [255-257]. Again, although only a few of the proteins found to be differentially expressed in the resistant compared with the parent are described here it does however indicate the major potential for this technique.

DLKP and A549 resistant variants were selected under different conditions and so display different resistance profiles. It was of interest to see if any of the proteins found to be differentially expressed in the resistant cell lines compared with parents overlapped between DLKP-A and A549-T. One of these proteins, the coxsackievirus and adenovirus receptor, has recently been identified as having a significantly higher level of expression in NSCLC patient samples compared with normal tissues [258]. It functions as an important receptor for entry of coxsackie B viruses and adenoviruses into the cell and high levels of staining has been associated with an increased proliferative activity of the tumour in an endometrial adenocarcinoma. Although evidence of its up-regulation in chemotherapy resistance has not been previously reported and these results are preliminary, it is important to note if this were to hold true it could present an opportunity in the face of resistance as it renders the cells more sensitive to potential adenoviral mediated gene therapy [259]. Integrin beta-4 which was mentioned previously to contribute to chemotherapy resistance by protecting the cell from apoptosis with cell-cell interactions was also found in both DLKP-A and A549-T only.

While these results are of a preliminary nature, they offer a taste of the great potential of this technique and its potential ability to identify membrane proteins with important roles in resistance that were previously difficult to detect by other methods.

4.3.6. Differentially expressed proteins with lapatinib treatment

Previously in this thesis, lapatinib has been shown to induce alterations in membrane proteins and so using the same method described above membrane proteins identified from lapatinib treated A549-T cells were compared with those found in the A549-T sample. Again, it is important to note that these samples were only analysed by mass spectrometry once, leading to the identification of large quantities of proteins and thus to a large number of differentially expressed proteins.

It was unexpected that the P-gp protein was not detected in the lapatinib-treated A549-T MS-analysed sample as it was shown to be induced in this cell line by Western blot (figure 3.1.5.2). This raises questions over the sensitivity of the method. On a similar note it is also important to bear in mind that this protein spans the membrane several times and so is difficult to analyse particularly when in low abundance. MRP3 (ABCC3) was detected in the lapatinib treated sample. It functions in the transport of organic compounds conjugated to glutathione, sulfate, or glucuronate and can eliminate xenobiotics after their conjugation with glucoronic acid [260]. Another ATP-binding cassette transporter identified after lapatinib treatment in A549-T was ABCA5 and although its function remains poorly understood it has been detected in various tumour types [261]. Calrecticulin, which can be found on the surface of cells under stress, is a crucial determinant of the phagocytosis of the dying cell by macrophages and was found in the proteins identified from lapatinib treated A549-T sample. This protein has been shown to travel to the cell surface in response to some cell death inducers and so maybe the expression of this protein is in response to the toxic insults of lapatinib [262]. As mentioned before, it would be preferable to do repeats and some validation before any hard conclusions are drawn from these data.

There are many different aspects of this method that require optimisation and further analysis but, time constraints did not allow this to be carried out for this thesis. However, these findings suggest; the MDLC method employed is adequate in

separating the peptides, the MS method is unable to fully deal with the complexity of the sample and ETD and CID should both be used and data analysed in unison. When fully validated and optimised this method should provide a very powerful tool for studying membrane proteins.

Chapter 5 Conclusions and Future Work

5.1. Conclusions

5.1.1. Lapatinib and EGF in resistant lung cancer

1. Lapatinib has a potential clinical role in combination with chemotherapy drugs in P-gp positive, non EGFR/HER-2 over-expressing cancers. This is based on results from combination toxicity assays in the resistant cell lines DLKP-A and A549-T which have little or no growth factor receptor expression and high to moderate expression of P-gp, respectively. Combinations of lapatinib with epirubicin, paclitaxel, docetaxel and vinblastine resulted in an increased toxicity compared with chemotherapy agents alone. This decrease in cell survival was associated with an increase in apoptosis, and so lapatinib increased the cytotoxic effects of the chemotherapy drugs. Synergistic toxicity was not observed with the non P-gp substrate drug 5-fluorouracil.

2. Lapatinib has the ability to alter transmembrane drug transporter expression levels which might be thought to have substantial implications in the clinic. It induced an increase in P-gp expression in a dose-responsive manner and this effect was residual in nature. RT-PCR analysis concluded this change in P-gp protein level was not occurring at a transcriptional level. Assays investigating the effect of lapatinib in combination with a chemically induced reduction in protein synthesis indicated that lapatinib is most likely causing an increase in P-gp levels by inducing synthesis of the protein, although does not rule out the possibility of preventing its degradation

3. Lapatinib was shown to have an effect on the P-gp protein level; however, it is entirely possible that this P-gp was non-functional for some reason as toxicity assays indicated. The lapatinib-induced change in P-gp expression had little or no negative impact on chemotherapy sensitivity. Pre-treating the cells with lapatinib did not alter chemotherapy drug accumulation or efflux or sensitivity to any great extent. Of note also, the positive synergistic effects were only observed with simultaneous combinations as opposed to pre-treatment with lapatinib.

4. Lapatinib has the ability to alter the MRP1 transporter pump expression. Lapatinib caused a reduction in MRP1 levels in both cells lines tested and RT-PCR results confirmed this alteration was not occurring at a transcriptional level.

5. The ability of lapatinib to alter the growth factor receptors EGFR and HER-2 and their phosphorylated counterparts was analysed and the findings suggested that lapatinib can slightly alter the levels of total EGFR and HER-2 and phosphorylated EGFR and HER-2 although this did not reach significance.

6. The EGFR and HER-2 ligand, EGF, was shown to reduce the expression levels of the drug transporter pumps P-gp and MRP1. This had little impact on chemotherapy sensitivity in the cell models.

7. EGF had more potent actions on the levels of growth factor receptors, causing a reduction in total levels of EGFR and HER-2.

8. Lapatinib and EGF actions on drug transporter expression levels were determined to be unlikely due to signalling through the EGFR or HER-2 pathways.

5.1.2. SiRNA techniques and chemotherapy resistance

1. SiRNA-mediated gene knockdown was coupled successfully with drug accumulation assays and it proved a very useful technique to study resistance in our cell models.

2. The inhibitor of DNA binding protein 3 may play a small role in chemotherapy resistance.

5.1.3. Membrane proteomic technique

1. Overall this technique proved a powerful one, resulting in the identification of many membrane proteins in cancer cell lines.

2. Although, not directly investigated, the extraction of membrane proteins and subsequent solubilisation and digestion proved successful based on the large numbers of membrane proteins identified from all the samples.

3. Multidimensional liquid chromatography was determined to be consistent, yield good separation, and led to the successful separation of proteins.

4. Mass spectrometry proved to be the limiting factor in the handling of such a complex sample and this may have contributed to the relatively small overlap in protein identifications in technical repeats was largely due to this.

5. The statistical parameters employed in the analyses have huge implications for the identifications of proteins. Analysing ETD and CID data together proved an important approach to ensure identifications were not over-looked.

6. The optimal XCorr scores in analysing our samples were 1.5 for single, 1.9 for double, 2.5 for triple and 3 for quadruple charged peptides. These settings may be altered further, in order to improve the detection of samples by the mass spectrometry.

7. Many comparisons were made between resistant and sensitive cell lines, implicating potential roles for many proteins in resistance. Further optimisation is required before hard conclusions can be drawn from these results. It does however provide a good insight to the capabilities of such a technique.

5.2. Future work

1. Literature evidence and findings in this thesis suggest there is a possibility that lapatinib-induced alterations of P-gp expression may be related to the proteasome-ubiquitination pathway and so further work to establish this is necessary.

2. The findings in this thesis indicate that the increase in P-gp level, in response to lapatinib has no effect in altering chemotherapy sensitivity. It is likely there is a complex relationship between lapatinib and P-gp, and work to expand this, such as longer treatments and continuous exposure mimicking therapy in the clinics and examining *in vivo* bioavailability of drugs following lapatinib treatment could be beneficial.

3. This thesis established that lapatinib can alter levels of the P-gp and MRP1 drug pumps. However, it does not clarify if this TKI can alter BCRP levels and so utilising a BCRP expressing cell line it should be established if it has modulatory actions on the expression of this drug transporter also.

4. Findings in this research suggest a possible role of ID3 in chemotherapy resistance and this warrant further study. This could be further explored by generating a stable transfection of ID3 cDNA in the parental cell line to see if this confers resistance to chemotherapy.

5. Time constraints did not allow sufficient repeats of the membrane proteomic samples and so this should be carried out so more substantial conclusions can be drawn from the data.

6. The membrane proteomic work showed huge promise but could be expanded much further. Firstly, validation by Western blot is vital in order to confirm some of the findings. Also, in order to achieve better resolution of the peptides, the inclusion of more salt fractions and a longer run time would also be beneficial.

7. Chymotrypsin, which allows the generation of more hydrophobic peptides, should be tried with trypsin to give more complex digestion, making peptides easier to separate and detect.

8. Ideally this technique could be progressed to a quantitative method when coupled with a quantitative technique such as SILAC (Stable isotope labeling with amino acids in cell culture).

Output generated from thesis

Publications – Manuscript in preparation

Title: Modulation of P-glycoprotein expression by Lapatinib.

Authors: Gráinne Dunne, Laura Breen, Denis M Collins, Sandra Roche, Martin Clynes and Robert O'Connor.

Poster Presentations

Irish Association for Cancer Research (IACR) – 2009 Annual Meeting, Athlone, 5th – 6th March 2009

Title: Modulation of Drug Transporters by Lapatinib

Authors: Gráinne Dunne, Denis M Collins, Sandra Roche, Martin Clynes and Robert O'Connor.

Oral Presentations

The Centre for Applied Science for Health Postgraduate Day – June 5th 2009

Title: Investigating the Effects of Lapatinib in Resistant Cancer Cell Models

Authors: Gráinne Dunne, Denis M Collins, Sandra Roche, Martin Clynes and Robert O'Connor.

Abbreviations

5-Fu	5-Fluorouracil
ABC	ATP-binding Cassette
ADP	Adenosine Diphosphate
AR	Amphiregulin
ATCC	American Tissue Culture Collection
ATP	Adenosine Triphosphate
BCRP	Breast Cancer Resistance Protein
BSA	Bovine Serum Albumin
BTC	Betacellulin
cDNA	Complementary DNA
CID	Collision Induced Dissociation
CML	Chronic Myeloid Leukaemia
CRIP	Cysteine-Rich Protein
CRYZ	Crystallin-Zeta
DMEM	Dulbecco's Minimum Essential Medium
DMSO	Dimethyl Sulfoxide
DNA	Deoxyribonucleic Acid
EDTA	Ethylene diamine tetracetic acid
EGF	Epidermal Growth Factor
EGFR	Epidermal Growth Factor Receptor
ELISA	Enzyme-linked Immunosorbant Assay
EPR	Epiregulin
ERK	Extracellular signal-Regulated Kinase
ETD	Electron Transfer Dissociation
FCS	Fetal Calf Serum
GSH	Glutathione
HB-EGF	Heparin-Binding EGF
HER-2	Human Epidermal Growth Factor Receptor 2
HCL	Hydrochloric Acid
HEPES	4-(2-hydroxyethyl)-piperazine ethane sulphonic acid
HPLC	High Performance Liquid Chromatography

IC50	Inhibitory Concentration 50%
ID3	Inhibitor of DNA Binding 3
IgG	Immunoglobulin
IMS	Industrial Methylated Spirits
kDa	Kilo Daltons
LC	Liquid Chromatograpy
MAPK	Mitogen Activated Protein Kinase
MDLC	Multi-Dimensional Liquid Chromatography
MDR	Multi-Drug Resistance
MEM	Minimum Essential Medium
MRP	Multidrug Resistance-associated Protein
mRNA	Messenger RNA
MS	Mass Spectrometry
mTOR	Mammalian Target of Rapamycin
MW	Molecular Weight
NaCl	Sodium Chloride
$NaHCO_3$	Sodium Bicarbonate
NaOH	Sodium Hydroxide
NFB	Nucleotide Binding Folds
NSAID	Nonsteroidal anti-inflammatory drug
NSCLC	Non-small cell lung cancer
PAGE	Polyacrylamide Gel Electrophoresis
PBS	Phosphate Buffered Saline
PCR	Polymerase Chain Reaction
P-gp	P-glycoprotein
PI3K	Phosphatidylinositol 3 Kinase
PLD	Phospholipase D
PMSF	Phenylmethanesulphonyl Fluoride
RNA	Ribonucleic Acid
RT-PCR	Reverse Transcriptase-PCR
SCLC	Small cell lung cancer
SD	Standard Deviation
SDS	Sodium Dodecyl Sulphate
siRNA	Small interfering RNA

STAT	Signal Transducer and Activator of Transcription
TEMED	N, N, N', N'-Tetramethyl-Ethylenediamine
TGF-α	Transforming Growth Factor-α
TKI	Tyrosine Kinase Inhibitor
TNM	Tumour Node Metastasis
TRIS	Tris(hydroxymethyl)aminomethane
VEGF	Vascular Endothelial Growth Factor
UHP	Ultra high purity water

Bibliography

1. Parkin, D.M., et al., *Global cancer statistics, 2002.* CA Cancer J Clin, 2005. **55**(2): p. 74-108.
2. Hanahan, D. and R.A. Weinberg, *The hallmarks of cancer.* Cell, 2000. **100**(1): p. 57-70.
3. Brambilla, E., et al., *The new World Health Organization classification of lung tumours.* Eur Respir J, 2001. **18**(6): p. 1059-68.
4. Karim-Kos, H.E., et al., *Recent trends of cancer in Europe: a combined approach of incidence, survival and mortality for 17 cancer sites since the 1990s.* Eur J Cancer, 2008. **44**(10): p. 1345-89.
5. Rom, W.N., et al., *Molecular and genetic aspects of lung cancer.* Am J Respir Crit Care Med, 2000. **161**(4 Pt 1): p. 1355-67.
6. Hecht, S.S., *Cigarette smoking and lung cancer: chemical mechanisms and approaches to prevention.* Lancet Oncol, 2002. **3**(8): p. 461-9.
7. Travis, W.D., L.B. Travis, and S.S. Devesa, *Lung cancer.* Cancer, 1995. **75**(1 Suppl): p. 191-202.
8. Mountain, C.F., *Staging classification of lung cancer. A critical evaluation.* Clin Chest Med, 2002. **23**(1): p. 103-21.
9. Beadsmoore, C.J. and N.J. Screaton, *Classification, staging and prognosis of lung cancer.* Eur J Radiol, 2003. **45**(1): p. 8-17.
10. Chua, Y.J., C. Steer, and D. Yip, *Recent advances in management of small-cell lung cancer.* Cancer Treat Rev, 2004. **30**(6): p. 521-43.
11. Hoffman, P.C., A.M. Mauer, and E.E. Vokes, *Lung cancer.* Lancet, 2000. **355**(9202): p. 479-85.
12. Dancey, J. and T. Le Chevalier, *Non-small cell lung cancer: an overview of current management.* Eur J Cancer, 1997. **33 Suppl 1**: p. S2-7.
13. Riedel, R.F. and J. Crawford, *Small-cell lung cancer: a review of clinical trials.* Semin Thorac Cardiovasc Surg, 2003. **15**(4): p. 448-56.
14. Socinski, M.A., *Cytotoxic chemotherapy in advanced non-small cell lung cancer: a review of standard treatment paradigms.* Clin Cancer Res, 2004. **10**(12 Pt 2): p. 4210s-4214s.
15. Heymach, J.V., et al., *Epidermal growth factor receptor inhibitors in development for the treatment of non-small cell lung cancer.* Clin Cancer Res, 2006. **12**(14 Pt 2): p. 4441s-4445s.
16. Katzung, B.G., *Chapter 55, Basic and Clinical Pharmacology*, in *Basic and Clinical Pharmacology*. 1998. p. 893 - 904.
17. Hande, K.R., *Topoisomerase II inhibitors.* Cancer Chemother Biol Response Modif, 2003. **21**: p. 103-25.
18. Verrill, M., *Anthracyclines in breast cancer: therapy and issues of toxicity.* Breast, 2001. **10**: p. 8-15.
19. Jordan, M.A. and L. Wilson, *Microtubules as a target for anticancer drugs.* Nat Rev Cancer, 2004. **4**(4): p. 253-65.
20. Miller, M.L. and I. Ojima, *Chemistry and chemical biology of taxane anticancer agents.* Chem Rec, 2001. **1**(3): p. 195-211.
21. Hait, W.N., E. Rubin, and S. Goodin, *Tubulin-targeting agents.* Cancer Chemother Biol Response Modif, 2005. **22**: p. 35-59.
22. Gligorov, J. and J.P. Lotz, *Preclinical pharmacology of the taxanes: implications of the differences.* Oncologist, 2004. **9 Suppl 2**: p. 3-8.

23. Cragg, G.M. and D.J. Newman, *Plants as a source of anti-cancer agents.* J Ethnopharmacol, 2005. **100**(1-2): p. 72-9.
24. Gidding, C.E., et al., *Vincristine revisited.* Crit Rev Oncol Hematol, 1999. **29**(3): p. 267-87.
25. Longley, D.B. and P.G. Johnston, *Molecular mechanisms of drug resistance.* J Pathol, 2005. **205**(2): p. 275-92.
26. Michor, F., M.A. Nowak, and Y. Iwasa, *Evolution of resistance to cancer therapy.* Curr Pharm Des, 2006. **12**(3): p. 261-71.
27. Juliano, R.L. and V. Ling, *A surface glycoprotein modulating drug permeability in Chinese hamster ovary cell mutants.* Biochim Biophys Acta, 1976. **455**(1): p. 152-62.
28. Sparreboom, A., et al., *Pharmacogenomics of ABC transporters and its role in cancer chemotherapy.* Drug Resist Updat, 2003. **6**(2): p. 71-84.
29. Schinkel, A.H. and J.W. Jonker, *Mammalian drug efflux transporters of the ATP binding cassette (ABC) family: an overview.* Adv Drug Deliv Rev, 2003. **55**(1): p. 3-29.
30. Hipfner, D.R., R.G. Deeley, and S.P. Cole, *Structural, mechanistic and clinical aspects of MRP1.* Biochim Biophys Acta, 1999. **1461**(2): p. 359-76.
31. Gottesman, M.M., I. Pastan, and S.V. Ambudkar, *P-glycoprotein and multidrug resistance.* Curr Opin Genet Dev, 1996. **6**(5): p. 610-7.
32. Sorrentino, B.P., *Gene therapy to protect haematopoietic cells from cytotoxic cancer drugs.* Nat Rev Cancer, 2002. **2**(6): p. 431-41.
33. van Tellingen, O., *The importance of drug-transporting P-glycoproteins in toxicology.* Toxicol Lett, 2001. **120**(1-3): p. 31-41.
34. Skovsgaard, T., et al., *Cellular resistance to cancer chemotherapy.* Int Rev Cytol, 1994. **156**: p. 77-157.
35. Chen, X., T.K. Yeung, and Z. Wang, *Enhanced drug resistance in cells coexpressing ErbB2 with EGF receptor or ErbB3.* Biochem Biophys Res Commun, 2000. **277**(3): p. 757-63.
36. Sharom, F.J., *The P-glycoprotein efflux pump: how does it transport drugs?* J Membr Biol, 1997. **160**(3): p. 161-75.
37. Cole, S.P., et al., *Overexpression of a transporter gene in a multidrug-resistant human lung cancer cell line.* Science, 1992. **258**(5088): p. 1650-4.
38. Doyle, L.A., et al., *A multidrug resistance transporter from human MCF-7 breast cancer cells.* Proc Natl Acad Sci U S A, 1998. **95**(26): p. 15665-70.
39. Ozvegy, C., et al., *Functional characterization of the human multidrug transporter, ABCG2, expressed in insect cells.* Biochem Biophys Res Commun, 2001. **285**(1): p. 111-7.
40. Krishna, R. and L.D. Mayer, *Multidrug resistance (MDR) in cancer. Mechanisms, reversal using modulators of MDR and the role of MDR modulators in influencing the pharmacokinetics of anticancer drugs.* Eur J Pharm Sci, 2000. **11**(4): p. 265-83.
41. Thomas, H. and H.M. Coley, *Overcoming multidrug resistance in cancer: an update on the clinical strategy of inhibiting p-glycoprotein.* Cancer Control, 2003. **10**(2): p. 159-65.
42. Pusztai, L., et al., *Phase II study of tariquidar, a selective P-glycoprotein inhibitor, in patients with chemotherapy-resistant, advanced breast carcinoma.* Cancer, 2005. **104**(4): p. 682-91.

43. Choi, B.H., et al., *Curcumin down-regulates the multidrug-resistance mdr1b gene by inhibiting the PI3K/Akt/NF kappa B pathway.* Cancer Lett, 2008. **259**(1): p. 111-8.
44. Angelini, A., et al., *Reversal of P-glycoprotein-mediated multidrug resistance in human sarcoma MES-SA/Dx-5 cells by nonsteroidal anti-inflammatory drugs.* Oncol Rep, 2008. **20**(4): p. 731-5.
45. Dai, C.L., et al., *Sensitization of ABCB1 overexpressing cells to chemotherapeutic agents by FG020326 via binding to ABCB1 and inhibiting its function.* Biochem Pharmacol, 2009. **78**(4): p. 355-64.
46. Yu, X.N., et al., *Reversion of P-glycoprotein-mediated multidrug resistance in human leukemic cell line by carnosic acid.* Chin J Physiol, 2008. **51**(6): p. 348-56.
47. Li, X., et al., *Reversal of p-glycoprotein-mediated multidrug resistance by macrocyclic bisbibenzyl derivatives in adriamycin-resistant human myelogenous leukemia (K562/A02) cells.* Toxicol In Vitro, 2009. **23**(1): p. 29-36.
48. Shi, Z., et al., *Sipholenol A, a marine-derived sipholane triterpene, potently reverses P-glycoprotein (ABCB1)-mediated multidrug resistance in cancer cells.* Cancer Sci, 2007. **98**(9): p. 1373-80.
49. Breen, L., *Drug resistance, and the role of p53, in lung cancer cell lines (Thesis)*, in *National Institute for Cellular Biotechnology*. 2005, Dublin City University. p. 299.
50. Sikder, H.A., et al., *Id proteins in cell growth and tumorigenesis.* Cancer Cell, 2003. **3**(6): p. 525-30.
51. Wilson, J.W., et al., *Expression of Id helix-loop-helix proteins in colorectal adenocarcinoma correlates with p53 expression and mitotic index.* Cancer Res, 2001. **61**(24): p. 8803-10.
52. Gonzalez, P., P.V. Rao, and J.S. Zigler, Jr., *Organization of the human zeta-crystallin/quinone reductase gene (CRYZ).* Genomics, 1994. **21**(2): p. 317-24.
53. Tumminia, S.J., et al., *Xenobiotic induction of quinone oxidoreductase activity in lens epithelial cells.* Biochim Biophys Acta, 1993. **1203**(2): p. 251-9.
54. Hempe, J.M. and R.J. Cousins, *Cysteine-rich intestinal protein binds zinc during transmucosal zinc transport.* Proc Natl Acad Sci U S A, 1991. **88**(21): p. 9671-4.
55. Khoo, C., et al., *Human cysteine-rich intestinal protein: cDNA cloning and expression of recombinant protein and identification in human peripheral blood mononuclear cells.* Protein Expr Purif, 1997. **9**(3): p. 379-87.
56. Hao, J., et al., *Identification and rational redesign of peptide ligands to CRIP1, a novel biomarker for cancers.* PLoS Comput Biol, 2008. **4**(8): p. e1000138.
57. Rosa, D.D., et al., *Molecular-targeted therapies: lessons from years of clinical development.* Cancer Treat Rev, 2008. **34**(1): p. 61-80.
58. Schlessinger, J., *Cell signaling by receptor tyrosine kinases.* Cell, 2000. **103**(2): p. 211-25.
59. Herbst, R.S., *Review of epidermal growth factor receptor biology.* Int J Radiat Oncol Biol Phys, 2004. **59**(2 Suppl): p. 21-6.
60. Hynes, N.E., et al., *The ErbB receptor tyrosine family as signal integrators.* Endocr Relat Cancer, 2001. **8**(3): p. 151-9.
61. Wells, A., *EGF receptor.* Int J Biochem Cell Biol, 1999. **31**(6): p. 637-43.

62. Aaronson, S.A., *Growth factors and cancer.* Science, 1991. **254**(5035): p. 1146-53.
63. Datta, S.R., et al., *Akt phosphorylation of BAD couples survival signals to the cell-intrinsic death machinery.* Cell, 1997. **91**(2): p. 231-41.
64. Bogdan, S. and C. Klambt, *Epidermal growth factor receptor signaling.* Curr Biol, 2001. **11**(8): p. R292-5.
65. Herbst, R.S., M. Fukuoka, and J. Baselga, *Gefitinib--a novel targeted approach to treating cancer.* Nat Rev Cancer, 2004. **4**(12): p. 956-65.
66. Saranath, D., et al., *Amplification and overexpression of epidermal growth factor receptor gene in human oropharyngeal cancer.* Eur J Cancer B Oral Oncol, 1992. **28B**(2): p. 139-43.
67. Hetzel, D.J., et al., *HER-2/neu expression: a major prognostic factor in endometrial cancer.* Gynecol Oncol, 1992. **47**(2): p. 179-85.
68. Slamon, D.J., et al., *Human breast cancer: correlation of relapse and survival with amplification of the HER-2/neu oncogene.* Science, 1987. **235**(4785): p. 177-82.
69. Hirsch, F.R., et al., *Epidermal growth factor receptor in non-small-cell lung carcinomas: correlation between gene copy number and protein expression and impact on prognosis.* J Clin Oncol, 2003. **21**(20): p. 3798-807.
70. Nicholson, R.I., J.M. Gee, and M.E. Harper, *EGFR and cancer prognosis.* Eur J Cancer, 2001. **37 Suppl 4**: p. S9-15.
71. Zandi, R., et al., *Mechanisms for oncogenic activation of the epidermal growth factor receptor.* Cell Signal, 2007. **19**(10): p. 2013-23.
72. Pedersen, M.W., et al., *Expression of a naturally occurring constitutively active variant of the epidermal growth factor receptor in mouse fibroblasts increases motility.* Int J Cancer, 2004. **108**(5): p. 643-53.
73. Olayioye, M.A., et al., *The ErbB signaling network: receptor heterodimerization in development and cancer.* Embo J, 2000. **19**(13): p. 3159-67.
74. Park, J.W., et al., *Unraveling the biologic and clinical complexities of HER2.* Clin Breast Cancer, 2008. **8**(5): p. 392-401.
75. Ignatoski, K.M., et al., *ERBB-2 overexpression confers PI 3' kinase-dependent invasion capacity on human mammary epithelial cells.* Br J Cancer, 2000. **82**(3): p. 666-74.
76. Spencer, K.S., et al., *ErbB2 is necessary for induction of carcinoma cell invasion by ErbB family receptor tyrosine kinases.* J Cell Biol, 2000. **148**(2): p. 385-97.
77. Dennis, P.A. and M.B. Kastan, *Cellular survival pathways and resistance to cancer therapy.* Drug Resist Updat, 1998. **1**(5): p. 301-9.
78. McCubrey, J.A., et al., *Roles of the RAF/MEK/ERK and PI3K/PTEN/AKT pathways in malignant transformation and drug resistance.* Adv Enzyme Regul, 2006. **46**: p. 249-79.
79. Dickstein, B., et al., *Increased epidermal growth factor receptor in an estrogen-responsive, adriamycin-resistant MCF-7 cell line.* J Cell Physiol, 1993. **157**(1): p. 110-8.
80. Yang, J.M., G.F. Sullivan, and W.N. Hait, *Regulation of the function of P-glycoprotein by epidermal growth factor through phospholipase C.* Biochem Pharmacol, 1997. **53**(11): p. 1597-604.
81. Lee, D.C., et al., *Transforming growth factor alpha: expression, regulation, and biological activities.* Pharmacol Rev, 1995. **47**(1): p. 51-85.

82. Pinkas-Kramarski, R., I. Alroy, and Y. Yarden, *ErbB receptors and EGF-like ligands: cell lineage determination and oncogenesis through combinatorial signaling.* J Mammary Gland Biol Neoplasia, 1997. **2**(2): p. 97-107.
83. Beerli, R.R. and N.E. Hynes, *Epidermal growth factor-related peptides activate distinct subsets of ErbB receptors and differ in their biological activities.* J Biol Chem, 1996. **271**(11): p. 6071-6.
84. Arteaga, C.L., *ErbB-targeted therapeutic approaches in human cancer.* Exp Cell Res, 2003. **284**(1): p. 122-30.
85. Goldenberg, M.M., *Trastuzumab, a recombinant DNA-derived humanized monoclonal antibody, a novel agent for the treatment of metastatic breast cancer.* Clin Ther, 1999. **21**(2): p. 309-18.
86. Rossi, A., P. Maione, and C. Gridelli, *Cetuximab in advanced non-small cell lung cancer.* Crit Rev Oncol Hematol, 2006. **59**(2): p. 139-49.
87. Wong, S.F., *Cetuximab: an epidermal growth factor receptor monoclonal antibody for the treatment of colorectal cancer.* Clin Ther, 2005. **27**(6): p. 684-94.
88. Madhusudan, S. and T.S. Ganesan, *Tyrosine kinase inhibitors in cancer therapy.* Clin Biochem, 2004. **37**(7): p. 618-35.
89. Wakeling, A.E., et al., *ZD1839 (Iressa): an orally active inhibitor of epidermal growth factor signaling with potential for cancer therapy.* Cancer Res, 2002. **62**(20): p. 5749-54.
90. Pao, W., V.A. Miller, and M.G. Kris, *'Targeting' the epidermal growth factor receptor tyrosine kinase with gefitinib (Iressa) in non-small cell lung cancer (NSCLC).* Semin Cancer Biol, 2004. **14**(1): p. 33-40.
91. Chang, G.C., et al., *Molecular mechanisms of ZD1839-induced G1-cell cycle arrest and apoptosis in human lung adenocarcinoma A549 cells.* Biochem Pharmacol, 2004. **68**(7): p. 1453-64.
92. Cohen, M.H., et al., *FDA drug approval summary: erlotinib (Tarceva) tablets.* Oncologist, 2005. **10**(7): p. 461-6.
93. Grunwald, V. and M. Hidalgo, *Development of the epidermal growth factor receptor inhibitor Tarceva (OSI-774).* Adv Exp Med Biol, 2003. **532**: p. 235-46.
94. Smith, J., *Erlotinib: small-molecule targeted therapy in the treatment of non-small-cell lung cancer.* Clin Ther, 2005. **27**(10): p. 1513-34.
95. Ling, Y.H., et al., *Erlotinib, an effective epidermal growth factor receptor tyrosine kinase inhibitor, induces p27KIP1 up-regulation and nuclear translocation in association with cell growth inhibition and G1/S phase arrest in human non-small-cell lung cancer cell lines.* Mol Pharmacol, 2007. **72**(2): p. 248-58.
96. Xia, W., et al., *Anti-tumor activity of GW572016: a dual tyrosine kinase inhibitor blocks EGF activation of EGFR/erbB2 and downstream Erk1/2 and AKT pathways.* Oncogene, 2002. **21**(41): p. 6255-63.
97. Konecny, G.E., et al., *Activity of the dual kinase inhibitor lapatinib (GW572016) against HER-2-overexpressing and trastuzumab-treated breast cancer cells.* Cancer Res, 2006. **66**(3): p. 1630-9.
98. Moy, B. and P.E. Goss, *Lapatinib: current status and future directions in breast cancer.* Oncologist, 2006. **11**(10): p. 1047-57.
99. Ryan, Q., et al., *FDA drug approval summary: lapatinib in combination with capecitabine for previously treated metastatic breast cancer that overexpresses HER-2.* Oncologist, 2008. **13**(10): p. 1114-9.

100. Sedlak, J., et al., *Protein kinase inhibitor-induced alterations of drug uptake, cell cycle and surface antigen expression in human multidrug-resistant (Pgp and MRP) promyelocytic leukemia HL-60 cells.* Leuk Res, 1997. **21**(5): p. 449-58.
101. Hegedus, T., et al., *Interaction of tyrosine kinase inhibitors with the human multidrug transporter proteins, MDR1 and MRP1.* Biochim Biophys Acta, 2002. **1587**(2-3): p. 318-25.
102. Kitazaki, T., et al., *Gefitinib, an EGFR tyrosine kinase inhibitor, directly inhibits the function of P-glycoprotein in multidrug resistant cancer cells.* Lung Cancer, 2005. **49**(3): p. 337-43.
103. Yang, C.H., et al., *Gefitinib reverses chemotherapy resistance in gefitinib-insensitive multidrug resistant cancer cells expressing ATP-binding cassette family protein.* Cancer Res, 2005. **65**(15): p. 6943-9.
104. Leggas, M., et al., *Gefitinib modulates the function of multiple ATP-binding cassette transporters in vivo.* Cancer Res, 2006. **66**(9): p. 4802-7.
105. Shi, Z., et al., *The epidermal growth factor tyrosine kinase inhibitor AG1478 and erlotinib reverse ABCG2-mediated drug resistance.* Oncol Rep, 2009. **21**(2): p. 483-9.
106. Coley, H.M., et al., *Receptor tyrosine kinase (RTK) inhibition is effective in chemosensitising EGFR-expressing drug resistant human ovarian cancer cell lines when used in combination with cytotoxic agents.* Biochem Pharmacol, 2006. **72**(8): p. 941-8.
107. Tiwari, A.K., et al., *Nilotinib (AMN107, Tasigna) reverses multidrug resistance by inhibiting the activity of the ABCB1/Pgp and ABCG2/BCRP/MXR transporters.* Biochem Pharmacol, 2009. **78**(2): p. 153-61.
108. Dai, C.L., et al., *Lapatinib (Tykerb, GW572016) reverses multidrug resistance in cancer cells by inhibiting the activity of ATP-binding cassette subfamily B member 1 and G member 2.* Cancer Res, 2008. **68**(19): p. 7905-14.
109. Collins, D.M., et al., *Tyrosine kinase inhibitors potentiate the cytotoxicity of MDR-substrate anticancer agents independent of growth factor receptor status in lung cancer cell lines.* Invest New Drugs, 2009.
110. Polli, J.W., et al., *The role of efflux and uptake transporters in [N-{3-chloro-4-[(3-fluorobenzyl)oxy]phenyl}-6-[5-({[2-(methylsulfonyl)ethy l]amino}methyl)-2-furyl]-4-quinazolinamine (GW572016, lapatinib) disposition and drug interactions.* Drug Metab Dispos, 2008. **36**(4): p. 695-701.
111. Shimoyama, T., et al., *Effects of different combinations of gefitinib and irinotecan in lung cancer cell lines expressing wild or deletional EGFR.* Lung Cancer, 2006. **53**(1): p. 13-21.
112. Sirotnak, F.M., et al., *Efficacy of cytotoxic agents against human tumor xenografts is markedly enhanced by coadministration of ZD1839 (Iressa), an inhibitor of EGFR tyrosine kinase.* Clin Cancer Res, 2000. **6**(12): p. 4885-92.
113. Takabatake, D., et al., *Tumor inhibitory effect of gefitinib (ZD1839, Iressa) and taxane combination therapy in EGFR-overexpressing breast cancer cell lines (MCF7/ADR, MDA-MB-231).* Int J Cancer, 2007. **120**(1): p. 181-8.
114. Chen, J., et al., *Antitumor activity of HER1/EGFR tyrosine kinase inhibitor erlotinib, alone and in combination with CPT-11 (irinotecan) in human*

colorectal cancer xenograft models. Cancer Chemother Pharmacol, 2007. **59**(5): p. 651-9.
115. Higgins, B., et al., *Antitumor activity of erlotinib (OSI-774, Tarceva) alone or in combination in human non-small cell lung cancer tumor xenograft models.* Anticancer Drugs, 2004. **15**(5): p. 503-12.
116. Saigal, B., B.S. Glisson, and F.M. Johnson, *Dose-dependent and sequence-dependent cytotoxicity of erlotinib and docetaxel in head and neck squamous cell carcinoma.* Anticancer Drugs, 2008. **19**(5): p. 465-75.
117. Awada, A., et al., *New anticancer agents and therapeutic strategies in development for solid cancers: a clinical perspective.* Expert Rev Anticancer Ther, 2004. **4**(1): p. 53-60.
118. Giaccone, G., et al., *Gefitinib in combination with gemcitabine and cisplatin in advanced non-small-cell lung cancer: a phase III trial--INTACT 1.* J Clin Oncol, 2004. **22**(5): p. 777-84.
119. Herbst, R.S., et al., *Gefitinib in combination with paclitaxel and carboplatin in advanced non-small-cell lung cancer: a phase III trial--INTACT 2.* J Clin Oncol, 2004. **22**(5): p. 785-94.
120. Burton, A., *What went wrong with Iressa?* Lancet Oncol, 2002. **3**(12): p. 708.
121. Dutta, P.R. and A. Maity, *Cellular responses to EGFR inhibitors and their relevance to cancer therapy.* Cancer Lett, 2007. **254**(2): p. 165-77.
122. Herbst, R.S., et al., *TRIBUTE: a phase III trial of erlotinib hydrochloride (OSI-774) combined with carboplatin and paclitaxel chemotherapy in advanced non-small-cell lung cancer.* J Clin Oncol, 2005. **23**(25): p. 5892-9.
123. Geyer, C.E., et al., *Lapatinib plus capecitabine for HER2-positive advanced breast cancer.* N Engl J Med, 2006. **355**(26): p. 2733-43.
124. Cristofanilli, M., et al., *A phase II combination study of lapatinib and paclitaxel as a neoadjuvant therapy in patients with newly diagnosed inflammatory breast cancer (IBC).* Breast Cancer Research and Treatment, 2006. **100**: p. S5-S5.
125. Di Leo, A., et al., *Phase III, double-blind, randomized study comparing lapatinib plus paclitaxel with placebo plus paclitaxel as first-line treatment for metastatic breast cancer.* J Clin Oncol, 2008. **26**(34): p. 5544-52.
126. Amir, E., et al., *Lapatinib plus paclitaxel as first-line therapy for patients with human epidermal growth factor receptor 2-positive metastatic breast cancer: inappropriate conclusions from a company-sponsored study?* J Clin Oncol, 2009. **27**(11): p. 1919; author reply 1920-1.
127. McHugh, L.A., et al., *Combined treatment of bladder cancer cell lines with lapatinib and varying chemotherapy regimens--evidence of schedule-dependent synergy.* Urology, 2007. **69**(2): p. 390-4.
128. Siegel-Lakhai, W.S., et al., *Phase I pharmacokinetic study of the safety and tolerability of lapatinib (GW572016) in combination with oxaliplatin/fluorouracil/leucovorin (FOLFOX4) in patients with solid tumors.* Clin Cancer Res, 2007. **13**(15 Pt 1): p. 4495-502.
129. LoRusso, P.M., et al., *Phase I and pharmacokinetic study of lapatinib and docetaxel in patients with advanced cancer.* J Clin Oncol, 2008. **26**(18): p. 3051-6.
130. Molina, J.R., et al., *Evaluation of lapatinib and topotecan combination therapy: tissue culture, murine xenograft, and phase I clinical trial data.* Clin Cancer Res, 2008. **14**(23): p. 7900-8.

131. Chun, P.Y., et al., *Synergistic effects of gemcitabine and gefitinib in the treatment of head and neck carcinoma.* Cancer Res, 2006. **66**(2): p. 981-8.
132. Morelli, M.P., et al., *Sequence-dependent antiproliferative effects of cytotoxic drugs and epidermal growth factor receptor inhibitors.* Ann Oncol, 2005. **16 Suppl 4**: p. iv61-68.
133. Nelson D.L., a.C.M.M., *Biological Membranes and Transport*, in *Principles of Biochemistry*. 2005, W.H Freeman and Company. p. 370-375.
134. Lodish H., B.A., Zipursky L.S., Matsudaira P., Baltimore D. and Darnell J., *Protein Structure and Function*, in *Molecular Cell Biology*. 2000, W.H. Freeman: New York.
135. Lu, B., et al., *Strategies for shotgun identification of integral membrane proteins by tandem mass spectrometry.* Proteomics, 2008. **8**(19): p. 3947-55.
136. Rabilloud, T., *Membrane proteins and proteomics: love is possible, but so difficult.* Electrophoresis, 2009. **30 Suppl 1**: p. S174-80.
137. Gygi, S.P. and R. Aebersold, *Mass spectrometry and proteomics.* Curr Opin Chem Biol, 2000. **4**(5): p. 489-94.
138. Cho, W.C., *Proteomics technologies and challenges.* Genomics Proteomics Bioinformatics, 2007. **5**(2): p. 77-85.
139. Blonder, J., et al., *Enrichment of integral membrane proteins for proteomic analysis using liquid chromatography-tandem mass spectrometry.* J Proteome Res, 2002. **1**(4): p. 351-60.
140. Molloy, M.P., et al., *Extraction of Escherichia coli proteins with organic solvents prior to two-dimensional electrophoresis.* Electrophoresis, 1999. **20**(4-5): p. 701-4.
141. Zhang, N., et al., *Comparison of SDS- and methanol-assisted protein solubilization and digestion methods for Escherichia coli membrane proteome analysis by 2-D LC-MS/MS.* Proteomics, 2007. **7**(4): p. 484-93.
142. Motoyama, A. and J.R. Yates, 3rd, *Multidimensional LC separations in shotgun proteomics.* Anal Chem, 2008. **80**(19): p. 7187-93.
143. Snyder, L.R.a.K., J.J., *Introduction to Modern Liquid Chromatography*. 2nd Edition ed. 1979: John Wiley and Sons, Inc. 839.
144. Claessens, H.A. and M.A. van Straten, *Review on the chemical and thermal stability of stationary phases for reversed-phase liquid chromatography.* J Chromatogr A, 2004. **1060**(1-2): p. 23-41.
145. Stroobant, H.a., *Mass Spectrometry*. Second Edition ed. 2003: John Wiley and Sons.
146. Glish, G.L. and R.W. Vachet, *The basics of mass spectrometry in the twenty-first century.* Nat Rev Drug Discov, 2003. **2**(2): p. 140-50.
147. Shukla, A.K. and J.H. Futrell, *Tandem mass spectrometry: dissociation of ions by collisional activation.* J Mass Spectrom, 2000. **35**(9): p. 1069-90.
148. Syka, J.E., et al., *Peptide and protein sequence analysis by electron transfer dissociation mass spectrometry.* Proc Natl Acad Sci U S A, 2004. **101**(26): p. 9528-33.
149. Mikesh, L.M., et al., *The utility of ETD mass spectrometry in proteomic analysis.* Biochim Biophys Acta, 2006. **1764**(12): p. 1811-22.
150. Zubarev, R.A., A.R. Zubarev, and M.M. Savitski, *Electron capture/transfer versus collisionally activated/induced dissociations: solo or duet?* J Am Soc Mass Spectrom, 2008. **19**(6): p. 753-61.

151. Sobott, F., et al., *Comparison of CID Versus ETD Based MS/MS Fragmentation for the Analysis of Protein Ubiquitination.* J Am Soc Mass Spectrom, 2009.
152. Donoghue, P.M., et al., *Nonionic detergent phase extraction for the proteomic analysis of heart membrane proteins using label-free LC-MS.* Proteomics, 2008. **8**(18): p. 3895-905.
153. Pasini, E.M., et al., *Red Blood Cell (RBC) membrane proteomics - Part II: Comparative proteomics and RBC patho-physiology.* J Proteomics, 2009.
154. Roesli, C., et al., *Comparative analysis of the membrane proteome of closely related metastatic and nonmetastatic tumor cells.* Cancer Res, 2009. **69**(13): p. 5406-14.
155. Leth-Larsen, R., et al., *Metastasis-related plasma membrane proteins of human breast cancer cells identified by comparative quantitative mass spectrometry.* Mol Cell Proteomics, 2009. **8**(6): p. 1436-49.
156. Josic, D., et al., *Membrane proteins as diagnostic biomarkers and targets for new therapies.* Curr Opin Mol Ther, 2008. **10**(2): p. 116-23.
157. Breen, L., et al., *Development of taxane resistance in a panel of human lung cancer cell lines.* Toxicol In Vitro, 2008. **22**(5): p. 1234-41.
158. Law, E., et al., *Cytogenetic comparison of two poorly differentiated human lung squamous cell carcinoma lines.* Cancer Genet Cytogenet, 1992. **59**(2): p. 111-8.
159. Clynes, M., et al., *Multiple drug-resistance in variant of a human non-small cell lung carcinoma cell line, DLKP-A.* Cytotechnology, 1992. **10**(1): p. 75-89.
160. Towbin, H., T. Staehelin, and J. Gordon, *Electrophoretic transfer of proteins from polyacrylamide gels to nitrocellulose sheets: procedure and some applications.* Proc Natl Acad Sci U S A, 1979. **76**(9): p. 4350-4.
161. Wall, R., et al., *Rapid and sensitive liquid chromatography-tandem mass spectrometry for the quantitation of epirubicin and identification of metabolites in biological samples.* Talanta, 2007. **72**(1): p. 145-54.
162. *Guava Package Insert. Guava Technologies TUNEL Kit.* 2006.
163. Doyle, L.A. and D.D. Ross, *Multidrug resistance mediated by the breast cancer resistance protein BCRP (ABCG2).* Oncogene, 2003. **22**(47): p. 7340-58.
164. Sanchez, C., et al., *Expression of multidrug resistance proteins in prostate cancer is related with cell sensitivity to chemotherapeutic drugs.* Prostate, 2009.
165. Collins, D.M., *Docetaxel uptake and modulation of P-gp-mediated docetaxel efflux by tyrosine kinase inhibitors in human lung carcinoma cell lines (Thesis)*, in *National Institute for Cellular Biotechnology*. 2007, Dublin City University. p. 354.
166. Haslam, I.S., et al., *Induction of P-glycoprotein expression and function in human intestinal epithelial cells (T84).* Biochem Pharmacol, 2008. **76**(7): p. 850-61.
167. Burdon, R.H., *Temperature and animal cell protein synthesis.* Symp Soc Exp Biol, 1987. **41**: p. 113-33.
168. Labroille, G., et al., *Cytometric study of intracellular P-gp expression and reversal of drug resistance.* Cytometry, 1998. **32**(2): p. 86-94.
169. Adams, J., *The proteasome: structure, function, and role in the cell.* Cancer Treat Rev, 2003. **29 Suppl 1**: p. 3-9.

170. MacCoss, M.J., C.C. Wu, and J.R. Yates, 3rd, *Probability-based validation of protein identifications using a modified SEQUEST algorithm.* Anal Chem, 2002. **74**(21): p. 5593-9.
171. Link, A.J., et al., *Direct analysis of protein complexes using mass spectrometry.* Nat Biotechnol, 1999. **17**(7): p. 676-82.
172. Mayya, V., et al., *Systematic comparison of a two-dimensional ion trap and a three-dimensional ion trap mass spectrometer in proteomics.* Mol Cell Proteomics, 2005. **4**(2): p. 214-23.
173. Moore, R.E., M.K. Young, and T.D. Lee, *Qscore: an algorithm for evaluating SEQUEST database search results.* J Am Soc Mass Spectrom, 2002. **13**(4): p. 378-86.
174. Shen, Q., et al., *NAT10, a nucleolar protein, localizes to the midbody and regulates cytokinesis and acetylation of microtubules.* Exp Cell Res, 2009. **315**(10): p. 1653-67.
175. Zolfaghari, R. and A.C. Ross, *Recent advances in molecular cloning of fatty acid desaturase genes and the regulation of their expression by dietary vitamin A and retinoic acid.* Prostaglandins Leukot Essent Fatty Acids, 2003. **68**(2): p. 171-9.
176. Keenan, J., et al., *Proteomic analysis of multidrug-resistance mechanisms in adriamycin-resistant variants of DLKP, a squamous lung cancer cell line.* Proteomics, 2009. **9**(6): p. 1556-66.
177. Good, D.M., et al., *Post-acquisition ETD spectral processing for increased peptide identifications.* J Am Soc Mass Spectrom, 2009. **20**(8): p. 1435-40.
178. Perkins, D.N., et al., *Probability-based protein identification by searching sequence databases using mass spectrometry data.* Electrophoresis, 1999. **20**(18): p. 3551-67.
179. Laity, J.H., B.M. Lee, and P.E. Wright, *Zinc finger proteins: new insights into structural and functional diversity.* Curr Opin Struct Biol, 2001. **11**(1): p. 39-46.
180. Ogata, M., et al., *Effects of overexpression of PTP36, a putative protein tyrosine phosphatase, on cell adhesion, cell growth, and cytoskeletons in HeLa cells.* J Biol Chem, 1999. **274**(18): p. 12905-9.
181. Frese, M.A., S. Schulz, and T. Dierks, *Arylsulfatase G, a novel lysosomal sulfatase.* J Biol Chem, 2008. **283**(17): p. 11388-95.
182. Kucharczak, J., et al., *R-Cadherin expression inhibits myogenesis and induces myoblast transformation via Rac1 GTPase.* Cancer Res, 2008. **68**(16): p. 6559-68.
183. Gillet, J.P., T. Efferth, and J. Remacle, *Chemotherapy-induced resistance by ATP-binding cassette transporter genes.* Biochim Biophys Acta, 2007. **1775**(2): p. 237-62.
184. O'Connor, R., *The pharmacology of cancer resistance.* Anticancer Res, 2007. **27**(3A): p. 1267-72.
185. Shi, Z., et al., *Erlotinib (Tarceva, OSI-774) antagonizes ATP-binding cassette subfamily B member 1 and ATP-binding cassette subfamily G member 2-mediated drug resistance.* Cancer Res, 2007. **67**(22): p. 11012-20.
186. Rusnak, D.W., et al., *The effects of the novel, reversible epidermal growth factor receptor/ErbB-2 tyrosine kinase inhibitor, GW2016, on the growth of human normal and tumor-derived cell lines in vitro and in vivo.* Mol Cancer Ther, 2001. **1**(2): p. 85-94.

187. Moyer, J.D., et al., *Induction of apoptosis and cell cycle arrest by CP-358,774, an inhibitor of epidermal growth factor receptor tyrosine kinase.* Cancer Res, 1997. **57**(21): p. 4838-48.
188. Kim, J.W., et al., *The growth inhibitory effect of lapatinib, a dual inhibitor of EGFR and HER2 tyrosine kinase, in gastric cancer cell lines.* Cancer Lett, 2008. **272**(2): p. 296-306.
189. Palayekar, M.J. and T.J. Herzog, *The emerging role of epidermal growth factor receptor inhibitors in ovarian cancer.* Int J Gynecol Cancer, 2008. **18**(5): p. 879-90.
190. Pallis, A.G., et al., *Targeted therapies in the treatment of advanced/metastatic NSCLC.* Eur J Cancer, 2009.
191. Fojo, A.T., et al., *Expression of a multidrug-resistance gene in human tumors and tissues.* Proc Natl Acad Sci U S A, 1987. **84**(1): p. 265-9.
192. Thiebaut, F., et al., *Cellular localization of the multidrug-resistance gene product P-glycoprotein in normal human tissues.* Proc Natl Acad Sci U S A, 1987. **84**(21): p. 7735-8.
193. Sikic, B.I., et al., *Modulation and prevention of multidrug resistance by inhibitors of P-glycoprotein.* Cancer Chemother Pharmacol, 1997. **40 Suppl**: p. S13-9.
194. Safran, H., et al., *Lapatinib/gemcitabine and lapatinib/gemcitabine/oxaliplatin: a phase I study for advanced pancreaticobiliary cancer.* Am J Clin Oncol, 2008. **31**(2): p. 140-4.
195. Maglich, J.M., et al., *Comparison of complete nuclear receptor sets from the human, Caenorhabditis elegans and Drosophila genomes.* Genome Biol, 2001. **2**(8): p. RESEARCH0029.
196. Vos, T.A., et al., *Up-regulation of the multidrug resistance genes, Mrp1 and Mdr1b, and down-regulation of the organic anion transporter, Mrp2, and the bile salt transporter, Spgp, in endotoxemic rat liver.* Hepatology, 1998. **28**(6): p. 1637-44.
197. Bark, H., et al., *P-glycoprotein down-regulates expression of breast cancer resistance protein in a drug-free state.* FEBS Lett, 2008. **582**(17): p. 2595-600.
198. Choi, C.H., et al., *Drug concentration-dependent expression of multidrug resistance-associated protein and P-glycoprotein in the doxorubicin-resistant acute myelogenous leukemia sublines.* Mol Cells, 1999. **9**(3): p. 314-9.
199. Zhang, Z., et al., *Regulation of the stability of P-glycoprotein by ubiquitination.* Mol Pharmacol, 2004. **66**(3): p. 395-403.
200. Schuetz, E.G., W.T. Beck, and J.D. Schuetz, *Modulators and substrates of P-glycoprotein and cytochrome P4503A coordinately up-regulate these proteins in human colon carcinoma cells.* Mol Pharmacol, 1996. **49**(2): p. 311-8.
201. Herzog, C.E., et al., *Increased mdr-1/P-glycoprotein expression after treatment of human colon carcinoma cells with P-glycoprotein antagonists.* J Biol Chem, 1993. **268**(4): p. 2946-52.
202. Stang, E., et al., *Polyubiquitination of the epidermal growth factor receptor occurs at the plasma membrane upon ligand-induced activation.* J Biol Chem, 2000. **275**(18): p. 13940-7.
203. Scaltriti, M., et al., *Lapatinib, a HER2 tyrosine kinase inhibitor, induces stabilization and accumulation of HER2 and potentiates trastuzumab-dependent cell cytotoxicity.* Oncogene, 2009. **28**(6): p. 803-14.

204. Wartenberg, M., et al., *Down-regulation of intrinsic P-glycoprotein expression in multicellular prostate tumor spheroids by reactive oxygen species.* J Biol Chem, 2001. **276**(20): p. 17420-8.
205. Joh, T., et al., *Physiological concentrations of human epidermal growth factor in biological fluids: use of a sensitive enzyme immunoassay.* Clin Chim Acta, 1986. **158**(1): p. 81-90.
206. Meyers, M.B., P. Yu, and J. Mendelsohn, *Crosstalk between epidermal growth factor receptor and P-glycoprotein in actinomycin D-resistant Chinese hamster lung cells.* Biochem Pharmacol, 1993. **46**(10): p. 1841-8.
207. Han, Z., et al., *Phospho Akt mediates multidrug resistance of gastric cancer cells through regulation of P-gp, Bcl-2 and Bax.* J Exp Clin Cancer Res, 2007. **26**(2): p. 261-8.
208. Gan, H.K., et al., *The epidermal growth factor receptor (EGFR) tyrosine kinase inhibitor AG1478 increases the formation of inactive untethered EGFR dimers. Implications for combination therapy with monoclonal antibody 806.* J Biol Chem, 2007. **282**(5): p. 2840-50.
209. Wang, Q., G. Villeneuve, and Z. Wang, *Control of epidermal growth factor receptor endocytosis by receptor dimerization, rather than receptor kinase activation.* EMBO Rep, 2005. **6**(10): p. 942-8.
210. Taverna, D., et al., *erbB-2 expression in estrogen-receptor-positive breast-tumor cells is regulated by growth-modulatory reagents.* Int J Cancer, 1994. **56**(4): p. 522-8.
211. Seth, D., et al., *Complex post-transcriptional regulation of EGF-receptor expression by EGF and TGF-alpha in human prostate cancer cells.* Br J Cancer, 1999. **80**(5-6): p. 657-69.
212. Beguinot, L., et al., *Down-regulation of the epidermal growth factor receptor in KB cells is due to receptor internalization and subsequent degradation in lysosomes.* Proc Natl Acad Sci U S A, 1984. **81**(8): p. 2384-8.
213. Goldberg, H., et al., *Reduced cyclosporin accumulation in multidrug-resistant cells.* Biochem Biophys Res Commun, 1988. **152**(2): p. 552-8.
214. Kohno, K., et al., *Vincristine-resistant human cancer KB cell line and increased expression of multidrug-resistance gene.* Jpn J Cancer Res, 1988. **79**(11): p. 1238-46.
215. Keizer, H.G., et al., *Correlation of multidrug resistance with decreased drug accumulation, altered subcellular drug distribution, and increased P-glycoprotein expression in cultured SW-1573 human lung tumor cells.* Cancer Res, 1989. **49**(11): p. 2988-93.
216. Kato, S., et al., *Mechanisms involved in the development of adriamycin resistance in human leukemic cells.* Leuk Res, 1990. **14**(6): p. 567-73.
217. Loo, T.W. and D.M. Clarke, *The human multidrug resistance P-glycoprotein is inactive when its maturation is inhibited: potential for a role in cancer chemotherapy.* Faseb J, 1999. **13**(13): p. 1724-32.
218. Hyafil, F., et al., *In vitro and in vivo reversal of multidrug resistance by GF120918, an acridonecarboxamide derivative.* Cancer Res, 1993. **53**(19): p. 4595-602.
219. Lage, H., *An overview of cancer multidrug resistance: a still unsolved problem.* Cell Mol Life Sci, 2008. **65**(20): p. 3145-67.
220. Lo, Y.L., C.Y. Hsu, and J.D. Huang, *Comparison of effects of surfactants with other MDR reversing agents on intracellular uptake of epirubicin in Caco-2 cell line.* Anticancer Res, 1998. **18**(4C): p. 3005-9.

221. Xia, J.R., N.F. Liu, and N.X. Zhu, *Specific siRNA Targeting the Receptor for Advanced Glycation End Products Inhibits Experimental Hepatic Fibrosis in Rats.* Int J Mol Sci, 2008. **9**(4): p. 638-61.
222. Peng, Z., et al., *Reversal of P-glycoprotein-mediated multidrug resistance with small interference RNA (siRNA) in leukemia cells.* Cancer Gene Ther, 2004. **11**(11): p. 707-12.
223. Wu, H., W.N. Hait, and J.M. Yang, *Small interfering RNA-induced suppression of MDR1 (P-glycoprotein) restores sensitivity to multidrug-resistant cancer cells.* Cancer Res, 2003. **63**(7): p. 1515-9.
224. Kamalian, L., et al., *Increased expression of Id family proteins in small cell lung cancer and its prognostic significance.* Clin Cancer Res, 2008. **14**(8): p. 2318-25.
225. Asirvatham, A.J., M.A. Schmidt, and J. Chaudhary, *Non-redundant inhibitor of differentiation (Id) gene expression and function in human prostate epithelial cells.* Prostate, 2006. **66**(9): p. 921-35.
226. Norton, J.D. and G.T. Atherton, *Coupling of cell growth control and apoptosis functions of Id proteins.* Mol Cell Biol, 1998. **18**(4): p. 2371-81.
227. Fernandez, M.R., et al., *Human and yeast zeta-crystallins bind AU-rich elements in RNA.* Cell Mol Life Sci, 2007. **64**(11): p. 1419-27.
228. Olsen, J.V., S.E. Ong, and M. Mann, *Trypsin cleaves exclusively C-terminal to arginine and lysine residues.* Mol Cell Proteomics, 2004. **3**(6): p. 608-14.
229. Russell, W.K., Z.Y. Park, and D.H. Russell, *Proteolysis in mixed organic-aqueous solvent systems: applications for peptide mass mapping using mass spectrometry.* Anal Chem, 2001. **73**(11): p. 2682-5.
230. Lohaus, C., et al., *Multidimensional chromatography: a powerful tool for the analysis of membrane proteins in mouse brain.* J Proteome Res, 2007. **6**(1): p. 105-13.
231. Coon, J.J., et al., *Tandem mass spectrometry for peptide and protein sequence analysis.* Biotechniques, 2005. **38**(4): p. 519, 521, 523.
232. Pisitkun, T., et al., *Tandem mass spectrometry in physiology.* Physiology (Bethesda), 2007. **22**: p. 390-400.
233. Good, D.M., et al., *Performance characteristics of electron transfer dissociation mass spectrometry.* Mol Cell Proteomics, 2007. **6**(11): p. 1942-51.
234. Hirosawa, M., et al., *MASCOT: multiple alignment system for protein sequences based on three-way dynamic programming.* Comput Appl Biosci, 1993. **9**(2): p. 161-7.
235. Altelaar, A.F., et al., *Improved identification of endogenous peptides from murine nervous tissue by multiplexed peptide extraction methods and multiplexed mass spectrometric analysis.* J Proteome Res, 2009. **8**(2): p. 870-6.
236. Taylor, G.K. and D.R. Goodlett, *Rules governing protein identification by mass spectrometry.* Rapid Commun Mass Spectrom, 2005. **19**(23): p. 3420.
237. Kohli, B.M., et al., *An alternative sampling algorithm for use in liquid chromatography/tandem mass spectrometry experiments.* Rapid Commun Mass Spectrom, 2005. **19**(5): p. 589-96.
238. Chen, H.S., et al., *Enhanced characterization of complex proteomic samples using LC-MALDI MS/MS: exclusion of redundant peptides from MS/MS analysis in replicate runs.* Anal Chem, 2005. **77**(23): p. 7816-25.

239. Van der Bliek, A.M., et al., *Genes amplified and overexpressed in human multidrug-resistant cell lines.* Cancer Res, 1988. **48**(21): p. 5927-32.
240. Duan, Z., K.A. Brakora, and M.V. Seiden, *Inhibition of ABCB1 (MDR1) and ABCB4 (MDR3) expression by small interfering RNA and reversal of paclitaxel resistance in human ovarian cancer cells.* Mol Cancer Ther, 2004. **3**(7): p. 833-8.
241. Garrido, C., et al., *Heat shock proteins 27 and 70: anti-apoptotic proteins with tumorigenic properties.* Cell Cycle, 2006. **5**(22): p. 2592-601.
242. Verrills, N.M., et al., *Proteome analysis of vinca alkaloid response and resistance in acute lymphoblastic leukemia reveals novel cytoskeletal alterations.* J Biol Chem, 2003. **278**(46): p. 45082-93.
243. Kraus, A.C., et al., *In vitro chemo- and radio-resistance in small cell lung cancer correlates with cell adhesion and constitutive activation of AKT and MAP kinase pathways.* Oncogene, 2002. **21**(57): p. 8683-95.
244. Bon, G., et al., *Loss of beta4 integrin subunit reduces the tumorigenicity of MCF7 mammary cells and causes apoptosis upon hormone deprivation.* Clin Cancer Res, 2006. **12**(11 Pt 1): p. 3280-7.
245. Howard, E.W., et al., *Decreased adhesiveness, resistance to anoikis and suppression of GRP94 are integral to the survival of circulating tumor cells in prostate cancer.* Clin Exp Metastasis, 2008. **25**(5): p. 497-508.
246. Verma, A. and K. Mehta, *Tissue transglutaminase-mediated chemoresistance in cancer cells.* Drug Resist Updat, 2007. **10**(4-5): p. 144-51.
247. Kajiyama, H., et al., *Chemoresistance to paclitaxel induces epithelial-mesenchymal transition and enhances metastatic potential for epithelial ovarian carcinoma cells.* Int J Oncol, 2007. **31**(2): p. 277-83.
248. Shah, A.N., et al., *Development and characterization of gemcitabine-resistant pancreatic tumor cells.* Ann Surg Oncol, 2007. **14**(12): p. 3629-37.
249. Sabbah, M., et al., *Molecular signature and therapeutic perspective of the epithelial-to-mesenchymal transitions in epithelial cancers.* Drug Resist Updat, 2008. **11**(4-5): p. 123-51.
250. Frank, N.Y., et al., *ABCB5-mediated doxorubicin transport and chemoresistance in human malignant melanoma.* Cancer Res, 2005. **65**(10): p. 4320-33.
251. Shen, D.W., et al., *Identification of cytoskeletal [14C]carboplatin-binding proteins reveals reduced expression and disorganization of actin and filamin in cisplatin-resistant cell lines.* Mol Pharmacol, 2004. **66**(4): p. 789-93.
252. Zhang, J.T. and Y. Liu, *Use of comparative proteomics to identify potential resistance mechanisms in cancer treatment.* Cancer Treat Rev, 2007. **33**(8): p. 741-56.
253. Duffy, M.J., et al., *The role of ADAMs in disease pathophysiology.* Clin Chim Acta, 2009. **403**(1-2): p. 31-6.
254. Edwards, D.R., M.M. Handsley, and C.J. Pennington, *The ADAM metalloproteinases.* Mol Aspects Med, 2008. **29**(5): p. 258-89.
255. Martinez-Balibrea, E., et al., *Increased levels of copper efflux transporter ATP7B are associated with poor outcome in colorectal cancer patients receiving oxaliplatin-based chemotherapy.* Int J Cancer, 2009. **124**(12): p. 2905-10.
256. Furukawa, T., et al., *Copper transport systems are involved in multidrug resistance and drug transport.* Curr Med Chem, 2008. **15**(30): p. 3268-78.

257. Safaei, R., et al., *Cross-resistance to cisplatin in cells with acquired resistance to copper.* Cancer Chemother Pharmacol, 2004. **53**(3): p. 239-46.
258. Gu, A.K., et al., *[Expression of coxsackievirus and adenovirus receptor in non-small cell lung cancer and its significance].* Zhonghua Zhong Liu Za Zhi, 2009. **31**(4): p. 278-81.
259. Giaginis, C.T., et al., *Coxsackievirus and adenovirus receptor expression in human endometrial adenocarcinoma: possible clinical implications.* World J Surg Oncol, 2008. **6**: p. 59.
260. Borst, P., C. de Wolf, and K. van de Wetering, *Multidrug resistance-associated proteins 3, 4, and 5.* Pflugers Arch, 2007. **453**(5): p. 661-73.
261. Ohtsuki, S., et al., *Correlation of induction of ATP binding cassette transporter A5 (ABCA5) and ABCB1 mRNAs with differentiation state of human colon tumor.* Biol Pharm Bull, 2007. **30**(6): p. 1144-6.
262. Tesniere, A., et al., *Molecular characteristics of immunogenic cancer cell death.* Cell Death Differ, 2008. **15**(1): p. 3-12.